Genetic and neuropathological study of primary and secondary dystonic syndromes

Reema Paudel

Department of Molecular Neuroscience

Institute of Neurology

University College London

Queen Square, London

WC1N 3BG

Submitted to

University College London

For the Degree of Philosophy, PhD

Declaration

I, Reema Paudel, confirm that the work presented in this thesis is my own. Where information has been derived from other sources, I confirm that this has been indicated in the thesis.

Acknowledgements

I would like to thank Professor Henry Houlden and Professor Janice L. Holton for giving me this opportunity to conduct research in their laboratories. This thesis would not have been possible without immense help and support from Prof Holton and her quiet assurances that everything will be fine.

Thank you to everyone at Department of Molecular Neuroscience, QSH and QSBB for embracing me and helping me around in the lab. Special thanks to Kate and Rob for their immense help.

Thank you to my family and friends who stood by me. I have annoyed most of them with the word 'PhD' in the last four years.

Thank you to my son for those lovely cuddles at difficult times. And to my husband for his love and generosity.

Thesis Outline

This thesis will examine monogenetic forms of primary dystonia related to *TOR1A, THAP1* and *GCH1* genes with a focus on genetic and neuropathological investigation. Further, this thesis discusses the neuropathology of genetic disorders under the neurodegeneration with brain iron accumulation (NBIA) spectrum, Beta-propeller protein associated neurodegeneration (BPAN) and neuroacanthocytosis. The genetics of spinocerebellar ataxia 8 will be discussed. This thesis also discusses the possibility of a common pathology for the lysosomal storage disorders (LSDs) impinging on ceramide pathway.

Table of contents

List of Tables

List of Figures

Abstracts

Dystonia 1 (DYT1) abstract

Early onset primary dystonia, DYT1 is linked to a three base pair deletion (ΔGAG) mutation in the *TOR1A* gene. Clinical manifestation includes intermittent muscle contraction leading to twisted movements or abnormal postures. Neuropathological studies on DYT1 cases are limited, most showing no significant abnormalities. In one study, brainstem intraneuronal inclusions immunoreactive for ubiquitin, torsinA and lamin A/C were described. Using the largest cohort of DYT1 cases reported to date we aimed to identify consistent neuropathological features in the disease and determine whether we would find the same intraneuronal inclusions as previously reported. Sanger sequencing was used to screen all the cases for (ΔGAG) mutation in *TOR1A* gene. Using immunohistochemistry seven DYT1 cases and five age and sex matched controls were studied for the presence of ubiquitinated inclusions in the brainstem and other anatomical regions implicated in dystonia. The pathological changes of brainstem inclusions reported in DYT1 dystonia were not replicated in our cohort. Other anatomical regions implicated in dystonia showed no disease-specific pathological intracellular inclusions or evidence of more than mild neuronal loss. Our findings suggest that the intracellular inclusions described previously in DYT1 dystonia may not be a hallmark

feature of the disorder. In DYT1, biochemical changes may be more relevant than the morphological changes.

Dystonia 6 (DYT6) abstract

Mutations in the thanatos-associated protein domain containing, apoptosis associated protein 1 gene (*THAP1*) are responsible for the adult-onset primary dystonia (DYT6). However, no neuropathological descriptions of genetically proven DYT6 cases have been reported to our knowledge. We report the clinical, genetic and neuropathological features of two DYT6 cases. The two DYT6 cases were genetically screened for the *THAP1* gene mutations using standard Sanger polymerase chain reaction sequencing. A detailed neuropathological assessment of the cases was performed using histochemical and immunohistochemical preparations. Both DYT6 cases showed no significant neurodegeneration and no specific disease-related pathology. This is the first detailed neuropthological investigation carried out on adult-onset primary dystonia, DYT6 brains. We did not identify any neuropathological features that could be defined as hallmark features of DYT6 dystonia. Our study supports the notion that in primary dystonia there is no significant neurodegeneration or associated neuropathological lesions.

Dopa-responsive dystonia (DRD) abstract

Autosomal dominant hereditary dopa-responsive dystonia (DYT5) is a rare movement disorder which presents typically in childhood with lower limb dystonia and subsequent generalization. Mutations in the *GCH1* gene on chromosome 14 q21.1-q22.2 are pathogenic in DYT5. The hallmark of the disease is an excellent and sustained response to small doses of levodopa, generally without the occurrence of motor fluctuations. The majority of DRD associated mutations lie within the coding region of the *GCH1* gene, but three additional single nucleotide sequence substitutions have been reported within the 5' untranslated (5'UTR) region of the gene. To determine if noncoding mutations in the 5' upstream region of *GCH1* gene are pathogenic in DYT5 dystonia Sanger sequencing of the region was carried out in a cohort of DRD cases negative for mutation in the coding regions of the *GCH1* gene. Two unrelated cases were identified with both -39C>T and -132C>T mutations in the 5' UTR of *GCH1* gene. However, one of the cases has an affected sibling without these mutations. Functional study identified negligible effect of these two mutations. Hence, in the DRD cohort studied, there is not enough evidence to conclude that the two non-coding variants underlie the disease manifestation.

Spinocerebellar ataxia type 8 (SCA8) abstract

SCA8 is characterized by repeat instability and presents as an ataxia with slow progression that largely spares brainstem and cerebral function. There is no anticipation observed and penetrance is reduced as the expansion can also be found in healthy individuals. Potentially pathogenic alleles contain 85 or more combined CTA/CTG repeats. However, repeats of this size are surprisingly frequent in the general population and also occur in asymptomatic relatives of ataxia individuals. This study examined the length of SCA8 repeats in English ataxia patients, English controls and in diversity (from 25 different countries) controls. In the ataxia cohort investigated, 6 out of 631 cases were in the potentially pathogenic range. However, a case out of 631 English controls and 3 cases out of 1148 individuals in diversity control cohort also fall in the same range.The significant difference (p= 0.018) in occurrence of SCA8 repeat expansions in ataxia patients compared with English controls but not with the diversity controls (p=0.192) suggests that the pathogenicity of SCA8 repeat expansion is not only dependent on the repeat size but also on the population, environment and the genetic modifiers. This study demonstrates that the presence of a SCA8 expansion cannot be used to predict whether or not an asymptomatic individual will develop ataxia as the control cases were asymptomatic at the time of study.

Beta-propeller protein associated neurodegeneration (BPAN) abstract

Neurodegenerative disorders with high iron in the basal ganglia encompass a single gene disorders collectively known as NBIA disorders. NBIA-5 (also known as BPAN) is linked to the mutations in the WD repeat domain 45 (*WDR45*) gene on chromosome Xp11. This study describes the genetic, clinical and neuropathological features of a case of BPAN. The clinical history of the case matches to other BPAN cases described which is characterized by global developmental delay and intellectual deficiency in early childhood then followed by further neurological and cognitive regression in early adulthood, with dystonia, and sometimes ocular defects and sleep perturbation. A cranial computed tomography (CT) revealed generalised brain atrophy and bilateral generalised mineralisation of the globi pallidi and substantia nigri that are likely to represent iron deposition on subsequent magnetic resonance imaging (MRI). The major pathological findings in this case were severe neuronal loss with gliosis affecting the substantia nigra, iron deposition in the substantia nigra and globus pallidus, axonal swellings in the substantia nigra, gracile nucleus and cuneate nucleus and very extensive phospho-tau deposition. Tau pathology was in the form of neurofibrillary tangles, pre-tangles and neuropil threads and histological studies indicated that many of the tau immunoreactive structures contained fibrillary protein (Gallyas silver positive and AT100 immunoreactive) and contained both 3-and 4-repeat tau isoforms similar to the tau deposits of Alzheimer's disease. This finding was confirmed by immunoblotting of non-dephosphorylated tangle extractions which showed the

classical triplet band as observed in AD cases (i.e. 3R+4R). When dephosphorylated, the tau isoform composition is almost identical to the AD case with 0N3R, 0N4R, 1N3R and 1N4R tau-isoforms. This study supports the involvement of beta–propeller protein (encoded by *WDR45* gene) in autophagy as has been documented in yeast and mammalian cells. The increased accumulation of LC3-II protein in brain tissue of the BPAN case compared to the three control cases implies that the autophagosome formation is hindered. BPAN represents the first direct link between autophagy mechanism and neurodegeneration. However, the role of iron in this process is still elusive.

Lewy bodies (LBs) in Lysosomal storage disorders (LSDs)

Inherited metabolic disorders which have been linked to lysosomal dysfunction belong to a family of diseases identified as sphingolipidoses, a class of LSDs. The main members of sphingolipidoses are Niemann-Pick disease, Krabbe disease, Gaucher disease, Fabry disease, Tay-Sachs disease, Sadhoff diasease and Metachromatic leukodystrophy. LSDs occurring due to the enzyme dysfunction in ceramide pathway develop Lewy body pathology, for example, Niemann-Pick disease, Krabbe disease, and Gaucher disease. This study investigated the possibility that LSDs, G_{M1}, Tay-Sachs disease, Sandhoff disease, Fabry disease and Metachromatic leukodystrophy which also occur due to the enzyme dysfunction in the ceramide pathway may mimic the Lewy body pathology suggesting that this may be a common theme for pathogenesis. Small changes in the molecular structure of ceramide can regulate its biological function and can contribute in development of age-related, neurological and neuroinflammatory disease. The negative alpha-synuclein immunohistochemistry observed in each case of LSD suggested that Lewy body pathology is not the hallmark of the LSDs in the ceramide pathway. However, a possibility is that Lewy bodies are a result of a stress created by free ceramides. Cells seek a balance of free ceramides and a slight tilt may be pathogenic.

Abbreviations

AD	Alzheimer's disease
ADCA	autosomal dominant inherited ataxias
Aβ	beta-amyloid
APP	amyloid precursor protein
BPAN	beta-propeller associated neurodegeneration
BTBDD	Brain and Tissue Banks for Developmental Disorders, Baltimore
CAA	cerebral amyloid angiopathy
CEPH	Foundation Jean Dausset-Centre d'Etude du Polymorphisme Humain
CERAD	Consortium to Establish a Registry for Alzheimer's Disease
ChAc	chorea-acanthocytosis
Ct	threshold cycle
CT	computerised tomography
DAB	diaminobenzidine
DBS	deep brain stimulation
DNA	deoxyribonucleic acid
DRD	dopa-responsive dystonia
DRPLA	dentatorubral-pallidoluysian atrophy
DTI	diffusion tensor imaging

DYT	dystonia
DYT1	dystonia 1
DYT6	dystonia 6
ECC	eyeblink classical conditioning
EEG	Electroencephalography
EMG	electromyography
FDG-PET	[18F]-fluorodeoxyglucose positron-emission tomography
Fe-S	iron-sulfur
FFPE	formalin-fixed-paraffin-embedded tissue
Ft	ferritin
GABA	gamma-amino butyric acid
GBA	glucocerebrosidase
GCH1	guanosine triphosphate cyclohydrolase 1 gene
GFAP	glial fibrillary acidic protein
GPe	globus pallidus external segment
GPi	globus pallidus internal segment
HBB	Harvard Brain Bank
HeLa	human epithelial cervical cancer
HGDP	human genome diversity project
HUVECs	human umbilical vein endothelial cells

IHC	immunohistochemistry
iPS	induced pluripotent stem cell
LAP1	lamina-associated polypeptide 1
LB/s	Lewy body/bodies
LC3	microtubule-associated protein 1A/1B-light chain 3
LSDs	lysosomal storage disorders
LULL1	luminal domain-like LAP-1
MLS	McLeod syndrome
MN-A	Amish-mennonite
MNCV	motor nerve conduction velocities
MRI	magnetic resonance imaging
mRNA	messenger ribonucleic acid
NA	neuroacanthocytosis
NBIA	neurodegeneration with brain iron accumulation
NCIs	neuronal cytoplasmic inclusions
NFTs	neurofibrillary tangles
NHNN-lab	National Hospital for Neurology and Neurosurgery
NPC	Niemann-Pick type C
PAR-4	prostate apoptosis response protein 4
PCR	polymerase chain reaction

PD	Parkinson's disease
PET	positron-emission tomography
PHF-tau	phosphorylated tau
PML	promyelocytic leukemia
qPCR	quantitative real-time polymerase chain reaction
QSBB	Queen Square Brain Bank
ROS	reactive-oxygen species
RT	room temperature
SAP	standard automated perimetry
SCAs	spinocerebellar ataxias
SENDA	static encephalopathy of childhood with neurodegeneration in adulthood
SH-SY5Y	neuroblastoma cells
SNpc	substantia nigra pars compacta
SNpr	substantia nigra pars reticulata
SPR	sepiapterin reductase
SVD	small vessel disease
TDP-43	TAR DNA-binding protein 43
TH	tyrosine hydroxylase
THAP1	thanatos-associated domain-containing apoptosis-associated protein 1

TOR1A	torsinA
VBM	voxel-based morphometry
WB	western blot
WDR45	WD repeat domain 45
ΔCt	normalised expression

Chapter 1. Introduction

1.1. Motor systems

The ease with which we make most of our movements contradicts the enormous sophistication and complexity of the motor system. Much of the brain and nervous system is devoted to the processing of sensory input, in order to construct detailed representations of the external environment; this is then integrated with the motor system to respond. This impact on the countless varieties of actions that make up our daily lives, for example: running, walking, expression of our feelings with concerted actions of facial muscles, communications through coordinated vocal cords and the movements of hands and digits and postural adjustments.

The sensory information-integrating capabilities of a brain highlight its centralized role in the motor systems. A very large proportion of the brain matter is dedicated to the motor function in lower mammalian species while in primates, motor areas are relatively small due to the huge cortical expansion. The cerebellum, a structure heavily involved in motor coordination, alone contains around 80% of the brain neurons (1).

In summary, motor function is supported through the functional integration across an extended motor system involving the cortical motor network, the cortico-spinal

tracts, the cortico-basal ganglia-thalamo-cortical loops and the cortico-cerebellar circuits. Any disorders of the motor system dramatically affect the quality of the life of the affected person as it hinders everyday actions that are naturally executed smoothly and unconsciously. One motor execution is comprised of many components (Figure 1.1) to deliver a precise orchestrated action. When one or more components involved in the motor system are subjected to noise, the motor output is still possible but slightly variable in response to the changing circumstances.

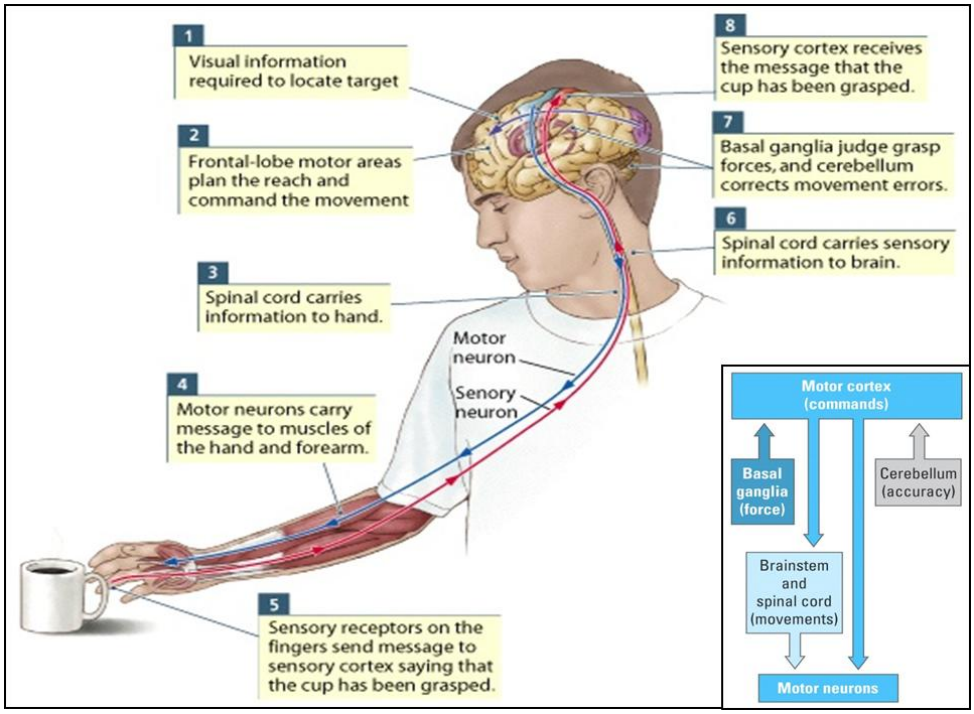

Figure 1.1: Steps in motor system components to execute a motor function (2).

The adaptive nature of the motor system means that there are many potential points of fault where motor disturbance and disorders may arise. For example: dysfunction of the basal ganglia leads to too little (Parkinsonian features) or excessive (dystonia, chorea) movement, abnormal cerebellar activity may lead to

unbalanced postures or a release of movement patterns inappropriate to the current context, degeneration of neurons and nerves innervating muscles (as can occur in diabetes or hereditary neuropathies) or aberrant ion homeostasis influencing muscle contractility.

In this study, I have focused on dystonia and in particular primary dystonia, where torsion dystonia is the main clinical symptom with the exception of tremor. Dystonia is traditionally believed to be a basal ganglia disorder however; the emerging role of cerebellum in dystonia needs consideration.

1.2. Dystonia overview

Dystonia is an umbrella term for a range of motor disorders characterised by sustained or intermittent muscle contractions causing abnormal, often repetitive, movements, postures, or both. These dystonic movements are typically patterned, twisting and may be tremulous. Dystonia is often initiated or worsened by voluntary action and associated with overflow muscle activation (3–7). The prevalence of dystonia is unknown, although it is probably more common than is generally appreciated. Total prevalence rates vary from 127 per million to 329 per million (8,9). Approximately 70,000 people in the UK are affected by dystonia including 8000 children and young adults (10). The prevalence of generalized isolated dystonia was reported to be 3.4 per 100,000 individuals in an epidemiological study of dystonia in Rochester, Minnesota, (8) and an annual prevalence of 15.2 per 100,000 individuals in Europe (11). New 'next generation' sequencing technologies have massively increased the speed of genetic discoveries

in recent years. Table 1.2 tabulates different dystonia (DYT) genes linked to the hereditary forms of dystonia till date.

Table 1.1 The current DYT loci with brief description of associated phenotype, gene, locus and mode of inheritance (Adapted from(12))

Locus symbol	Phenotype	Gene	Locus	Mode of inheritance
PURE PRIMARYTORSION DYSTONIA				
DYT1	Early-onset generalized limb onset dystonia	*TOR1A*	9q34	AD
DYT2	Early-onset generalized dystonia with prominent cranio-cervical involvement	-		AR
DYT4	Whispering dysphonia	*TUBB4a*	19p13.12–13	AD
DYT6	Generalized cervical and upper-limb-onset dystonia	*THAP1*	8p11.21	AD
DYT7	Adult-onset cervical dystonia	-	18p	AD
DYT13	Cervical and upper-limb dystonia	-	1p36.32–p36.13	AD
DYT17	Segmental or generalized dystonia with prominent dysphonia	-	20p11.2–q13.12	AR
DYT21	Adult-onset generalized or multifocal dystonia, often starting with blepharospasm	-	2q14.3–q21.3	AD
DYT23	Adult-onset cervical dystonia	*CIZ1*	9q34	AD
DYT24	Cranio-cervical dystonia with laryngeal and upper-limb involvement	*ANO3*	11p14.2	AD
DYT25	Adult-onset cervical dystonia	*GNAL*	18p11	AD
PRIMARY DYSTONIA-PLUS SYNDROME				
DYT5	Dopa-responsive dystonia	*GCH1*	14q22.2	AD
THD	Dopa-responsive dystonia	*TH*	11p15.5	AR
DYT11	Myoclonus-dystonia	*SGCE*	7q21.3	AD
DYT12	Rapid-onset dystonia parkinsonism	*ATP1A3*	19q13.2	AD
DYT15	Myoclonus-dystonia	-	18p11	AD
DYT16	Early-onset dystonia parkinsonism	*PRKRA*	2q31.2	AR
PAROXYSMAL SYNDROME				
DYT8	Paroxysmal non-kinesigenic dyskinesia (PNKD)	*MR1*	2q35	AD
DYT9/ DYT18	Paroxysmal dyskinesias with episodic ataxia and spasticity/paroxysmal exercise-induced dystonia (PED)	*SLC2A1*	1p34.2	AD
DYT10	Paroxysmal kinesigenic dyskinesia (PKD)	*PRRT2*	16p11.2	AD
DYT19	Paroxysmal kinesigenic dyskinesia 2 (PKD2)	-	16q13-q22.1	AD
DYT20	Paroxysmal non-kinesigenic dyskinesia 2 (PNKD2)	-	16q13–q22.1	AD
HEREDODEGENERATIVE DYSTONIA SYNDROME				
DYT3	Dystonia parkinsonism	*TAF1*	16q13–q22.1	X-R

*AD, autosomal dominant; AR autosomal recessive: X-R, X linked recessive. *DYT7 locus on chromosome 18p has been recently questioned (Winter et al., 2012).*

The European Federation of Neurological Societies recommended dystonia classification scheme based on one of the four major variables: (i) age of onset (early versus adult onset); (ii) distribution of affected body parts (focal, multifocal, segmental or generalized); (iii) the underlying cause (primary, secondary or heredodegenerative); or (iv) special clinical features (paroxysmal, exercise-induced, task-specific or DOPA-responsive)(13). This classification scheme was considered in this study Table 1.2.

Table 1.2 Classification of dystonia, based on the European Federation of Neurological Societies (13)

By aetiology	
Primary dystonia	
1.1 Primary pure dystonia	Torsion dystonia is the only clinical sign (apart from tremor) and there is no identifiable exogenous cause or other inherited or degenerative disease
1.2 Primary plus dystonia	Torsion dystonia is a prominent sign but is associated with another movement disorder, for example myoclonus or parkinsonism. There is no evidence of neurodegeneration.
1.3 Primary paroxysmal dystonia	Torsion dystonia occurs in brief episodes with normalcy in between. Three main forms are known depending on the triggering factor.
2. Heredodegenerative dystonia	Dystonia is a feature, among other neurological signs, of a heredodegenerative disorder, such as Wilson's disease
3. Secondary dystonia	Dystonia is a symptom of an identified neurological condition, such as a focal brain lesion, exposure to drugs or chemicals, e.g. dystonia because of a brain tumour, off-period dystonia in Parkinson's disease.
By age at onset	
1. Early onset (<30 years of age)	Usually starts in a leg or arm and frequently progresses to involve other limbs and the trunk
2. Late onset	Usually starts in the neck (including the larynx), the cranial muscles or one arm. Tends to remain localized with restricted progression to adjacent muscles
By distribution of affected body parts	
1. Focal	Single body region (e.g. writer's cramp, blepharospasm)
2. Segmental	Contiguous body regions (e.g. cranial and cervical, cervical and upper limb)
3. Multifocal	Non-contiguous body regions (e.g. upper and lower limb, cranial and upper limb)
4. Generalized	Both legs and at least one other body region (usually one or both arms)
5. Hemidystonia	Half of the body (usually secondary to a lesion in the contralateral basal ganglia)

Primary dystonias are the cases where dystonia is the main clinical consequence without any evidence of neurodegeneration or any obvious secondary cause (e.g. trauma, autoimmune, post-infectious etc). Primary dystonias are further categorised into primary pure where torsion dystonia is the only clinical sign (for example: DYT1/Oppenheim's Dystonia, DYT6 dystonia); primary plus where torsion dystonia is associated with another neurological disorder (for example: DYT11, DYT12, DYT16); and primary paroxysmal where torsion dystonia occurs in brief episodes (for example: DYT8, DYT10, DYT18). *Heredodegenerative dystonia* comprises a large number of complex neurological disorders of which dystonia can sometimes be a significant feature, such as Huntington's disease and Wilson's disease (7, 8). *Secondary dystonia* occurs as a downstream consequence of a brain injury often resulting in the dysfunction of the basal ganglia, such as stroke, tumours or the effect of drugs, toxins or infection (16).

The age at onset of dystonia varies. Childhood onset cases have a tendency to affect the whole body (generalized dystonia) with a more severe course whereas in adulthood onset cases, dystonia typically remains focal or segmental (5). Focal dystonias generally arise later in life around 40-60 years of age and affect small, discrete muscle groups: for example, focal hand dystonias such as writer's cramp or musician's dystonia manifest only during writing or playing musical instrument, respectively (17,18). Focal dystonias allow the patients a relative normal lifestyle (20). Generalised dystonias are of early onset (19), affect nearly all muscle group and are strongly enabling. Generalised dystonias severely reduce the quality of life

(21). Environmental factors have been investigated for possible association with primary dystonia. Evidence for possible contributions of environmental factors to early-onset primary dystonia is limited. However, in specific forms of primary adult onset focal dystonia, there is reasonable epidemiological evidence that some environmental factors are risk-modifying factors compared to control subjects. Namely, eye diseases, sore throat, idiopathic scoliosis, and repetitive upper limb motor action seem to be associated with blepharospasm, laryngeal dystonia, cervical dystonia, and upper limb dystonia, respectively (22). The pathophysiology of dystonia most likely arises due to abnormal processing of motor commands as a consequence of brain lesions or dysfunction of motor pathways involving basal ganglia and cerebellum (23,24).

1.3. The Basal Ganglia and their involvement in dystonia

The basal ganglia are known to be associated with various motor functions (5,25–28), any disruption of the basal ganglia's normal function is hypothesized to lead to some movement impairment. The basal ganglia are comprised of the caudate and putamen, globus pallidus, substantia nigra and subthalamic nucleus (Figure 1.2). The globus pallidus is divided into external segment (GPe), and an internal segment (GPi); the substantia nigra is composed of a pigmented region, the substantia nigra pars compacta (SNpc) and an unpigmented region, substantia nigra pars reticulata (SNpr) (25,28). The basal ganglia have specific input, output and intrinsic nuclei, which are modulated by several neurotransmitters. Among these, both the

inhibitory gamma-amino butyric acid (GABA) and dopamine are significant to the proper functioning of the basal ganglia (5).

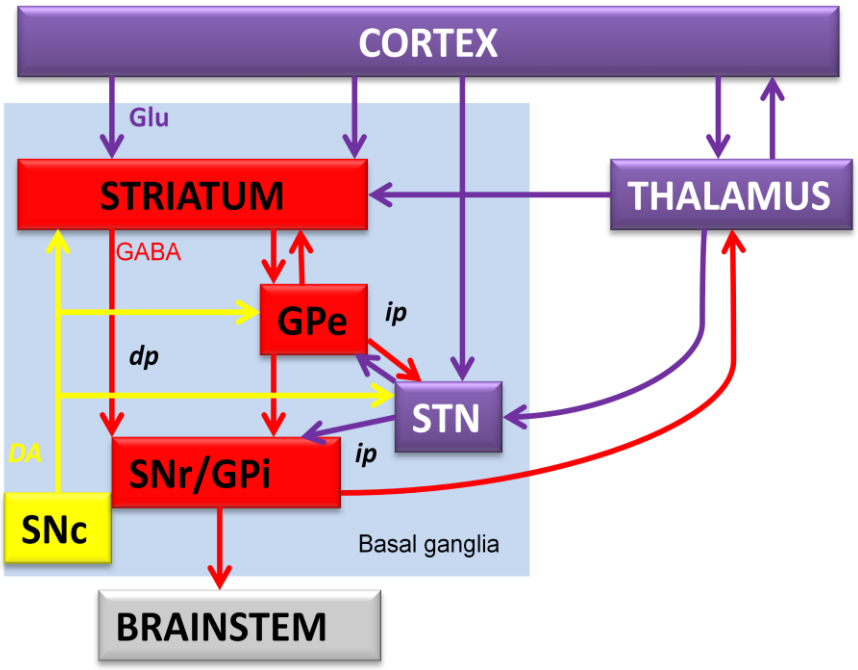

Figure 1.2 Organization of the basal ganglia, an ensemble of tightly interconnected sub-cortical nuclei. In blue are represented the glutamatergic (Glu) structures, in red the GABAergic (GABA) nuclei and in yellow the dopaminergic (DA) nucleus. GPe: external part of the globus pallidus; GPi: internal part of the globus pallidus; SNr: substantia nigra pars reticulata; SNc: substantia nigra pars compacta; dp: direct pathway; ip: indirect pathway. Adapted from (28).

The principal region that receives inputs is the striatum. GPi and SNpr are the output regions projecting beyond the basal ganglia. The input and output regions are connected by two basic pathways: direct and indirect. The former being implicated in movement facilitation and the latter in movement inhibition. In the

basal ganglia, the putamen receives information from all parts of the cerebral cortex. This information projects through an indirect pathway, containing GPe, STN, or direct pathway to the GPi. The striatal output of the basal ganglia has an ascending component to the thalamic nuclei that in turn are connected with the premotor and prefrontal cortical areas, and a descending component to the mesencephalon that projects to the lower brainstem and spinal cord (29,30).

The basal ganglia have been focused on in dystonia research and multiple publications have implicated basal ganglia dysfunction in the condition (5,31,32). Neuropathological studies showed defects in basal ganglia of individuals with secondary dystonia (33,34) well supported by focal lesions observed in putamen in neuroimaging studies (35). In total, dystonia occurred in 36% of 240 cases with basal ganglia lesions described in literature (36). Abnormalities in the basal ganglia have been documented for a wide variety of different forms of dystonia by positron-emission tomography (PET) studies of regional metabolic activity detected with [^{18}F]-fluorodeoxyglucose (FDG-PET) uptake or regional blood flow, voxel-based morphometry (VBM), magnetic resonance imaging (MRI), and diffusion tensor imaging (DTI) (37–40). Clinical associations of dystonia with other movement disorders have also pointed to the basal ganglia. For example, dystonia often co-exists with parkinsonism in idiopathic Parkinson's disease (PD) and several Parkinson-plus syndromes (41–44) where the primary pathology involves dysfunction of dopaminergic and other basal ganglia pathways (43,45). Dysfunction of nigrostriatal pathways is also thought to be responsible for both acute dystonic

reactions and tardive dystonia associated with antagonists of dopamine receptors. Dystonia similarly co-exists with chorea, for example in Huntington's disease where there is prominent degeneration of the striatum (46). Evidence from deep brain stimulation (DBS) of the same region is particularly compelling, since dystonia remits when stimulation is turned on, and returns when stimulation is turned off (47,48). Benefits are not universal but occur in primary generalized and focal dystonias, dystonia-plus syndromes, tardive dystonia, and some developmental or degenerative disorders.

Finally, animal studies frequently have implicated the basal ganglia in dystonia, as noted in several reviews (49–51). For example, selective lesions of the nigrostriatal dopamine pathway with the toxins 6-hydroxydopamine or MPTP result in dystonic movements in both rodents (52) and primates (53,54). Lesions of the striatum with the toxin 3-nitropropionic acid similarly cause dystonia in both rodents (55) and primates (56–58). In primates, focal destructive lesions of the posterior putamen also result in dystonia (59). In aggregate, these results provide strong converging support that the basal ganglia play an important role in dystonia.

1.4. The cerebellum and its role in dystonia

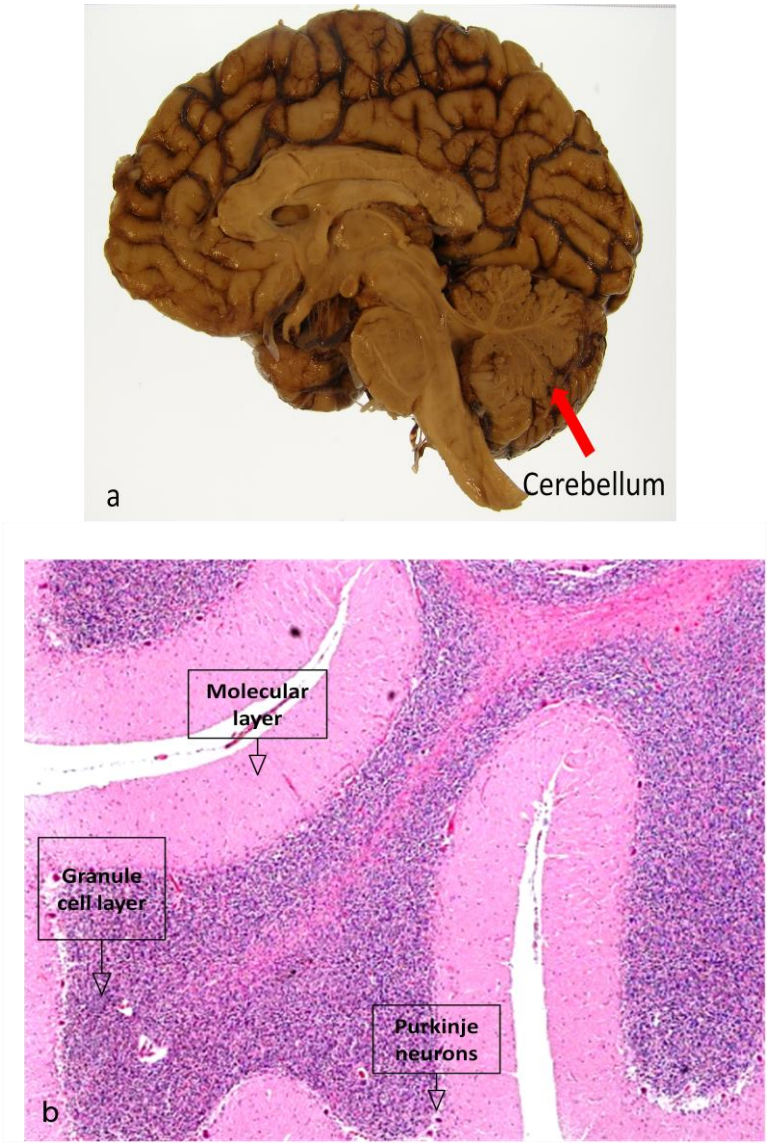

Figure 1.3 Cerebellum. (a) Macroscopic image of a half brain, cerebellum is located at the base of the brain (arrow, from the QSBB repository) (b) cellular layers of the cerebellum.

The cerebellum (Latin 'Little brain') plays an important role in motor control by modulating the primary motor cortex as well as spinally projecting brainstem regions to make movements integrated and seamless. The cerebellum directly excites the brainstem reticular formation, the red nucleus and the ventrolateral

thalamus to influence and regulate movements (60). The cerebellum is a compact structure at the base of the brain which despite its relatively small size comprises 80% of the neurons in the human brain (1) which are densely arranged in a highly ordered fashion (Figure 1.3).

In recent years, the cerebellum has emerged as a key player in dystonia. It has been reported that in some cases dystonia arises after injury to the cerebellum (61) and in some cases of genetic cerebellar degeneration dystonia is the predominant disease phenotype (62). In DYT1 mutation carriers, imaging studies revealed alterations in metabolic brain activity not only in the basal ganglia but also in the cerebellum (63–65). The hypothesis of cerebellar involvement in dystonia is further supported by a study in patients with focal dystonia. The patients were found to have impaired eyeblink classical conditioning, which is believed to be cerebellum-dependant (66). During eyeblink classical conditioning (ECC), a tone or light signal is repetitively paired with an airpuff to the eye until this unconditioned stimulus itself is sufficient to elicit an anticipatory eyeblink. Learning of the association between light/tone and airpuff is dependent on the cerebellum (67) but not on the basal ganglia: PD patients perform as well as healthy controls (68). Hence, this supports cerebellar abnormality to be present in at least some dystonias and rules out basal-ganglionic pathology in the dystonia patients. It is yet to determine if the aberrant cerebellar function is causal or secondary to a dystonic phenotype. Animal model provided evidence for a more casual role of abnormal cerebellar activity in dystonia: in a genetic mouse model of dystonia, the tottering mouse,

pharmacological stimulation of cerebellar structures has been found sufficient to elicit dystonia postures (69) and surgical ablation of the cerebellum abolished the dystonic phenotype (70). The tottering mice suggests that in this mouse model at least, cerebellar involvement is both sufficient and necessary for the generation of dystonia. The cerebellum has been suggested to have a prominent role in modulating cortical plasticity (71,72) so that developmental structural abnormalities in the cerebellum and its outflow pathways may give rise to alteractions in cortical activation responses during movement and learning, leading to the functional changes seen in dystonia.

Recently, the anatomical interconnection between the basal ganglia and cerebellum were shown using retrogradely transmitted viral tracers (73,74) which revealed their capability of directly interacting with each other. The exact nature of this interaction and whether cerebellar activity is casual, correlated or compensatory to abnormalities of the basal ganglia in the etiology of dystonia still remains unclear. A disynaptic link interconnecting cerebellum and basal gnglia from dentate nucleus to striatum and a reciprocal projection from the basal ganglia to the cerebellum has also been described which may allow abnormalities of the cerebellum to affect the basal ganglia and vice-versa (74).

The accumulating evidence reviewed above renders traditional models that focus on basal ganglia circuits as the central cause for all forms of dystonia obsolete. It is becoming increasingly clear that many brain regions contribute to dystonia, including the cerebral cortex, cerebellum, thalamus, and midbrain/brainstem. It

also is becoming increasingly clear that etiological heterogeneity among dystonias is important, as the relative importance of different brain regions seems to vary among them. Current challenges are to develop a model for understanding physiological interactions for how the different brain regions may contribute to different forms of dystonia, whether different dystonias can be subdivided into subgroups depending on how these regions are affected, and whether there is a final common pathway for all dystonias.

1.5. Primary pure dystonia

(This section will provide a brief review on primary pure dystonia and associated genes, in particular TOR1A and THAP1.)

Primary pure dystonia is usually defined as a syndrome in which dystonia is the only clinical feature (except for tremor of the arms or head and neck) without any evidence of neurodegeneration or any obvious secondary cause (e.g. trauma, autoimmune, post-infectious etc). In United States, the prevalence of generalized primary dystonia was reported to be 3.4 per 100,000 individuals and of focal primary dystonia, 29.5 per 100,000 individuals (8). In 1999, an epidemiological study of dystonia in Europe showed an annual prevalence of 15.2 per 100,000 individuals with the majority having focal dystonia , 11.7 per 100,000 (ESDE Collaborative Group).Genes linked to primary pure dystonia are summarized in Table 1.3.

Table 1.3 Primary pure dystonia genes described in literature (12)

Gene	Typical age range for onset	Typical distribution of dystonia (at onset)	Generalization or progression?	Clinical clues or other special features
TOR1A (DYT1)	Childhood	Legs ≫ arms	Often Generalizes	Jewish ancestry; dystonia progressing to fixed deformity; laryngeal or cranial sparing
THAP1 (DYT6)	Adolescence to early adulthood	Laryngeal, cervical or brachial	Generalization common	Laryngeal or brachial onset with progression
CIZ1	Adult	Cervical	No generalization	Only reported in pure focal cervical dystonia
ANO3 (DYT23)	Adolescence to early adulthood	Craniocervical or brachial	No generalization	Prominent head, voice or arm tremor
TUBB4A (DYT4)	Adolescence to early adulthood	Laryngeal, craniocervical	Generalization observed	Ataxic, hobbyhorse gait; extrusional tongue dystonia; single family
GNAL	Adolescence to mid-life	Craniocervical	Generalization observed	–

TOR1A: torsinA *; THAP1:* thanatos associated protein domain containing, apoptosis associated protein 1; *CIZ1:* CDKN1A interacting zinc finger protein 1; *ANO3:* anoctamin 3; *TUBB4A:* β-tubulin 4; *GNAL:* Guanine nucleotide-binding protein G(olf) subunit alpha

1.5.1. *TOR1A* Mutations (DYT1/Oppenheim's Disease)

Genetics and clinical features

DYT1 dystonia is the most common inherited form of early onset primary dystonia. The symptoms typically present in childhood or adolescence with only a few cases in adulthood and it has an autosomal dominant mode of inheritance (75).

In 1911, Oppenheim proposed the term 'dystonia musculorum deformans' to describe a syndrome in children with twisting or jerking movements, muscular spasm, and gait abnormalities that often progressed to a fixed postural deformity. The hereditary nature of the condition was subsequently recognized and in 1990, the disease was linked to chromosome 9q32-34 and designated with the first dystonia locus (DYT1) (76). It was quickly realized that this locus was associated with a significant proportion of all childhood-onset dystonia, particularly in Ashkenazi Jews (76,77). Seven years later the gene responsible for the condition was identified and named *TOR1A* (78).

The most frequent genetic cause of early-onset, generalized dystonia is a GAG deletion in exon 5 of the *DYT1* gene leading to deletion of a glutamic acid residue in the gene product torsinA (78). This mutation has been shown to be responsible for ~80% of all primary, early-onset dystonia in Ashkenazi Jewish populations and up to 50% of primary, early-onset dystonia in non-Jewish populations (79,80). Only two other missense variants (p.A288G and p.F205I) and one frameshift, 4-base pair

deletion (c.934_937delAGAG) in this gene have since been reported to cause dystonia, though their pathogenicity is by no means certain (81,82). Phenotypic presentation can vary widely within families (83) and between ethnic groups, with increased prevalence and severity found in the Ashkenazi Jewish population. Common clinical features include dystonic muscle contractions causing posturing of a foot, leg, or arm and in most cases this evolves to generalized dystonia with severe disability (84).

The penetrance of the GAG deletion is notably low, with current estimates somewhere within the region of 30–40% (76,79). In manifesting carriers, the spectrum of severity of the symptoms is wide, ranging from mild focal dystonia to severe and disabling generalized dystonia. The exact mechanism underlying this variability remains unclear, but is presumed that other genetic or environmental modifiers must exist that influences the penetrance and presentation of the disease.

Clinically, DYT1-related dystonia typically presents in childhood with dystonic posturing of the foot or leg and evolves to generalized dystonia with fixed deformities. However, late-onset or much milder forms of the disorder are recognized (80). There is generally a family history consistent with autosomal dominant inheritance, albeit with reduced penetrance, but apparently sporadic early and late onset cases are also seen (85). In general, symptoms of early-onset generalized dystonia can include:

- Twisted postures, for example in the torso or limbs
- Turning in of the foot or arm
- Unusual walking with bending and twisting of the torso
- Muscle spasms, with or without pain
- Rapid, sometimes rhythmic, jerking movements (often 'myoclonic jerks')
- Progression of symptoms leading to areas of the body remaining in sustained or fixed postures

TorsinA

The *DYT1*/*TOR1A* gene encodes a protein torsinA, a member of the AAA+ family of ATPases which resides in the lumen of the endoplasmic reticulum and nuclear envelope (78,86). However, when the mutant form of torsinA, torsinAΔ*E*, is overexpressed, it concentrates in the perinuclear space of the nuclear envelope, forming inclusions in both neuronal and nonneuronal cells (Figure 1.4) (33,87–89). It is believed to be involved in maintenance of both structural integrity and/or normal protein processing and trafficking (90–92). Molecular chaperone-like activities of torsinA have been reported using *in vitro* or *in vivo* protein aggregation models. Overexpression of torsinA prevents aggregation of luciferase *in vitro* (93), accumulations of α-synuclein in cultured mammalian cells (94), and polyglutamine-repeat proteins in *Caenorhabditis elegans* (95), suggesting torsinA has molecular chaperone activities.

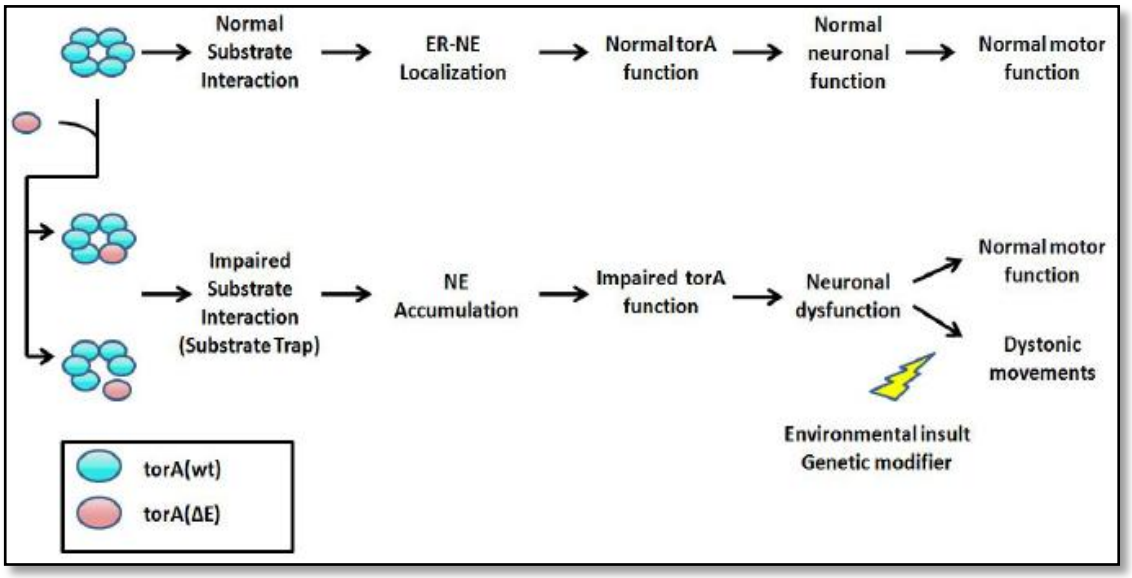

Figure 1.4: Putative mechanism by which mutant torsinA asserts dystonic movements. Mutant torsinA acts like a substrate trap and accumulates that in the nuclear membrane. The impaired tosinA function leads to neuronal dysfunction. Further environmental insults or genetic modifiers can then lead to the development of dystonia. (Adapted from (96)).

Of the four torsins that are encoded in the human genome (TorsinA, TorsinB, Torsin2A, Torsin3A), torsinA is by far the best characterized (97). TorsinA has a highly homologous family member torsinB, which is encoded by *TOR1B* located adjacent to *TOR1A* on human chromosome 9q34 (98) sharing 61% amino acid identity. TorsinA is expressed throughout the central nervous system in humans, but is found at particularly high levels in the dopaminergic neurons of substantia nigra pars compacta, locus coeruleus, Purkinje cells, cerebellar dentate nucleus, basis pontis, thalamus, hippocampal formation, oculomotor nuclei and frontal cortex (Figure 1.5 (99–101)). Since the discovery of the *TOR1A* gene, a number of cellular processes have been associated with torsinA, albeit the specific molecular

mechanism through which mutated torsinA leads to DYT1 dystonia remains unclear. There is accumulating data to suggest that torsinA has an important role in several cellular compartments and pathways, including the cytoskeleton, the nuclear envelope, the secretory pathway and the synaptic vesicle machinery (102–105). Recently a new function for torsinA in endoplasmic reticulum-associated degradation has been reported (106).

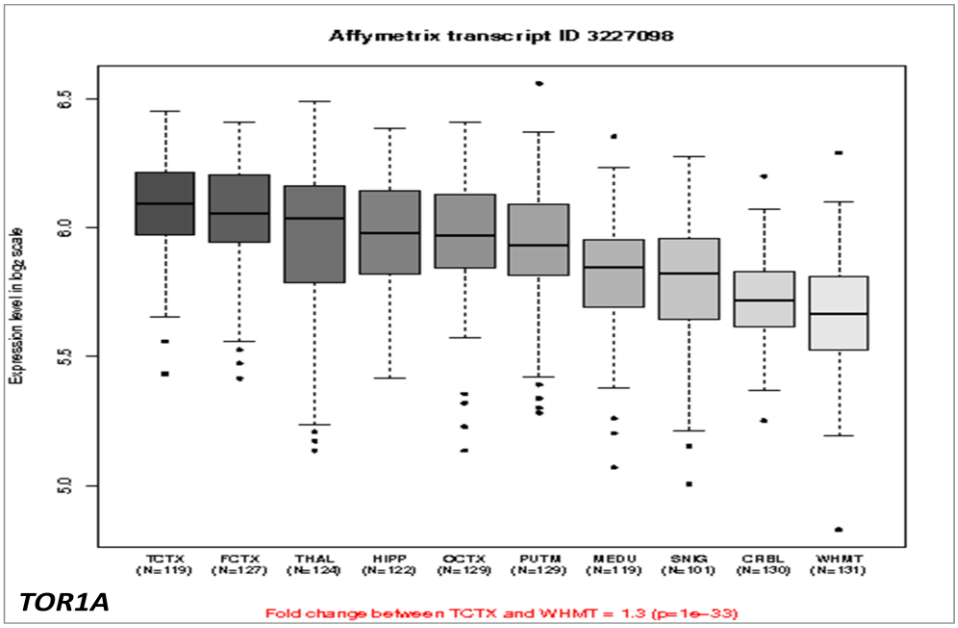

Figure 1.5: *TOR1A* gene expression pattern in different brain regions of neuropathologically confirmed healthy controls (HEX databse). Of the regions studied, *TOR1A* expression is highest in the temporal cortex.

Models of DYT1 dystonia

Several murine models of DYT1 dystonia have been developed, and characterized to various degrees. These models include DYT1 knock-out (102), cortex-specific DYT1 knock-out (107), torsinA knock-down (108), transgenic overexpression of mutant and wild-type torsinA (109,110) and DYT1 ΔGAG knock-in (102,111) mouse models. Whereas common features exist among some of these models, inconsistencies have been noticed. Morphological studies of *TOR1A* knock-out and homozygous *TOR1A* ΔGAG knock-in revealed that they are embryonically lethal (103,111). The heterozygous ΔGAG knock-in mice showed abnormal motor behaviours in 6-month old males with ubiquitin and torsin A positive aggregates in neurons of the pontine nuclei (111). Similar findings were reported in a cortex-specific DYT1 knock-out model (107). Dystonic movement of limbs with self-clasping, circling behavior, and hyperactivity was reported in 40% of the transgenic mouse models along with ubiquitin and torsinA-positive inclusions in the pedunculopontine nucleus, periaqueductal grey matter and pons (109,110). Prion protein promoter was reported to affect the torsinA expression in another DYT1 transgenic mouse model (110). Recently, mice that lacked the *TOR1A* gene in the entire central nervous system were generated and observed to develop striking abnormal twisting movements indicative of dystonia (112). In a genetic mouse model of dystonia, the tottering mouse, pharmacological stimulation of cerebellar structures has been found sufficient to elicit dystonia postures (69) and surgical ablation of the cerebellum abolished the dystonic phenotype (70) suggesting that in

this mouse model at least, cerebellar involvement is both sufficient and necessary for the generation of dystonia.

Alteration in the normal cytoplasmic localization to a perinuclear inclusion morphology was reported when mutant porcine torsinA was overexpressed in neuroblastoma cells (105). A similar observation was reported where transfection of mutant torsinA into cells resulted in re-distribution of the wild-type protein to the nuclear envelope (102). Severe abnormalities were also observed in the neurons from both torsinA null and homozygous disease mutant knockin mice (50). These observations suggest that DYT1 dystonia may be one of a group of diseases associated with defects in nuclear membrane structure and function (89).

DYT1 *in vitro* studies suggested that torsinA interacts with several proteins within the endoplasmic reticulum/nuclear envelope space, including lamina-associated polypeptide 1 (*LAP1*), luminal domain-like LAP-1 (*LULL1*), nesprins, and printor (113–116). Recent study has shown physical interaction of *TOR1A* with *LAP1* and *LULL1* where overexpression of these cofactors profoundly changes the subcellular localization of torsinA (117).

Neuropathology of DYT1 cases

Neuropathological studies of dystonia are sparse, partly due to the low availability of post-mortem tissue from these patients and the labour intensive nature of exploratory neurological examination of the entire human brain. Only a few studies

have examined neuropathological abnormalities in a handful of dystonia patients, providing limited information regarding the relationship between functional/structural brain changes and underlying neuropathology. However, neuropathological research has been unrewarding in providing information on disease processes.

Despite the studies implicating the caudate, putamen and globus pallidus in dystonia (36,118,119) neuropathological investigation of primary pure dystonia has not provided consistent evidence of neurodegeneration affecting these structures. There are relatively few published neuropathological studies of primary pure dystonia and the major contributors to the literature have been summarized in Table 1.4. Early studies lack genetic investigation and are based only on clinical classification of patients. The majority of primary pure dystonia cases that have undergone neuropathological investigation showed no abnormalities (120,121). Meige syndrome (a condition characterized by blepharospasm with facial, mandibular, oral, lingual, and laryngeal spasms) has been associated with neuronal loss in brainstem nuclei including the substantia nigra and with brainstem LB pathology (122,123). In one Meige syndrome case rod-shaped intranuclear inclusions were observed in neurons in the midbrain tectum. However, the nature of these inclusions is uncertain as immunohistochemical staining was not available at that time and the finding does not appear to have been replicated in more recent studies (122) . Decreased dopamine turnover in the substantia nigra,

striatum and nucleus accumbens, similar to that found in PD, was also described in one of the cases with Meige syndrome associated with Lewy bodies (LBs) (123).

Histopathological changes of neurofibrillary tangles (NFTs) with mild neuronal loss in the locus coeruleus and occasional NFTs identified by Congo red and Bielschowsky silver stains in the substantia nigra, pedunculopontine nucleus and dorsal raphe nucleus were reported in the brain of a 29 year old male with onset of dystonia at the age of 14 years. He had sustained a head injury aged 23 and additional neuropathological findings included old contusions in frontal and temporal lobes (121). NFTs have been described in the hippocampal formation and neocortex of patients as young as 27 years following a single episode of head trauma, however, brain stem regions have not been studied in such cases and it is therefore uncertain whether the brain stem NFTs could relate to the episode of trauma in this case (124). Neurofibrillary tangle pathology does not seem to be a consistent finding in dystonia, although in a series of 6 cases aged 65 – 84 years neurofibrillary tangle pathology and amyloid-β peptide deposition were observed in patients corresponding to the diagnosis of intermediate-high likelihood of Alzheimer's disease (AD). These changes were regarded as incidental and related to age rather than representing the pathology underlying dystonia (125). No significant neuropathological abnormalities were reported for clinical cases with spasmodic torticollis, blepharospasm with oromandibular dystonia (44) and oromandibular dystonia with torticollis (121,126). one of the cases with Meige syndrome associated with LBs (123).

Neuropathological examination of genetically confirmed DYT1 cases was disappointing as no evidence of neuronal loss, inflammation or altered localization of torsinA could be identified (101,120,127,128) (Table 1.4). Evaluation of a single DYT1 case demonstrated a modest reduction in dopamine content in the rostral putamen and caudate (127). A further study, which described 3 cases of DYT1 dystonia, also demonstrated a reduction in striatal dopamine, but this was not statistically significant when compared with controls. These authors were able to demonstrate evidence of increased dopamine turnover and a trend towards reduced D1R and D2R binding (128). A study of 5 DYT1 cases showed no apparent loss of pigmented neurons in the substantia nigra, however, using a semi-quantitative approach to estimate the size of pigmented neurons it was suggested that these may show an increase in size. Detailed morphometric analysis would be required to validate this observation (101).

One of the most interesting neuropathological studies of DYT1 dystonia described the novel finding of neuronal cytoplasmic inclusions (NCIs) immunoreactive for ubiquitin, torsinA and lamin A/C in the periaqueductal grey matter, cuneiform and pedunculopontine nuclei. These inclusions were identified in four genetically confirmed DYT1 dystonia cases and were absent from normal controls. Tau immunoreactive inclusions likely to represent age-related NFTs were also observed in the substantia nigra and locus coeruleus (129). In the light of current functional studies suggesting that torsinA interacts with nuclear membrane proteins, the presence of both torsinA and lamin A/C in the DYT1-associated intracytoplasmic

inclusions is of considerable interest (129,130). Although this report represents the most significant neuropathological observation in DYT1 dystonia to date, the findings have never been replicated due to the shortage of cases available for post-mortem investigations. Support for these observations has been provided by reports of similar inclusions in some DYT1 mouse models produced by expression of transgenic human torsinA (92,109).

Current treatments for DYT1 dystonia

Early diagnosis and start of treatment for dystonia, though not proven to alter its course or increase the likelihood for remission, may improve quality of life and alleviate the disability of patients with dystonia. Anticholinergic drugs, dopamine modulators, baclofen, muscle relaxants, and other pharmacologic agents have been used for a long time to treat dystonia. The introduction of botulinum toxin and DBS clearly revolutionized the symptomatic treatment of this neurological movement disorder (131). Therapy of dystonia can be divided into the following categories: (1) physical, supportive, and ancillary therapy; (2) pharmacologic treatment; (3) chemodenervation with botulinum toxin; and (4) peripheral and central surgery such as DBS. Anticholinergics block the neurotransmitter acetylcholine and have been shown moderately effective in patients with either generalized or focal dystonia (132,133). A second treatment modality involves injection of botulinum toxin directly into affected muscle regions. Botulinum toxin acts to block neuronal signals that tell the muscles to contract, thereby allowing the hypercontracted muscles of DYT1 patients to relax. Though shown to be quite effective for treating

focal dystonia, it is not practical for generalized dystonia and effects are transient, lasting 3-6 months.

The final treatment option shown to be effective is DBS of the globus pallidus, a nucleus within the basal ganglia, particularly for severe cases of generalized dystonia (134,135). Electrode leads are placed within the brain and the patient receives electrical impulses to the targeted region of the brain. The mechanism by which DBS operates is not currently understood. Some drawbacks of this treatment include the invasive nature of the surgery and variable effectiveness between patients.

Although several treatments are currently available for DYT1 patients, none of them are universally effective or curative and are associated with potentially severe and sometimes poorly characterized adverse effects. Given these limitations further therapies should be investigated.

Table 1.4 Summary of neuropathological studies in primary dystonia in literature

References	Cases	Diagnostic method	Clinical phenotype	Age at death, years	Sex	Neuropathology reported
(136)	1	Clinical	Spasmodic torticollis	65	F	No abnormality observed.
(121)	1	Clinical	Dystonia musculorum defomans	29	M	Numerous NFTs and mild neuronal loss in the LC. Occasional NFTs in the SNpc, pedunculopontine nucleus & dorsal raphe nucleus
	2	Clinical	Meige syndrome	68	M	Moderate to severe neuronal loss in brainstem nuclei including the SNpc, LC, raphe nuclei & pedunculopontine nucleus.
	3	Clinical	Dystonia musculorum defomans	10	M	No abnormality observed.
	4	Clinical	Spasmodic torticollis	50	F	No abnormality observed.
(126)	1	Clinical	Cranial dystonia (blephararospasm & oromandibular dystonia)	67	M	No abnormality observed.
	2	Clinical	Cranial dystonia (blephararospasm & oromandibular dystonia)	68	M	No abnormality observed.
	3	Clinical	Cranial dystonia (blephararospasm only)	73	M	Angioma in dorsal pons involving the central tegmental tract (represents secondary dystonia).
	4	Clinical	Oromandibular dystonia with retrocollis	68	F	No abnormality observed.
(122)	1	Clinical	Meige syndrome	72	M	Mild to moderate cell loss in the SNpc & LC, midbrain tectum & dentate nucleus. Frequent LBs in SN & LC. Rod-shaped intranuclear inclusions in neurons in midbrain tectum.
(123)	1	Clinical	Meige syndrome	69	M	LB pathology in the nucleus ambigus, LC, SN & nucleus basalis of Meynert. Mild neuronal loss in SN & LC.

M= male, F = female; Meige syndrome (focal adult onset torsion dystonia variant with cranial dystonia), SN-substantia nigra, SNpc-substantia nigra par compacta, LC-locus coeruleus, CN-cuneiform nucleus, PAG-periaqueductal gray matter, LB-Lewy body, DA- dopamine

Table 1.4 Summary of neuropathological studies in primary dystonia in literature continued...

References	Cases	Diagnostic method	Clinical phenotype	Age at death, years	Sex	Neuropathology reported
(120)	1	Genetic, DYT1	Generalized dystonia	33	M	No abnormality in localization of torsinA, no other significant pathological changes.
	2	Clinical, DYT1-ve	Cervical & possible brachial dystonia	68	N/A	No abnormality observed.
	3	Clinical, DYT1-ve	Cranial segmental dystonia	72	N/A	No abnormality observed.
	4	Clinical, DYT1-ve	Cranial segmental dystonia	45	N/A	Occasional pyknotic neurons in putamen & thalamus.
(101)	1	Genetic, DYT1	Dystonia musculorum defomans	83	F	No difference in the pattern of torsinA immunoreactivity between dystonia & control brains. No loss of pigmented neurons in the SN but increased neuronal size suggested by semiquantative analysis. Cases 1, 2,4,5,7 & 8 used for IHC. Cases 4, 5 & 6 are DYT1 negative.
	2	Genetic, DYT1	Focal non-progre-ssive dystonia	86	M	
	3	Genetic, DYT1	Dystonia musculorum defomans	29	M	
	4	Genetic, DYT1	Dystonia musculorum defomans	78	M	
	5	Genetic, DYT1	Spastic dysphonia	80	F	
	6	Genetic, DYT1	Torsion dystonia	67	F	
	7	Genetic, DYT1	Dystonia musculorum defomans	78	M	
	8	Genetic, DYT1	Torsion dystonia	67	F	
(127)	1	Genetic, DYT1	Generalized dystonia	10	M	No pathological abnormalities, normal content of dopamine with exception of a modest reduction in the rostral putamen & caudate.
(128)	1	Genetic, DYT1	Early onset generalized dystonia	67	F	Normal content of DA, changes in DA metabolites suggestive of increased DA turnover. Case 4 showed neuronal loss in the SN with no LBs. Mutation in parkin gene was excluded
	2	Genetic, DYT1		83	F	
	3	Genetic, DYT1		86	M	
	4	Genetic, DYT1	Parkinsonism	79	F	

M= male, F = female; Meige syndrome (focal adult onset torsion dystonia variant with cranial dystonia), SN-substantia nigra, SNpc-substantia nigra par compacta, LC-locus coeruleus, CN-cuneiform nucleus, PAG-periaqueductal gray matter, LB-Lewy body, DA- dopamine

Table 1.4 Summary of neuropathological studies in primary dystonia in literature continued..

References	Cases	Diagnostic method	Clinical phenotype	Age at death, years	Sex	Neuropathology reported
(129)	1	Genetic, DYT1	Dystonia musculorum defomans	83	F	Ubiquitin, laminA/C & torsinA positive inclusions within neurons in the brainstem, including the pedunculopontine nucleus, CN & the PAG. Tau & ubiquitin positive inclusions likely to represent NFTs noted in pigmented neurons in the SN & LC.
	2	Genetic, DYT1	Focal non-progre-ssive dystonia	86	M	
	3	Genetic, DYT1	Dystonia musculorum defomans	78	M	
	4	Genetic, DYT1	Generalized dystonia	33	M	
(125)	1	Clinical, DYT1-ve	Blepharospasm, subsequent right arm dystonia (late onset)	84	F	Neuronal inclusions were not identified in brainstem nuclei. No apparent neuronal loss in the striatal striosome compartment. Case 2: Frequent neuritic plaques, Braak & Braak stage IV tau pathology & brainstem predominant LB pathology. Cases 1, 3 & 5: minor degree of Alzheimer pathology. Cases 3, 4 & 5: small vessel disease, severe in case 3 with infarct in caudate nucleus.
	2	Clinical	Retrocollis, facial dystonia (late onset)	72	M	
	3	Clinical, DYT1-ve	Torticollis, dystonic head & hand tremor, later jaw opening dystonia (late onset)	79	F	
	4	Clinical	Axial dystonia, later laryngeal dystonia (late onset)	65	M	
	5	Clinical, DYT1-ve	Torticollis (late onset)	80	F	
	6	Clinical	Blepharospasm (late onset)	78	F	

M= male, F = female; Meige syndrome (focal adult onset torsion dystonia variant with cranial dystonia), SN-substantia nigra, SNpc-substantia nigra par compacta, LC-locus coeruleus, CN-cuneiform nucleus, PAG-periaqueductal gray matter, LB-Lewy body, DA- dopamine

1.5.2. *THAP1* mutations (DYT6)

Genetics and clinical features

Another distinct form of primary pure dystonia is dystonia 6 (DYT6). Affected individuals, who were negative for *TOR1A* mutations, tend to have an older age of onset during adolescence. Cases presented clinically with predominantly cranio-cervical or focal dystonia affecting the upper limbs.

The *DYT6* locus was localized to chromosome 8p21-q22 by linkage analysis in two Mennonite families (137,138) and linked to mutations in the DYT6 gene, also known *THAP1* (thanatos-associated domain-containing apoptosis-associated protein 1) in a non-Amish-Mennonite German family with primary torsion dystonia (138). DYT6/*THAP1* mutations are either missense or out of frame deletions, usually non-recurrent and have now been reported across many ethnicities (138). Inheritance is autosomal dominant with reduced penetrance. The disease penetrance was found to be 60% in three Amish-Mennonite families (75,137,139) but this may not be true of all populations or mutations (139).

The clinical spectrum of *THAP1* mutations is wide. Presentation with oromandibular, cranio-cervical and laryngeal dystonia is common, but presentations with focal dystonia of the limbs, segmental or generalised dystonia are also described in the literature (5,140).

THAP1

The THAP1 protein is a 213 amino acid protein characterized by an N-terminal THAP domain (amino acids 1 to 81) with DNA binding properties, followed by a proline-rich region (amino acids 90 to 110) and a nuclear localization signal (amino acids 146 to 162) (141). The THAP domain is conserved in both vertebrates and invertebrates (142). It has DNA binding properties and is thought to be involved in the regulation of transcription, either on its own or in concert with other proteins. Thus, one possible mechanism by which mutations in *THAP1* might cause dystonia is by dysregulated transcription of key genes. THAP1 protein is also known to interact with the prostate apoptosis response protein 4 (PAR-4), which is a transcription regulator involved in apoptosis (143). Under conditions of cellular stress or toxicity, this protein is rapidly upregulated and it has been linked to neurodegeneration in a number of disease models (144–146). Two spliced messenger ribonucleic acid (mRNA) variants that produce functional proteins have been reported (*THAP1a*: CCDS6136 and *THAP1b*: CCDS6137)(147). The first 2.2Kb isoform contains 3 exons, whereas the second corresponds to an alternatively spliced isoform that lacks exon 2 (2 kb mRNA). This second isoform encodes a truncated THAP1 protein without the C-terminus of the THAP domain (Figure 1.6). The two isoforms are expressed in many tissues suggesting that THAP1 has a widespread, although not ubiquitous, distribution in humans.

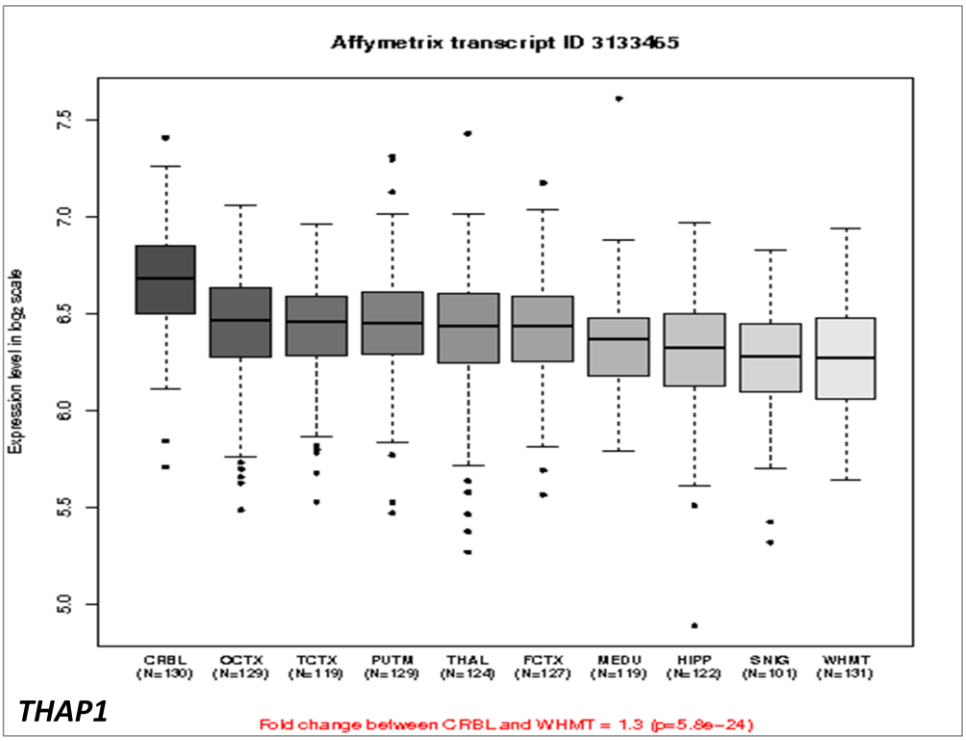

Figure 1.6: *THAP1* gene expression pattern in different brain regions of neuropathologically confirmed healthy controls (HEX databse).

One intriguing finding has been that THAP1 may regulate transcription of *TOR1A* by binding to one of the two sites in its promoter region suggesting a link *via* transcriptional regulation of other dystonia genes (148). Mutations in *THAP1* have been shown to disrupt binding to the *TOR1A* promoter and decrease *TOR1A*-driven luciferase expression, thus suggesting that under some conditions *TOR1A* is negatively regulated by THAP1 protein and that mutations in *THAP1* may lead to abnormally high levels of torsinA (149). Although these data come from experimental cell lines and thus are of uncertain physiological significance, this does at least raise the possibility that the disease mechanisms in DYT1 and DYT6 dystonia may be linked. However, if this is the case, the question arises as to how to link this mechanistically with the prevailing idea that the GAG-deletion in *TOR1A*

leads to a loss of function of the protein (103). One possibility is that *TOR1A* expression must be maintained within a set range in relation to its binding partners and that dysfunction may result from either increased expression or loss of function (150). Indeed, transgenic mice overexpressing wild-type *TOR1A* have been shown to display evidence of neurohistological, neurochemical and behavioural abnormalities, which may provide some support for this hypothesis (110). It has also been suggested that if there is a link between two monogenic forms of dystonia, mutations or other sequence variations in *THAP1* might influence the penetrance of DYT1 dystonia (151).

1.5.3. *THAP1*/DYT6 and *TOR1A*/DYT1 interaction

(This section reviews the emerging role of THAP1 protein. We aim to ifentify the interaction between two primary pure dystonia genes, TOR1A and THAP1 thereby predicting a common pathology in primary dystonia.)

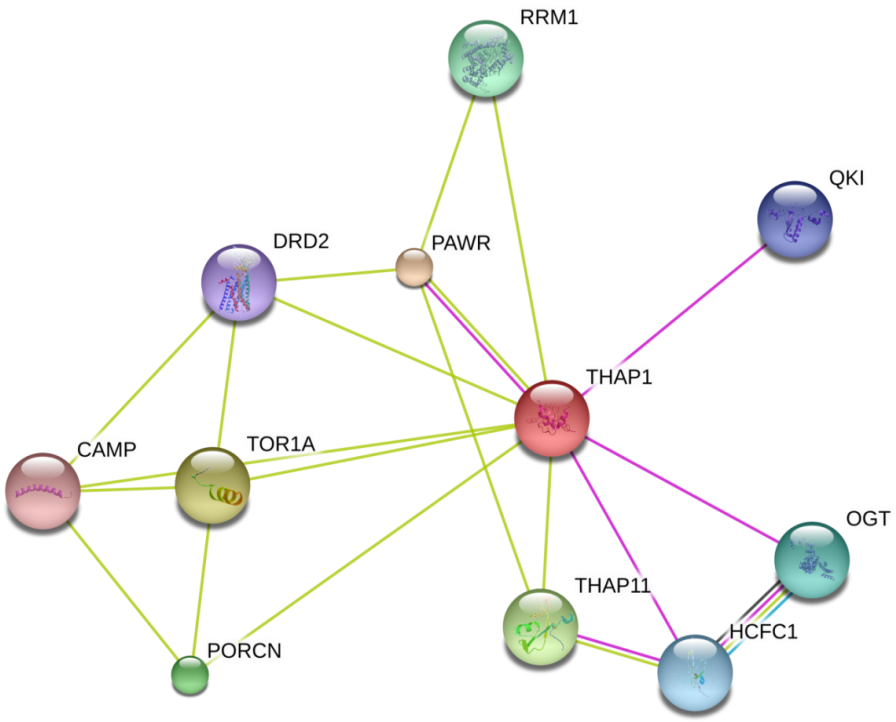

Figure 1.7: THAP1 Protein interaction prediction model generated by SIFT software predicting TOR1A interaction. Prediction based on **Neighbourhood, Gene fusion, Co-occurance, Co-expression, Experiments, Data-bases, Text-mining, and Homology.**

The phenotypic variability of primary dystonia suggests genetic heterogeneity. However clinical overlaps, not only in early-onset but also with the more common focal/segmental dystonias, suggest that common pathogenic mechanisms may be involved. Indeed, recent functional studies have demonstrated that *THAP1* and *TOR1A* interact in a common pathway (148,149).

Torsion dystonias are mostly associated with dysfunction in CNS regions controlling movement. The precise nature of this dysfunction is unclear, although it is believed that it may involve imbalances in neurotransmission within certain circuits, particularly in the basal ganglia, sensorimotor cortex, brainstem, and cerebellum (5,152). THAP1 is a nuclear transcription factor that can regulate endothelial cell proliferation (153) but its function in the brain is still unknown. *In vitro* studies have shown that *THAP1* physically interacts with *TOR1A* and represses torsinA expression by binding to the *TOR1A* promoter; this interaction is abolished by pathogenic mutations, leading to a decreased repression (149). However, the role of *THAP1* as a major genetic modifier in DYT1-dystonia has been recently questioned (154). Molecular analysis of *THAP1* as a genetic modifier for DYT1 has shown no sequence variation in coding regions and untranslated regions of the *THAP1* gene among affected and non-manifesting carriers of the DYT1 GAG deletion carriers (155). In line with this, *THAP1* is predicted to regulate several other gene targets, including the *TAF1* gene implicated in DYT3 dystonia (156). *THAP1* has been reported to co-localise with the apoptosis response protein

PAWR/PAR-4 in promyelocytic leukemia (PML) nuclear bodies, and function as a proapoptotic factor that links PAWR to PML nuclear bodies (143) Figure 1.7.

Although, the sequences and predicted functional domains of the two proteins causing DYT1 and DYT6 do not reveal obvious relationships among them, the mutations produce overlapping clinical phenotypes. In DYT1 symptoms starts before the age of 28 (157,158). Onset most often begins in legs and in the majority of the cases, symptoms spread to involve multiple body regions with segmental, multifocal or generalized dystonia (75). In DYT6 onset occurs across a much broader span, ranging from 10 to 80 years. The arm is the most common site of onset for DYT6, with subsequent spread to craniofacial muscles, leg, and neck (159). A common feature of DYT6 is laryngeal dystonia, producing severe speech defects, which is not often seen in DYT1 (157,159).

The initial efforts to map torsinA expression in human brain found particularly high mRNA levels in dopaminergic nigrostriatal neurons (160,161). However, no pathologic lesions were detected (33) in DYT1 in dopaminergic cell bodies in the substantia nigra, or in any other regions in CNS region, although one study reported apparent enlargement of dopaminergic neurons in DYT1 brains relative to controls (101). Inconsistent results were obtained from the multiple DYT1 mouse models and similarly monitored striatal tissue content of dopamine and metabolites (108–111,162–164). However, inconsistent results were obtained even in the same mouse model when analyzed by separate labs (162,164). Although a recent report describing a specific interaction between torsinA and tyrosine hydroxlase (163,165)

indicates this may still be a possibility. Moreover, a particularly striking finding is that even greater reductions in D2R availability were apparent in brains of DYT6 patients compared to controls than for the DYT1 patients, independent of clinical disease status (166). These data provide one of the first direct links between DYT6 and a potential dopamine-related defect, while further suggesting that D2R availability may be a critical factor in both DYT1 and DYT6 dystonias. in promyelocytic leukemia (PML) nuclear bodies, and function as a proapoptotic factor that links PAWR to PML nuclear bodies (143).

A recent hypothesis linking DYT1 and DYT6 is that THAP1 may regulate transcription of torsinA (148,149). *In vivo* method using human epithelial cervical cancer (HeLa) and neuroblastoma cells (SH-SY5Y) demonstrated the interaction between *THAP1* and *TOR1A* promoter (149). Cell lines overexpressing THAP1 was transfected with a plasmid containing a 977bp TOR1A promoter/exon1 fragment litigated to a reporter gene. A THAP1-mediated dose dependent decrease in activity of the promoter construct was reported; however failed to replicate the same effect in a more direct experiment. A small interfering RNA (siRNA)-mediated repression of *THAP1* did not have any effect on the cellular level of TOR1A mRNA. THAP1 and TOR1A interaction was also demonstrated by electrophoretic mobility shift assay (EMSAs) using nuclear extracts from the cells overexpressing wild-type THAP1 which bound to the TOR1A promoter sequences, whereas multiple DYT6 mutant forms did not (148). Human umbilical vein endothelial cells (HUVECs) and T98G glioblastoma cell lines were used for the purpose. THAP1 modulation of TOR1A

expression in lymphoblast cell lines derived from subjects with *THAP1* mutations, in 293T cells, or in HUVEC cells was not demonstrated. Thus, it is possible that the *THAP1/TOR1A* interaction is important in the CNS only. in promyelocytic leukemia (PML) nuclear bodies, and function as a proapoptotic factor that links PAWR to PML nuclear bodies (143).

Hence the recent hypothesis that THAP proteins most likely function as transcriptional repressors contrasts markedly with the prevailing DYT1 pathogenesis which proposes that *TOR1A* mutation results in a loss of torsinA function (96,103) as DYT6 mutations which decrease its DNA binding could theoretically lead to abnormally high levels of torsinA protein.

However, in studies of torsinA's role in trafficking of the DA transporter (DAT), overexpression of wild-type torsinA decreased surface expression of DAT, presumably by trapping it within the endoplasmic reticulum (113). In addition, phenotypic abnormalities were observed in transgenic mice overexpressing either mutant human torsinA or wild-type torsinA, indicating that at high expression levels, the wild-type protein may also interfere with protein processing (110). A potential hypothesis would then be that torsinA expression levels must be maintained within a certain stoichiometry relative to its binding partners and that perturbations in either direction might lead to imbalances that cause dysfunction.

1.6. Primary plus dystonia, Dopa-responsive dystonia (DYT5)

(This section reviews dopa-responsive dystonia with mutations in GCH1 gene. This project aims to identify if non-coding mutations in the 5'UTR of the gene are pathogenic in dopa responsive dystonia.)

To date, three genes have been convincingly shown to cause DOPA-responsive dystonia (DRD): *GCH1* (guanosine triphosphate cyclohydrolase 1 gene), *TH* (tyrosine hydroxylase) and *SPR* (sepiapterin reductase) (167–169). All three genes are bound together aetiologically by their connection to the endogenous pathway for the synthesis of dopamine, which accounts for their shared clinic characteristic of an improvement in symptoms in response to treatment with oral l-DOPA. We discuss *GCH1* gene in relation to dopa responsive dystonia in detail hereafter as mutations in *GCH1* gene are the commonest cause of dopa-responsive dystonia (DYT5).

Genetics and clinical features

DYT-5 dystonia is an autosomal dominant hereditary DRD (170), a rare movement disorder which presents typically in childhood with lower limb dystonia and subsequent generalization (171). DYT5 is linked to the mutations in the *GCH1* on chromosome 14 q21.1-q22.2 (167,172). More than 200 mutations have been reported in the gene (refer The Human Gene Mutation Database [HGMD]: http://www.hgmd.cf.ac.uk/ac/gene.php?gene = GCH1 for a complete published list of mutations). The hallmark of the disease is an excellent and sustained response to small doses of levodopa, generally without the occurrence of motor fluctuations. (170–173).

Clinical presentation is typically with lower limb dystonia and gait disturbance in the first decade of life, which occasionally leads to misdiagnosis as cerebral palsy or spastic paraparesis (174). Diurnal fluctuation in the severity of the dystonia is common, though this may abate with age. With time there is usually gradual generalization, and parkinsonism and dystonic tremor are possible complications of the condition (175,176). In a subgroup of patients, the dystonia is mild, progresses only very slowly and may require no treatment (177). Infrequently, patients may present later in life with a dystonic tremor or akinetic-rigid Parkinsonism (172,177). There is some evidence that subtle neuropsychiatric features may be associated with mutations in this gene. In one recent study of 18 patients, major depressive and sleep disorders occurred in about half of those over 20 years of age, whereas obsessive–compulsive disorder was found in 25% of cases (178). In terms of treatment, the response even to low doses of l-DOPA is generally excellent (70–100% improvement in clinical symptoms), sustained and is not generally associated with the late-onset dyskinesias that often accompany prolonged use of l-DOPA in other conditions, such as PD (179). Diagnosis can be confirmed on the basis of reduced cerebrospinal fluid levels of pterins, dopamine and serotonin metabolites (180), or an abnormal phenylalanine loading test (181,182).

Inheritance is usually autosomal dominant with reduced penetrance. Mutations in this gene account for ~60–80% of autosomal dominant DRD (183). Penetrance is incomplete and lower for males (~40–50%) than females (~80%)(184). Autosomal recessive mutations in *GCH1* have also been reported, resulting in no detectable

enzyme activity in the liver. As might be expected the phenotype is generally distinct and much more severe, with complex neurological dysfunction, including developmental delay, spasticity, seizures and physiological hyperphenylalaninaemia, which is generally picked up on routine screening of newborn infants (185). DRD shares some similarities with primary torsion dystonia such as frequent onset in childhood and initial involvement of lower limbs.

Noncoding mutations have also been reported spanning the 5' upstream region of *GCH1* gene. One subject had 2 mutations, -39C>T and -132C>T and another had a single mutation, -22 C>T. One family of Irish/French-Canadian ethnicity with DRD was studied where -22 C>T mutation segregate in the family with disease affected status (181,186). This makes it likely that the -22 C>T mutation is pathogenic and results in DRD. Of the above three mutations only -22 C>T mutation is evolutionarily conserved between human, rat and mouse (Figure 1.8).

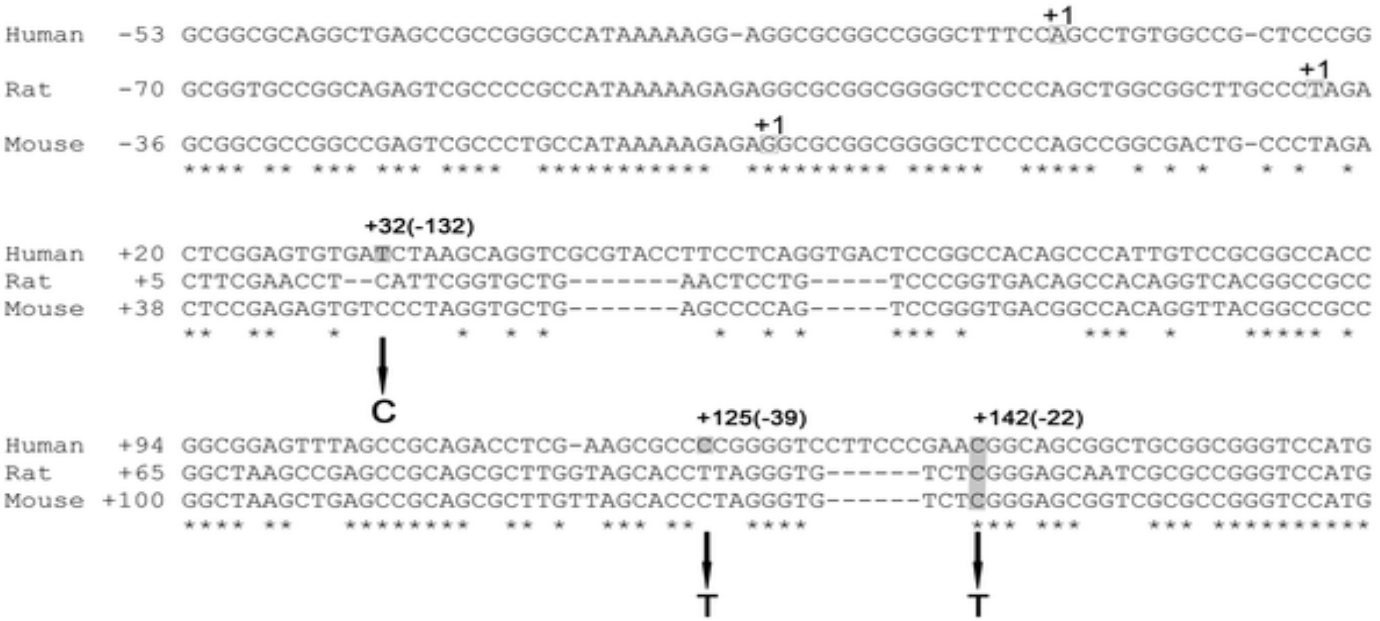

Figure 1.8: Alignment of the human, mouse and rat 5' upstream *GCH1* region. Nucleotides are numbered from the transcription start site (+1) as previously identified for the human, rat and mouse *GCH1* genes. Substitutions identified to date is shaded and the nucleotide substitution is shown beneath the sequence.(Adapted from **(187)**).

GTP cyclohydrolase 1 (GTPCH)

GCH1 gene encodes the enzyme guanosine triphosphate cyclohydrolase 1 gene, the enzyme controlling the first and rate-limiting step of the biosynthesis of tetrahydrobiopterin, essential cofactor for the ativity of tyrosine hydroxylase, and for dopamine production in nigrostriatal cells (188).

Neuropathology

Neuropathological examination, in a limited number of dystonia cases, revealed marked reduction of melanin pigment and dopamine content in nigrostriatal neurons, but no evidence of nigral cell loss or degeneration (189).

1.7. Genetics of Spinocerebellar ataxia type 8 (SCA8)

The autosomal dominant inherited ataxias (ADCA) constitute a clinically and genetically heterogeneous group of neurodegenerative diseases (190). ADCA is commonly denoted as Spinocerebellar ataxias (SCAs) and numbered chronologically following publication date from SCA1 found in 1993 (191) up to SCA35 and SCA36 described in 2011 (192,193) and SCA37 described in 2013 (194). SCAs are a group of late-onset neurodegenerative disorders characterized by slowly progressive ataxia that eventually leads to severe gait, speech, coordination and sensory loss (190). Polyglutamine expansion (a type of trinucleotide repeat expansion) in the encoded protein is the main mutational mechanism behind SCA1-3, SCA6-7 and Dentatorubral-Pallidoluysian Atrophy (DRPLA). However, trinucleotide repeat

expansions in the non-translated region of the genes causes gait ataxia in SCA8, 10, 12, 31 and 36 (192,195).

Identification of the SCA8 CTG/CAGrepeat expansion mutation

SCA8 is a dominantly inherited, slowly progressive neurodegenerative disorder caused by expression of a CTG/CAG repeat expansion mutation from opposite strands producing CUG expansion transcripts (*ATXN8OS*) and a polyglutamine expression protein (*ATXN8)* in the 3' UTR of the SCA8 gene (196). SCA8 has been classified into a new class of degenerative disorder in which microsatellite repeat expansion within a non-coding region of the gene results in an altered RNA product with a deleterious effect. The mutation for SCA8 was initially identified in 1999 as a CTG/CAG expansion mapping to chromosome 13q21 (197). The initial sequence analysis of the SCA8 CTG/CAG repeat region identified no likely open reading frames in the CTG or CAG direction but it was demonstrated that the SCA8 repeat mutation was transcribed in the CTG direction and that transcripts containing the CAG repeat were primarily expressed in the CNS and cerebellum (197). The CTG/CAGrepeat is adjacent to a CTA/TAG repeat that is highly polymorphic but stable when transmitted from one generation to the next (197–199). Although the SCA8 repeat is conserved in chimpanzees, gorillas, and orang-utans the genomic region containing the SCA8 repeat is not conserved in the mouse (200–202).

Evidence for SCA8 CTG expansion causing ataxia

It has been suggested that the CTG/CAG expansion is not involved in the SCA8 disease process and is simply a non-pathogenic polymorphism in linkage disequilibrium with another mutation that causes ataxia (203,204). However, using RAPID cloning SCA8 CTG/CAG expansion was isolated directly from the DNA of a single ataxia patient (197,205). Similar SCA8 expansions were subsequently found in additional ataxia families including a seven generation Amish-mennonite (MN-A) family (197,206). This study allowed 92 family members to genetically confirm that the mutation and the clinical disease map to the same locus (197,205,207). The relationship between repeat length and disease was observed in MN-A family members having longer CTG repeat tract (mean 116) than 21 asymptomatic expansion carriers (mean 90). The high frequency of SCA8 expansion was observed among apparently unrelated ataxia families worldwide with an incidence of 2-5% (197,208–212). SCA8 transcripts are primarily expressed in CNS tissue, including cerebellum (197,206).

Clinical features of SCA8

SCA8 presents as an ataxia with slow progression that largely spares brainstem and cerebral function (197,206–209,213,214). In the MN-A family, disease onset ranges from 13-60 years of age with the most frequently reported symptom being gait incoordination. Disease progression is relatively slow with significantly limited mobility occurring approximately 20 years after the initial symptoms, but without shortening life expectancy. Moderate to severely affected patients present with

dysarthric speech and commonly manifest oculomotor deficits (206,213,215). Severely affected individuals can present with hyperflexia and occasionally present mild myoclonic finger and arm jerks. Mild sensory loss is observed as indicated by decreased vibratory perception (206,213).

MRI analysis shows atrophy of the cerebellar hemispheres and vermis in affected SCA8 individuals (206,214,216), with little or no involvement of the brainstem, cerebral hemispheres and basal ganglia. Results from MRI studies are variable but generally show little change in affected individuals over decades of life, being consistent with the slowly progressive disease course (206). Analysis of a carrier of a SCA8 expansion, who is clinically unaffected, showed cerebellar atrophy indicating that asymptomatic individuals with the SCA8 mutation may have mild cerebellar atrophy (216).

Reduced Penetrance in SCA8

The SCA8 mutation is transmitted in an autosomal dominant pattern with reduced penetrance. The linkage data and the biological relationship between the repeat length and disease status in the MN-A family have supported the hypothesis that CTG/CAG repeat length is directly associated with ataxia. Affected members of the large MN-A family have significantly longer expansions (110-127, mean=119) than unaffected MN-A expansion carriers (73-104, mean=90) (206), indicating penetrance is influenced by CTG/CAGrepeat length (197,206).

A more complex pattern of inheritance emerges in other SCA8 families with more individuals that are carriers for the SCA8 expansion being asymptomatic (197,206,214,216,217). In small families with multiple affected individuals, the repeat mutation co-segregates with ataxia but far fewer expansion carriers develop ataxia (197,206,213,214,216–218). Additionally, the tight correlation between repeat size and pathogenesis found in the MN-A family has not been found in other reported SCA8 ataxia families with unaffected expansion carriers commonly having repeat sizes that exceed the pathogenic threshold observed in the MN-A family (218). These findings, and others, demonstrate that SCA8 expansions cannot be used to predict ataxia in asymptomatic expansion carriers (199,204,218).

SCA8 allele sizes

The precise number of the pathogenic (CTG)n repeat is technically difficult to determine due to its localization adjacent to a non-pathogenic but highly polymorphic, stably transmitted (CTA)n repeat (198). Therefore the current reference ranges are based on the total number of both the (CTA)n and (CTG)n repeats. *Normal alleles*: In general population, more than 99% of the alleles have 16-37 combined repeats (197). *Expanded alleles*: The reduced penetrance is found for SCA8 repeats of all sizes (219). The combined repeat length of the alleles with ataxia ranges from 68 to >1000 repeats, mostly 85-130 (203,218). Although the length of the repeat tract does not correlate with the age of onset, severity, symptoms or disease progression, within the repeat range 85-130, affected individuals tend to have longer repeat tracts than asymptomatic individuals.

However large SCA8 repeat allele has been reported in healthy controls and in non-ataxia neurological and neuropsychiatric patients (203,204,217,220,221).

1.8. Neurodegeneration with brain iron accumulation (NBIA)

(Neurodegeneration with brain iron accumulation (NBIA) brain is a movement disorder with a hallmark feature of iron deposition in the basal ganglia observed in magnetic resonance imaging. Neuroacanthocytosis (NA) is progressive movement disorder where presence of acanthocytes, spiky red cells with a poorly-understood membrane dysfunction in blood is a hallmark feature. The neuropathology of these two disorders, NBIA and NA will be discussed.)

Neurodegenerative disorders with high levels of iron in the basal ganglia encompass a group of single gene disorders collectively known as NBIA (neurodegeneration with brain iron accumulation) disorders. NBIA is a group of heterogeneous disorders primarily characterized by progressive extrapyramidal deterioration and excess iron accumulation in the basal ganglia (222). The hallmark clinical manifestations of NBIA are progressive dystonia, dysarthria, spasticity and parkinsonism. To date there are nine genes associated with the NBIA disorders (Table 1.5). Despite important differences, several genetically diverse forms of NBIA share common features in addition to iron deposition, such as the presence of neuroaxonal spheroids suggesting axonal dysfunction (223). Also reported are tau or α-synuclein pathology (223). Beta-propeller protein (*WDR45*) will be the focus of this chapter.

Table 1.5 Types of NBIA (224)

Disease name	Gene	Inheritance	Pattern of iron deposition	Other key features
Pantothenate kinase-associated neurodegeneration (PKAN) (225)	*PANK2*	AR	GP, SN	Eye-of-the-tiger sign in GP
PLA2G6-associated neurodegeneration (226)	*PLA2G6*	AR	Variable GP, SN (some cases have no iron accumulation)	Cerebellar atrophy
Mitochondrial membrane protein-associated neurodegeneration (227,228)	*C19orf12*	AR	GP, SN	Cerebellar and cortical atrophy; on T_2-weighted images hyperintense streaking of the medial medullary lamina between the globus pallidus interna and externa
Beta-propeller protein-associated neurodegeneration (229)	*WDR45*	XLD	GP, SN	T_1-weighted signal hyperintensity with a central band of hypointensity in the SN; SN iron > GP iron
Fatty acid hydroxylase-associated neurodegeneration (230)	*FA2H*	AR	GP, SN	Pontocerebellar atrophy
Kufor-Rakeb syndrome (231)	*ATP13A2*	AR	Variable GP, putamen, caudate (some cases have no iron accumulation)	Cerebral, cerebellar, and brain stem atrophy
Neuroferritinopathy (232)	*FTL*	AD	GP, putamen, caudate, dentate, thalamus	Cystic cavitation; mild cortical and cerebellar atrophy
Aceruloplasminemia (233)	*CP*	AR	GP, putamen, caudate, thalamus, RN, dentate	Cerebellar atrophy
Woodhouse-Sakati syndrome (234)	*DCAF17*	AR	GP	No additional key features
COASY protein-associated neurodegeneration (CoPAN) (235)	*COASY*	AR	GP, SN	T_2-weighted images: hyperintense caudate, putamina, medial and posterior thalami in early disease; GP calcifications

GP: globus palligus; SN: substantia nigra; RN: red nucleus

1.8.1. **Beta-propeller protein associated neurodegeneration (BPAN)**

Mutations in the WD repeat domain 45 (*WDR45*) gene on chromosome Xp11 are linked to BPAN, a type of NBIA (229). Previously referenced as "SENDA" (static encephalopathy of childhood with neurodegeneration in adulthood), BPAN has X-linked inheritance and is characterized by global developmental delay in early childhood that is essentially static, with slow motor and cognitive gains until adolescence or early adulthood (229). In young adulthood, affected individuals develop progressive dystonia, parkinsonism, extrapyramidal signs and dementia resulting in severe disability. Brain MRI shows iron accumulation in the globus pallidus and substantia nigra. A characteristic finding is T1-weighted hyperintensity surrounding a central band of hypointensity in the substantia nigra. Cerebral and cerebellar atrophy are also observed (229,236).

Genetics

All BPAN cases reported to date harboured *de novo* mutations in the *WDR45* gene encoding a beta-propeller protein. In a study of 20 unrelated patients (17 females and 3 males) with BPAN, 19 different hemizygous or heterozygous *de novo* mutations in the *WDR45* gene were identified located throughout the coding sequence, most of the mutations were truncating but 2 were missense mutations affecting highly conserved residues (229). Another study identified 5 different *de novo* heterozygous truncating mutations in the *WDR45* gene in 5 unrelated women with NBIA5 (236). Although molecular analysis has shown it to be X-linked dominant, both affected males and females exhibited a homogeneous phenotype (236). Since *WDR45* is on the X chromosome, the males must be somatic mosaic for

the mutation (229). Presumably, males with germline *WDR45* mutations are nonviable. Females may either harbor germline or somatic mutations, and several affected females had evidence of skewed X-inactivation. All of these factors may contribute to disease manifestations.

Neuropathology

Macroscopic features reported in a single BPAN case were mild cerebellar atrophy, thinned cerebral peduncles and a dark grey-brown appearance of substantia nigra and, to a much lesser extent, the globus pallidus. Microscopic findings included that the globus pallidus and substantia nigra stained strongly for iron and demonstrated numerous large axonal spheroids, siderophages, reactive astrocytes and severe neuronal loss. Axonal spheroids were seen also in the pons, medulla and thalamus but were fewer in number. The putamen and thalamus showed gliosis and mild neuronal loss. Significant loss of Purkinje cells with axonal 'torpedoes' was evident. Numerous tau-positive NFTs were seen in the hippocampus, neocortex, putamen, and hypothalamus, with fewer seen in remaining neurons in globus pallidus, substantia nigra, pons and thalamus. No amyloid-β plaques or LBs were observed (237).

Iron

Iron participates in a wide array of cellular functions including cytokinesis, myelination, electron transport, antioxidant enzyme activity and biogenic amine metabolism. It is essential for normal neuroembryogenesis (238). In normal human brain, iron is regionally distributed and is highest in the globus pallidus, substantia

SNpr, dentate nucleus, and red nucleus. Though very little iron is typically stored in neurons, and since neuronal iron is transported along axons and dendrites, iron overload may cause both neuronal cell death and axonal degeneration (239). In NBIA iron accumulates abnormally in the brain regions that are typically iron-rich, substantia nigra and globus pallidus (240). The electronic properties of this transition metal enable iron to take part in chemical reactions that may be injurious to neural and other cellular substrates. Owing to iron's ability to donate electrons to oxygen, increased iron levels can lead to the formation of hydroxyl radicals and hydroxyl anions via the Fenton Reaction ($Fe^{2+} + H_2O_2 \rightarrow Fe^{3+} + OH\cdot + OH^-$). Increased iron levels also can generate peroxyl/alkoxyl radicals due to Fe^{2+}-dependent lipid peroxidation (241). These reactive-oxygen species (ROS) can damage cellular macromolecules including proteins, lipids, and DNA. Under normal conditions, several detoxification systems and antioxidant defence mechanisms exist to prevent this damage; for example, catalase and glutathione peroxidase quickly convert H_2O_2 to water, helping to ensure that ROS-induced damage is minimal in the brain (242). However, when the formation of ROS exceeds the cells' detoxification/antioxidant systems, the cell experiences oxidative stress. Iron-induced oxidative stress is particularly dangerous because it can cause further iron release from iron-containing proteins such as ferritin (Ft)**,** heme proteins, and iron-sulfur (Fe-S) clusters, forming a destructive intracellular positive-feedback loop that exacerbates the toxic effects of brain iron overload (246). Iron has been shown to progressively accumulate in the brain with normal aging, and iron-induced oxidative stress can also cause neurodegeneration (243). However, the brain iron

uptake and the cellular and intercellular iron transport mechanisms in the central nervous system are still poorly understood. In NBIA, where iron deposition is considered as the biomarker, it is yet to be understood if the iron directly contributes to the functional consequences, for example, tissue damage or is solely an epiphenomenon.

Beta-propeller protein and autophagy

In the case of BPAN, the *WDR45* gene is postulated to have an important role in the autophagy pathway, which is the major intracellular degradation system by which cytoplasmic materials are packaged into autophagosomes and delivered to lysosomes for degradation in autophagy (236). *WDR45* is the first NBIA gene directly linked to autophagy.

Beta-propeller protein encoded by the *WDR45* gene is one of the four mammalian homologs of yeast Atg18, an important regulator of autophagy. Its involvement in autophagy has been documented in yeast and mammalian cells, where it interacts with ATG2 (244), and in *C. elegans*, where its deletion leads to accumulation of early autophagosome (245). In lymphoblast cells from BPAN patients, accumulation of LC3-II protein and its co-localization with ATG9a in enlarged membrane structures was observed suggesting autophagosome formation is hindered at an early stage (236). Hence, BPAN represents the first direct link between the autophagy mechanism and neurodegeneration. Further functional studies may provide a link between iron homeostasis and autophagy as neuronal autophagy is essential for the elimination of accumulated and aggregating proteins.

1.8.2. **Neuroacanthocytosis**

Neuroacanthocytosis (NA) encompasses a group of genetically heterogeneous disorders characterized by neurologic signs and symptoms associated with acanthocytosis, an abnormality of red blood cells in which a certain percentage of erythrocytes (typically 10-30%) have an unusual starlike appearance with spiky- or thorny-appearing projections (246,247). Neurologic problems usually consist of either movement disorders or ataxia, personality changes, cognitive deterioration (248,249), axonal neuropathy, and seizures (250).

The first form of NA to be well described in the medical literature is Bassen-Kornzweig disease, or abetalipoproteinemia which is an autosomal recessive abnormality of lipoprotein metabolism resulting in ataxia combined with acanthocytosis (246). Bassen-Kornzweig disease was compared with a better known condition, Friedreich ataxia. The two are rather similar except that patients with Bassen-Kornzweig disease have acanthocytosis. The second type of neuroacanthocytosis was described in two separate North American kindreds known as Levine-Critchley syndrome (251,252). Levine-Critchley syndrome resembled Huntington disease with prominent choreiform or choreoathetoid movements, progressive dementia, and, in the original descriptions, autosomal dominant inheritance.

The first recognised neurological association was a result from inherited abetalipoproteinaemia and sometime referred to as hereditary acanthocytosis

(246). However, casaes with acanthocytosis and neurological impairment have been reported without lipoprotein abnormalities (253).

Genetics

The inheritance of NA has been described as autosomal recessive, autosomal dominant and as part of an X-linked disorder called McLeod syndrome (MLS). The autosomal recessive type, called chorea-acanthocytosis (ChAc), is the most common form of NA and is linked to the mutations in *VPS13A* gene (251,252,254,255). The *VPS13A* gene spans a 250kb region on chromosome 9q21 and consists of 73 exons encoding chorein (255,256). Chorein is believed to be involved in protein trafficking at the trans-golgi network for maintenance of the plasma membrane (255,257). The localization of chorein has been demonstrated in wild-type mice by western blot (WB) and immunohistochemical (IHC) analyses (258).

Neuropathology

The degeneration of the basal ganglia is a consistent feature of NA. On autopsy of NA cases, the cerebral cortex appears unaffected. Macroscopically, bilateral atrophy of the caudate nucleus, the putamen and the globus pallidus was observed. This corresponds to neuronal loss and gliosis, which was particularly severe in the caudate and less so in the putamen and the external and internal pallidum (259–261). Pronounced neuronal loss in the substantia nigra was the likely neuropathological correlate of Parkinsonism. Gliosis and extraneuronal melanin

pigment without LBs were reported in the substantia nigra. The locus coeruleus, inferior olives, and cerebellum appeared unaffected. Loss of spinal cord anterior horn cells, a correlate of neurogenic muscle atrophy, was seen in some of the autopsies of individuals with ChAc. Gliosis may also occur in the thalamus.

Acanthocyte

Acanthocytic deformation of red cells is an intriguing feature and may possibly provide an essential clue for the understanding of their pathophysiology. The acanthocytic protrusion of parts of the cell membrane appears to be the result of disorganized membrane-cytoskeleton interactions due to defective endosomal trafficking and sorting, autophagic flux and autolysosomal degradation in late stage erythropoiesis. The protrusions and thorns of acanthocytes could perhaps be viewed as an arrested state among a multitude of continuously changing states of membrane deformation, thus potentially providing insights into basic mechanisms of cell biology (262).

1.9. Lewy bodies (LBs) in Lysosomal storage disorders (LSDs)

Classically, the approach taken to the study of genetic forms of diseases has relied on the clinical features associated with each genetic locus. A great deal of attention has been focused on the assignment of the locus on the clinical basis. However, to identify the pathways of pathogenicity for a given disorder, arguably, one should start by analyzing the genetics of disease based on pathology. We are more likely to find a common pathway if there is a common pathology rather than common clinical characteristics. In this regard, LB diseases sharing the common role in ceramide metabolism are discussed based on Figure 1.9.

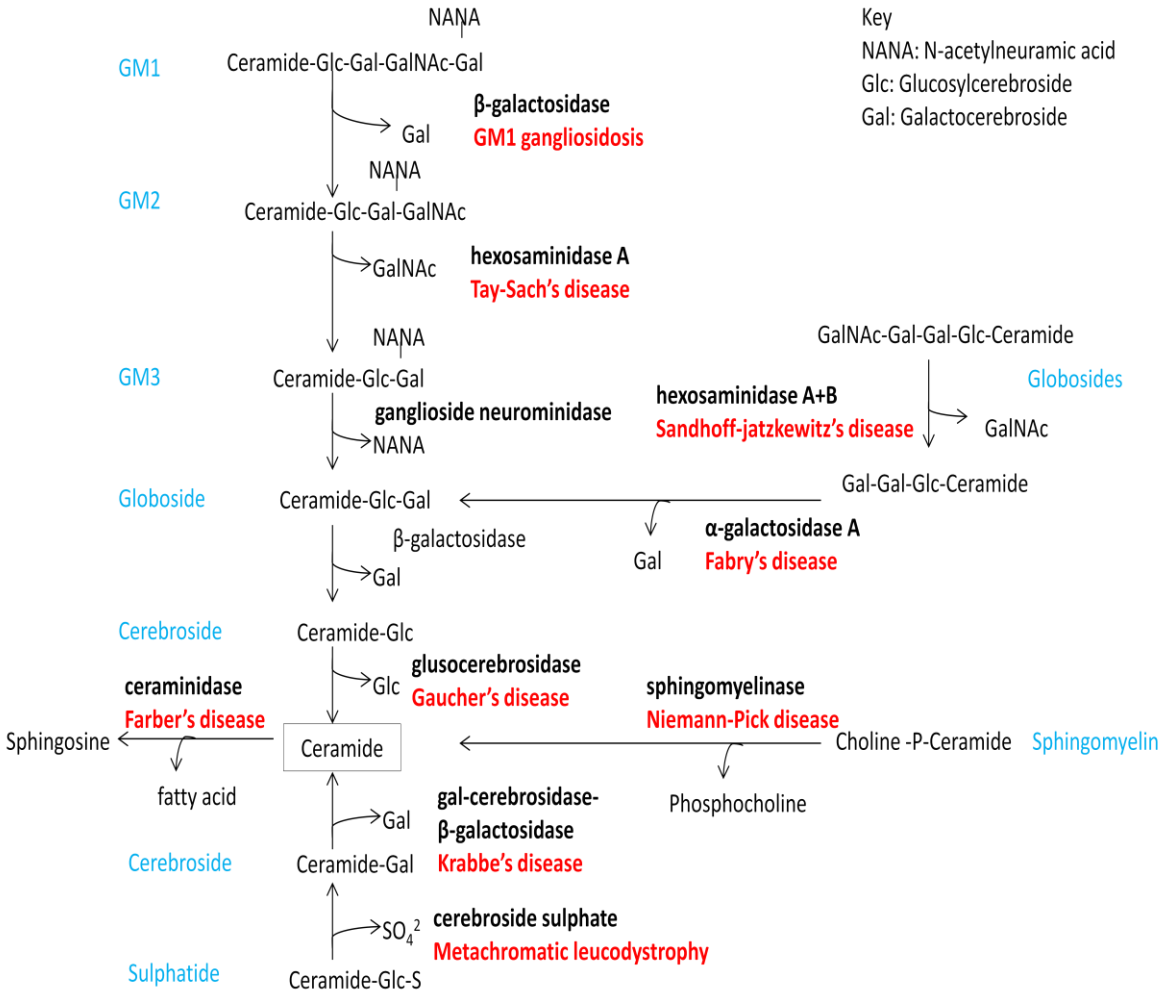

Figure 1.9: Ceramide pathway with lysosomal storage disorders (highlighted in red) along the pathway. The defective enzymes are in bold. Adapted from (263).

Ceramide

Ceramide, the precursor of all complex sphingolipids, is a potent signaling molecule that mediates key events of cellular pathophysiology. In the nervous system, the sphingolipid metabolism has an important impact on neural tissue. All sphingolipids are synthesized from ceramides and are hydrolyzed to ceramides using specific acid exohydrolases. Deficiency or malfunctioning of one of these enzymes results in accumulation of the corresponding lipid substrate in the lysosomal compartment

leading to cellular enlargement, dysfunction and death. Their abnormal storage and slow turnover results in severe dementia and mental retardation. Ceramides are able to induce apoptosis by changing the phospholipid membrane properties, increasing the membrane permeability leading to an efflux of lysosomal proteases and inhibits the mitochondrial respiratory chain (264–266). Appropriate lipid membrane homeostasis is crucial for lysosomal, mitochondria and myelin sheath arrangement. Lysosomes are linked to iron in the cell, as they degrade cytosolic ferritin and its disruption would damage cellular iron recycling (267). In turn the free iron would overload phagocytosing cells and increase reactive oxygen species. Oligodendrocytes contain the highest iron content of all the brain cells; they are highly energy and lipid demanding. Disruption of these supplies may lead to dysfunction of myelin production or maintenance (268).

Levels of cellular ceramide are regulated by the *de novo* pathway and the recycling pathway (269). The former relates to the synthesis of ceramide through the condensation of palmitate and serine in a series of reactions that are ultimately dependent on Co-Enzyme A. The latter pathway is slightly more intricate, since several outcomes are possible depending on the enzymes involved (269).

LSDs

Lysosomes are acidic intracellular compartment that provide inherent protein, nucleic acid and pathogen degrading activities for the cell. They receive their substrates from endocytosis, phagocytosis and autophagy and are active participants in bulk degeneration of metabolic waste products (270). Lysosomal

activities are rate-limiting, induced under stress and the major force in clearance of damaged or aggregated proteins. The autophagy-lysosomal pathway is essential for maintaining protein and energy homeostasis (271).

Inherited metabolic disorders which have been linked to lysosomal dysfunction belong to a family of diseases identified as sphingolipidoses, a class of LSDs (272,273). The main members of the sphingolipidoses are NPC disease, Krabbe disease, Gaucher disease, Fabry disease, Tay-Sachs disease, Sandhoff disease and metachromatic leukodystrophy. They are generally inherited in an autosomal recessive fashion, but notably Fabry disease is X-linked. Taken together, sphingolipidoses have an incidence of approximately 1 in 10,000, but substantially more in certain populations such as Ashkenazi Jews. Enzyme replacement therapy is available to treat mainly Fabry disease and Gaucher disease, and people with these types of sphingolipidoses may live well into adulthood. The other types are generally fatal by age 1 to 5 years for infantile forms, but progression may be mild for juvenile- or adult-onset forms (274).

Table 1.6 Comparison of the main sphingolipidoses					
Disease (reference)	**Inheritance**	**Deficient enzyme**	**Accumulated products**	**Clinical symptoms**	**Treatment**
Niemann-Pick (275)	Autosomal recessive	Sphingomyelinase	Sphingomyelin in brain & red blood cell	Mental retardation, spasticity, seizures, hepatosplenomegaly, thrombocytopenia, ataxia	Limited, usually fatal by the age of approx 1.5years
Fabry disease (276)	X-linked	α-galactosidase A	Glycolipids, particularly ceramide trihexoside, in brain, heart, kidney	Ischemic infarction in affected organs, acroparesthesia, angiokeratomas hypohidrosis	Enzyme replacement therapy (but expensive), life expectancy among males of approximately 60 years
Krabbe disease (277)	Autosomal recessive	Galactocerebrosida-se	Glycolipids, particularly galactocerebroside, in oligodendrocytes	Spasticity, neurodenegeration(leading to death), hypertonia, hyperreflexia, decerebration-like posture, blindness and deafness	Limited, generally fatal before age 2 for infants
Gaucher disease (278)	Autosomal recessive	Glucocerebrosidase	Glucocerebrosides in red blood cells, liver and spleen	Hepatosplenomegaly, pancytopenia, bone pain, erlenmeyer flask deformity	Enzyme replacement therapy (but expensive), may live well into adulthood
Tay-Sachs disease (279)	Autosomal recessive	Hexosaminidase A	GM2 gangliosides in neurons	Neurodegeneration, developmental disability, early death	Death by approximately 4 years for infantile Tay–Sachs
Sandhoff disease (280)	Autosomal recessive	Hexosaminidase A + B	Globosides in neurons and spinal cord	Developmental disability, seizures, ataxia, speech problems, early death	Infantile Sandhoff usually live only into early childhood
Metachromatic leukodystrophy (MLD) (277)	Autosomal recessive	Arylsulfatase A or prosaposin	Sulfatide compounds in neural tissue, demyelinisation in central and peripheral nervous system	Mental retardation, motor dysfunction, ataxia, hyporeflexia, seizures	Death by approximately 5 years for infantile MLD

Niemann-Pick type C (NPC) disease is an autosomal recessive lipid storage disorder characterized by progressive neurodegeneration with a highly variable clinical phenotype. Patients with the 'classic' childhood onset type C usually appear normal for 1 or 2 years with symptoms appearing between 2 and 4 years. They gradually develop neurologic abnormalities which are initially manifested by ataxia, seizures, and loss of previously learned speech. Spasticity is striking and seizures are common (281). Approximately 95% of cases are caused by mutations in the *NPC1* gene, referred to as type C1. This gene encodes a putative integral membrane protein containing motifs consistent with a role in intracellular transport of cholesterol to post-lysosomal destinations. Cells from NPC subjects show a decrease in acid sphingomyelinase activity, leading to the accumulation of sphingomyelin (282). Since one of the pathways for ceramide recycling is the sphingomyelin pathway, it is conceivable that associated to the accumulation of sphingomyelin, a decrease of ceramide may also be present. Some cases of NPC1 were described as having LBs (283).

Krabbe disease is an autosomal recessive disorder caused by deficiency of the enzyme galactocerebrosidase. The disease most often affects infants, with onset before age 6 months, but can occur in adolescence or adulthood. The build up of undigested fats affects the growth of the myelin sheath and causes severe deterioration of mental and motor skills. Other symptoms include muscle weakness, hypertonia, myoclonic seizures, spasticity, irritability, unexplained fever, deafness, optic atrophy and blindness, paralysis, and difficulty when swallowing. In

infants, the disease is generally fatal before age 2. Patients with a later onset form of the disease have a milder course and live significantly longer. Galactocerebrosidase is responsible for the liposomal hydrolysis of galactolipids formed during white matter myelination. The pathologic changes in the peripheral and CNS (globoid cell formation and decreased myelin) appear to result from the toxic nature of accumulated psychosine (galactosylsphingosine) and galactocerebroside (galactosylceramide) that cannot be degraded because of the galactocerebrosidase deficiency. In vitro assays demonstrated that psychosine, the neurotoxic sphingolipid accumulated in Krabbe brain, accelerated the fibrillization of α-synuclein. Hence, the occurrence of neuronal deposits of fibrillized proteins including α-synuclein, identified Krabbe disease as a new α-synucleinopathy (277,284).

Gaucher disease is the most common form of the sphingolipidoses caused by a homozygous or a compound heterozygous mutation in the glucocerebrosidase gene (GBA). The gene GBA encodes a lysosomal enzyme, glucocerebrosidase, that catalyses the breakdown of the glycolipid glucosylceramide to ceramide and glucose (285). Over 200 mutations have been described in GBA, most of which are known to cause Gaucher disease, in the homozygous or compound heterozygous condition (286). Manifestations may include an enlarged spleen and liver, liver malfunction, skeletal disorders and bone lesions that may be painful, severe neurologic complications, swelling of lymph nodes and (occasionally) adjacent joints, distended abdomen, a brownish tint to the skin, anemia, low blood platelets

and yellow fatty deposits on the sclera (287,288). Gaucher patients typically present enlarged macrophages resulting from the intracellular accumulation of glucosylceramide. The fact that these patients show increased levels of the enzyme's substrate indicates that pathogenic variants act as loss-of-function mutations. GBA mutations, in addition to causing Gaucher disease when homozygous, have recently been established to act as a risk factor for PD (289,290) and for LB disorders (291).

Fabry disease, also known as alpha-galactosidase-A deficiency, causes a build-up of glycolipids in the autonomic nervous system, eyes, kidneys, and cardiovascular system. Fabry disease is the only X-linked lipid storage disease. Onset of symptoms is usually during childhood or adolescence. Neurological signs include burning pain in the arms and legs and the build up of excess material in the clear layers of the cornea. Glycolipids storage in blood vessel walls may impair circulation, putting the patient at risk for stroke or heart attack. Other manifestations include heart enlargement, progressive kidney impairment leading to renal failure, gastrointestinal difficulties, decreased sweating, fever and angiokeratomas.

The **gangliosidoses** are comprised of two distinct groups of genetic diseases, monosialoganglioside 1 (**G_{M1}**) and 2 (**G_{M2}**). Both are autosomal recessive and affect males and females equally. The **G_{M1} gangliosidoses** are caused by a deficiency of the enzyme beta-galactosidase, resulting in abnormal storage of acidic lipid materials particularly in the nerve cells in the central and peripheral nervous

systems. G_{M1} gangliosidosis has three clinical presentations: early infantile, late infantile, and adult. Symptoms may vary with the age at onset but mainly include neurodegeneration, seizures, liver and spleen enlargement, coarsening of facial features, skeletal irregularities, joint stiffness, distended abdomen, muscle weakness, gait ataxia, dementia, angiokeratomas and difficulties with speech, muscle atrophy, corneal clouding in some patients, and dystonia.

The **G_{M2}** gangliosidoses represent a heterogeneous autosomal recessive group of disorders caused by deficiency of the lysosomal enzyme beta- hexosaminidase. The resulting accumulation of ganglioside G_{M2} occurs primarily in neuronal cells and coincides with a progressive broad spectrum of neurologic deterioration (292,293). The G_{M2} disorders include:

Tay-Sachs disease (also known as G_{M2} gangliosidosis-variant B) and its variant forms are caused by a deficiency in the enzyme hexosaminidase A. The incidence is particularly high among Eastern European and Ashkenazi Jewish populations, as well as certain French Canadians and Louisianan Cajuns (294). Affected children appear to develop normally for the first few months of life. Symptoms begin by 6 months of age and include progressive loss of mental ability, dementia, decreased eye contact, increased startle reflex to noise, progressive loss of hearing leading to deafness, difficulty in swallowing, blindness, cherry-red spots in the retinas, and some paralysis. Seizures may begin in the child's second year and often die by age 4 from recurring infection. A rarer form of the disorder, called late-onset Tay-Sachs

disease, occurs in patients in their twenties and early thirties and is characterized by unsteadiness of gait and progressive neurological deterioration.

Sandhoff disease (variant AB) is a severe form of Tay-Sachs disease. Onset usually occurs at the age of 6 months and is not limited to any ethnic group. Neurological signs may include progressive deterioration of the CNS, motor weakness, early blindness, marked startle response to sound, spasticity, myoclonus (shock-like contractions of a muscle), seizures, macrocephaly (an abnormally enlarged head), and cherry-red spots in the eye. Children generally die by age 3 from respiratory infections.

Metachromatic leukodystrophy (MLD) is an autosomal recessive deficiency comprised of several allelic disorders. The variant with cerebroside sulfate deficiency results in accumulation of the myelin lipid sulfatide in oligodendrocytes and Schwann cells (295). Patients are normal up to age one or two years, and then develop progressive peripheral neuropathy, psychomotor retardation, and blindness. Signs of white matter involvement (spasticity, brisk tendon reflexes, extensor plantar responses) are prominent. Less severe variants cause adult onset dementia, psychiatric disorders, and neuropathy (295).

LBs

Intracellular proteinaceous inclusions called LBs and Lewy neurites are the common pathological features in the brainstem and cortical areas in PD and dementia. Alpha-synuclein is the major component of LBs and diseases with mutations in

SNCA gene have extensive LBs since these mutations are known to increase aggregation of the protein (296,297). Alpha-synuclein may also be involved, albeit in a more indirect manner, in the ceramide pathway. It has been shown that deletion of the gene decreases brain palmitate uptake (298) and that the presence of palmitic acid increases the *de novo* synthesis of ceramide significantly (299). However, known pathogenic mutations in *SNCA* gene are likely gain-of-function mutations, suggesting that, in these cases, the mutations drive the aggregation of α-synuclein, while in cases where ceramide metabolism is affected, LB inclusions may be a cellular response to this altered ceramide metabolism. Also connecting the ceramide pathway to α-synuclein deposition is the recent description of an increase in alpha-synuclein inclusions in *C. elegans* when LASS2, a ceramide synthase, is knocked-down (300). This result should obviously be taken with some caution, since it was obtained in a non-mammalian organism, but nevertheless it further connects ceramide to synuclein deposition.

LSDs occurring due to the enzyme dysfunction in the ceramide pathway also develop Lewy body pathology, for example, NPC, Krabbe disease, and Gaucher disease. Hence, a possibility is that LSDs, G_{M1}, Tay-Sachs disease, Sandhoff disease, Fabry disease and metachromatic leukodystrophy which occur due to enzyme dysfunction in the ceramide pathway may mimic the Lewy body pathology suggesting that this may be a common theme for pathogenesis.

1.10. Thesis Aims and objectives

This primary aim of this thesis is to significantly contribute to the field of neuroscience by identifying causes of the neurodegenerative diseases via classical methods. In this regard genetics and neuropathology of dystonia, NBIA, SCA 8 and LSDs in ceramide pathway were investigated.

The specific aims include:

A) To investigate genetic and neuropathological aspects of primary dystonia cases and provide a detailed neuropathological study on primary pure dystonia through a unique resource of genetically confirmed 7 DYT1 cases and 2 DYT6 cases. The approach taken is to provide a clinical-genetic-pathological description of these cases.

B) To investigate interaction between two primary pure dystonia genes, *TOR1A* and *THAP1*, thereby determining whether there is a common mechanistic pathway in primary dystonia. The approach taken is from genetic to pathophysiological prediction.

C) To investigate whether the non coding mutations in the 5'UTR region of *GCH1* gene is pathogenic in dopa responsive dystonia. The approach taken is from genetic to clinical correlation.

D) To investigate the trinucleotide repeat expansion length for SCA8 in ataxia patients to determine whether the repeat length is directly related to the disease pathogenesis. The approach taken is from repeat length to clinical and pathogenicity prediction.

E) To investigate the neuropathology of NBIA cases, neuroacanthocytosis and *WDR45* case. The approach taken is from clinical to genetic and pathological description.

F) To investigate if disease with an enzyme dysfunction in a specific pathway may have a shared pathology. In this regard, LSDs in the ceramide pathway were investigated for LB pathology. This approach taken is from neuropathology to genetic and clinical description.

Chapter 2. Materials and method

2.1. Research cohorts

Dystonia cohort

This project was approved by the Joint Local Research Ethics Committee of the National Hospital for Neurology and Neurosurgery and the UCL Institute of Neurology. Autopsy specimens were received from the Brain and Tissue Banks for Developmental Disorders, Baltimore (BTBDD), Queen Square Brain Bank (QSBB) at University College London, and Harvard Brain Bank (HBB) and stored with appropriate consent. Ethical consent was also approved from all the participants. The research cohort consisted of 89 clinically diagnosed generalized dystonia patients (Table 2.1). Brain tissue samples were collected for 57 patients from BTBDD, 7 from HBB and 14 from QSBB. Genomic DNA was received for 11 patients from National Hospital for Neurology and Neurosurgery (NHNN-lab).

Table 2.1 Dystonia cases received from different brain banks

Source	UMB#	Sex	Age at death	Disease Onset	Clinical diagnosis
NICHD-BTB	187	M	83	Adolescence	Dystonia, Generalized, Familial
NICHD-BTB	593	F	57	Adolescence	Dystonia, Meige Syndrome, Focal
NICHD	741	F	52	N/A	Dystonia, Spasmodic Torticollis
NICHD	785	M	69	Adulthood	Dystonia, Generalized
NICHD	837	F	52	N/A	Dystonia
NICHD	842	F	79	Adulthood	Dystonia, Spasmodic Torticollis
NICHD	851	M	70	N/A	Dystonia, Spasmodic Torticollis
NICHD	855	M	80	Adulthood	Dystonia, Blepharospasm
NICHD	903	F	68	Adulthood	Dystonia, Meige Syndrome, Focal
NICHD	999	F	79	N/A	Dystonia, Spasmodic Torticollis
NICHD	1017	F	84	Adulthood	Dystonia, Spasmodic Torticollis
NICHD	1019	M	44	Adulthood	Dystonia
NICHD	1020	M	71	Childhood	Dystonia
NICHD	1048	F	44	N/A	Dystonia, Medication Induced
NICHD	1099	F	75	Adult onset	Dystonia, Blepharospasm
NICHD	1125	F	77	Adult onset	Dystonia, Familial Tremor
NICHD	1141	F	82	Childhood	Dystonia, Generalized, Familial,
NICHD	1162	F	>90	N/A	Dystonia, Meige Syndrome
NICHD	1187	M	>90	N/A	Dystonia , Myoclonic Dystonia
NICHD	1235	F	87	Adult onset	Dystonia, Blepharospasm
NICHD	1353	M	78	Childhood	Dystonia, Acquired, Post Traumatic
NICHD	1457	M	72	N/A	Dystonia
NICHD	1458	M	62	N/A	Dystonia
NICHD	1481	F	62	Late	Dystonia
NICHD	1513	F	81	Adulthood	Dystonia, Spasmodic Torticollis
NICHD	1554	F	59	Adulthood	Dystonia
NICHD	1559	F	78	Adulthood	Dystonia, Spasmodic Torticollis
NICHD	1629	F	73	N/A	Dystonia, Blepharospasm, Meige Syndrome
NICHD	1688	F	81	N/A	Dystonia, Spasmodic Torticollis
NICHD	1705	F	>90	N/A	Dystonia, Blepharospasm
NICHD	1716	F	>90	N/A	Dystonia, Spasmodic Dysphonia
NICHD	1837	F	81	N/A	Dystonia, Meige Syndrome
NICHD	1850	F	50	Adult onset	Dystonia
NICHD	1899	M	81	Adult onset	Dystonia, Generalized, Meige Syndrome
NICHD	4518	F	82	N/A	Dystonia, Spasmodic Torticollis
NICHD	4520	F	68	N/A	Dystonia, Blepharospasm
NICHD	4635	M	76	Adult onset	Dystonia, Familial
NICHD	4690	F	>90	N/A	Dystonia, Spasmodic Dysphonia
NICHD	4700	F	75	Early onset	Dystonia, Spasmodic Torticollis
NICHD	4763	F	60	N/A	Dystonia, Meige Syndrome
NICHD	4835	M	>90	Adult onset	Dystonia, Meige syndrome, Familial
NICHD	4880	F	44	N/A	Dystonia, Generalized
NICHD	4881	M	70	Adult onset	Dystonia, Generalized/Dementia
NICHD	4897	F	49	N/A	Dystonia, Generalized
NICHD	5145	F	84	Adult onset	Dystonia
NICHD	5154	F	>90	N/A	Dystonia
NICHD	5155	F	86	N/A	Dystonia, Spasmodic Torticollis
NICHD	5159	F	85	N/A	Dystonia, Spasmodic Torticollis
NICHD	5221	F	61	Late onset	Dystonia
NICHD	5281	F	32	N/A	Dystonia, Spasmodic Torticollis
NICHD	881	F	67	Childhood	Dystonia, Generalized
NICHD	1512	F	89	N/A	Dystonia, DYT1
NICHD	1619	F	87	Adult onset	Dystonia, DYT1
NICHD	4628	F	77	Childhood	Dystonia, DYT1
NICHD	4877	F	>90	Late onset	Dystonia, DYT1
NICHD	4896	F	>90	N/A	Dystonia, DYT1
NICHD	5200	F	88	N/A	Dystonia, DYT1

Table 2.1 Dystonia cases received from different brain banks continued...

Source	Case	Sex	Age at death	Disease Onset	Clinical diagnosis
HBB	HB1	M	30	N/A	Dystonia
HBB	HB2	F	57	N/A	Dystonia
HBB	HB3	F	79	N/A	Dystonia
HBB	HB4	M	58	N/A	Dystonia
HBB	HB5	M	56	N/A	Dystonia
HBB	HB6	M	88	N/A	Dystonia
HBB	HB7	M	57	N/A	Dystonia
QSBB	QS1	M	69	Adulthood	Dystonia
QSBB	QS2	F	76	Adulthood	Dystonia
QSBB	QS3	F	76	Childhood	Dystonia
QSBB	QS4	F	74	Adulthood	Dystonia
QSBB	QS5	F	70	Late	Dystonia
QSBB	QS6	F	77	Childhood	Dystonia
QSBB	QS7	M	91	Late	Dystonia
QSBB	QS8	M	79	Adulthood	Dystonia
QSBB	QS9	F	81	Late	Dystonia
QSBB	QS10	F	86	Late	Dystonia
QSBB	QS11	F	84	Late	Dystonia
QSBB	QS12	F	76	Adulthood	Dystonia
QSBB	QS13	M	61	N/A	Dystonia
NHNN	NH1	N/A	N/A	N/A	Dystonia
NHNN	NH2	N/A	N/A	N/A	Dystonia
NHNN	NH3	N/A	N/A	N/A	Dystonia
NHNN	NH4	N/A	N/A	N/A	Dystonia
NHNN	NH5	N/A	N/A	N/A	Dystonia
NHNN	NH6	N/A	N/A	N/A	Dystonia
NHNN	NH7	N/A	N/A	N/A	Dystonia
NHNN	NH8	N/A	N/A	N/A	Dystonia
NHNN	NH9	N/A	N/A	N/A	Dystonia
NHNN	NH10	N/A	N/A	N/A	Dystonia
NHNN	NH11	N/A	N/A	N/A	Dystonia

The dystonia cohort for the gene interaction project consisted of 6 DYT1 and 2DYT6 cases along with 5 age and sex matched controls. Brains regions available and used for the study are summarized in Table 2.2.

Table 2.2 Dystonia cohort for gene interaction study										
Cases	Frontal cortex	Superior temporal gyrus	Cerebellum	Globus pallidus	Caudate	Putamen	Medulla	Pons	Hippo-campus	Midbrain
DYT1	X									
DYT1	X	x	X	x		x		x		
DYT1	X	x								
DYT1	X	x	X	x		x	x	x		x
DYT1	X	x	X					x		
DYT1	X	x	X	x		x	x	x		x
DYT6	X	x	X	x	x	x	x			x
DYT6	X	x	X	x	x	x	x		x	
Ctrl	x	x	X	x	x	x	x	x	x	x
Ctrl	x	x	X				x	x	x	x
Ctrl	x		X					x	x	x
Ctrl	x		X		x	x	x	x	x	
Ctrl	x		X		x			x	x	x

DYT1 and DYT6 cohorts for neuropathological study

Table 2.3 DYT1 and DYT6 cohorts for neuropathological study			
UMB#	Sex	Age at death	Brain regions available
DYT1 cases			
1512	F	89	Frontal cortex , basal ganglia, Superior temporal gyrus , motor cortex BA4, cerebellum with dentate nucleus
1619	F	87	Frontal cortex, basal ganglia, superior temporal gyrus, pons with locus coeruleus, cerebellum with dentate nucleus
4628	F	77	Frontal cortex, basal ganglia, superior temporal gyrus, motor cortex BA4, pons with locus coeruleus, cerebellum with dentate nucleus
4877	F	90	Frontal cortex, basal ganglia, superior temporal gyrus, motor cortex BA4, midbrain/pons, medulla, cerebellum with dentate nucleus
4896	F	90	Frontal cortex, basal ganglia, superior temporal gyrus, motor cortex BA4, midbrain/pons, cerebellum with dentate nucleus
5200	F	88	Frontal cortex, basal ganglia, superior temporal gyrus, motor cortex BA4, cerebellum with dentate nucleus
DYT6 cases			
1020	M	71	Frontal cortex , basal ganglia, superior temporal gyrus , medulla, cerebellum with dentate nucleus
HB5	M	56	Multiple brain regions

DRD cohort

The DRD cohort consisted of 192 clinically diagnosed DRD cases. These cases were negative for mutations in the coding regions of *GCH1* gene. The dystonia cohort described above was also screened for mutations in the *GCH1* coding regions and the promoter region.

Ataxia cohort

Written consent was obtained from all the patients to perform molecular studies. The ataxia cohort comprised 630 cases of clinically diagnosed sporadic cases with progressive cerebellar ataxia from the NHNN.

English control cohort

English cohort consisted of 631 normal individuals of English origin obtained from Wellcome trust.

Human genome diversity project (HGDP) control cohort

HGDP of worldwide control cases consisted of 1148 control individuals of diverse ethnicities (including individual from China, India, Pakistan, South Africa, Brazil etc) and was obtained from The Foundation Jean Dausset-Centre d'Etude du Polymorphisme Humain (CEPH).

Neuroacanthocytosis case

Paraffin blocks representing multiple brain regions from a post mortem case of NA were obtained from QSBB.

Neurodegeneration with brain iron accumulation -BPAN case

Paraffin blocks representing multiple brain regions from a post mortem case of BPAN were obtained from QSBB.

Lewy body in LSDs

To investigate if LBs are hallmark feature of LSDs in ceramide pathway, the cohort consisted of the following cases:

Table 2.4 LSD cohort to access Lewy body pathology

Disease	UMB#	Age/Sex	Ethnicity	Fixed tissue available
Leukodystrophy, Metachromatic	1231	60M	Caucasian	frontal cortex, hippocampus, substantia nigra, pons
Sandhoff Disease	1814	1M	Caucasian	frontal cortex, hippocampus
Fabry's Disease	4299	50M	Caucasian	frontal cortex, hippocampus, substantia nigra, pons
Tay-Sachs Disease	5094	27M	Caucasian	frontal cortex, hippocampus, substantia nigra, pons
Gangliosidosis, GM1	5384	19M	Caucasian	frontal cortex, hippocampus, substantia nigra, pons

2.2. Genetics

2.2.1. Extraction of nucleic acids

Genomic deoxyribonucleic acid (DNA) was extracted from brain tissues using DNeasy kit. Genomic DNA was extracted from peripheral blood leucocytes by standard method at the NHN-lab where only blood samples were available for the study. DNA concentration was measured using Nanodrop and diluted to (~20ng/uL) for use in the polymerase chain reaction (PCR).

2.2.2. **Candidate Gene Screening**

All exons and exon-intron boundaries were PCR amplified using primers already published. The target genomic DNA sequence was amplified by using a PCR and gel electrophoresis was done for quality control. PCR amplified fragments were purified using PCR Cleanup Filter Plates (Millipore, MA, USA) and a direct dye terminator sequencing (BigDye v3.1; Applied Biosystems, CA, USA) was performed as per the manufacturer's instructions. The resulting reactions were cleaned with PCR Cleanup Filter Plates (Millipore, MA, USA) before processing on a 3730xl DNA Analyzer 84 (Applied Biosystems, CA, USA) and analysed with Sequencher™ software (version 4.1.4; Gene Codes Corporation, MI, USA). The dystonia cohort was screened for the 3-bp ΔGAG mutation in exon 5 of *TOR1A,* three exons in *THAP1*, twelve exons in *GNAL,* seventeen exons in *CIZ1* and two exons in *PRRT2* using direct sequencing as described above. The DRD cohort was sequenced for five exons in *GCH1* gene and a promoter region.

2.2.3. **PCR amplification**

PCR were performed on Eppendorf thermocycler. Typical volumes of PCR amplification reactions are as follows:

TOR1A conditions, Exons 3, 4 and 5 PCR reagents for each reaction are as follows: 12µl Roche mix, 2µl forward/reverse primer (5µM), 3µl dH20, 1µl DNA (~20ng/ul). PCR was run on a 62 touchdown 57 programme.

THAP1 conditions, Exon1 PCR reagents for each reaction are as follows: , 2.5µl x10 PCR buffer, 5µl x5 Q buffer mix, 2.5µl DNTPs (2mM), 3µl forward/reverse primer (5µM), 0.5µl Taq polymerase,0.8µl DMSO, 6.2µl ddH20, and 1µl DNA (~20ng/ µl). PCR was run on a 62.5 touchdown 55 programme. Exons 2 and 3 PCR reagents for each reaction are as follows: 12µl Roche mix, 2µl forward/reverse primer (5µM), 2µl dH20, 2µl DNA (~20ng/ul). PCR was run on a 60 touchdown 50 programme.

CIZ1 conditions, Exons 2-17 PCR reagents for each reaction are as follows: 12µl Roche mix, 2µl forward/reverse primer (5µM), 2µl dH20, 2µl DNA (~20ng/ µl). Exon 1 PCR reagents for each reaction are as follows: 12µl Roche mix, 2µl forward/reverse primer (5µM), 1.2µl dH20, 0.8µl DMSO, 2µl DNA (~20ng/ul). PCR was run on a 65 touchdown 55 programme. Primers used were published before(301).

GNAL conditions, Exons 2-12 PCR reagents for each reaction are as follows: 12µl Roche mix, 2µl forward/reverse primer (5µM), 2µl dH20, 2µl DNA (~20ng/ µl). PCR was run on a 60 touchdown 50 programme. Primers used were published before (302).

TUBB4a conditions, Exons 1-4 PCR reagents for each reaction are as follows: 12µl FastStart Mastermix (Roche), 1µl (10pM) forward and reverse primers, 1µl DMSO, 4µl PCR grade water, 1µl DNA (30ng/µl). Primers used were published before (303).

GCH1 conditions, Exons 1-5 PCR reagents for each reaction are as follows: 12µl Roche mix, 2µl forward/reverse primer (5µM), 2µl dH20, 2µl DNA (~20ng/ µl). PCR

was run on a 60touchdown50 programme. Promoter region PCR reagents for each reaction is as follows: 2.5µl x10 PCR buffer, 5µl x5 Q buffer mix, 3µl DNTPs (2mM), 5µl forward/reverse primer (5µM), 0.2µl Taq polymerase, 1.3µl ddH20, and 3µl DNA (~20ng/ µl). PCR was run on a 60 touchdown 50 programme.

SCA8 conditions, PCR reagents for each reaction are as follows: 12µl Roche mix, 2µl forward/reverse primer (5µM), 0.8 µLDMSO, 1.2µl dH20, 2µl DNA (~20ng/ µl). PCR was run on a 60 touchdown 50 programme. Primer set used was published before (197).

Table 2.5 Primers used for sequencing and fragment analysis

Primary Antibody	Forward	Reverse	Primary Antibody	Forward	Reverse
TOR1A_exon5	AAGGAGCTGATTGATGGC	GGGTGCAGGATTAGGAAC	CIZ1_exon15	GATATGGGAGGGTCATGTGG	TGGAAATCAAGGGGATTCTG
THAP1_exon1	GCTTCCCAGGAAACGTACC	TTCCAGGAGCGCGAGAAAC	CIZ1_exon16	ACCCGAATCAGCTTGGATTA	TGGTACAGCGCGTGAGTGGCT
THAP1_exon2	TAAGATATTTCCTAAGCTGG	CCAGGCACATTTATTCTC	CIZ1_exon17	TGGGAACTGCACAGCCAAACTACC	CAGAGAGGCCGAGTGCATCACGCA
THAP1_exon3	TAGGATTATAGGCATGAGC	AATGAAACTCCTTTACAGG	GNAL_exon1-2	AAACGCCTGCTCTGAATCGGAA	ACTCTGGGAGAGAGACGAAGTTT
CIZ1_exon1	GCATCCCAGTCCCTAGAAGA	CCGCCATCCCTGTCTTAGTC	GNAL_exon3-4	AACCTTTGCAGATGTCTTGG	CCTCTTATGCATTTAGAGAGCTGG
CIZ1_exon2	TCCGAGACATGGGTCTGAGT	AGCAGGCCTGACTTATGGTG	GNAL_exon5	TCACACTAAACATAGAGTAGGTGCAT	TTATTCATTCCTTGCACTCAAG
CIZ1_exon3	GTGGCTGTGTGGAGTTGAGA	CTTGGGGAAGAAGGAAGGTC	GNAL_exon6	ACTCACTTCAGCTTCTTGGCCT	ATGACCAATCCACRCACACACA
CIZ1_exon4	AGCTTCTTTTTGCCAACCAA	GGGGGATGGATGTTTTATGG	GNAL_exon7	ATGCTCGGCCAATGTTGGTT	TGGGCCATGCAGCTCTTAACAA
CIZ1_exon5	GGCATAAAGGGAGTGTGACC	TGCCTGACCCTACCTTCTGC	GNAL_exon8	ATGTGTGAACGCTGGAACCT	GCAGTGCTGAGTGTTAGAATTCAC
CIZ1_exon6	TGCCTCTATCACCTGCTGACCC	GGGTGGGTATTGGATGTCAA	GNAL_exon9	TGCAGGCTGATCTGTGACT	AGAGATACTTCGTACGGTTCTGG
CIZ1_exon7	TAAGGCCTTCCTCCAAATCA	CCCATCTCTTGGAGGTCAGA	GNAL_exon10	ACAGATGGAATGAGGATACTGGTG	GGGATCCAATTACAAATAGGACCTTG
CIZ1_exon8$_1$	ACCCAGTCAGGGGAGGAAT	GCAAACACAGACCTCTCCAG	GNAL_exon11	GCTGGGAATATACAGCAGTCTAACA	TGAAGTCTAGCCCATCCAAG
CIZ1_exon8$_2$	CTGTGTGTGGACCTGTGGAT	GGGCCTCTTTGAAGACATGA	GNAL_exon12	TGCATTGAGACCATTCCTGCCT	GGGAGGCTGTATTCAATGACAACA
CIZ1_exon9	GACGCACAACAGCAAGAGG	ACGGAGAAGGCAGCTCTTG	GCH1_exon1	CCGGGCCATAAAAAGGAG	CGCCAAAAGTGAGGCAACTC
CIZ1_exon10	GAGGGCAGGCTGGGCATTCCACGC	GGCTGGCCCACTATAAGTACA	GCH1_exon2	TTAACGTTCGTTTATGTTGACTGTC	ACCTGAGATATCAGCAATTGGCAGC
CIZ1_exon11	TGTTACAGGCAGGGAAAACTG	CCTTGCCCACTGTTCTGG	GCH1_exon3	AGATGTTTTCAAGGTAATACATTGTCG	TAGATTCTCAGCAGATGAGGGCAG
CIZ1_exon12	AACTGGGGCTCTGTGTTGTC	TGTCTTTCTGGCGTCACATT	GCH1_exon4	GTCCTTTTTGTTTTATGAGGAAGGC	GGTGATGCACTCTTATAATCTCAGC
CIZ1_exon13	GGGCTGGGATAAACCTCAAC	GTGCTAGTCAGGGGGCTTG	GCH1_exon5	CTCTGTGGCCCAGTCAGC	AGGCTCAGGGATGGAAATCT
CIZ1_exon14	GCACTTCACAGTAATCAGTTGTGGC	CAAGGCTGTGTAGCAAGTTGAGGTTTA	GCH1_exon6	CATTTGTGTAAGAAGGGATATTTCG	AGTGACAAGGAATAAAGTTCACATC

2.2.4. Gel electrophoresis

Amplified products were run on an agarose gel to ensure that PCR amplification efficiency and fragment size. Red dye was added to the gel to enable visualization and orangeG was used as a loading buffer (5µl product +5µl OrangeG). Gel electrophoresis was done in a 1.5% agarose gel along with a corresponding molecular weight standard (100bp ladder) to estimate the size of the DNA fragments. The electrophoresis was run at 100V for 40 mins in 1x TBE buffer. Gels were visualised using a UV transilluminator and images were taken with Syngene Bioimaging System.

2.2.5. PCR Clean Up

Samples were centrifuged briefly for 30secs to collect condensation formed during PCR. ddH_20 was added up to a total of 100µl and diluted PCRs transferred to the MultiScreen-PCR 96 filter plates (Millipore). The filter plate was placed under vacuum until all fluid was removed (20-25inHg). Further 20µl ddH20 water was added to each well to reconstitute the PCR and placed on a shaker for 10mins. The purified PCR products were transferred to a clean 96-well reaction plate and stored at -20°C until further use.

2.2.6. Sanger Sequencing

DNA sequencing reactions were performed based on the principle of the chain termination method. Sequencing reagents for each 10µl reaction are as follows: 2µl Big dye buffer 5X, 0.5µl Big Dye v3.1, 0.5µl forward/reverse primer (5µM), 5µl clean PCR product, 2µl ddH20. The sequencing reaction was run on Eppendorf

thermocycler and a big dye termination programme used is as follows: Initial denaturation 96°C x5mins, denaturation 96°C x10secs, primer annealing 50°C x5secs, extension 60°C x 4mins.

2.2.7. **Sequencing cleanup**

Samples were centrifuged briefly for 30secs to collect condensation formed during sequencing reaction. Double distilled water was added up to a total of 100µl and diluted sequencing reaction was transferred to the MultiScreen-PCR 96 filter plates (Millipore). The filter plate was placed under vacuum until all fluid was removed (20-25inHg). Further 20µl ddH20 water was added to each well to reconstitute the sequencing reaction and placed on a shaker for 10mins. The purified sequencing products were transferred to a clean 96-well reaction plate and processed on a 3730xl DNA Analyzer 84 (Applied Biosystems, CA, USA) and analysed with Sequencher™ software (version 4.1.4; Gene Codes Corporation, MI, USA).

2.2.8. **Fragment analysis**

Fragment analysis was carried out to determine the SCA8 repeats. The 5' terminal of SCA8 forward primer was labeled with FAM™ fluorescent dye. PCR amplification and gel electrophoresis was carried out as described above. GeneScan™ Liz-500 (Applied Biosystems) was used as a size standard. Amplified PCR products were visualised by automated fragment size analysis on an ABI 3730XL Genetic Sequencer (Applied Biosystems). Each reaction consisted of 12 µl L Formamide,0.3 µl Liz marker 500 and 7 µl of amplified PCR product. The fragment size data was collected and analysed using GENESCAN™672 Data Collection Software version

1.2.1 (Applied Biosystems). The alleles were sized manually in relation to a fluorescent-labelled size standard in a GeneMapper version 3.7 software.

2.3. Neuropathology

2.3.1. Tissue processing

Paraffin-wax embedded blocks were requested from Maryland brain bank for the genetically confirmed DYT1 and DYT6 cases. Formalin fixed half brain received for a DYT6 case from Harvard Brain Bank was processed and embedded in paraffin wax at Queen Square brain bank using routine protocols. Paraffin-wax embedded blocks were also obtained from age-matched neurologically normal control individuals from QSBB.

2.3.2. Histology stains Dewaxing and rehydration of sections procedure

Eight-micrometer-thick sections were cut, deparaffinized in three changes of xylene (10mins, 5mins and 5mins respectively) and then rehydrated using graded alcohols (100, 95, and 70%) for 2mins in each. Sections were washed for 2mins in running water before proceeding for appropriate immunohistochemical procedure. The procedure is reversed to dehydrate section to xylene.

2.3.3. Haematoxylin and Eosin (H&E) Staining

Deparaffinized and rehydrated sections as described above were placed in Gills haematoxylin for 5mins, rinsed under running water until excess dye has cleared, and quick dips in 1% acid-alcohol until tissue appeared red/purple in colour.

Sections were washed under cold running water to 'blue' tissue and incubated in eosin for 5mins. After a brief wash in water, sections were rehydrated as described above and mounted in DPX and cover. Haematoxylin is a basic dye, highlights nuclei. Eosin is an acidic dye, highlights cytoplasmic components of the cell.

2.3.4. Immunohistochemistry (IHC) on Formalin-fixed-paraffin-embedded (FFPE) tissue

Eight-micrometer-thick sections were deparaffinised and rehydrated as described above. Endogenous peroxidase activity was blocked using 0.3% peroxide in methanol for ten minutes, followed by several washes in distilled water. Pretreatment was carried out according to the appropriate IHC protocol for each antibody used. Sections were then placed in 10% non fat milk for 30 min at room temperature (RT) to reduce non-specific binding, followed by incubation in the primary antibody. After washes in PBS, the sections were incubated with secondary antibodies (dilution of 1:200) for 30 min at RT. The secondary antibody was washed off then the sections were incubated in the avidin-biotin complex solution for 30 min at RT. After washes in PBS, they were treated in the diaminobenzidine (DAB) solution for 2-5 min. The DAB solution was washed off and the tissues were counterstained in Mayer's hematoxylin for 30 sec. The tissue sections were then dehydrated in graded alcohol (70%, 90%, and absolute alcohol), cleared in three changes of xylene, and then mounted with DPX mounting medium. Primary antibodies with pre-treatment conditions, dilutions and incubation times are described below (Table 2.1).

2.3.5. **Gallyas silver staining**

Sections were dewaxed and rehydrated as described above. Sections were placed in several changes of distilled water, incubated in 5% periodic acid for 5mins, washed in several changes of distilled water, incubated in alkaline silver iodide solution for 1min and then washed in 0.5% acetic acid for 5mins. Further sections were incubated in developer solution until the sections turned dark brown/black (5-45mins), wash again in 0.5% acetic acid for 5mins, followed by a 5min wash in distilled water. Sections were 'toned' in 0.2% gold chloride until the excess dark colour has disappeared, washed again in distilled water, fixed in 1% sodium thiosulphate solution and finally washed in distilled water. Sections were then counterstained in Mayer's haematoxylin for 1min and excess dye was washed off in the running water. Finally, the sections are dehydrated, cleared and mounted as previously described. This technique highlights NFTs, plaques neurites, and neuropil threads as black.

2.3.6. **Luxol Fast Blue/ cresyl violet (LFB/CV) procedure**

Thirteen-micrometer-thick sections were cut and require longer time in xylene (30mins) to clear the wax. Sections were incubated in filtered LFB solution overnight at 60°c. Sections were then rinsed briely in 95% IMS, rinsed again in distilled water, differentiated in lithium carbonate solution for 30secs, followed by 30secs in 70% IMS and rinsed in distilled water. Sections were counter stained with prewarmed (60°C) cresyl violet for 20mins, rinsed in distilled water, followed by a

final 5mins incubation in 95% IMS. Finally, the sections are dehydrated, cleared and mounted as previously described.

2.3.7. **Evaluation of IHC**

Neuronal loss, gliosis and concomitant pathologies: tau, beta-amyloid (Aβ), LBs, cerebral amyloid angiopathy (CAA), TAR DNA-binding protein 43 (TDP-43), and small vessel disease (SVD) were assessed in a semi-quantitative manner according to published criteria (304–307) and summarized in Table 2.6. A score scale of 0 - +3 was used to indicate increasing pathology.

Table 2.6 Semi-quantitative scale	
Parameter	**Scale**
GCI and NCI burden	0 Absent +1 1-5 inclusions +2 6-19 inclusions +3 ≥20 inclusions
Neuronal loss	0 No neuronal loss +1 Slight neuronal loss +2 Moderate neuronal loss +3 Severe neuronal loss
Gliosis	0 No gliosis +1 Astrocytes around blood vessels and sub-pial +2 Astrocytes around blood vessels and sub-pial and extending into intervening parenchyma +3 Greater burden than ++'
CAA	0 No amyloid +1 Scattered vessels in leptomeninges or cortex with patchy deposition +2 As '+' with occasional vessels having circumferential deposition +3 Widespread circumferential deposition +4 Severe deposition of amyloid accompanied by projection of amyloid into the adjacent parenchyma
SVD	0 Vessels normal +1 Occasional vessels affected +2 A significant proportion of small vessels affected with few or no sequelae noted +3 A significant proportion of the small vessels affected with obvious sequelae

2.3.8. **Western blot (WB)**

Research cohorts

Human brain lysates were extracted from normal human controls available at QSBB for optimizing the antibodies. Mouse and cell lysates used in antibody optimization were kindly given in the lab. For tau-blot cohort, cases included were: *WDR45*, AD and Pick's disease. For LC3-blots, cohort consisted of *WDR45* case and 3x age and sex matched control human brains.

Preparation of homogenates/extractions

For immunoblotting, the frontal cortex was homogenised in 50mMTris-HCl pH7.5, 150mM NaCl, 5mM EDTA, 1%tritonX-100, 2% SDS, complete protease inhibitor and Phosphatase inhibitor (Roche). Lysates were obtained after centrifugation of homogenised samples at 10000g for 15 min. Protein concentration was determined using Bio-RAD protein assay kit.

Tau extraction: Sarkosyl-insoluble tangle phosphorylated (PHF) tau was isolated from brain samples as previously described (308). Insoluble PHF-tau was enriched from frontal cortex of the cases as previously described (309,310). For Sarkosyl-insoluble tangle PHF-tau preparation, tissue samples (frontal cortex) were weighed and homogenized in 10 volumes of homogenization buffer (NP-40 lysis buffer supplemented with protease inhibitors (Complete Mini Protease inhibitors, Roche). The homogenized samples were spun at 15,000 rpm for 20 min; the supernatants were collected; and aliquots were resuspended in 5X sample buffer (32% 1M Tris, pH6.8, 5% SDS, 50% glycerol, and 1% β-mercaptoethanol) for analysis as the starting material. The rest of the sample was used for extraction of PHF-tau using the sarkosyl extraction of insoluble material (309). Briefly, the supernatants of the brain homogenates were centrifuged at 35,000 rpm for 1 hr at 23°C; the resulting pellets were resuspended in 1% sarkosyl (Fisher Scientific) in TBS and incubated on shaker for 30 min at RT, and then centrifuged at 35,000 rpm for 1 hr at 23°C.

WB run

Gel samples were prepared by the addition of 5x sample buffer (0.625 M Tris-HCl, pH 6.8, 50% glycerol, 10% (w/v) SDS, bromophenol blue and 10% b-mercaptoethanol). Samples were denatured in at 98°C for 10 minutes and 20ug of protein was loaded. Proteins were then separated on 6% SDS gels and transferred to PVDF membrane. Membranes were blocked with PBS/0.1% Tween 20 (PBS-T) containing 10% milk for 30mins to 1 hour, washed briefly in PBS-T and then incubated overnight at 4°C. The membranes were washed five times in PBS-T and then incubated at room temperature for 60mins with secondary antibody in PBS-T with 1% milk. Membrane were then washed in PBS a further five times and developed in Odyssey scanner.

Table 2.7 Primary and secondary antibodies used in IHC staining and WB

Primary Antibody	Species	Company	Pre-treatment	Dilution	Usage	Incubation time
Glial fibrillary acidic protein (GFAP)	Rabbit	DakoCytomation, Denmark (M0872)	Proteinase K	1/1000	IHC	1 hour
CD68	Mouse	Dako	Citrate Buffer	1/150	IHC	1 hour
Ubiquitin	Rabbit	Dako	Citrate Buffer	1/200	IHC	1 hour
Tau (AT8)	Mouse	Source Bioscience, UK (90206)	Citrate Buffer	1/600	IHC	1 hour
P62	Mouse	Bio Sciences	Citrate Buffer	1/100	IHC	1 hour
AT100 tau	Mouse	Autogen bioclear	Citrate Buffer	1/1000	IHC	1 hour
β-Amyloid (Aβ)	Mouse	DakoCytomation,Denmark (M0872)	Formic acid and Citrate Buffer	1/100	IHC	1 hour
α-synuclein	Mouse	VectorLaboratories, (VP A106)	Formic acid and Citrate Buffer	1/50	IHC	1 hour
α-synuclein	Mouse	BD transduction (610787)	Formic acid	1/1000	IHC	Overnight
TAR DNA-binding protein 43 (TDP-43)	Rabbit	Protein Tech (12892-1-AP)	Citrate Buffer	1/2000	IHC	1 hour
TDP-43 phosph	Rabbit	Protein Tech	Citrate Buffer	1/2000	IHC	1 hour
α-internexin	Mouse		Citrate Buffer	1/75	IHC	1 hour
Tau (rabbit anti-human)	Rabbit	DakoCytomation,Denmark (A0024)	-	1:20000	WB	Overnight
αβ crystalline	Mouse		Citrate Buffer	1:300	IHC	1 hour
SMI31	Mouse	Sternberger	Citrate Buffer	1:5000	IHC	1 hour
Neurofilament cocktail	Mouse		-	1:20	IHC	1 hour
Amyloid precursor protein (APP)	Mouse		Citrate Buffer	1:100	IHC	1 hour
Microtubule-associated protein 1A/1B light chain 3 (LC3)	Rabbit	Novus Biologicals	-	1:2000	WB	Overnight
B-actin	Mouse	Sigma	-	1:10000	WB	Overnight

Table 2.7 Primary and secondary antibodies used in IHC staining and WB continued..					
Secondary Antibody	**Species**	**Company**	**Dilution**	**Usage**	**Incubation time**
Biotinylated rabbit anti-mouse IgG	Goat	DakoCytomation, Denmark (E0354)	1:200	IHC	1 hour
Biotinylated swine anti-rabbit IgG	Goat	DakoCytomation, Denmark (E0353)	1:200	IHC	1 hour
IRDye800CW Donkey anti-Rabbit IgG (H+L)	Donkey	Li-Cor(926-32213)	1:10000	WB	1 hour
IRDye800CW Goat anti-Rabbit IgG (H+L)	Goat	Li-Cor	1:15000	WB	1 hour
IRDye680CW Donkey anti-Mouse IgG (H+L)	Donkey	Li-Cor	1:15000	WB	1 hour

2.4. RNA - Quantitative real-time PCR (qPCR)

2.4.1. RNA Extraction

RNA was extracted using Qiagen RNEasy kit *www.qiagen.com/hb/rneasymini.* 700 µL of QIAzol was added to the tissue sample, which was then disrupted and homogenized using TissueRuptor (Qiagen). The homogenized sample was then left at RT for 5 min. To the homogenized sample, 140 µL of chloroform was added, vortexed for 30 sec, incubated at RT for 2-3 min and centrifuged at 12000*g* at 4°C for 15 min. The aqueous phase (upper layer) was then transferred to a sterile 2 mL RNase free tube, added 100% ethanol (1.5x the volume of the aqueous phase) and mixed with pipette to precipitate the RNA. Samples were then purified into the spin column (including any precipitate) and centrifuged at 10000 rpm at RT for 1 min. The flow-through was discarded. The samples were washed for salt traces and impurities by adding 700µL of the RWT solution and centrifuged at 10000 rpm at RT for 1 min. The flow-through was discarded. 500µL RPE solution was added to the column and centrifuged at 10000 rpm at RT for 1 min. The flow-through was discarded. The washing step was repeated. The flow-through was discarded and 500µL RPE solution was added to the column and centrifuged at 10000 rpm at RT for 2 min. The column as transferred to a new 1.5 mL RNase free tube. 15µL RNase-free water was added to the column and let to stand for 1-2 min at RT, then centrifuged at 10000 rpm at RT for 1 min. The elute is the extracted RNA. RNA quality and concentration was assessed using the nanodrop and Agilent Bioanalyser 2100. RNA samples with 260/280 ratio > 1.9 were used for reverse transcription - PCR.

2.4.2. **Reverse transcription**

This procedure is carried out to convert total RNA to first strand DNA. RNA is reverse transcribed to form cDNA using SuperScript® VILO™ cDNA Synthesis Kit (Invitrogen, UK). According to manufacturer's instructions, following components are mixed for each reaction: 4 µl 5X VILO Reaction Mix, 2 µl 10X SuperScript Enzyme Mix, RNA (up to 2.5 µg), DEPC-treated water to make up 20 µl total reaction volume. After gently mixing the tube contents, incubation was done at 42°C for 60 min followed by termination at 85°C for 5 min. Samples were stored -20°C until further use. For multiple reactions, a mater mix was prepared without RNA. cDNA was then diluted 1:10 for use in qPCR.

2.4.3. **Primer design**

Primers were designed to detect the most common isoforms for *THAP1* and *TOR1A* genes and where possible primers were used from rt-primer database (http://www.rtprimerdb.org/). Careful primer design is necessary in SYBR green detection is of utmost importance because of the sensitivity of real-time detection. Primers were designed across exon-exon boundary, reducing contamination through amplification of genomic DNA. Housekeeping genes (*RPLP0, UBC, GAPDH, and beta-actin*) were used to ensure reliability of the experiment and for adjustment of relative expression data. Real-time PCR was performed on Stratagene MX3000p (Agilent technologies, CA) using Power SYBR Green Master Mix (Applied Biosystems). In addition to the software output, qPCR products were also checked by running them on agarose gels. Primers used are listed in Table 2.8.

Table 2.8 Primers used in qPCR			
Housekeeping genes:		Genes of interest:	
GAPDH (amplicon 120 bp)		TOR1A_q1 (amplicon 117 bp)	
GAPDH_q1F:	GAAATCCCATCACCATCTTCCAGG	TOR1A_q1F:	TACAGTTGTGGATTCGAGGCA
GAPDH _q1R:	GAGCCCCAGCCTTCTCCATG	TOR1A_q1R:	AATAGTCGAGGAAAGGCTTGATG
Rplp0 (amplicon 130 bp)		TOR1A_q2 (amplicon 113 bp)	
Rplp0_q1F:	GCTGCTGCCCGTGCTGGTG	TOR1A_q2F:	GCACAGCAGCTTAATTGACCG
Rplp0_q1R:	TGGTGCCCCTGGAGATTTTAGTGG	TOR1A_q2R:	CATAGCCTCGGGACTGCATT
UBC (amplicon 133 bp)		THAP1_q1 (amplicon 95 bp)	
UBC_q1F:	ATTTGGGTCGCGGTTCTTG	THAP1_q1F:	TGCAAGAACCGCTACGACAA
UBC_q1R:	TGCCTTGACATTCTCGATGGT	THAP1_q1R:	CTGACAGCTGCCTCCCATTC
ATCB (amplicon 107 bp)		THAP1_q2 (amplicon 117 bp)	
ATCB_q1F:	ATGTGGCCGAGGACTTTGATT	THAP1_q2F:	GCAGTCCTGCTCCGCCTACG
ATCB_q1R:	AGTGGGGTGGCTTTTAGGATG	THAP1_q2R:	CTGACAGCTGCCTCCCATTC

2.4.4. **Validation of primers and efficiency of the qPCR**

The standard curve was created using a cDNA pool with the primers listed above to determine the efficiency of the primers for genes of interest and housekeeping genes using conventional PCR method. Each PCR reaction contained 12/ uL 5xRoche mix, 2uL of each primer (5uM), 2ul of ddh20 and 2ul of cDNA template (~30ng/uL). The cycling conditions were as follows: Initial denaturation 95°C x5mins; 40 cycles of denaturation 95°C x15secs, primer annealing 60°C x60secs, extension 72°C x 45secs; and the final extension at 72°C x 10mins. The PCR product was purified with Millipore plate and verified on 1% agarose gel run at 100V for 1 hr. The purified product was quantified with Nanodrop spectrophotometer and diluted to the first working standard 10^8. The stock is then diluted serially from 10^1 – 10^7. The serial dilutions are used as a template for qPCR to generate a standard curve.

2.4.5. **qPCR**

SYBR Green is a dye that fluoresces upon intercalation with double-stranded DNA. It is used to detect the threshold cycle (Ct) during PCR when the level of fluorescence gives a signal over the background and is in the linear portion of the amplified curve. The Ct value is responsible for the accurate quantification of the PCR. The PCR amplification mixture for each 20 μL reaction was prepared as follows: 10 μL Power SYBR Green PCR Master Mix, 1 μL forward primer (500nM), 1 μL reverse primer (500nM), 3 μL molecular biology grade water and 5 μL cDNA (1:15 dilution). Cycling conditions: : Initial denaturation 95ºC 10min; denaturation 95ºC 15secs, primer annealing 60ºC 1min for 40 cycles. Melting curve analysis: Initial denaturation 95°C x5mins, denaturation 95°C x30secs, primer annealing 60°C x45secs, extension 72°C x 45secs and the final extension at 72°C x 10mins. The PCR was run for 40 cycles and kept at -20 and away from light.

2.4.6. **ΔΔCt method**

Semi-quantitative real-time PCR was used in this study to determine a fold change of gene expression levels. The relative expression of mRNA is calculated by measuring the cycle in the log phase of PCR, at which amplified DNA reaches a significant fluorescence threshold (Ct) and was determined for each sample using Maxpro software. Due to technical variability between experiments the Ct needs to be normalised against the housekeeping genes. Comparing the normalised expression (ΔCt) of three conditions (in this case THAP1, TOR1A and control) it was possible to calculate the fold change of the gene expression (2^-ΔΔCt). The fold

change is the expression ratio: a positive changes means a gene is upregulated, a negative fold change represents a downregulation (Livak and Schmittgen 2001). 5 healthy age and sex matched controls were used as a calibrator.

Fold change (2^-ΔΔCt) = 2 exp {ΔCt sample (target gene- reference gene) -ΔCt calibrator (target gene – reference gene)}

Chapter 3. Genetics of primary dystonia

3.1. Background

The dystonias are a heterogenous group of movement disorders, characterized by involuntary sustained muscle contractions affecting one or more sites of the body, which lead to twisting and repetitive movements or abnormal postures of the affected body part. It is the third most common movement disorder worldwide (3–6). Approximately 70 000 people are affected by dystonia in the UK alone, including some 8000 children and adolescents (311). Affected individuals can suffer considerable physical and psychosocial distress, which has been demonstrated to have a significant impact on their quality of life (12). New 'next generation' sequencing technologies have massively increased the speed of genetic discoveries in recent years and this has made itself felt in the field of dystonia research as in many others. To date, genes associated with primary pure dystonia are *TOR1A/DYT1* (torsinA), *THAP1/DYT6* (thanatos associated protein domain containing, apoptosis associated protein 1), *CIZ1* (CDKN1A interacting zinc finger protein 1), *ANO3/DYT23* (anoctamin 3), *TUBB4A/DYT4* (β-tubulin 4) and *GNAL* (α-activating activity polypeptide, olfactory type). Dystonia gene, *ANO3* is not included in this study (Chapter1, 1.2).

3.2. Aims and Hypothesis

Hypothesis

- Primary pure dystonia is caused by a mutation in one of the primary dystonia genes described in literature: *TOR1A, THAP1, CIZ1, TUBB4,* or *GNAL*
- The nature of the mutation will influence the clinico-pathological phenotype

Aims

- To locate and obtain clinically diagnosed primary dystonia cases
- Investigate clinical and genetic correlation

3.3. Methods

Primary dystonia genes were screened using Sanger sequencing (described in Chapter 2).

3.4. Results

Tissues were initially requested from cases clinically diagnosed as primary dystonia from Maryland Brain Bank, Baltimore, USA, Queen Square Brain Bank and Harvard Brain Bank. Consent for research was obtained from all the participants. A cohort of 90 patients clinically diagnosed as primary dystonia was screened for primary pure dystonia genes, *TOR1A, THAP1, CIZ1, GNAL* and *TUBB4*. Dystonia cohort was not screened for *ANO3*. The cohort was also sequenced for *PRRT2.*

The disease onset in the cohort varied from early to adult onset and was in the ratio of 1:4. Age at death ranged from 32 to 91 years old and male to female ratio was 1:3.

3.4.1. Genetic screening and mutation analysis

DNA was extracted using the Qiagen Tissue extraction kit. All exons in each of the genes were amplified using polymerase chain reaction and Sanger sequencing was carried out to identify the mutations. Mutations identified are summarized in the Table 3.1.

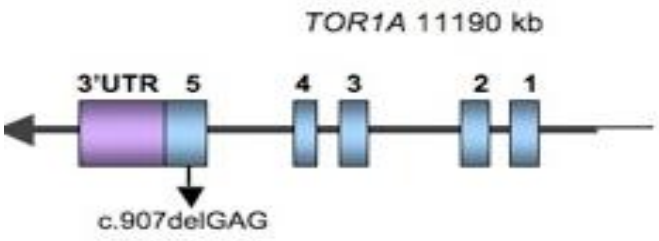

Figure 3.1 The location of the recurring 3basepair deletion (ΔGAG) mutation in exon 5 of *TOR1A*.

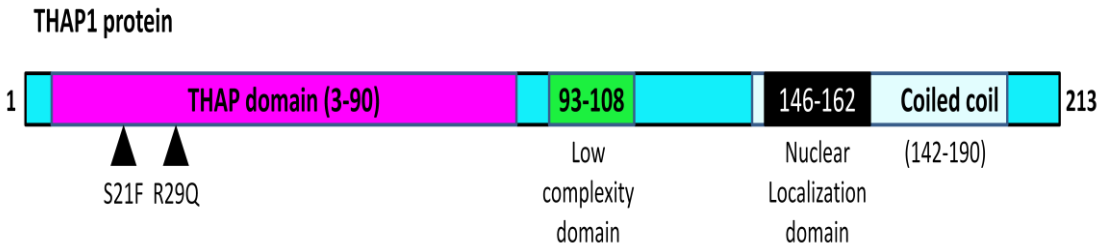

Figure 3.2 Structure of THAP1 protein and location of *THAP1* mutations in the cases studied.

Table 3.1 Mutations identified in the cohort

Case	Mutation					Clinical diagnosis
	TOR1A	*THAP1*	*CIZ1*	*GNAL*	*TUBB4*	
1	p.303-/Glu304	-	-	-	-	Dystonia, DYT-1 GAG deletion carrier
2	p.303-/Glu304	-	-	-	-	Dystonia, DYT-1 GAG deletion carrier
3	p.303-/Glu304	-	-	-	-	Familial congenital Dystonia, generalized, childhood onset
4	p.303-/Glu304	-	-	-	-	Dystonia, DYT-1 GAG deletion carrier
5	p.303-/Glu304	-	-	-	-	Dystonia, generalized
6	p.303-/Glu304	-	-	-	-	Dystonia, DYT-1 GAG deletion carrier
7	p.303-/Glu304	-	-	-	-	Dystonia, DYT-1 GAG deletion carrier
8	p.303-/Glu304	-	-	-	-	Dystonia, DYT-1 GAG deletion carrier
9	-	p.Arg29Gln	-	-	-	Dystonia, childhood onset
10	-	p.Ser21Phe	-	-	-	Dystonia
11	p.303-/Glu304	-	-	-	-	Dystonia
12	p.Lys275Glu	-	-	-	-	-

Ten cases were identified with heterozygous mutation p.303-/Glu304 in exon 5 of the *TOR1A/DYT1* gene (Figure 3.1). This mutation is a recurring mutation in DYT1 cases and has been described as pathogenic in human and animal studies (background information on the mutation in chapter 1).

Two cases were identified with heterozygous mutations, p.Arg29Gln or p.R29Q and p.Ser21Phe or p.S21F respectively, in the coding region of *THAP1/DYT6* gene (Figure 3.2). p.R29Q mutation variant predicted to be damaging by Mutation taster (score: 43), Polyphen (score: 0.867) and SIFT (score: 0.004). This mutation has previously been described as pathogenic in dystonia (312,313). Case 2 had a novel variant p. S21F, predicted to be disease causing by Mutation taster (score: 155), Polyphen (score: 0.981) and SIFT (score: 0.01). A pathogenic mutation in the amino acid 21 was reported before but involving a different nucleotide than reported above. Both amino acids are conserved across several species (chimpanzee,

monkey, mouse, chicken, zebrafish and xenopus). Mutations identified are summarized in Table 3.1.

3.4.2. **Clinical details**

Case1: This Caucasian female (ΔGAG mutation carrier) was 89 years old at death. Despite having a strong family history of dystonia she was clinically unaffected. Her grandson had primary dystonia and torticollis. Her sister (case 2) and niece were positive for the ΔGAG mutation. She had a medical history of hypertension, coronary artery disease, arteriovascular insufficiency involving left arm and developed cognitive impairment.

Case 2: A Caucasian woman (ΔGAG mutation carrier) who died at the age of 87 years had a past medical history of hypertension, hyperlipidemia, coronary artery disease, pulmonary embolism, hypothyroidism, osteoarthritis and dementia. Although unaffected herself, she had a strong family history of dystonia. Her sister (case 1) and niece were both positive for ΔGAG mutation. She died following a right middle cerebral artery infarction confirmed prior to death by imaging studies

Case 3: This Caucasian female, positive for ΔGAG mutation, had a clinical diagnosis of congenital dystonia with life-long disability. Dystonic symptoms started at the age of 9 or 10 and were slowly progressive. She had a similarly affected sibling but no other family history was available. By 73 years of age she was weak bilaterally in the upper and lower limbs and wheelchair bound. Abnormal involuntary movements affected both upper extremities. She complained of progressive

bilateral hearing loss and episodic problems with her vision and speech. Neurological examination reported no facial asymmetry, weakness in the both upper and both lower extremities, more severe proximally than distally. Deep tendon reflexes were diminished in the upper extremities, but symmetrical. Sensory evaluation showed intact pinprick and vibration sensation in both hands and right foot but these were absent in the left leg. No obvious cerebellar dysfunction was reported. She died at the age of 77.

Case 4: A Caucasian female (ΔGAG mutation carrier) of Jewish ancestry died at the age of 90 years. She had been well until the age of 89 when she developed left sided weakness, expressive aphasia and dysphagia secondary to cerebrovascular accident. She also had intermittent confusion and paranoia. MRI reportedly showed an infarct involving the right internal capsule, thalamus and white matter. She did not have a history of movement disorder; however, her grandson had a diagnosis of dystonia.

Case 5: A Caucasian female with a clinical diagnosis of dystonia died at the age of 90 years. Her son had a confirmed ΔGAG mutation. No further medical history was available.

Case 6: This Caucasian female was a ΔGAG mutation carrier and died aged 88 years. No further medical history was available.

Case 7: This Caucasian male (ΔGAG mutation carrier) was unaffected by dystonia and died at the age of 75. No further clinical history was available.

Case 8: This Caucasian female, positive for ΔGAG mutation had a clinical diagnosis of torsion dystonia. The symptoms initially started at approximately 12-15 years of age but diagnosed as a psychiatric condition. Diagnosis of dystonia was made when she was 34 years old and narrowed down to torsion dystonia when she was approximately 57 years old. The symptoms largely took the form of tremors of the body, not of the neck or head and were described as a mild case of cerebral palsy. At the end of her life, 67 years old dystonia did not get any worse and no other treatments were offered.

Case 9: This Caucasian male with p.Arg29Gln mutation in *THAP1/DYT6* gene had a history of multi-infarct dementia, chronic obstructive pulmonary disease with severe dystonia and incontinence. He was negative for DYT1 dystonia and the onset of the dystonic symptoms was at the age of 17. He developed absence seizures late in life, at approximately, the onset of his Alzheimer's symptoms. He died of two violent seizures three hours apart at the age of 71.

Case 10: This Caucasian male with p.Ser21Phe mutation in *THAP1/DYT6* gene, was 59 years old at death with clinical diagnosis of dystonia. No further clinical details were available.

Case 11 and 12 were with clinical diagnosis of dystonia. No further clinical details were available.

3.5. Discussion

New 'next generation' sequencing technologies have massively increased the speed of genetic discoveries in recent years. Till date, 25 different loci for dystonia are reported in literature. The genes involved in monogenic forms of dystonia reflect the clinical heterogeneity. Although the genes identified to date are diverse and at present, the underlying functions of most of these genes and how they lead to dystonia remain elusive, their identification has fostered basic research (development of animal and cellular models) aimed at understanding the pathophysiology of dystonia.

There is an accumulating evidence for genetic and clinical heterogeneity in primary dystonia. However, due to extremely reduced penetrance of primary dystonia mild cases may remain undiagnosed. A recurring mutation (ΔGAG) in the *TOR1A* gene causes the loss of an amino acid, glutamic acid, in the torsinA protein which is responsible for primary dystonia DYT1. Several heterozygous mutations along the coding regions of *THAP1* gene are linked to primary dystonia DYT6.

In total, 90 cases clinically diagnosed as primary dystonia were screened for primary dystonia genes *TOR1A*, *THAP1*, *CIZ1*, *TUBB4* and *GNAL*. The disease onset in the cohort varied from early to adult onset and was in the ratio of 1:4. Age at death ranged from 32 to 91 years old and male to female ratio was 1:3. *TOR1A* mutations were identified in ten cases (11.1%) (9 cases with recurring mutation p.303-/Glu304 and a case with p.Lys275Glu) and two cases (2.2%) have mutation in the *THAP1* gene (p.Arg29Gln and p.Ser21Phe). p.303-/Glu304 is a recurring mutation in DYT1

dystonia. The *THAP1* mutations observed in cases 9 and 10 are predicted to be pathogenic by prediction softwares. One of the DYT1 cases has also a mutation in *CIZ1* gene.

Among the ten cases presented here, medical records and brain tissues were not available for cases 9 and 10 hence excluded from further study. Of the 8 cases, three cases (cases 3, 5, 8) are symptomatic and five of them are carriers for DYT1 dystonia (cases 1, 2, 4, 6, and 7). Monogenic inheritance is most often seen in early-onset cases, where a family history can often be elicited. Among eight cases in our cohort, cases 1, 2 and 8 belong to a same family tree. However, the reduced penetrance of DYT1 mutation means that many apparently sporadic cases may also fall into this category.

Although the clinical phenotype associated with DYT1 dystonia can vary from severe dystonic storm to mild writer's cramp, a typical phenotype has been described across ethnic groups characterized by early (mean age at onset, 13 years; with the majority before 26 years) limb (arm or leg is affected first in 90% of cases) onset, progressing to generalized/multifocal (65%) involvement, with spread to cranial muscles less common (15%–20%) (75). Symptomatic cases in the dystonia cohort: case 3 had no family history of dystonia, disease onset was in childhood affecting limbs (arms and leg) and progressed to generalized involvement; case 5 had no clinical details available; case 8 had no family history of dystonia, disease onset was in childhood in the form of tremors of the body. Cases 1, 2, 4, 6, and 7 are DYT1 mutation carriers where dystonic symptoms were absent.

Comparing clinical symptoms in mutation carriers, a typical DYT6 phenotype is characterized by early onset (mean, 16 years; range, 5–62 years); onset most often in an arm (50%), followed by cranial muscles (about 25%) or the neck (about 25%). In the dystonia cohort, a DYT6 symptomatic case (case 9) with a *THAP1* mutation had onset at 17 years with severe dystonia and incontinence.

Mutations in primary dystonia genes *TUBB4, GNAl* and *CIZ1* are rare. Sanger sequencing of the primary dystonia genes mentioned above suggest that *GNAL, TUBB4* and *CIZ1* mutations do not represent a common cause of dystonia (in at least US and UK population) and that the frequency of mutations may vary with the population under consideration.

Recent international consensus has proposed a new classification system for dystonia to address an increased understanding of the various clinical manifestations and etiologies (7). Owing to the serious shortcomings with assigning the DYTn loci based on statistical associations (314), the new classification system highlights the importance of biological phenomenon in understanding the disorders. The classification system is based on two axes: (a) clinical characteristics: age at onset, body distribution, temporal pattern, associated features (isolated or combined with another movement disorder), (b) etiology: nervous system pathology and inherited or acquired. The new classification system groups the previously 'pure' or 'primary' dystonias into isolated dystonias and 'dystonia plus' or 'heredodegenerative' dystonias into combined dystonia. Hence, by combining phenomenology and biological mechanism in the same classification, it becomes

easier for diagnostic testing and clinical recognition of dystonia syndromes. This will also help to keep the clinical practice and scientific discoveries in the same pace.

Nevertheless, studying the genetics of dystonia will not only help refine diagnostic and reproductive technology applications, but it also contributes greatly to our understanding of dystonia and quest for better treatments and a cure.

Chapter 4. Neuropathology of DYT1 dystonia

4.1. Background

Neuropathological reports on genetically confirmed DYT1 dystonia are few in number and results are inconsistent. The absence of histological confirmation of changes in the basal ganglia, cerebral cortex and brainstem has made it even more difficult to support the traditional view of dystonia being a basal ganglia disorder. The evidence of perinuclear inclusion bodies in some of the neurons of pedunculopontine nucleus, the cuneiform nucleus and periaqueductal gray, but not in substantia nigra pars compacta, striatum, hippocampus and neocortex in four manifesting DYT1 carriers is by far the most interesting finding in the neuropathology of DYT1 dystonia (129). However, these findings are not replicated till date (Chapter 1, 1.5).

DYT1 dystonia is caused by a heterozygous three base pair deletion in exon 5 of *TOR1A* gene with autosomal dominant inheritance. It encodes protein torsinA which resides in endoplasmic reticulum while the mutant form has been reported to reside in the nuclear envelope. The exact function of torsinA is still unknown but it is believed to take part in chaperone-like activities. Though DYT1 dystonia is more frequently observed in the clinics, the penetrance of the disease is only 30-40%. The low penetrance makes it difficult to draw a clinic-genetic-pathological correlation.

4.2. Aims and Hypothesis

Hypothesis

- That the ΔGAG deletion mutation in DYT1 dystonia influence the clinico-pathological phenotype and include perinuclear inclusions in brainstem, which have been previously described (129).
- The emerging role of cerebellum in dystonia will influence clinico-pathological phenotype in cerebellum.
- That a consistent neuropathology such as tau pathology or LBs, can be identified amongst seven genetically confirmed cases of DYT1 dystonia.

Aim

- To obtain both paraffin fixed and frozen tissues from brain regions of interest for genetically confirmed DYT1 cases.
- To characterize the neuropathology of DYT1 cases.
- To determine whether there is any corelation between clinical, genetic and pathological features.

4.3. Methods

Cohort

Ten DYT1 cases were identified by genetic screening (described in Chapter 3) of the dystonia cohort. We selected the first seven cases for neuropathological examination as brain tissues were not available for the case 8, 11 and 12 (Table 3.1). Autopsy specimens of 7 DYT1 confirmed cases were received from the

BTBDD. Neurologically normal controls (n=5) were selected from the collection of the QSBB. Clinical details, macroscopic findings and neuropathology reports were provided by the respective institutions. To our knowledge, none of the DYT1 cases have been previously reported. Formalin fixed, paraffin embedded brain tissue was available in all dystonia cases although systematic sampling of multiple regions for each case was not possible due to the retrospective nature of the study. Where possible the frontal and temporal cortices, striatum, globus pallidus, thalamus, subthalamic nucleus, cerebellum, midbrain, pons, and medulla were investigated. Brain regions available for study in each case are indicated in Table 2.3 DYT1 and DYT6 cohorts for neuropathological studyTable 2.3. The midbrain was absent in cases 2 and 3 and was only partially represented in case 6. The pons including the reticular formation was present in all cases except case 6.

IHC

Histological staining and and IHC methods carried out are described in detail in Chapter 2. In brief, paraffin embedded tissue sections (7 µm) were cut and stained using routine methods, including hematoxylin and eosin, Gallyas silver and Luxol fast blue/cresyl violet. IHC staining was performed according to a standard avidin-biotin complex protocol using the following antibodies: ubiquitin (1:200, Dako, Ely,UK), tau (1:600, AT8, Autogen Bioclear, Calne, UK); AT100 (1:200, Innogenetics, Gent, Belgium), glial fibrillary acidic protein (GFAP; 1:1,000, Dako), Aβ (1:200, Dako), α-synuclein (1:50, Novacastra, Newcastle, UK), α-synuclein (1:1000, BD Transduction Biolabs, Oxford, UK), p62 (1:100, BD Bioscience, Oxford, UK), CD68 (1:150, Dako), and TDP-43 (1:2000, Protein Tech, Manchester, UK). Antibodies to

ubiquitin, p62, and tau required pretreatment with pressure cooking in sodium citrate buffer, pH 6.0, for 10 minutes before IHC staining. Sections to be used for IHC staining with antibodies to α-synuclein and Aβ were treated with formic acid for 30 minutes before pressure cooking as described above. For GFAP IHC, pretreatment with proteinase K was used. Antibody binding sites were visualized using the chromogen diaminobenzidine, and sections were counterstained using Mayer's hematoxylin.

Assessment

The staining protocol was designed to detect intracellular inclusions as previously described in DYT1 dystonia (129). In all cases brain regions including the midbrain and pons were stained with antibodies to ubiquitin and p62 to assess the presence of intraneuronal inclusions in the periaqueductal grey matter, pedunculopontine nucleus, cuneiform nucleus, and reticular formation (129). Due to limited tissue availability the periaqueductal grey matter was not available in all cases (absent in cases 2, 3 and 6). The pontine tegmentum was available in all cases except case 6. Cases were systematically screened for additional neuropathological changes. Using Aβ IHC vascular and parenchymal Aβ deposition was determined in the frontal cortex and diffuse and mature plaque load was assessed based on the criteria of the Consortium to Establish a Registry for Alzheimer's Disease (CERAD)(304). NFT pathology was determined using tau IHC and staged where possible according to the method of Braak and Braak (305). Vascular pathology was assessed and tau, ubiquitin, and α-synuclein IHC were performed in selected regions to exclude progressive supranuclear palsy, corticobasal degeneration,

Parkinson disease and multiple system atrophy as described previously (306). Where brainstem LBs were identified cortical LB pathology was also determined (307).

4.4. Results

Demographics and clinical reports obtained from the respective brainbanks for each case is described in detail in Chapter 3 and summarized in Table 4.1

Table 4.1 Demographics and **clinical report of DYT1 cases and controls**

Case	***Sex***	***Ethnicity***	*Phenotype*	*Family history*	***Age at onset, y***	***Age at death, y***	***Cause of death***
1	F	American Caucasian	Non-manifesting	+	N/A	89	Natural
2	F	American Caucasian	Non-manifesting	+	N/A	87	Stroke
3	F	American Caucasian	Affected	-	~9-10	77	Complications of disorder
4	F	American Caucasian	Non-manifesting	+	N/A	90	Stroke
5	F	American Caucasian	Affected	+	N/A	90	Natural
6	F	American Caucasian	Non-manifesting	N/A	N/A	88	N/A
7	M	American Caucasian	Non-manifesting	N/A	N/A	75	Natural
C1	M	English	Control	N/A	N/A	69	Myocardial infarction
C2	F	English	Control	N/A	N/A	93	Old age
C3	F	English	Control	N/A	N/A	87	Cancer
C4	F	English	Control	N/A	N/A	81	Respiratory tract infection
C5	F	English	Control	N/A	N/A	79	Cancer

N/A: not available

4.4.1. Macroscopic findings

The macroscopic details were available from the neuropathology reports supplied by the brain bank providing the case. In all the DYT1 cases the weight of the unfixed brains was in the normal range (315) or mildly reduced (range 1010 – 1200g, data available for cases 2-4 and 6). The blood vessels of the circle of Willis showed variable atherosclerosis in all cases except case 7. Mild cerebral cortical atrophy was evident in case 3 and generalized brain atrophy consistent with age was described in case 6. At brain slicing the cortical ribbon was well preserved in all cases. The ventricular system was unremarkable in cases 3 and 4 but there was moderate dilatation in case 2. Four cases showed cerebral infarction, this affected the right middle cerebral artery territory in case 2, frontal white matter in case 3, several infarcts of varying age with unspecified distribution in case 5, and multiple regions of cerebral white matter, occipital cortex and deep grey nuclei in case 4. Case 7 was found to have a diffuse leptomeningeal melanocytoma. Pigmentation of the substantia nigra and locus coeruleus was described in cases 2, 3, 4, and 6 where it was noted to be normal.

4.4.2. Histological findings

A summary of the pathological findings is given in Table 4.2 Examination of the midbrain and pons, represented in all cases except cases 6, using ubiquitin and p62 IHC showed no evidence of NCIs of similar distribution and morphology to those previously associated with early-onset DYT1 dystonia (129) in the 7 cases and 5

controls studied. Moreover a detailed systematic examination of additional brain regions did not reveal similar inclusions in other structures.

DYT1 cases were systematically assessed for other neuropathological abnormalities. Neuronal loss was generally inconspicuous in the regions studied. There was mild neuronal cell loss in the pigmented neurons of the substantia nigra pars compacta of case 1, 4, 5 and 7 and in the locus coeruleus of case 2, 4 and 5. Mild to moderate Purkinje cell loss was observed in the cerebellum of all the cases (Figure 4.2). Mild to moderate gliosis of the striatum was observed in all the cases and also in the substantia nigra of all cases in which it was available for analysis. The pontine base showed variable gliosis and this was severe in case 3. Vascular pathology and ischemic damage in the form of SVD, CAA and infarction was assessed in all cases. Cases 1, 4, 5 and 6 had mild SVD while this was severe in case 2. CAA was mild in cases 2 and 6 and moderate in case 4. Small areas of infarction were observed in 3 cases. In cases 2 and 4 infarcts involved the globus pallidus and in case 5 a small infarct was noted in the midbrain tegmentum. Using two different α-synuclein antibodies for IHC investigation on multiple regions to assess LB pathology, cortical and brainstem Lewy bodies were observed in case 5 and rare LBs were observed in substantia nigra of case 7. Braak staging of LB pathology could not be performed as only limited brain regions were available.

Full neuropathological assessment for AD was not possible due to the limited tissue available. Sparse diffuse Aβ plaques were noted in the cortex of case 1. In cases 2, 4, 5 and 6 both diffuse and mature cortical Aβ plaques were present (Figure 4.1).

Tau pathology in the form of NFTs and neuropil threads was evident in four cases (cases 4, 5, 6 and 7). Formal Braak and Braak staging could not be performed. Tufted astrocytes, astrocytic plaques and coiled bodies were not observed.

No consistent abnormalities were noted in the brain regions available for examination in this study including the midbrain, striatum, globus pallidus, cerebellum, and pons. Apart from AD and LB pathology as described above, none of the cases were found to have neuropathological features of any other neurodegenerative disease. In particular, multiple system atrophy, progressive supranuclear palsy and corticobasal degeneration were excluded.

Table 4.3 summarizes the semi-quantitative findings of the histological features of the seven DYT1 cases.

Table 4.2 Summary of pathological findings in DYT1 cases

Case	Brainweight, g*	Infarction	Aβ pathology		Tau pathology	Lewy body pathology	SVD	CAA	Final neuropathological diagnosis*
			D	M					
1	N/A	-	+	-	-	-	+	-	• moderate atherosclerosis of cerebral vessels • mild neuronal loss and gliosis in hippocampus between the CA1 region and the subiculum • mild loss of Purkinje cells in the cerebellum • mineralization of vessel walls in the dentate nucleus • non-specific neurodegenerative changes
2	1110	globus pallidus	+	+	-	-	+++	+	• mild cerebral artery atherosclerosis • right middle cerebral artery territory subacute infarct • possible AD
3	1200	-	-	-	-	-	-	-	• mild cortical atrophy • small areas of infarction • cerebral athero-arterio-arteriolosclerosis, remote frontal white matter infarct
4	1010	globus pallidus	+++	++	+ (cortex, striatum and brainstem)	-	+	++	• cerebral artho-arteriosclerosis • microinfarcts in cerebral white matter, deep gray nuclei and occipital cortex • macro infarct in right posterior internal capsule and pulvinar • hippocampal sclerosis
5	N/A	midbrain tegmentum	++	++	+ (cortex, striatum and brainstem)	++ (cortical and brainstem)	+	-	• diffuse LB disease (a) SN degeneration with LBs (b) neocortical LBs (c)AD neuropathology • cerebrovascular disease (a)numerous infartcs of different ages (b)atherosclerotic disease of circle of Willis arteries
6	1184	-	++	+	+ (cortex, striatum and brainstem)	-	+	+	• brain generalized atrophy • focal acute (perimortem) petechial hemorrhages
7	N/A	-	-	-	+ (brainstem)	+ (SN)	-	-	• melanocytic neoplasm with diffuse leptomeningeal and perineural spread

- = absent; + = occasional/mild; ++ = moderate; +++ = severe; N/A-not available; SVD- Small vessel disease ; CAA- Cerebral amyloid angiopathy; SN: Substantia nigra; Aβ : D-diffuse plaques, M-mature plaques; AD: Alzheimer's disease; LB: Lewy body; *: Derived from neuropathology report issued by BTDBB

Table 4.3 Semi-quantitative summary of neuronal loss (NL), gliosis pathology, Lewy bodies (LB), and Tau pathology in DYT1 cases

Brain regions	Case 1						Case 2						Case 3						Case 4					
	NL	Gliosis	Aβ		LB	Tau	NL	Gliosis	Aβ		LB	Tau	NL	Gliosis	Aβ		LB	Tau	NL	Gliosis	Aβ		LB	Tau
			D	M					D	M					D	M					D	M		
Frontal cortex	-	+	+	-	-	-	-	+++	+	+	-	-	-	++	-	-	-	-	-	++	++	+	-	+
Temporal cortex	-	+	-	-	-	-	-	-	+	+	-	-	-	-	-	-	-	-	-	++	++	+	-	-
Caudate	-	+	N/P		-	-	-	++	N/P		-	-	-	+	N/P		-	-	-	++	N/P		-	+
Putamen	-	+	N/P		-	-	-	++	N/P		-	-	-	++	N/P		-	-	-	++	N/P		-	++
Globus pallidus	-	++	N/P		-	-	-	+++	N/P		-	-	N/A	N/A	N/A		N/A	N/A	-	+++	N/P		-	-
Thalamus	-	+	N/P		-	-	-	-	N/P		-	-	N/A	N/A	N/A		N/A	N/A	-	++	N/P		-	-
Subthalamic nucleus	-	+	N/P		-	-	N/A	N/A	N/A		N/A	N/A	N/A	N/A	N/A		N/A	N/A	N/A	N/A	N/A		N/A	N/A
Midbrain tegmentum	-	++	N/P		-	N/P	N/A	N/A	N/A		N/A	N/A	N/A	N/A	N/A		N/A	N/A	-	-	N/P		-	+
Midbrain tectum	N/A	N/A	N/A		N/A	N/A	N/A	N/A	N/A		N/A	N/A	N/A	N/A	N/A		N/A	N/A	-	-	N/P		-	+
Reticular formation	-	++	N/P		-	N/P	-	-	N/P		-	-	-	-	N/P		-	-	-	-	N/P		-	+
Substantia nigra pars compacta	+	++	N/P		-	N/P	N/A	N/A	N/A		N/A	N/A	N/A	N/A	N/A		N/A	N/A	+	++	N/P		-	+
Red nucleus	-	-	N/P		-	N/P	N/A	N/A	N/A		N/A	N/A	N/A	N/A	N/A		N/A	N/A	N/A	N/A	N/A		N/A	N/A
Locus coeruleus	N/A	N/A	N/A		N/A	N/A	+	-	N/P		-	+	-	+++	N/P		-	+	+	+	N/P		-	+
Pontine tegmentum	-	++	N/P		-	N/P	-	-	N/P		-	+	-	++	N/P		-	-	-	++	N/P		-	-
Pontine base	-	++	N/P		-	N/P	-	-	N/P		-	-	-	+++	N/P		-	-	-	++	N/P		-	-
XIIth nerve nuclei	N/A	N/A	N/A		N/A	N/A	N/A	N/A	N/A		N/A	N/A	N/A	N/A	N/A		N/A	N/A	-	+	N/P		-	-
Dorsal motor nuclei Xth	N/A	N/A	N/A		N/A	N/A	N/A	N/A	N/A		N/A	N/A	N/A	N/A	N/A		N/A	N/A	-	-	N/P		-	-
Inferior olive	N/A	N/A	N/A		N/A	N/A	N/A	N/A	N/A		N/A	N/A	N/A	N/A	N/A		N/A	N/A	-	-	N/P		-	-
Pyramid	N/A	N/A	N/A		N/A	N/A	N/A	N/A	N/A		N/A	N/A	N/A	N/A	N/A		N/A	N/A	-	-	N/P		-	-
Periaqueductal gray	N/A	N/A	N/A		N/A	N/A	-	-	N/P		-	-	N/A	N/A	N/A		N/A	N/A	-	-	N/P		-	+
Cerebellum	+	+	N/P		N/P	-	+	+	N/P		N/P	-	+	++	N/P		N/P	-	+	++	N/P		N/P	-
Vermis	++	++	N/P		N/P	-	N/A	N/A	N/A		N/A	N/A	N/A	N/A	N/A		N/A	N/A	+	++	N/P		N/P	-
Dentate nucleus	+	-	N/P		N/P	-	-	-	N/P		N/P	-	-	+	N/P		N/P	-	-	+	N/P		N/P	-

Key: - = absent; + = occasional/mild; ++ = moderate; +++ = severe/frequent, Tau [- = absent; + = Neurofibrillary tangles/ abnormal neurites/neuropil threads; Aβ [D: diffuse plaques, M: mature plaques]; N/A: not available; N/P: not performed; Assessment: LB- α-syn, Tau- AT8, NL-H&E, Gliosis- GFAP.

Table 4.3: Semi-quantitative summary of neuronal loss (NL), gliosis pathology, Lewy bodies (LB), and Tau pathology in DYT1 cases continued..

Brain regions	Case 5						Case 6						Case 7					
	NL	Gliosis	Aβ		LB	Tau	NL	Gliosis	Aβ		LB	Tau	NL	Gliosis	Aβ		LB	Tau
			D	M					D	M					D	M		
Frontal cortex	-	+	+	++	-	+	-	+	++	+	-	+	-	++	N/P		-	-
Temporal cortex	-	++	++	++	-	+	-	++	+	++	-	+	N/A	N/A	N/A		N/A	N/A
Caudate	-	+	N/P		-	+	-	++	N/P		-	+	-	+	N/P		N/P	-
Putamen	-	++	N/P		-	-	N/A	N/A	N/A		N/A	N/A	-	+	N/P		N/P	-
Globus pallidus	-	++	N/P		-	-	-	-	N/P		-	-	-	++	N/P		N/P	N/P
Thalamus	N/A	N/A	N/A		N/A	N/A	-	+	N/P		-		N/A	N/A	N/A		N/A	N/A
Subthalamic nucleus	N/A	N/A	N/A		N/A	N/A	-	++	N/P		-	-	N/A	N/A	N/A		N/A	N/A
Midbrain tegmentum	+	++	N/P		+	-	N/A	N/A	N/A		N/A	N/A	-	+	N/P		-	N/P
Midbrain tectum	-	++	N/P		-	+	N/A	N/A	N/A		N/A	N/A	-	+	N/P		-	N/P
Reticular formation	-	-	N/P		-	-	N/A	N/A	N/A		N/A	N/A	-	++	N/P		-	-
Substantia nigra pars compacta	+	++	N/P		++	+	-	++	N/P		-	+	+	++	N/P		+	-
Red nucleus	-	+	N/P		-	-	-	+	N/P		-	+	-	+	N/P		-	N/P
Locus coeruleus	+	-	N/P		++	-	N/A	N/A	N/A		N/A	N/A	-	++	N/P		-	+
Pontine tegmentum	-	-	N/P		++	-	N/A	N/A	N/A		N/A	N/A	-	++	N/P		-	+
Pontine base	-	-	N/P		-	-	N/A	N/A	N/A		N/A	N/A	N/A	N/A	N/A		N/A	N/A
XIIth nerve nuclei	N/A	N/A	N/A		N/A	N/A	N/A	N/A	N/A		N/A	N/A	N/A	N/A	N/A		N/A	N/A
Dorsal motor nuclei Xth	N/A	N/A	N/A		N/A	N/A	N/A	N/A	N/A		N/A	N/A	N/A	N/A	N/A		N/A	N/A
Inferior olive	N/A	N/A	N/A		N/A	N/A	N/A	N/A	N/A		N/A	N/A	N/A	N/A	N/A		N/A	N/A
Pyramid	N/A	N/A	N/A		N/A	N/A	N/A	N/A	N/A		N/A	N/A	N/A	N/A	N/A		N/A	N/A
Periaqueductal gray	N/A	N/A	N/A		N/A	N/A	N/A	N/A	N/A		N/A	N/A	N/A	N/A	N/A		N/A	N/A
Cerebellum	++	++	N/P		N/P	-	+	++	N/P		N/P	N/P	+	++	N/P		-	-
Vermis	+	++	N/P		N/P	-	N/A	N/A	N/A		N/A	N/A	+	++	N/A		N/P	N/P
Dentate nucleus	-	-	N/P		N/P	-	-	+	N/P		N/P	-	-	-	N/P		-	-

Key: - = absent; + = occasional/mild; ++ = moderate; +++ = severe/frequent, Tau [- = absent; + = Neurofibrillary tangles/ abnormal neurites/neuropil threads; Aβ [D: diffuse plaques, M: mature plaques]; N/A: not available; N/P: not performed; Assessment: LB- α-syn, Tau- AT8, NL-H&E, Gliosis- GFAP; CAA- Aβ

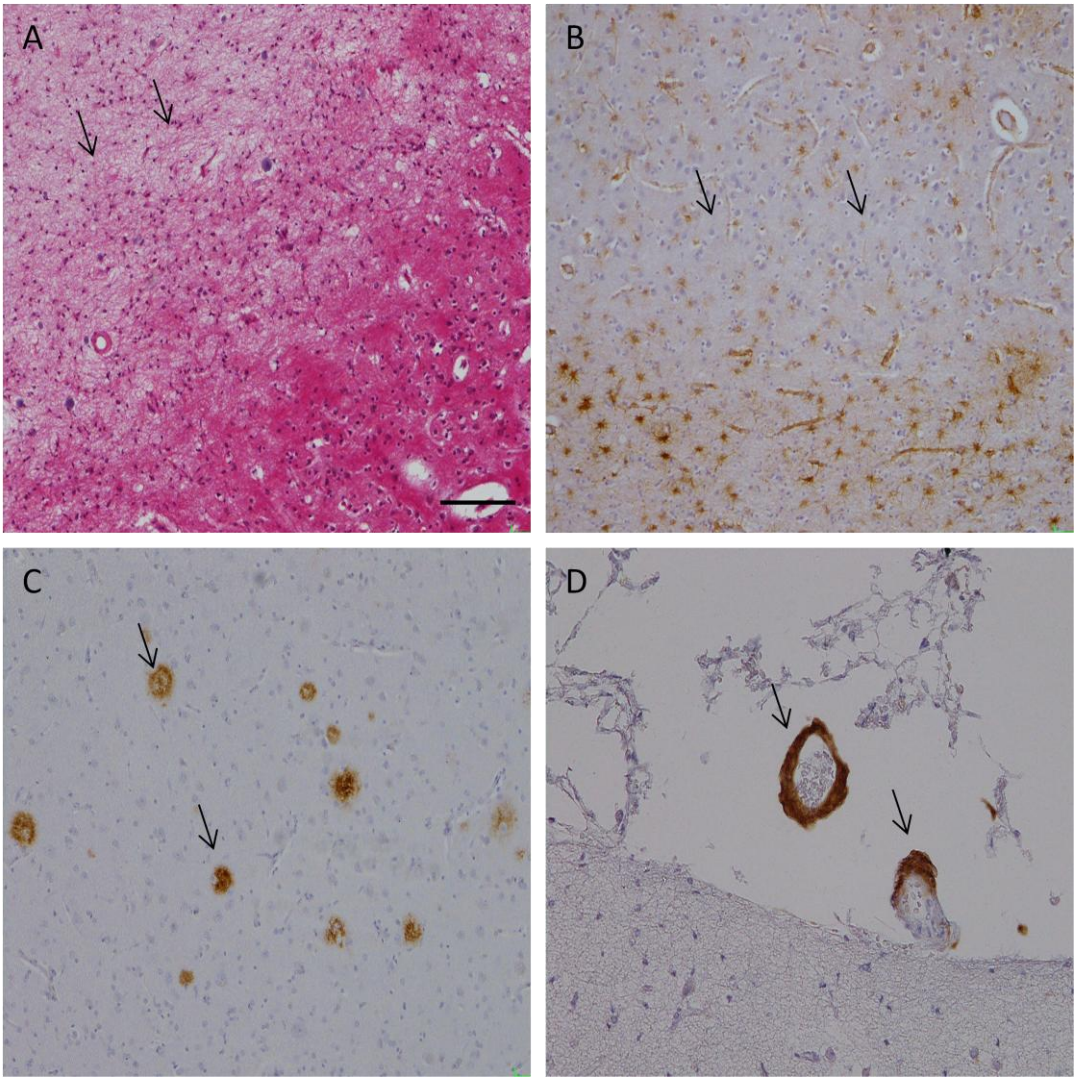

Figure 4.1 Histological findings in DYT1 cases. Neocortical regions examined and illustrated using the frontal cortex showed good preservation of neurons (A) and only mild gliosis (B). Aβ immunohistochemistry showed only sparse plaques (C) and mild cerebral amyloid angiopathy (D). Scale bar: A-C=60 µm, D=30µm. A-D represents phots from Case 4.

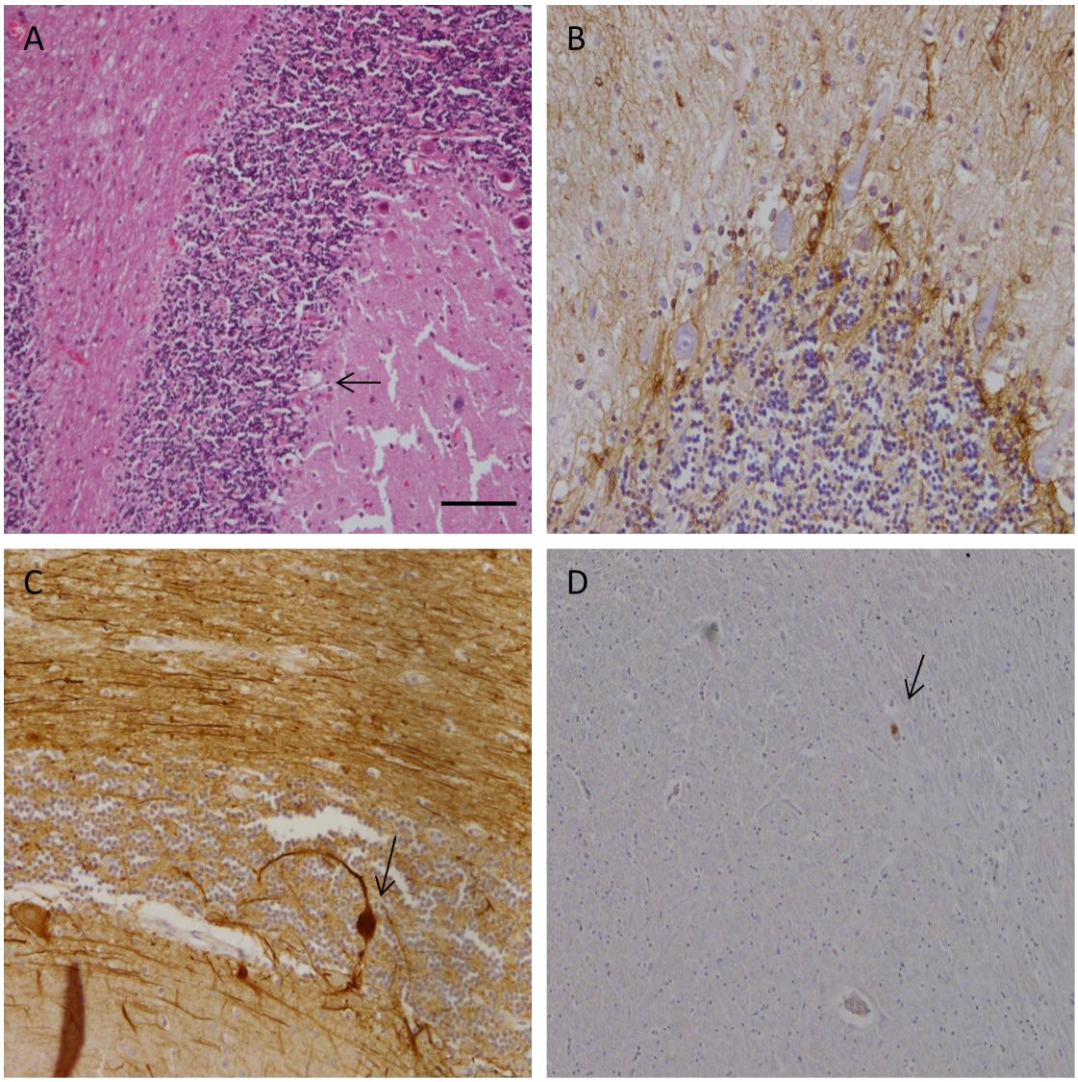

Figure 4.2 Histological findings in DYT1 cases. In the cerebellum there was mild Purkinje cell depletion (A) with associated gliosis (B) and occasional axonal swellings and torpedo bodies (C). Lewy body was observed in temporal cortex (D). A: haematoxylin and eosin; B: GFAP; C: Silver stain and D: alpha-synuclein Scale bar: A, D=60 µm, B, C=30µm. A, B and D represent photos from Case 4. C represents Case 1.

4.5. Discussion

This study provides a detailed neuropathological assessment of the largest cohort of genetically proven DYT1 cases ever evaluated. This is an important contribution as there are few neuropathological studies of genetically confirmed DYT1 mutation cases in the literature (311). I aimed to to determine whether consistent neuropathological features could be identified as a hallmark of the disease and to address the question of whether neuronal perinuclear inclusions of the type previously associated with early-onset DYT1 dystonia could be confirmed in our cohort to be a consistent disease marker (129).

I described in chapter 3 that all of the cases examined carry a 3-basepair deletion (ΔGAG) in exon 5 of the *TOR1A* gene which is a common mutation in DYT1 dystonia. Among the seven cases included in the neuropathology study, two cases (cases 3 and 5) were symptomatic and five were asymptomatic carriers for DYT1 dystonia (cases 1, 2, 4, 6, and 7). Case 3 had a clinical diagnosis of childhood onset slowly progressive dystonia and died at age of 77. Case 5 had a clinical diagnosis of dystonia and died at the age of 90. Cases 1, 2, 4, 5 and 6 were in good health for most of their lives with no chronic neurological disorder.

Neuropathological studies of dystonia are sparse, partly due to the low availability of post-mortem tissue from these patients and the labour intensive nature of the exploratory neurological examination of the entire human brain. Only a few studies have examined neuropathological abnormalities in a handful of dystonia patients, providing limited information regarding the relationship between

functional/structural brain changes and underlying neuropathology. Using a series of genetically confirmed DYT1 brains it was hoped to identifiy consistent neuropathological changes in the disease. Post-mortem human brain tissue was used to examine a number of brain regions (basal ganglia, cerebellum, dentate nucleus, locus coeruleus, frontal cortex, midbriain, substantia nigra, pons, and medulla) although not all regions were available in each case due to the retrospective nature of the study. Using a similar IHC approach to that applied in a previous neuropathological study of DYT1 dystonia (129) we were unable to replicate the finding of ubiquitin positive inclusions in the midbrain and pons with the exception of inclusions that were also immunoreactive for tau or α-synuclein, representing NFTs and Lewy bodies respectively. We also screened for intracellular inclusions in other brain regions and could not demonstrate abnormality other than Alzheimer pathology and sparse LB pathology. The remaining pathological features identified in the cases were those of gliosis, mild-moderate Purkinje cell depletion, CAA, SVD of varying severity and cerebral infarcts. None of these changes can be regarded as disease specific and are most likely to be due to the advanced age at death of the cases (75-90 years).

We examined anatomical regions implicated in dystonia and found no pathological intracellular inclusions or evidence of more than mild neuronal loss in the caudate, putamen, subthalamic nucleus, thalamus, substantia nigra and globus pallidus, other than that associated with small infarcts in the latter in two cases (316).

The reason that we failed to replicate the findings of McNaught *et al.* (129) is uncertain. With the exception of case 4 in the McNaught series, who was aged 33 years at death, the ages of our 2 case series were similar excluding the possibility that the inclusions observed are age related. One difference between the two studies is that all four cases described by McNaught *et al.* manifested clinical dystonia compared with only two cases in our series, the remaining five cases that we investigated were non-manifesting carriers of the gene mutation. If the neuronal inclusions are only present in patients with clinical dystonia this may have reduced the likelihood that we would have detected inclusions in our cases. An alternative explanation would be that different antibodies were used in the two studies and this remains a possibility. Given the limitation that only a small amount of tissue was available for study we chose ubiquitin and p62 as screening antibodies as they target abnormally folded proteins for degradation by the proteasome and autophagy respectively. As both are sensitive markers of inclusions formed from a wide variety of different proteins in neurodegenerative diseases and can recognise proteinaceous inclusions for which the principle protein component has not been identified we argued that if DYT1 dystonia is associated with intraneuronal inclusions these would be highlighted by one or both of these antibodies (317,318). Any inclusions identified could then have been further defined using other specific antibodies such as lamin A/C or torsinA and the affected neurons would have been immunophenotyped to determine whether cholinergic neurons were affected as described in the McNaught study. Assessment of cell inclusions using a reliable human specific torsinA antibody would be highly

desirable. During the study I characterized 4 different antibodies: torsinA (99,129,319), torsinA (TA913)(320), anti-torsinA (ab34540) and torsinA (santacruz s-20) using western blots, IHC and immunofluorescence (Chapter 5). However, none of these was found to be reliable and therefore hindered the further progress of this study.

Despite the limitations of this study due to its retrospective nature and the restricted tissue availability our observations support the previous findings that in primary dystonia, there is no overt neurodegeneration or cell loss (311). The pathological change of brainstem neuronal inclusions reported in DYT1 dystonia (129) was not replicated in our cohort. This study supports the hypothesis that dystonia may be a result of dysfunction of a wide variety of cellular pathways but these to not give rise to morphological changes identifiable using current methods. Hence emphasis should be placed on the need to understand the biochemical and cellular pathways involved in dystonia. In this regard, generation of cellular disease models using the induction of pluripotent stem (iPS) cells from patient skin fibroblast has opened new horizons (321,322). Understanding the cellular pathways influenced by particular mutations and the neuronal networks affected may inform future neuropathological studies.

Chapter 5. Neuropathology of DYT6 cases

5.1. Background

DYT6 dystonia is caused by the mutation in the coding region of *THAP1* (thanatos associated protein domain containing, apoptosis associated protein 1) gene (137,138). Missense, nonsense and frameshift mutations, spread throughout most of the coding portion of the gene, have all been associated with disease. Mutations in this gene have been detected in genetically diverse populations throughout the world (Chapter 1). To date, penetrance has only been measured in Amish–Mennonite families, where it appears to be ~60%, but this may not be true of all populations or mutations (139). Most mutations are found in the heterozygous state, but homozygotes are described (138,323).

THAP1 protein is thought to be involved in the regulation of transcription and hence dysregulated transcription of key genes is thought to be one of the mechanism by which *THAP1* mutations might cause dystonia. THAP1 protein is also known to interact with PAR-4, promoter region of *TOR1A/DYT1* and *TAF1/DYT3* gene.

Neuropathology of DYT6 has not been described in the literature so far. This is the first ever neuropathologcal examination carried out in two cases of DYT6 mutation human brains.

5.2. Aims and Hypothesis

Hypothesis

- The mutation and its location in *THAP1* gene influence the clinico-pathological phenotype in a DYT6 case.
- DYT6 and DYT1 dystonias are forms of primary pure dystonia, hence may share the pathology.
- The perinuclear inclusions described in brainstem for DYT1 dystonia may be true for DYT6 dystonia (129).
- The emerging role of cerebellum in dystonia will influence clinico-pathological phenotype in cerebellum.
- Description of a significant pathology in DYT6 may help in treatment of DYT6 dystonia since this is the first ever neuropathological examination carried out on DYT6 cases to date.

Aims

- Characterise neuropathology of DYT6 cases.
- Investigate clinico-genetic-pathological correlation

5.3. Methods

Two DYT6 cases were identified by genetic screening (described in Chapter 2 and 3) of the dystonia cohort. To carry out the detailed neuropathological examination, tissues for brain regions of interest were requested based on the previous studies (129,304,306,307,324). These include brainstem, midbrain, substantia nigra, frontal

cortex, motor cortex, cerebellum, dentate nucleus, pons, and medulla. However, brain regions studied were largely based on the availability of the tissue at the respective brain banks. Histological staining and and IHC methods carried out as described in detail in Chapter 2. Antibodies used for IHC include: ubiquitin (1:200, Dako, Ely,UK), tau (1:600, AT8, Autogen Bioclear, Calne, UK); AT100 (1:200, Innogenetics, Gent, Belgium), glial fibrillary acidic protein (GFAP; 1:1,000, Dako), Aβ (1:200, Dako), α-synuclein (1:50, Novacastra, Newcastle, UK), α-synuclein (1:1000, BD Transduction Biolabs, Oxford, UK), P62 (1:100, BD Bioscience, Oxford, UK), CD68 (1:150, Dako) and TDP-43 (1:2000, Protein Tech, Manchester, UK).

Neuropathological assessment

A detailed neuropathological study was carried out on both cases for the brain regions available. Semi-quantitative assessment of neuronal loss and gliosis was performed using haematoxylin and eosin staining and GFAP IHC respectively. The midbrain and pons were stained with antibodies to ubiquitin and p62 to assess the presence of intraneuronal inclusions in the periaqueductal gray matter, pedunculopontine nucleus, cuneiform nucleus and reticular formation where available (129). The Aβ cortical plaques were assessed based on CERAD criteria (304). Other concomitant pathological conditions including tau, CAA, TDP-43, α-synuclein pathology and SVD were assessed using published criteria (304,306,325–327).

5.4. Results

5.4.1. Clinical data

Table 5.1 Demographic and clinical details of DYT6 cases

Case	Sex	Ethnicity	Clinical diagnosis	DYT6 variant	Age at onset, years	Age at death, years	Cause of death
1	M	American Caucasian	Dystonia, affected	p.R29Q	17	71	Seizures
2	M	American Caucasian	Dystonia, affected	p.S21F	N/A	59	N/A

N/A: not available

Demographic and clinical data are summarized in Table 5.1.

Case 1 was a Caucasian male with onset of dystonia at the age of 17 which became severe. Later in life he developed seizures, chronic obstructive pulmonary disease and was thought to have multi-infarct dementia. Genetic testing was negative for DYT1 dystonia. He died following two seizures at the age of 71.

Case 2 was a 59 year old male with clinical diagnosis of dystonia. No further clinical details were available.

5.4.2. **Genetics**

Case 1 had a single heterozygous mutation, p.R29Q in the coding region of *THAP1*. The mutation variant is predicted to be damaging using prediction software (Mutation taster-score: 43, Polyphen -score: 0.867 and SIFT-score: 0.004). This mutation has previously been described as pathogenic in DYT6 (312,313).

Case 2 had a novel heterozygous variant p. S21F, predicted to be disease causing (Mutation taster-score: 155, Polyphen-score: 0.981 and SIFT-score: 0.01. The amino acids involved in each case are conserved across several species (Figure 5.1).

Species																																
Human	G	T	T	**T**	**C**	**T**	T	T	C	C	A	C	A	A	G	T	T	T	C	C	T	C	T	T	A	C	T	**C**	**G**	**A**	C	C	C
	-	V	-	**-**	**S**	**-**	-	F	-	-	H	-	-	K	-	-	F	-	-	P	-	-	L	-	-	T	-	**-**	**R**	**-**	-	P	-
Chimpanzee	G	T	T	**T**	**C**	**T**	T	T	C	C	A	C	A	A	G	T	T	T	C	C	T	C	T	T	A	C	T	**C**	**G**	**A**	C	C	C
	-	V	-	**-**	**S**	**-**	-	F	-	-	H	-	-	K	-	-	F	-	-	P	-	-	L	-	-	T	-	**-**	**R**	**-**	-	P	-
Gorilla	G	T	T	**T**	**C**	**T**	T	T	C	C	A	C	A	A	G	T	T	T	C	C	T	C	T	T	A	C	T	**C**	**G**	**A**	C	C	C
	-	V	-	**-**	**S**	**-**	-	F	-	-	H	-	-	K	-	-	F	-	-	P	-	-	L	-	-	T	-	**-**	**R**	**-**	-	P	-
Mouse	G	T	C	**T**	**C**	**C**	T	T	C	C	A	C	A	A	G	T	T	T	C	C	T	C	T	T	A	C	T	**C**	**G**	**C**	C	C	C
	-	V	-	**-**	**S**	**-**	-	F	-	-	H	-	-	K	-	-	F	-	-	P	-	-	L	-	-	T	-	**-**	**R**	**-**	-	P	-
Chicken	A	T	C	**T**	**C**	**T**	T	T	C	C	A	C	A	A	G	T	T	T	C	C	T	T	T	G	A	C	C	**A**	**G**	**G**	C	C	C
	-	I	-	**-**	**S**	**-**	-	F	-	-	H	-	-	K	-	-	F	-	-	P	-	-	L	-	-	T	-	**-**	**R**	**-**	-	P	-
Zebrafish	A	T	C	**T**	**C**	**C**	T	T	C	C	A	C	A	A	G	T	T	T	C	C	G	C	T	G	G	C	A	**C**	**G**	**G**	C	C	G
	-	I	-	**-**	**S**	**-**	-	F	-	-	H	-	-	K	-	-	F	-	-	P	-	-	L	-	-	A	-	**-**	**R**	**-**	-	P	-
Xenopus	A	T	C	**T**	**C**	**T**	T	T	T	C	A	C	A	A	G	T	T	T	C	C	C	C	T	T	A	A	A	**C**	**G**	**C**	C	C	G
	-	I	-	**-**	**S**	**-**	-	F	-	-	H	-	-	K	-	-	F	-	-	P	-	-	L	-	-	K	-	**-**	**R**	**-**	-	P	-

Figure 5.1 Mutations in *THAP1* gene considered in this study. Diagram showing conservation of the amino acids and the nucleotides of concern across different species in exon 1 of *THAP1,* c. 62C>T/ p. S21F and in exon 2 of *THAP1,* c. 86G>A / p. R29Q (the affected bases and codons are shown in boldface and red, respectively).

5.4.3. **Neuropathological assessment**

A summary of the pathological findings is given in Table 5.2 with details of the regional histological assessment provided in Table 5.3.

Macroscopic findings

Macroscopic findings were derived from the report provided by the BTDBB for case 1 and by direct observation of the brain slices provided for case 2. In case 1 mild to moderate generalised cerebral atrophy was described. The blood vessels of circle of Willis showed moderate atherosclerosis with no vascular anomalies. The cortical ribbon was of slightly reduced thickness and the hippocampal formation was mildly atrophic. Patchy areas of acute ischemia were observed in the deep gray matter structures but there was no evidence of established vascular lesions.

Case 2 showed no macroscopic abnormalities. The cortical ribbon, caudate, putamen, thalamus, subthalamic nucleus, globus pallidus, hippocampus, cerebellum, pons and medulla were all unremarkable. There were no focal lesions and no brain atrophy was observed.

Histology

In case 1 the cortex, cerebellum, dentate nucleus, basal ganglia, substantia nigra and medulla were well preserved with no detectable neuronal loss with the exception of mild Purkinje cell depletion. There was mild to moderate gliosis in several brain regions (Figure 5.2). Aβ deposits were most frequent in the frontal

cortex where there were frequent diffuse and sparse mature plaques. There was also mild cerebral amyloid angiopathy. Tau pathology of Alzheimer type (neurofibrillary tangles, neuropil threads and abnormal neurites) was mild in the temporal cortex but was not observed in subcortical regions. Formal analysis of the Aβ Thal phase and Braak and Braak tau staging was not possible due to the limited regions available for examination. There was no α-synuclein pathology in the form of either Lewy bodies or glial cytoplasmic inclusions and no TDP-43 immunoreactive inclusions were found. There was mild small vessel disease but no further evidence of vascular lesions. We sought to identify pathological neuronal cytoplasmic inclusions in the midbrain and pons as described previously in DYT1 dystonia cases using ubiquitin and p62 IHC, however, such inclusions were not identified.

In case 2 no neuronal loss was observed expect for mild loss of pigmented neurons in the substantia nigra and mild Purkinje cell depletion. Gliosis was restricted to the cerebellar cortex where it was of mild degree. Alzheimer pathology in the form of cortical Aβ deposition was observed in the parietal cortex where there were sparse diffuse deposits. There was moderate cerebral amyloid angiopathy in the parietal lobe. No tau immunoreactive inclusions were found in any region. Careful examination of the midbrain and pons showed no p62 or ubiquitin labelled neuronal cytoplasmic inclusions. No α-synuclein or TDP-43 pathology was found and there was no evidence of small vessel disease.

Table 5.2 Summary of neuropathological findings in DYT6 cases

Case	***Macroscopic features***	***Aβ***		***Tau***	***Lewy body***	***SVD***	***CAA***	***TDP-43***
		D	*M*					
1	Mild-moderate cerebral atrophy* Mild cortical and hippocampal atrophy* Patchy acute ischemic lesions *	+++	+	+	-	+	+	-
2	No abnormalities*	+	+	-	-	-	++	-

- = absent; + = mild; ++ = moderate; +++ = severe; SVD- Small vessel disease ; CAA- *Cerebral amyloid angiopathy*; D-diffuse, M-mature; *: Derived from neuropathology report issued by BTDBB for case 1 and QSBB for case 2

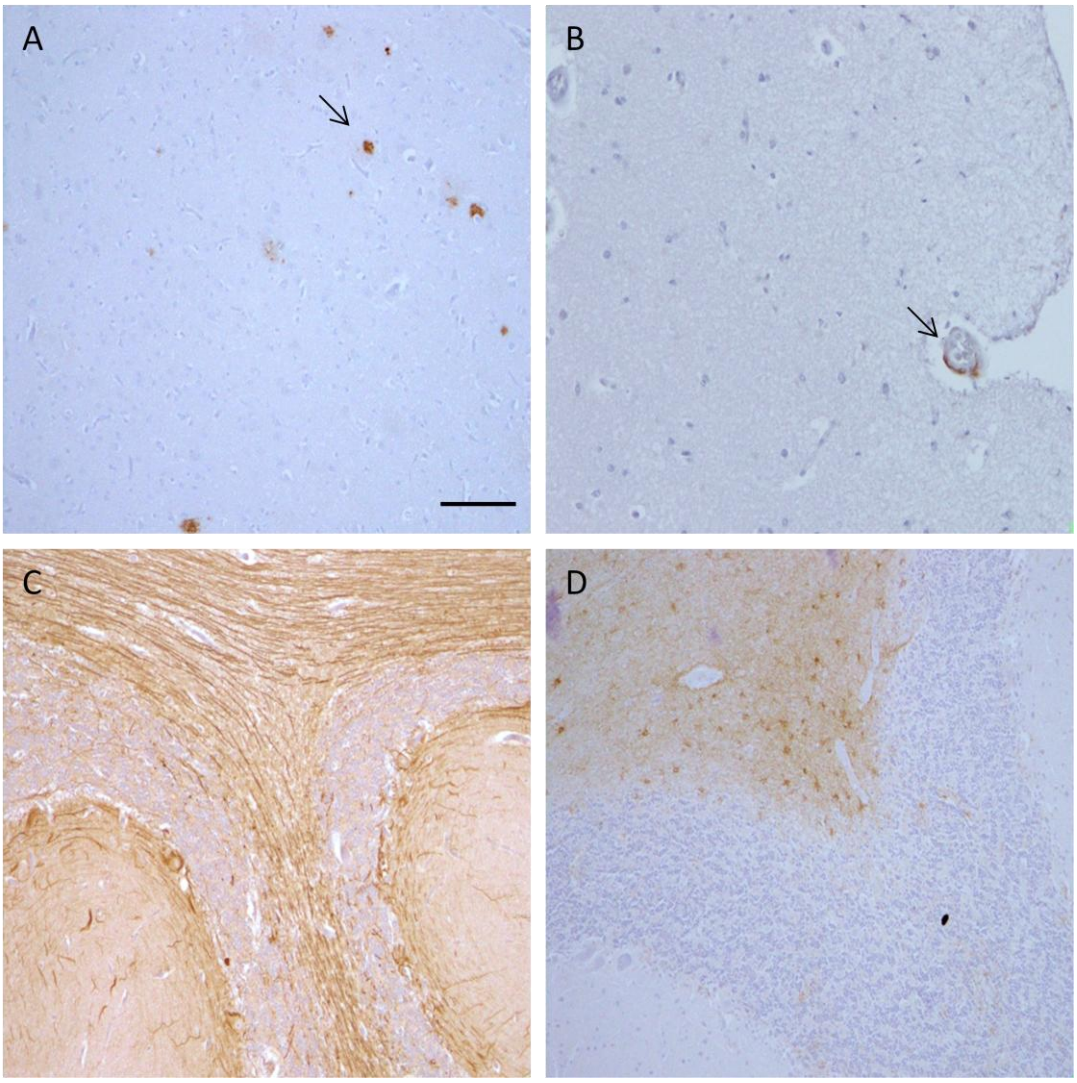

Figure 5.2 Histological findings in DYT6 cases. Sparse mature and frequent diffuse plaques were observed in frontal cortex (A) with moderate cerebral amyloid angiopathy in the parietal lobe (B). In the cerebellum there was mild Purkinje cell depletion and associated gliosis (C). Mild cortical gliosis was observed in cerebellum (D). A and B: Aβ IHC; C: alpha-internexin and D: GFAP. A=20, B=50, C and D=60 µm, A-B represent photos from Case 1 and C-D represents Case 2.

Table 5.3: Semi-quantitative summary of neuropathological changes in DYT6 cases

Regions	Case 1								Case 2							
	Neuronal loss	**Gliosis**	**Aβ**		**Lewy bodies**	**Tau**	**CAA**	**TDP43**	**Neuronal loss**	**Gliosis**	**Aβ**		**Lewy bodies**	**Tau**	**CAA**	**TDP43**
			D	M							D	M				
Cortex																
Frontal	-	+	+++	+	-	-	+	N/P	-	-	N/P	N/P	N/P	N/P	N/P	N/P
Motor	N/A	N/A	N/A		N/A	N/A	N/A	N/A	-	-	N/P		N/P	N/P	N/P	N/P
Temporal	-	+	+	-	-	+	+	N/P	-	-	-	-	N/P	-	N/P	N/P
Parietal	N/A	N/A	N/A		N/A	N/A	N/A	N/A	-	-	+	-		-	++	N/P
Hippocampal formation	N/A	N/A	N/A		N/A	N/A	N/A	N/A	-	-	N/P		-	-	N/P	N/P
Caudate	-	-	N/P		N/P	-	N/P	-	-	-	N/P		N/P	-	N/P	-
Putamen	-	+	N/P		N/P	-	N/P	-	-	-	N/P		N/P	-	N/P	-
Globus pallidus	-	+	N/P		N/P	-	N/P	-	-	-	N/P		N/P	-	N/P	-
Thalamus	N/A	N/A	N/A		N/A	N/A	N/A	N/A	-	-	N/P		N/P	-	N/P	N/P
Subthalamic nucleus	N/A	N/A	N/A		N/A	N/A	N/A	N/A	-	-	N/P		-	-	N/P	N/P
Substantia nigra	N/A	N/A	N/A		N/A	N/A	N/A	N/A	+	-	-		-	-	N/P	N/P
Locus coeruleus	N/A	N/A	N/A		N/A	N/A	N/A	N/A	-	-	N/P		-	N/P	N/P	N/P
Pontine nuclei	N/A	N/A	N/A		N/A	N/A	N/A	N/A	-	-	N/P		-	N/P	N/P	N/P
Dorsal motor nucleus of vagus	-	++	N/P		-	-	N/P	N/P	N/A	N/A	N/A		N/A	N/A	N/A	N/A
Twelfth nerve nucleus	-	++	N/P		-	-	N/P	N/P	-	-	N/P		-	N/P	N/P	N/P
Inferior olive	-	++	N/P		-	-	N/P	N/P	-	-	N/P		-	N/P	N/P	N/P
Cerebellar Purkinje cells	+	+	N/P		N/P	-	N/P	N/P	+	+	N/P		N/P	-	N/P	N/P
Dentate nucleus	-	+	N/P		N/P	-	N/P	N/P	-	-	N/P		N/P	-	N/P	N/P

Key: - = absent; + = mild; ++ = moderate; +++ = severe; D: diffuse plaques; M: mature plaques; N/A: not available; N/P: not performed; CAA: cerebral amyloid angiopathy

5.5. Discussion

The molecular genetics of primary dystonia syndromes have been the object of extensive analysis and a number of genes associated with autosomal dominant inheritance have now been identified. Despite these genetic advances which shed light on the disease pathogenesis there are few neuropathological descriptions of isolated dystonia in the literature and the neuropathology of DYT6 has not previously been described. In this study we undertook detailed neuropathological assessment of two DYT6 cases with confirmed *THPA1* mutations and could find no disease specific morphological abnormalities.

Both cases had missense mutations in the THAP1 domain of *THAP1* resulting in different amino acid changes, p. R29Q (312,313) and a novel mutation p. S21F respectively. In the latter case, a pathogenic mutation in this codon due to a different nucleotide change has previously been reported (159). The heterogeneity in the clinical spectrum of DYT6 dystonia is growing owing to the number of *THAP1* mutations reported in literature since the gene discovery. This has made it difficult to establish a genotype-phenotype correlation in terms of clinical phenotypes reported for each DYT6 case in literature. However, functional studies were more successful in demonstrating the mutation effect. Mutations in the THAP1 domain are thought to interrupt DNA binding causing transcriptional dysregulation of THAP1 target genes (328). A functional study on a THAP1 case with a frameshift mutation in NLS region of *THAP1* demonstrated impaired nuclear import of mutant THAP1 *in vitro*(329)*;* THAP1 is reported to interact with the promoters of *TOR1A*

(148) and *TAF1*, implicated in DYT3 dystonia (156) and recently THAP1 has been reported to autoregulate its own expression (330). Hence, studies of biochemical and cellular mechanisms may provide a link to abnormal motor control in DYT6 dystonia.

Our neuropathological investigation of these DYT6 cases utilised a similar immunohistochemical approach to that previously applied in *DYT1*-related dystonia cases (129) and adult-onset dystonia cases (125) with the specific aim of determining whether brainstem neuronal cytoplasmic inclusions are a common hallmark of isolated dystonias. We were unable to identify such inclusions in our study and, indeed, we found no neuropathological features that could be regarded as specific to dystonia in either case(129). As basal ganglia dysfunction gives rise to dystonia we examined these regions in detail but no significant pathological changes were found. Neurodegenerative diseases such as Parkinson's disease, progressive supranuclear palsy and corticobasal degeneration, which may sometimes present with dystonic symptoms, were excluded by detailed neuropathologic examination.

This study adds further evidence that morphological abnormalities detectable using current neuropathological techniques are not features of isolated dystonias and indicate that future advances in our understanding of the pathogenesis of group of diseases is more likely to come from biochemical and molecular biology studies. In this context, iPS cells may provide a good understanding of the cellular pathways and biochemical activities of the gene /protein under consideration. However, it

may be challenging to apply the results of such studies in a controlled setting to the clinical diseases.

5.6. Antibody optimization

5.6.1. Problem

The problems with the commercial antibodies is not unheard of (331). The quality control has been of utmost importance since we are in the era of off-the-shelf molecular and cellular biology. The list of commercially available antibodies for the protein of interest is long. However, the process of optimising any antibody to specifically detect your protein of interest within the correct conditions is arduous and frequently unsuccessful.

Primary dystonia genes, *TOR1A* and *THAP1* were known since 1997 and 2007 respectively. However, good quality antibodies which are human specific for respective genes are difficult to obtain. This is partly due to the unavailability of brain tissues of interest to carry out tests by respective companies and as well, these proteins are poorly characterized.

Four different TOR1A antibodies were tested: rabbit polyclonal *TOR1A* (ab34540), mouse monoclonal *TOR1A* (sc-373915), rabbit monoclonal *TOR1A* (kindly given to brainbank in 2007), rabbit polyclonal *TOR1A* (TA913 kindly given by Dr Angrez lab). For *THAP1*, a rabbit polyclonal *THAP1* (Proteintech) was tested.

Optimization conditions for IHC included:

- Different primary antibodies as listed above
- Different blocking solution: 1% and 10% milk, 5% BSA
- Different pre-treatments: formic acid/citrate buffer /proteinease k
- Different primary antibody incubation period: overnight/ an hour
- Different primary antibody dilutions: 1:10, 1:100, 1:500, 1:800, 1:1000, 1:5000
- Different staining material: frozen / paraffin embedded brain tissues
- Different species: human / mouse
- Other variations : tissues from control and affected individuals

Optimization for Immunoflourescence included

- Different paraffin embedded tissues : mouse / human
- Different secondary antibodies: goat / mouse /rabbit

Optimization for Western blot included

- Different species lysates: human, mouse, neuroblastoma cells
- Different primary antibody concentration: 1:100, 1:500, 1:800, 1:1000
- Different blocking solution : 1% milk, 5% BSA

5.6.2. **Results**

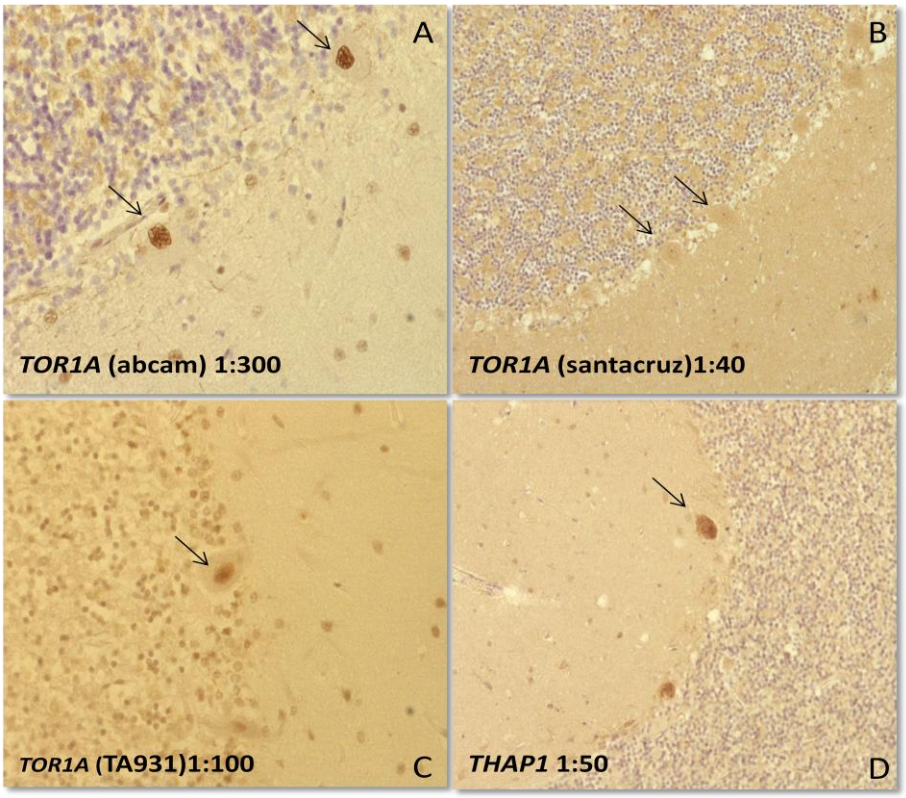

Figure 5.3 Immunohistochemical optimization of the TOR1A and THAP1 antibodies in normal human controls. Panel A, B and C represents three different TOR1A antibodies tested in this study. Each of the antibodies gave high background and stained whole of the nucleus (shown by arrows). Panel D represents THAP1 antibody tested.

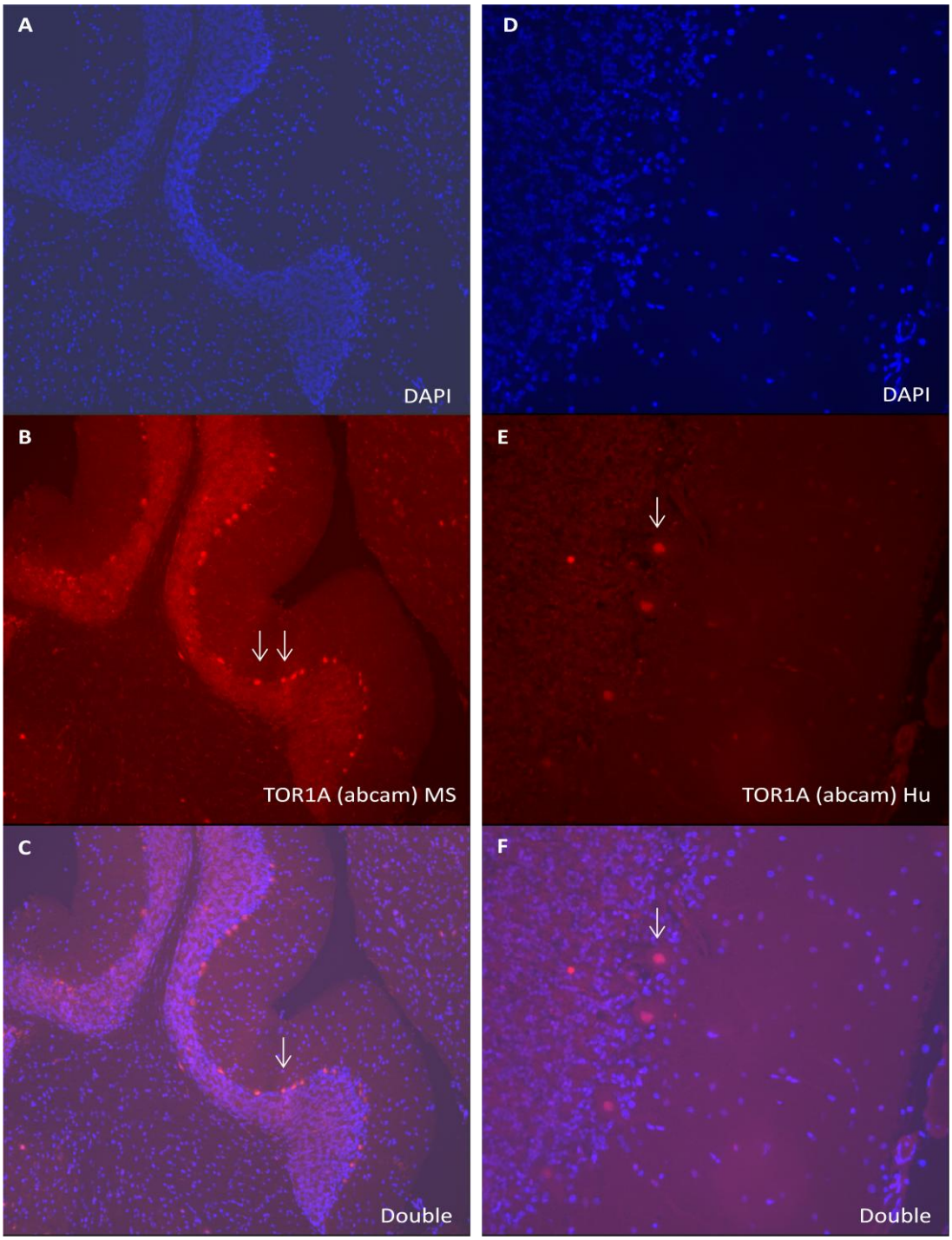

Figure 5.4 Immunofluorescence staining of TOR1A antibody in wildtype mouse (left panel) and human (right panel) paraffin-fixed tissues. Staining is with high background and the whole nucleus is stained making it difficult to localise the nuclear protein. Arrows showing stained nucleus.

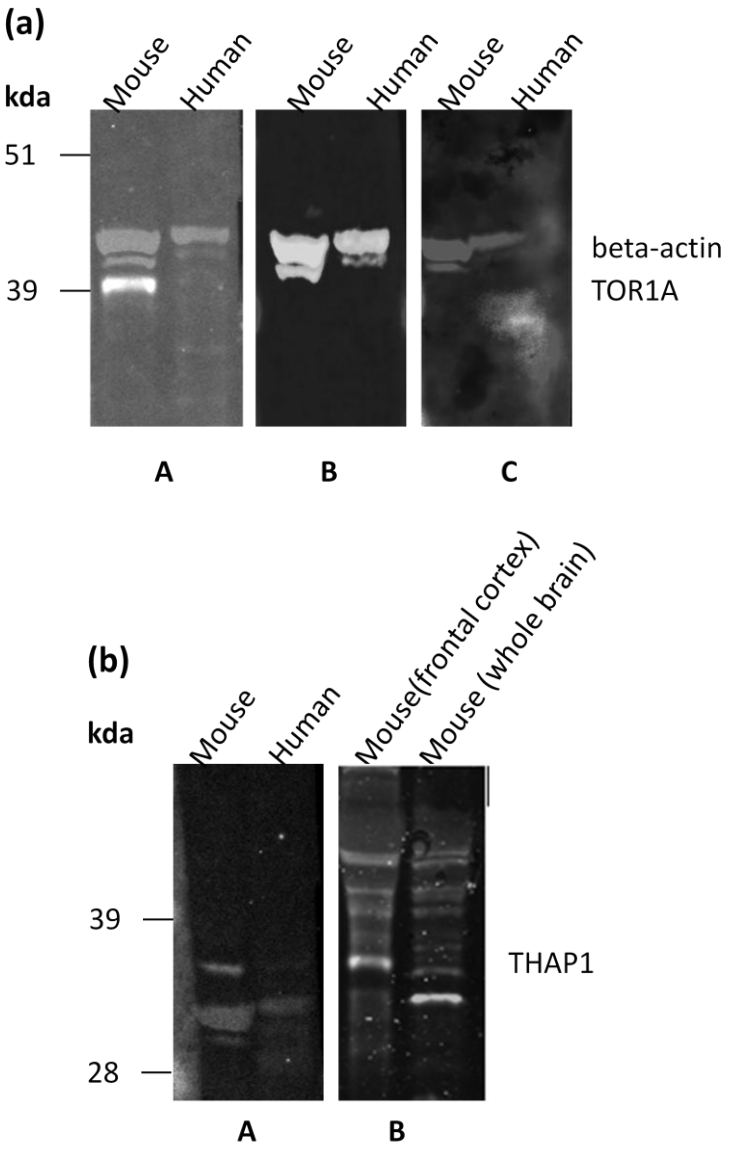

Figure 5.5 Antibody optimization. (a) represents western blots of three TOR1A antibodies for human and mouse lysates (a) TOR1a (abcam) showed TOR1A band at about 38kda in mouse but not in human (B) TOR1A (santacruz) did not show specific band (C) TOR1A-TA193 showed a fuzzy band for human but not for mouse. (b) represents western blots for a THAP1 antibody tested where bands were observed at various sizes in mouse lysate but did not work with human brain lysate.

The non-specific staining in both IHC and IF were observed (Figure 5.3). By WB, non-specific bands were observed in human brain lysates, however specific bands at the predicted molecular weight of THAP1 (25kda) and TOR1A (38kda) were detected in both mouse and cell lysates. The presence of non-specific bands in WB and a high background in IHC and IF for human brain samples meant that we could not be confident that any staining which we were detecting by IHC was specific and thus was the reason to stop pursuing staining using the above antibodies in our cohort.

5.6.3. **Discussion**

The use of IHC is ubiquitous in neuroscience. A list of antibodies for the protein of interest is available commercially. Antibodies that work are extremely valuable research tools. However, the search for such antibodies is made quite difficult by two different problems; the good antibody problem, the bad technique problem.

Despite cellular studies on torsinA and THAP1 proteins the exact function of the protein is still unknown. Also there is mismatched information on whether torsinA is nuclear or cytoplasmic protein which makes it difficult to test our hypothesis on humans in the IHC studies. Published reports which used *TOR1A* antibodies for immunofluorescence did not use human samples, further published reports which used the THAP1 antibodies used neither human or cellular samples. Hence, the first problem, “the good antibody problem” is that production of a good antibody is a difficult and a time consuming process and many researchers may not possess the skill necessary to make good antibodies or the time to make project specific

antibodies. During project conception, only one *THAP1* antibody was available commercially which is tested here. The commercial antibodies available for torsinA and THAP1 are not tested on humans due to the unavailability of the affected/control human brains though are predicted to work on human. The IHC studies on human *TOR1A* cases published used their own lab-specific *TOR1A* antibodies. Two of these antibodies were kindly given to us to use in this project. Hence, the second problem, "the bad technique problem" is that a good antibody may not "work" in all of the various antibody-based assays. This may occur because the antibody cannot detect its target in a particular type of assay (e.g. the antibody target may become denatured in formalin fixation, thus formalin fixation is a bad technique for this antibody). Alternatively, incorrect technique (or a bad technique) in an assay may interfere with the antibody binding to its target. Also, lot to lot variation in antibodies may alter protein conformation in different regions, expression below the level of detection. Also sometimes it is hard to replicate findings from other groups as they may use subtly different techniques which they do not fully describe in their papers.

Antibody characterization is the first step in any scientific projects. We ran WB with several protocol variations to characterize the protein of interest. TOR1A and THAP1 proteins are expected at of 38kda and 25kda, respectively. However, several nonspecific bands were observed and after running several WBs we were unable reach to a reasonable level of assurance that an antibody is actually recognizing what it is supposed to. However, the same antibodies, *TOR1A* (abcam) and *TOR1A*

(santacruz) provide an acceptable level of assurance with mouse brain tissue. Same is the case with THAP1 antibody. TA913 antibody is lab specific and is published as recognizing human TOR1A only (320). The WB result assured us as well as it did not recognize mouse but human TOR1A. However, this batch of antibody was not affinity purified and did not produce a strong band. Affinity purified TA913 was out of stock.

In parallel, variations in IHC and IF were carried out on fresh and fixed tissues of human and wild type mouse. High background caused by both non-specific staining and by non-specific secondary antibody binding made it difficult to describe the expression pattern of proteins in both human and mouse tissues.

The possible problem with the antibodies tested above is that they are likely to cross react with a number of different homologous proteins. For example, torsinB has 80% homology with torsinA and is reported to colocalise in humans CNS (100). Both proteins showed cytoplasmic distribution but torsinB was also perinuclear in some neurons. After several communications with the company the immunogen sequence was available for TOR1A (abcam): CKTVFTKLDYYLDD. NCBI BLAST of the immunogen sequence showed no significant homology to other torsin family members, including TOR1B. However, sequence alignment of the orthologs showed it was not exact match for human (highlighted region in the alignment below). Hence the lack of exact match of the immunogen sequence may be one of the reasons for the problems we have faced with the antibody.

The exact immunogen sequence for TorsinA (santacruz) was not available. However, the datasheet provides information on cross reaction to lesser extent with TorsinB. This explanation does not help much for researchers as the lab data provided in the datasheet showed no trace of torsinB in WB.

Orthologs	Immunogen sequence (319-332aa)
Human	CKTVFTKLDYYYDD
Mouse	CKTVFTKLDYYLDD
Rat	CKTVFTKLDYYLDD
Monkeys	CKTVFTKLDYYYDD

Figure 5.6 Alingment of the orthologs for the immunogen in TOR1A antibody (abcam).

Hence, the integrity of this neuropathological study was being threatened by the proliferation of poorly characterized antibodies that produce artifactual staining pattern.

5.7. DYT6 and DYT1 interaction

5.7.1. Background

In vitro studies have shown that *THAP1* physically interacts with *TOR1A* and represses torsinA expression by binding to the *TOR1A* promoter; this interaction is abolished by pathogenic mutations, leading to a decreased repression (149). However, this effect was not observed in fibroblasts from DYT1 patients. Thus it was likely that the interaction is possible in CNS only.

5.7.2. Aims and Hypothesis

Hypothesis

- There is a direct interaction between causative genes of DYT1 and DYT6 primary dystonia
- The dystonia gene *TOR1A* is repressed by the transcription factor THAP1
- The THAP1-TOR1A interaction is restricted to CNS in humans

Aims

- To obtain frozen brain tissues for brain regions of interest
- Define interaction using qPCR

5.7.3. Results

A total of 6 DYT1, 2 DYT6 and 5 control cases were included in this study. These cases were genetically confirmed for the mutations in *DYT1* and *DYT6* genes. In DYT1 cohort, all the cases have p.303-/Glu304 mutation in *TOR1A/DYT1* gene. Two cases included in DYT6 cohort have p.Arg29Gln and p.Ser21Phe mutations in *THAP1/DYT6* gene respectively and both are in zinc-dependent THAP domain (1-81 amino acids) of the THAP1 protein.

To validate the efficiency of the primers and qPCR reaction standard curve was generated. Keeping in consideration that there is no best match, primers for genes of interest (*TOR1A, THAP1*), and housekeeping genes (*GAPDH, ACTB, RPLP0, UBC*) were chosen to take forward as their efficiency matched to an agreeable level.

To determine whether THAP1 modulates TOR1A expression or vice-versa in human, we analysed *TOR1A* mRNA and *THAP1* mRNA levels in 6 DYT1 cases, 2 DYT6 cases,

normalised against 5 controls in brain regions. The availability of the brain regions vary in each case. Brain regions sampled for was based on the previous study and included cerebellum (Cbl), frontal cortex (Ftx), superior temporal gyrus (Gyrus), basal ganglia (BG), midbrain (MB), global pallidus (GP), putamen (Pu), caudate (Cau), pons, medulla (Med) and hippocampus (Hip). Brain regions included in the study was also based on the brain regions available for research for each case. Cases were normalized using reference genes (*GAPDH, ACTB, RPLP0, UBC*) and calibrated against age and sex matched healthy controls (calibrator).

Table 5.4 Student's t-test (p<0.05), p values to compare the difference in expression of TOR1A and THAP1 in each brain regions of DYT1 and DYT6 cohorts

Brain regions	**p values TOR1A vs THAP1 (Statistical significant p value defined as < 0.05)**	
	DYT1 cohort	**DYT6 cohort**
Frontal cortex	0.58	0.59
Superior temporal gyrus	0.13	0.19
Global pallidus	0.65	0.65
Putamen	0.19	0.023
Cerebellum w/dentate nuc.	0.82	0.64
Midbrain/S. Nigra	0.26	0.8
Medulla	0.6	0.12

Normalised expression of *TOR1A* and *THAP1* is ubiquitous in brain regions studied in controls, DYT1 and DYT6 cases (Figure 3.2). In controls, expression level of *TOR1A* is higher than *THAP1* in the brain regions studied. Expression of these two genes is lower in the DYT1 and DYT6 cases compared to controls except in few brain regions. Student's t-test revealed a significant difference in *TOR1A* and *THAP1* expression in putamen (0.023, p<0.05) of DYT6 cohort only. No significant difference in expression of the two genes was observed in other brain regions

studied in both cohorts. No significant pattern of *THAP1* and *TOR1A* was observed in both cohorts.

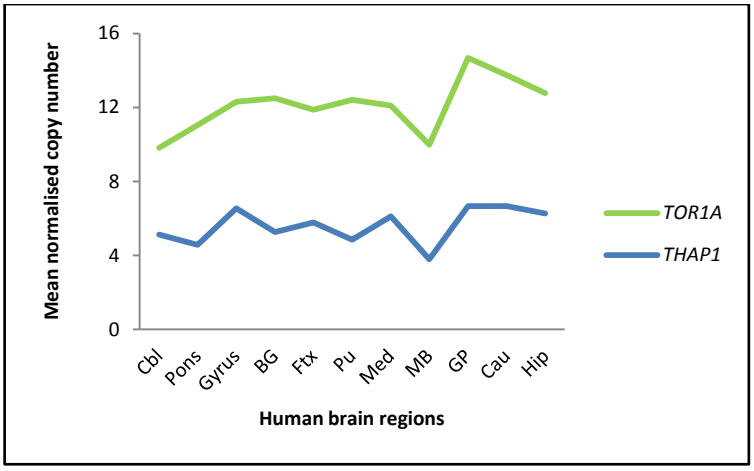

Figure 5.7 Mean normalized copy number of *THAP1* and *TOR1A* gene expression in controls.

In DYT6 case 1 and 2, THAP1 expression is lower compared to controls in the brain regions studied but expression was higher than in controls in globus pallidus and cerebellum of case 1. In both DYT6 cases, there is a marked increase in *TOR1A* expression in putamen compared to the controls. However similar pattern of genes expression was observed in an asymptomatic DYT1 case (case 6). Hence, it is difficult to conclude that the interaction is centered in putamen of DYT6 cohort. A 3bp mutation in *TOR1A* is described as a loss of function. Our data suggests that though loss of function, *TOR1A* expression is higher than normal in some CNS regions; globus pallidus, midbrain, pons, putamen. The lack of a consistent pattern of expression of these genes makes it difficult to pinpoint a region for interaction and thus supports the heterogeneity observed in primary dystonia.

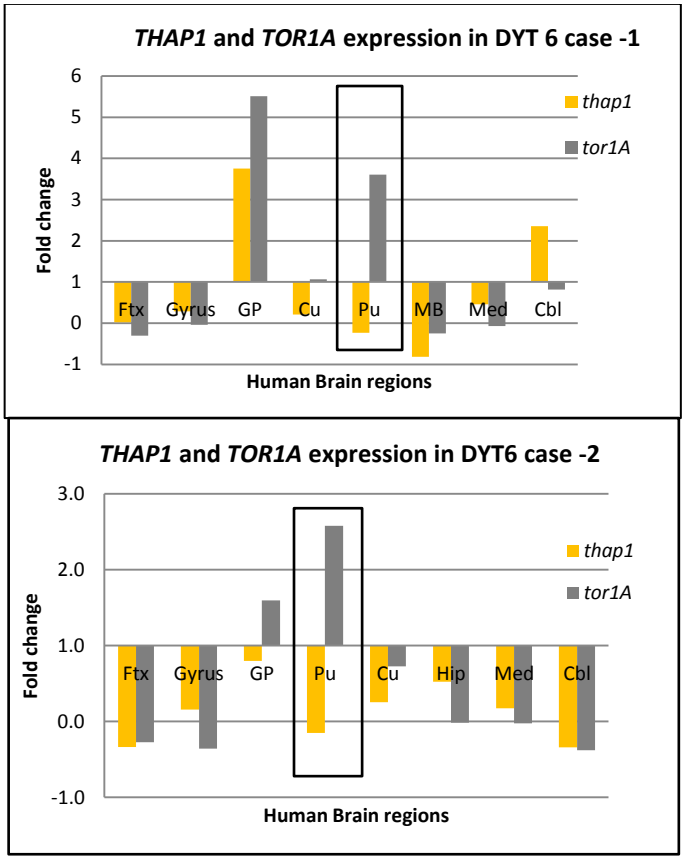

Figure 5.8 THAP1 and *TOR1A* expression in DYT6 patients. In putamen of both cases with decrease in expression of THAP1, there is a marked increase in expression of TOR1A. Student's t-test reveals a significant difference in expression compared to the controls (0.023, $p<0.05$).

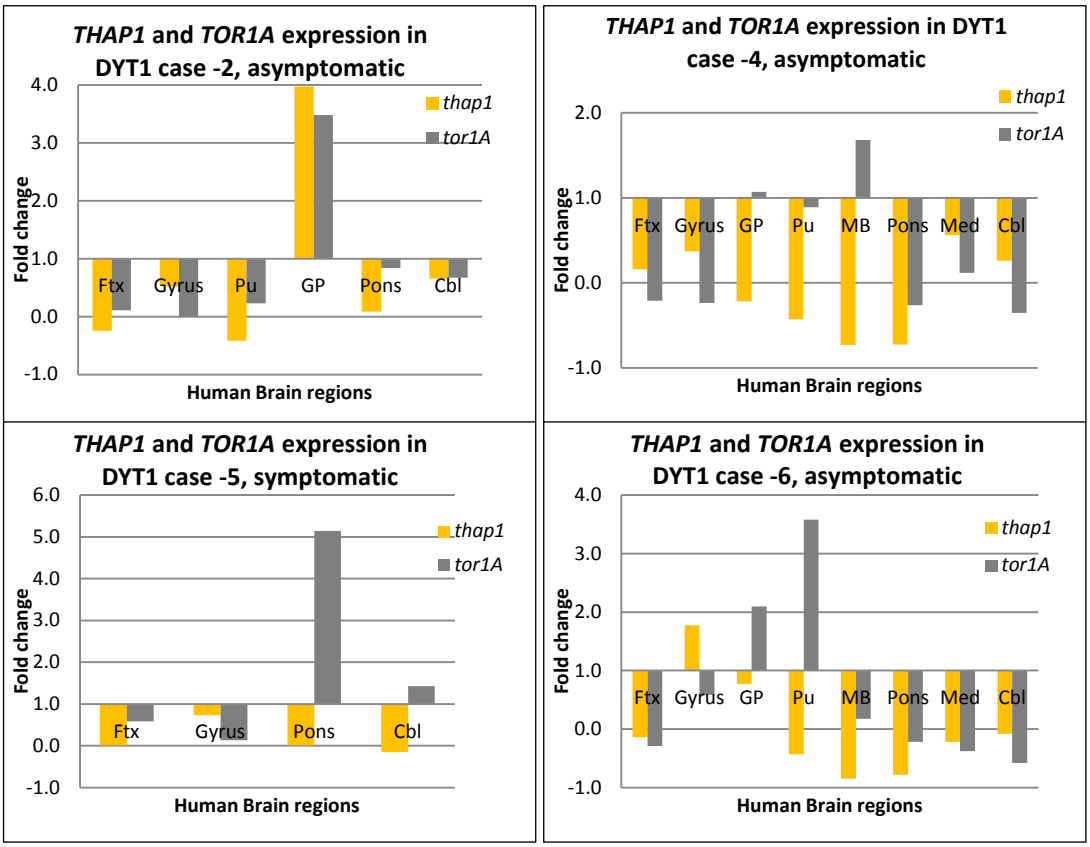

Figure 5.9 *THAP1* and *TOR1A* expression in DYT1 and DYT6 patients. The expression pattern doesnot follow a consistent pattern.

5.7.4. **Discussion**

The low penetrance of *THAP1* and *TOR1A* mutations has often been related to the phenotypic heterogeneity of the primary pure dystonia. A possible role of *THAP1* as a genetic modifier in DYT1 dystonia has been recently suggested as THAP1 was shown to bind to TOR1A promoter (148) and repress transcription of torsin A (149). The functional link between the two gene products suggesting the mechanism of transcriptional dysregulation as a cause of primary dystonia provided a breakthrough in understanding the primary pure dystonia. However, both studies failed to show the effect *in vivo* and the TOR1A modification was moderate *in vitro*. Genetic screening of the sequence variations in the *THAP1* gene and also the THAP1-binding sites of the TOR1A-promoter questioned the *THAP1* as a genetic modifier of DYT1 dystonia (332).

Our study aimed to address the possibility that dystonia being a CNS disorder, THAP1-TOR1A interaction may be centered within specific regions in CNS. *TOR1A* and *THAP1* gene expression is ubiquitous in the brain regions included in this study (Figure 1.5, Figure 1.6). Our results suggested a significant difference in expression of *THAP1* and *TOR1A* in putamen of DYT6 cohort, normalised against the healthy controls.

The basal ganglia traditionally have been implicated in human dystonia by studies showing correlations between dystonia and imaging or pathological evidence for basal ganglia dysfunction. The basal ganglia and especially the putamen are most frequently implicated among patients with dystonia and overt lesions in structural

imaging studies (35,36,333). Even when overt lesions cannot be identified, functional imaging studies such as fMRI or PET often reveal areas of abnormal activity in the basal ganglia for many types of dystonia (39,334). In primates, focal destructive lesions of the posterior putamen has been reported to cause dystonia (59). In putamen of the two DYT6 cases, there is a marked increase in *TOR1A* expression when *THAP1* expression decreased, compared to the control. This data matches the previous finding that *THAP1* may act as a repressor. In DYT6 cases, when *THAP1* is mutated, *TOR1A* is excessively expressed. However, similar pattern of *THAP1* and *TOR1A* expression was also observed in a DYT1 asymptomatic case (case 6). Hence, a possibility that *THAP1* not only represses *TOR1A* but a similar effect vice-versa is also possible. However, lack of a significant pattern among all the DYT1 cases makes it difficult to draw a conclusion. Another possibility is that a third modifier is necessary to make the effect pathogenic.

THAP1 has been shown to bind to the promoter region of a *TAF1* transcript (156). *TAF1* gene has been linked to another form of primary dystonia (adult onset X-linked dystonia parkinsonism) which is clinically very different (335,336). Hence it will be interesting to see if *THAP1* and *TAF1* gene show any potential functional link to associate with the clinical phenotype presented for each dystonia type.

Our data suggest a possible link between *THAP1* and *TOR1A* in putamen of DYT6 cohort and a possible role of *THAP1* gene as a repressor. However, similar pattern was observed in a DYT1 case, asymptomatic. There was no specific expression pattern of *THAP1* and *TOR1A* genes in the brain regions studied. Hence, it is difficult

to pinpoint putamen as a brain region for *THAP1* and *TOR1A* interaction and if repression is a feature of *THAP1* gene. Furthermore, a better understanding of *THAP1* and *TOR1A* protein function and cellular pathogenicity may address the interaction more precisely.

Chapter 6. Genetics of Primary plus dystonia, Dopa-responsive dystonia (DYT5)

6.1. Background

Mutations in the *GCH1* gene are associated with childhood onset, autosomal dominant hereditary DRD (170). Correct diagnosis of DRD is crucial, given the potential for complete recovery once treated with L-dopa. The majority of DRD associated mutations lie within the coding region of the *GCH1* gene, but three additional single nucleotide sequence substitutions have been reported within the 5' untranslated (5'UTR) region of the mRNA. One subject had 2 mutations, -39C>T and -132C>T and another had a single mutation, -22 C>T. One family of Irish/French-Canadian ethnicity with DRD was studied where -22 C>T mutation segregate in the family with disease affected status (181,186). This makes it likely that the -22 C>T mutation is pathogenic and results in DRD.

6.2. Methods

Sanger sequencing was carried out as described in Chapter 2 for the coding regions and the 5'UTR of the *GCH1* gene.

6.3. Aims and Hypothesis

Hypothesis

- Noncoding mutations in the 5' upstream region of *GCH1* gene are pathogenic in DYT5 dystonia
- Coding and noncoding mutations in *GCH1* gene may be observed in primary torsion dystonia due to some shared clinical phenotype

Aims

- To obtain DNA from DRD cases with no mutations reported in coding regions of the *GCH1* gene
- Screen dystonia cohort (described in chapter 2) for the coding and noncoding mutations in *GCH1* gene.
- Investigate the clinico-genetic correlation

6.4. Results

Of the total 192 clinically diagnosed DRD cases negative for mutations in the coding regions of *GCH1* gene, two noncoding point mutations, -39C>T and -132C>T were observed in the 5' UTR region. Both mutations were present in each of the cases.

Case 1 is a 21 year old Portuguese male clinically presenting as a recessive hereditary spastic paraplegia. He had mild disability during primary school and slowly progressed. At age of 15 he developed gait disturbance and became more forgetful. MR brain scan showed patchy signal change in the subcortical white matter with atrophy of the corpus callosum. He had very mild ptosis but also slight

exophthalmos. He had severe spasticity in both lower limbs but no weakness. There was no dystonia. He has an elder brother who is affected but his parents are well and not related. The elder brother had a partial transient response to levodopa.

Case 2 is a 25 year old Tunisian female. At the age of three weaknesses, unsteadiness and walking difficulties in both legs were noticed and progressed slowly. By the age of 14 her right arm became more affected than the left, her back was sore and tilted to the left. Over the years jerky movements affected her right hand and her trunk. Levodopa which had a dramatic initiation response but after a couple of years the effect wear off. She had mild distal dystonia of the right arm and slight dystonia at the left side.There was no dystonia of the face but her speech is slightly dystonic. Her lower limbs show only slight dystonia. Tendon jerks were reduced and symmetrical. Eye movements were normal. There was no known family history of dystonia and the parents are not related. She has a sister who is well.

6.5. Discussion

Human disease can result from single nucleotide polymorphisms that affect any step of its finely tuned regulatory system. However, the absence of mutations in the coding region or the splice sites in some classic cases of DRD has been observed (185,337). It has also been suggested that autosomal recessively inherited mutations of the tyrosine hydroxylase gene might also casue DRD (338), but genetic heterogeneity cannot explain the absence of *GCH1* mutations in families with

autosomal dominantly inherited DRD and linkage to the GCH1 locus. Hence, genetic analysis beyond the coding regions of the *GCH1* gene is necessary.

Three different mutations have been described in the 5' untranslated region (UTR) of the *GCH1* gene in literature. We report two cases with both mutations, -39C>T and -132C>T in the 5' UTR of *GCH1* gene. 5' UTR in other genes suggest that this region of the gene is important in the regulation of gene expression and that sequence change changes in this particular region of the gene can lead to decreased enzyme activity of the gene product (181).

Both cases were with childhood onset, slowly progressive, no family history of dystonia, non-consanguineous parents and the effect of levodopa not sustained. The first case is clinically a recessive HSP case and since DRD can mimic HSP a trial of levodopa was given where the effect was not sustained. His brother is affected but the mutations are not segregated. Hence, the pathogenicity of these non-coding mutations in 5' UTR of *GCH1* gene is less likely. In second case, though clinically dystonic symptoms are reported, the levodopa response was not sustained. Hence the non-coding mutations in *GCH1* gene cannot be directly associated with the disease phenotype. Deep brain stimulation of the internal part of globus pallidus has been considered as a next step.

In particular for diseases linked to non-coding substitutions, functional assays are required to establish a link between the substitution and the disease phenotype. The -39C>T and -132C>T substitutions were identified as co-existing in *cis* in a single

subject with DRD, making it impossible to independently determine hereditary disease association for each substitution (187). The negligible effects on luciferase activity for -39C>T and -132C>T substitutions in a single DRD patient was reported when tested either individually or combined into a single reporter construct (187). However, functional study on -22 C>T mutation showed reduced translational efficiency and likely leading to reduced wild type *GCH1* protein levels, underlying manifestation of DRD.

Nevertheless from this study we conclude that the effect of two non-coding mutations in the 5'UTR of *GCH1* gene described in above two cases is not significant to underline the manifestation of DRD.

Chapter 7. Genetics of spinocerebellar ataxia (SCA8)

7.1. Background

SCA8 is a dominantly inherited, slowly progressive neurodegenerative disorder caused by a CTG/CAG repeat expansion. The mutation for SCA8 was initially identified in 1999 as a CTG/CAG expansion mapping to chromosome 13q21 (197). Initial sequence analysis of the SCA8 CTG/CAG repeat region identified no likely open reading frames in the CTG or CAG direction, but it was demonstrated that the SCA8 repeat mutation was transcribed in the CTG direction and that transcripts containing the CAG repeat were primarily expressed in the CNS and especially in the cerebellum (197). The SCA8 repeat is conserved in chimpanzees, gorillas, and orang-utans but the genomic region containing the SCA8 repeat is not conserved in the mouse (200–202).

Clinically SCA8 presents as an ataxia with slow progression that largely spares brainstem and cerebral function (197,206–209,213,214). Disease progression is relatively slow with significantly limited mobility occurring approximately 20 years after the initial symptoms but does not shorten life. Moderate to severely affected patients present with dysarthric speech and commonly manifest oculomotor deficits (206,213,215). Severely affected individuals can present with hypereflexia and occasionally present with mild myoclonic finger and arm jerks. Mild sensory loss is observed as indicated by decreased vibratory perception (206,213).

The precise number of the pathogenic (CTG)n repeat is technically difficult to determine. This study will use a division of alleles in four classes: the small normal alleles (≤ 39 CTA/CTG repeats), the intermediate alleles (40-84 CTA/CTG repeats), large expanded alleles (85-400 CTA/CTG repeats), and very large expanded alleles (≥400 CTA/CTG repeats) (339).

7.2. Aims and Hypothesis

Hypothesis

- The (CTG)n repeat length determines the disease pathogenesis in SCA8.

Aims

- To determine SCA8 repeat size in a cohort of ataxia cases and normal controls.
- To determine if repeat size length is statistically significant to the disease pathogenesis.

7.3. Methods

Fragment analysis was carried out to analyse the SCA8 repeat alleles as described in Chapter 2.

7.4. Results

The study group comprised 630 cases of clinically diagnosed sporadic ataxia patients, 631 English controls and 1148 of diversity controls.

The distribution of the number of SCA8 repeats are shown in table 1. Very large expanded alleles (≥400 CTA/CTG repeats) were not observed in cases and controls. In clinically diagnosed ataxia patient cohort of 630 cases, large expanded SCA8 alleles (>84 CTA/CTG repeats) were noted in 6 (0.95%) cases, intermediate SCA8 alleles (40-84 CTA/CTG repeats) were noted in 6 (0.95%) and 618 (98.1%) cases were in the the small normal SCA8 repeat allele (≤ 39 CTA/CTG repeats) range. In the English control cohorts of 631 individuals, we identified an individual (0.16%) with a large expanded SCA8 allele, 5 (0.79%) individuals with intermediate alleles and 625 (99.04%) individuals in small normal allele range. In diversity control cohort of 1148 individuals, we identified 3 individuals (0.27%) with a large expanded SCA8 allele, 23 (2%) individuals with intermediate alleles and 1122 (97.7%) individuals in small normal allele range. Student's t-test showed there is no significant difference in SCA8 repeat expansion length between the diversity controls and the patients group at 0.05 level of significance (p= 0.192). However, occurrence of SCA8 repeat expansion in patients compared with English controls showed a significant difference at 0.05 level of significance (p= 0.018). Clinical data is summarized in the Table 7.1.

In diversity control cohort, cases with repeat expansion 84 are, case 1 (repeat genotypes 22/87) is a female of Chinese origin, case 2 (repeat genotypes 22/95) is a male of Pakistani origin, and case 3 (repeat genotypes 22/88) is a female of Middle Eastern origin (Israel).

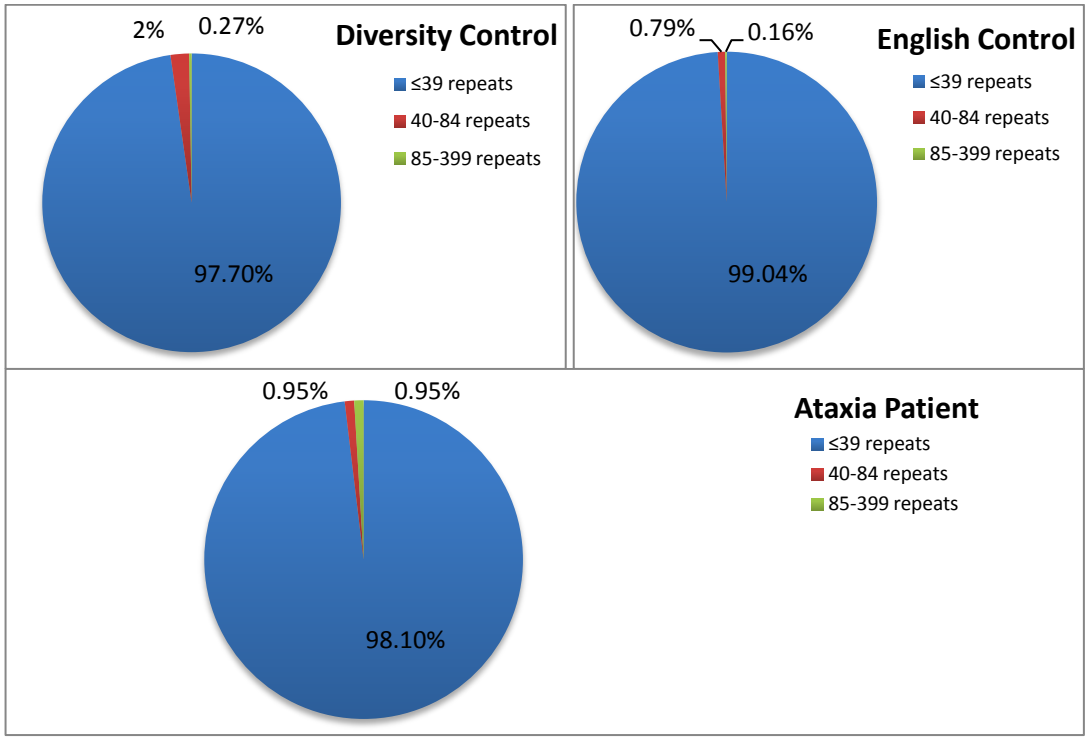

Figure 7.1 Distribution of SCA8 repeats expansion in ataxia cases and controls.

Table 7.1 Clinical details of cases with SCA8 repeat expansion in the range of 85-399 repeats along with two cases in the borderline.

Case No.	*Age/ Sex*	*Genotypes for SCA8 repeats*	*Family History*	*Dysathria*	*Cerebellar Ataxia*	*Gait Ataxia*	*Limb Ataxia*	*Nystagmus*	*Clinical diagnosis*
1	45F	28/87	-	+	-	+	+	+	Late onset cerebellar degeneration
2	63F	22/91	-	+	-	+	-	-	Progressive Parkinsons syndrome
3	43F	27/95	-	-	-	+	+	+	Idiopathic cerebellar ataxia with pyramidal signs
4	36F	27/96	-	+	+	+	+	+	Early onset spinocerebellar ataxia
5	67F	22/97	-	-	-	-	-	-	Craniocervical Dystonia, Blepharospasm
6	43M	22/103	+	+	-	+	-	+	Inherited ataxia
7	59F	24/83	-	+	+	+	+	+	Multi-system atrophy (MSA)
8	44F	24/84	-	+	+	+	+	+	Extrapyramidal signs probable MSA

Case 1 (SCA8 repeats 28/87) is a 45 year old female with idiopathic early onset cerebellar ataxia. She has subcortical slow speech with dysarthria. She has broken pursuit eye movements and gaze evoked nystagmus. She has finger nose and heel shin ataxia. She mobilises with a stick and her gait is ataxic. Tests for SCA 1-7, 12, 17, ataxia telangiectasia mutated (ATM), ataxia with oculomotor apraxia type 1 (AOA1) and ataxia with oculomotor apraxia type 2 (AOA2) were normal.

Case 2 (SCA8 repeats 22/91) is a 63 year old female with atypical Parkinsonism and no family history. She has progressive dysarthria and dysphonia and recurrent falls since 2006. There was a slight restriction of upward gaze, intermittent upbeat nystagmus bilaterally. She had spastic dysarthria and slow tongue movement. Her gait was slow, stooped and broad-based with poor-arm swing and turning. Over the two years she developed neck stiffness, a decline in her dexterity and a slowing of movement. She is imbalanced and occasionally has urinary incontinence. Brain MRI showed volume loss of the cerebral peduncles, pons, cerebellum, superior colliculi, frontal and temporal lobes. A DaTscan showed nigrostriatal degeneration.

Case 3 (SCA8 repeats 27/95) is a 43 year old female with clinical diagnosis of idiopathic cerebellar ataxia with pyramidal signs. She started to notice bumping into objects at the age of 38 and her balance became progressively worse. She had mild broad-based gait and gaze evoked nystagmus. There was no dysarthria and no limb ataxia. Tests were negative for SCA 1, 2, 3, 6, 7, 12, 17, AOA1, AOA2, and friedreich's ataxia (FRDA).

Case 4 (SCA8 repeats 27/96) is a 30 year old female with clinical diagnosis of early onset spinocerebellar ataxia. She had tremor of the head, jerky pursuit, gaze-evoked nystgamus and slight frontalis overreactivity. Saccades were slow and there was ataxia of in her upper and lower limbs. She had dysarthric speech pattern and bilateral horizontal nystgmus and jerky pursuit movements. Cerebellar signs were present on finger-nose testing and heel-knee-shin testing. Gait was broad based and only able to perform tandem walk. Tests were negative for SCA1, 2, 3, 6, and 7 and ATM.

Case 5 (SCA8 repeats 22/97) is a 67 year old female with clinical diagnosis of cranial cervical dystonia in addition to belpharospasm. She has restricted movements of the neck and had torticollis to the right and occasional rectrocollis.

Case 6 (SCA8 repeats 22/103) is a 40 year old male with inherited autosomal dominant cerebellar ataxia. He had experienced balance problems and on examination had mild broad-based gait with trunkal stiffness. He had a slightly asymmetric face and nystagmus. Speech was slightly slurred. In upper limbs, tone and power were normal with coordination showing dysmetria, dysdiadokinesia and intention tremor. Lower limbs were normal with mild dysmetria in the heel-to-shin test. A brain MRI showed severe atrophy of both cerebellar hemisphere and the vermis.

Case 7 (SCA8 repeats 24/83) is a 45 year female with multiple system atrophy (MSA). She had gradually deteriorating ataxia and bladder incontinence because of

MSA. Her gait deteriorated such that she needed frame to walk and now she is wheelchair bound. There were no problems with the vision, hearing, memory, blackouts or numbness or pins and needles in the limbs. She had occasional swallowing difficulty and bladder incontinence. Neurological examination revealed an ataxic dysarthria and finger-nose and heel-shin ataxia in the arms and legs. There was bilateral first-degree nystagmus and no clear cognitive deficit. A brain MRI showed atrophy of cerebellum and brainstem but little of the supratentorial structures and 'hot-cross-bun' changes in the brainstem, consistent with a diagnosis of MSA.

Case 8 (SCA8 repeats 24/84) is a 40 year old female with probable diagnosis of MSA. She showed clinical symptoms of slowly progressive cerebellar ataxia for three years, late-onset and acquired. In 2008, she had a mildly ataxia gait and limbs. She had increasing difficulties with balance, slurred speech, writing and problems with focus over the last two years. She had gaze instability due to nystagmus. A brain MRI showed a degree of mild cerebellar atrophy and vermian volume loss. Tests for SCA1, 2, 3, 6, 7 and FRDA were negative.

7.5. Discussion

The genetics underlying SCA8 is complex and not yet finally understood. SCA8 was the first published repeat expansion SCA (CAG or CTG) in an untranslated region. It is characterized by repeat instability and with no correlation between repeat length and penetrance. There is no anticipation observed and penetrance is reduced as

the expansion can also be found in healthy individuals. Thus, the diagnosis remains controversial (204).

Potentially pathogenic alleles contain 85 or more combined CTA/CTG repeats. However, repeats of this size are surprisingly frequent in the general population and also occur in asymptomatic relatives of ataxia individuals (197,204,206,211,340). The complex pattern of inheritance has resulted in unaffected carriers commonly having repeat sizes that exceed the pathogenic threshold making it difficult to ascertain clear ranges for pathogenic expansion (199,208). SCA8 may rarely coexist with SCA6 (339) or SCA1 (341) which makes it difficult to assign symptoms to a specific entity.

This study examined the length of SCA8 repeats in English ataxia patients, English controls and in diversity (from 25 different countries) controls. Alleles with >84 SCA8 repeats are potentially pathogenic and in the ataxia cohort investigated, 6 out of 631 cases were in this range. However, a case out of 631 English controls and 3 cases out of 1148 individuals in diversity control cohort were also in the potentially pathogenic range table .The range of SCA8 large alleles observed is not much different from that reported in the literature. The significant difference (p= 0.018) in occurrence of SCA8 repeat expansions in ataxia patients compared with English controls but not with the diversity controls (p=0.192) suggests that the pathogenicity of SCA8 repeat expansion is not only dependent on the repeat size but also on the population, environment and the genetic modifiers. Another

possibility is that the individuals with a large repeat expansion in ataxia cohort, English cohort and Diversity cohort may have shared the common founder. Hence, SCA8 sizes among affected and unaffected expansion carriers can be shorter or longer than the pathogenic threshold MN-A family defined in literature but the pathogenicity may also be influenced by other genetic modifiers. These data demonstrate that the presence of a SCA8 expansion cannot be used to predict whether or not an asymptomatic individual will develop ataxia as the control cases were asymptomatic at the time of study.

The six cases with SCA8 repeat expansion ≥85 repeats were characterized by high frequencies of gait ataxia, ataxic dysarthria, limb dysmetria, and gaze-evoked nystagmus. Pyramidal tract signs and reduced vibratory sense are observed less frequently. Other neurological signs are rare or absent. The clinical features of the SCA8 can be summarized as relatively pure cerebellar ataxia. The disease progression is typically very slow. When available, MRI scans showed cerebellar atrophy. However, two cases with SCA8 repeat in the large intermiediate range, 83 and 84 respectively, are in the borderline of the marked pathogenic ranges and were also looked into. They showed all the above clinical criteria. The brain MRI in one case showed features consistent with diagnosis of MSA and another case was diagnosed as MSA. Hence, SCA8 expansion may be a susceptibility factor for MSA. This data suggests that SCA8 repeat expansion length should not be the sole method of for diagnostic purposes.

The disease status in the MN-A family have supported the hypothesis that CTG/CAG repeat length is directly associated with ataxia (197,206) but was not true in other ethnicities. In our cohort, the largest SCA8 repeat allele was 103 in an inherited ataxia case but repeat length of 97 was found in a dystonia case with no other clinical symptoms of SCA8 described above. 96 repeat length was observed in early onset spinocerebellar ataxia case with the clinical symptoms of SCA8. The expanded allele ranged from 87-103 repeats and this is quite a narrow range to determine if the penetrance is directly related to the repeat length. Also, alleles in the pathogenic repeat length expansion range were observed in control population, the reduced penetrance of SCA8 is the most difficult genetic feature of the disease to understand.

Although the risk of developing ataxia is dependent on the size of the expansion and probably also on other factors that affect the penetrance of the mutation, neither family history nor the expansion repeat size can be used to accurately predict which offspring will develop symptoms of the disease. The length of the repeat tract does not correlate with the age of onset, severity, symptoms, or progression of the disease. Hence, along with the clinical symptoms, neurologic assessment, including neuroimaging (brain MRI or CT) and assessment of family pedigree is essential to establish a clinical prognosis.

Although next generation sequencing (NGS) is a very powerful diagnostic tool in genetic studies, there are also limitations in particular in the diagnostics of repeat

expansion SCAs. NGS are currently relatively poor in their ability to identify stretches of repetitive DNA sequence. It does currently not qualify for detection of these types of mutations. This weakness of NGS also reduces the chances to discover new repeat expansion SCAs in a research setting.

Chapter 8. Neuropathology of BPAN

8.1. Background

Neurodegeneration with brain iron accumulation (NBIA) is a group of inherited neurological disorders in which iron accumulates in the basal ganglia resulting in progressive dystonia, spasticity, Parkinsonism, neuropsychiatric abnormalities, and optic atrophy or retinal degeneration. Nine types and their associated genes are recognized. The age of onset ranges from infancy to late adulthood; the rate of progression varies. Cognitive decline occurs in some subtypes, but more often cognition is relatively spared. Cerebellar atrophy is a frequent finding in some subtypes. Recently, de novo mutations in a *WDR45* gene was identified causing a phenotypically distinct X-linked dominant form of NBIA, named BPAN (229). *WDR45* encodes a beta-propeller protein that serves a putative role in autophagy, a lysosomal process to degrade cellular components that is thought to be defective in many neurodegenerative disorders (244). Neuropathological features reported on a case of BPAN included positive iron staining in substantia nigra and globus pallidus with is a hallmark feature of NBIA. Axonal spheroids and tau-positive NFTs were reported but no amyloid-β plaques or LBs were observed (237).

In this chapter we will discuss Beta-propeller protein associated neurodegeneration (BPAN) and neuroacanthocytosis.

8.2. Aims and Hypothesis

Hypothesis

- Iron accumulation in basal ganglia is a feature of BPAN.
- Tau pathology as described in a case of BPAN is a consistent feature of the disorder.
- Delineation of tau-isoforms may determine similarities to other diseases.
- Beta-propeller protein participates in autophagy.

Aims

- To carry out a detailed neuropathological study of a case with mutation in *WDR45.*
- To carry our tau-blotting to determine the tau isoforms present.
- To investigate autophagy in a case of BPAN.

8.3. Methods

Paraffin blocks representing multiple brain regions from a post mortem case of BPAN were obtained from QSBB and investigated using routine histological staining and IHC methods as described in Chapter 2. Antibodies used for IHC included: ubiquitin (1:200, Dako, Ely,UK), tau (1:600, AT8, Autogen Bioclear, Calne, UK); AT100 (1:200, Innogenetics, Gent, Belgium), glial fibrillary acidic protein (GFAP; 1:1,000, Dako), Aβ (1:200, Dako), α-synuclein (1:50, Novacastra, Newcastle, UK), α-synuclein (1:1000, BD Transduction Biolabs, Oxford, UK), P62 (1:100, BD Bioscience, Oxford, UK), CD68 (1:150, Dako) and TDP-43 (1:2000, Protein Tech, Manchester,

UK). Neuropathological assessment of neuronal loss, gliosis and concomitant pathologies (tau, Aβ, LBs, CAA, TDP-43, and SVD) were carried out in a semi-quantitative manner according to published criteria (304–307). A score scale of 0 - +3 was used to indicate increasing pathology.

WB (as described in Chapter 2) was carried out to delineate the tau isoforms present and to investigate disturbances in autophagy by WB on LCI and LCII.

8.4. Results

8.4.1. Genetics

The case had a *de novo* mutation in the exon 9 of *WDR45*, c.694_703del, p.Leu232Alafs*53. The genetics and clinical history of this case have been previously published as case number HH84 (229,237).

8.4.2. Clinical details

The case was a female 51 years of age at death. She showed features of learning disability, mental retardation and progressive gait abnormalities since childhood. By the age of 13, she was moved to a special school for handicapped children. Her movement disorder symptoms started deteriorating significantly at the age of 29 with slowing of gait and reduction of arm-swing whilst walking. Her condition deteriorated and she developed dystonic features during her thirties. She developed behavioural difficulties with social withdrawal, self-mutilative tendencies and depression throughout the years. Disturbed sleep with early morning awakening occurred and the behavioural problems became more and

more prominent. There was reduced spontaneous speech and communication as well as reduced attention span. In the late stages of her disease, she was wheelchair-bound, had urinary and faecal incontinence and was totally dependent on the activities of daily living (ADL)-score. Family history was negative.

On examination she showed predominant extra-pyramidal symptoms with significant bradykinesia, hypomimia and hypophonia with signs of mild cerebellar disturbance. She had a bilateral grasp reflex. Her eye movements were normal. Brain imaging revealed generalised brain atrophy and bilateral generalised mineralisation of the globus pallidus. The globus pallidus and substantia nigra showed changes thought to represent iron deposition. Blood count revealed microcytic hypochromic anemia, normal platelets, white-cell count, negative acanthocytes, normal lactate and pyruvate.

8.4.3. **Macroscopic findings**

The macroscopic details were available from the neuropathology reports supplied by the QSBB. The brain weighed 1,117g. External examination of the left half of the brain showed frontal atrophy with preservation of parietal, temporal and occipital lobes. Coronal slices revealed mild dilatation of the frontal horn of the lateral ventricle and patchy thinning of the cortical ribbon in the frontal lobe. In the occipital cortex an area of cavitation with the appearance of an old infarct involved the primary visual cortex. White matter in the anterior frontal and temporal lobes showed mild atrophy. The globus pallidus was reduced in size with blurring of the

distinction between internal and external parts and showed dark discolouration anteriorly (Figure 1A, arrow). The caudate and putamen appeared normal. The thalamus and hippocampus showed mild atrophy and there was moderate reduction in bulk of the amygdala. There was marked abnormality of the substantia nigra which showed brown discolouration and had a gelatinous texture throughout (Figure 1B, double arrow). The locus coeruleus was indiscernible (Figure 1B, arrow). The medulla and cerebellum appeared normal.

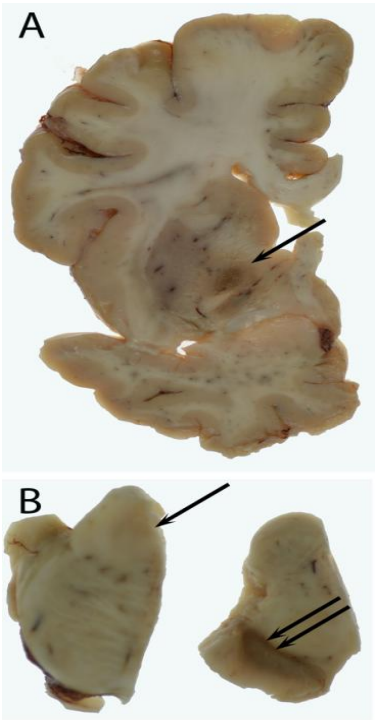

Figure 8.1 A coronal slice at the level of the anterior commissure shows atrophy and dark discolouration of the globus pallidus (A, arrow). There was loss of pigment in the locus coeruleus which was indiscernible (B, arrow). The substantia nigra was markedly abnormal with brown discolouration and a gelatinous texture (B, double arrow).

8.4.4. **Histological findings**

Histological examination showed mild superficial vacuolation in anterior frontal, temporal and parietal cortices. A full thickness cortical infarct with cavitation, infiltration of macrophages and surrounding gliosis was confirmed in the visual cortex. Neuronal loss was mild in neocortical regions (frontal, temporal, parietal, Table 2) and occasional swollen neurons were identified using αB-crystallin immunohistochemistry. Luxol fast blue staining confirmed good myelin preservation in the subcortical white matter. There was no cortical iron deposition identified using Perl's stain.

Neuronal populations in the hippocampus, amygdala, striatum, thalamus and subthalamic nucleus were well preserved. Examination of the globus pallidus showed extensive mineralisation of vessels including arteries, veins and capillaries. Perl's staining for iron was positive in areas of mineralisation and also in scattered cells with macrophage morphology. GFAP IHC showed marked gliosis of the globus pallidus and there was also an increase in CD68 immunoreactive microglia. No axonal swellings were identified using antibodies recognising neurofilaments.

Examination of the midbrain showed very severe loss of pigmented neurons in the substantia nigra accompanied by gliosis, macrophage infiltration and marked deposition of Perl's positive pigment. Numerous axonal swellings were present and were highlighted with IHC for amyloid precursor protein (APP), neurofilament cocktail, SMI31 and ubiquitin. Occasional swellings were α-internexin-positive

however, most were unstained in this preparation. In the pons the locus coeruleus showed mild neuronal loss, the pontine nuclei were well preserved. In the medulla the Xth and XIIth cranial nerve nuclei as well as the inferior olivary nucleus were well preserved. Axonal swellings were observed in the gracile and cuneate nuclei. The cerebellum showed mild Purkinje cell depletion with good preservation of the dentate nucleus and hemispheric myelin. There was no Aβ deposition in the hippocampus or neocortex. No α-synuclein pathology was found in brainstem or limbic regions and there was no TDP-43 pathology in limbic structures.

Tau pathology was extensive in the form of neurofibrillary tangles, pre-tangles and neuropil threads affecting cortical regions, white matter, deep grey nuclei, hippocampus, amygdala, brainstem structures and the cerebellum. Very rare coiled bodies were present in the sub-cortical white matter but there was no accumulation of tau in astrocytes. The type of tau pathology and semi-quantitative analysis of the tau burden in different brain regions is summarised in Table 2. Isoform specific antibodies demonstrated the expression of both 3- and 4-repeat tau isoforms. Immunoreactivity for AT100, which recognises Alzheimer–type paired helical filament tau, was also demonstrated. NFTs and neuropil threads are also identified using Gallyas silver staining further confirming the presence of fibrillary tau.

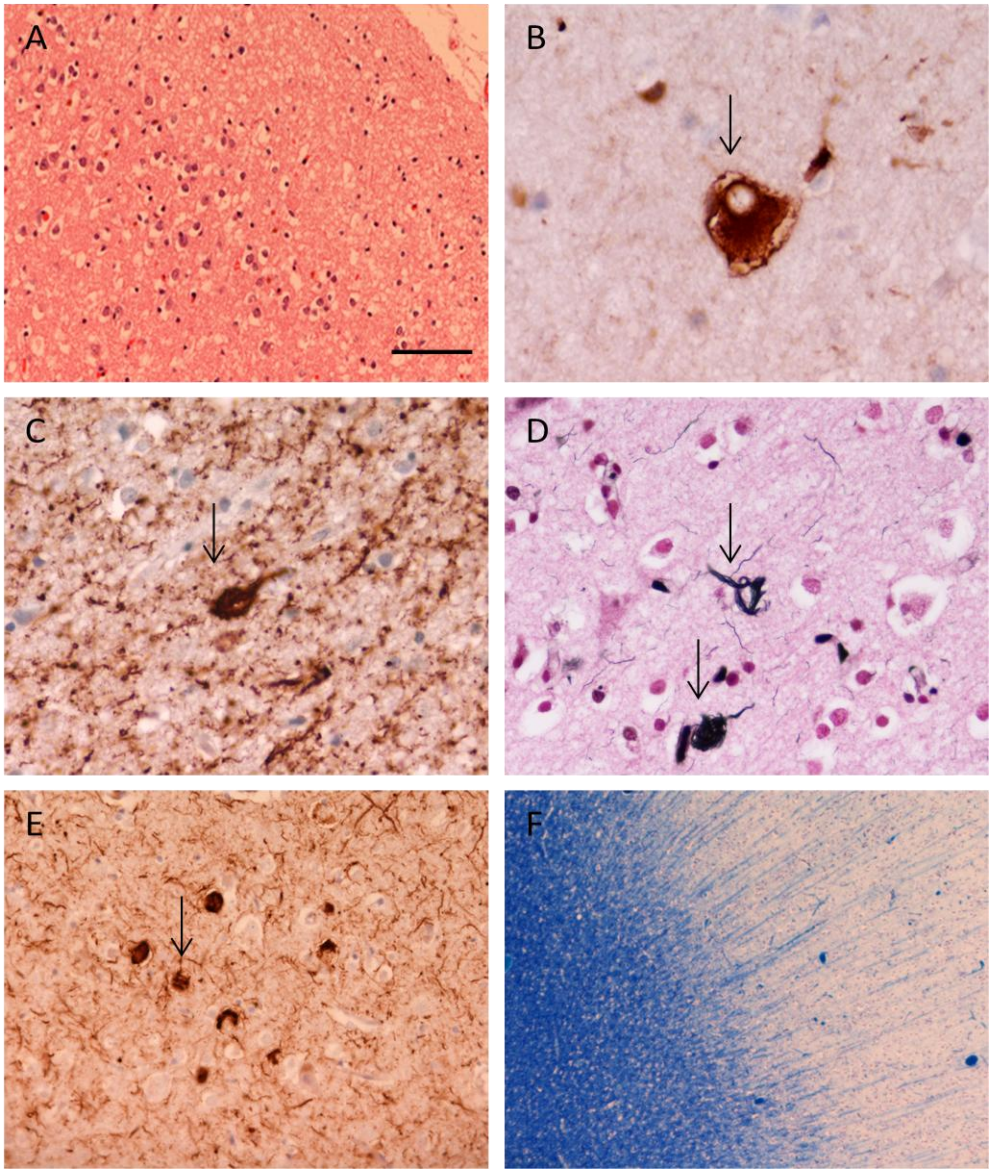

Figure 8.2 Histological findings in frontal cortex of BPAN case. Mild neuronal loss and vacuolation (A) with swollen neurons were observed (B). Tau pathology was extensive in the form of neurofibrillary tangles, pre-tangles and neuropil threads (C-D) and also showed immunoreactivty for Alzheimer–type paired helical filament tau (E). Good myelin preservation was observed in the subcortical white matter with fibres radiating towards cortex (F). Scale bar: A= 100µm, B-C &E=50 µm, D=25 µm and F=260 µm. A: H&E; B: αβ crystalline; C: AT8; D: Gallyas stain; E: AT100 and F: Luxol fast blue.

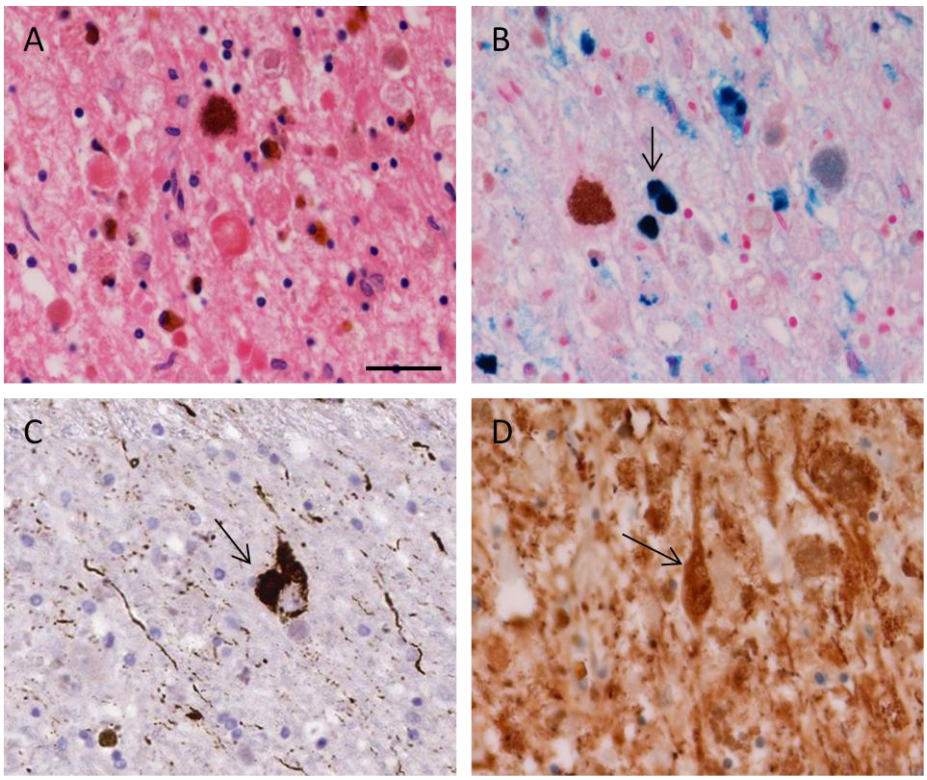

Figure 8.3 Histological findings in midbrain. Examination of the midbrain showed severe loss of pigmented neurons in the substantia nigra accompanied by gliosis, axonal swellings (A and D) and marked deposition of iron (B). Tau pathology was positive with NFTs and threads (C). Scale bar: A and C=50 µm, B and D=25 µm. A=H&E; B=Perl's stain; C=AT8 and D=phosphorylated SMI31 neurofilament.

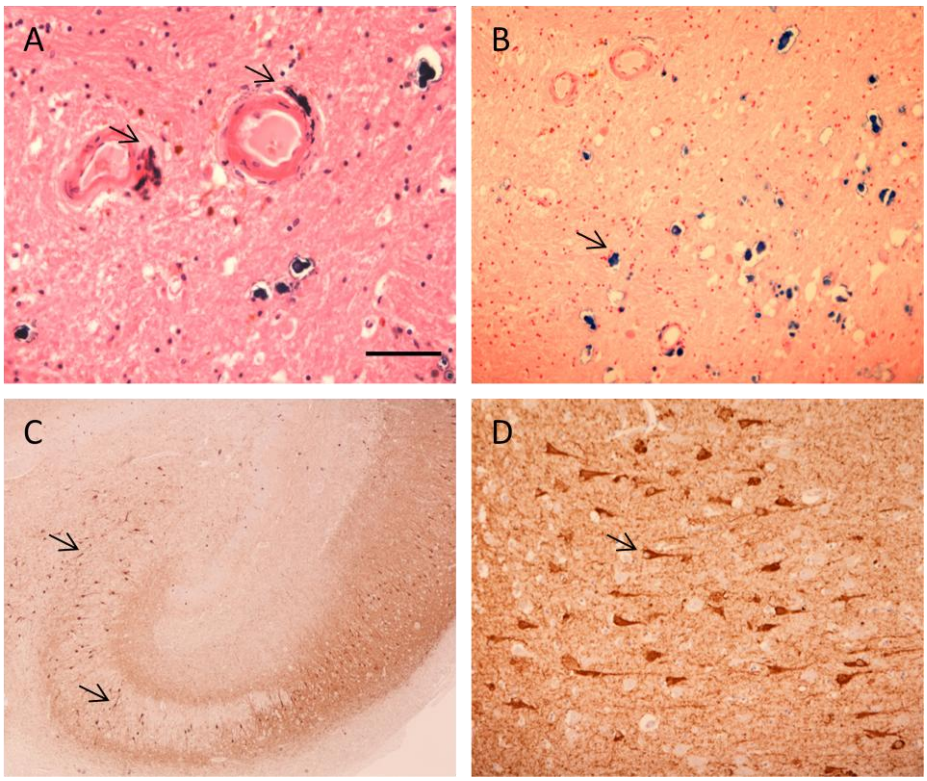

Figure 8.4 Histological findings in globus pallidus (top panel) and hippocampus (bottom panel). Examination of the globus pallidus showed extensive mineralisation of vessels including arteries, veins and capillaries (A) and iron deposition in the areas of mineralisation (B). Examination of the hippocampus showed extensive tau pathology in the form of neurofibrillary tangles, pre-tangles and neuropil threads (C). D represents tau pathology in CA1 region. Scale bar in A represents: A=50 µm, B=100, C =525 µm and D=25 µm. A=H&E; B= Perl's stain; C and D= AT8 IHC.

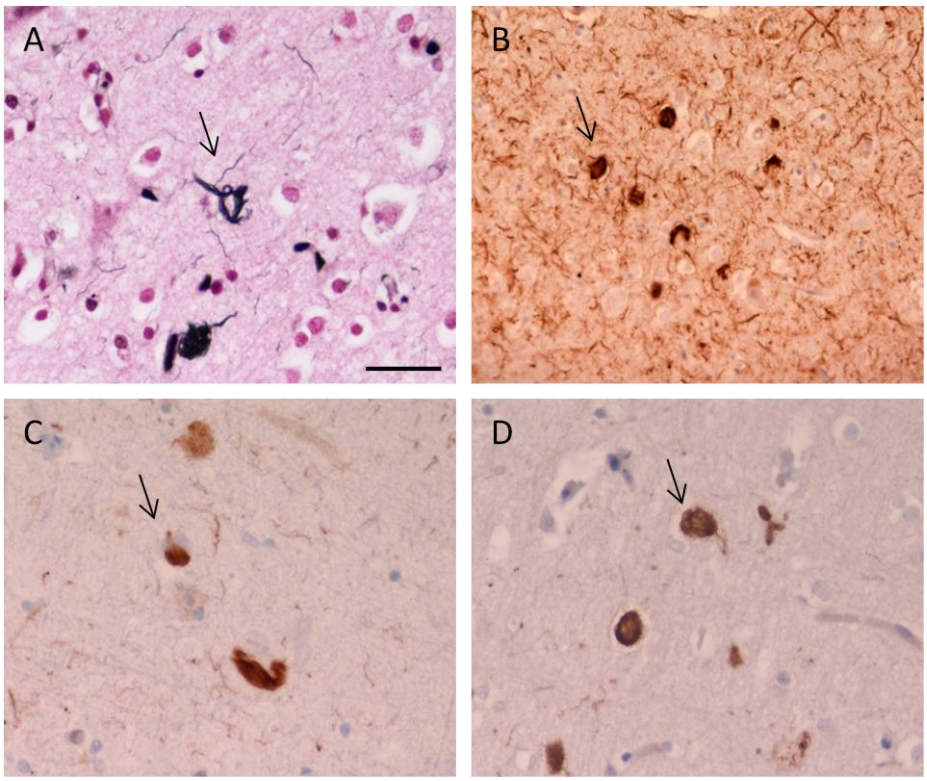

Figure 8.5 Tau deposition. Extensive tau pathology was observed in the form of neurofibrillary tangles, pretangles and threads and was of Alzheirmer-type tau deposition. Gallyas silver impregnation demonstrated the presence of fibrillar protein (A). Support for Alzheimer-type tau deposition was provided using the AT100 antibody, recognising tau phosphorylated at Thr212 and Ser214 with paired helical filament conformation, which labelled a proportion of NFTs (B) and by isoform specific antibodies, which showed a mixture of 3- repeat (**C**) and 4-repeat (**D**) tau isoforms. Scale bar in A represents: A,C-D= 25 µm and B= 50 µm.

Table 8.1 Summary of neuronal loss and semi-quantitative assessment of tau pathology in different brain regions

		Tau pathology		
	Neuronal loss	***Threads***	***Pre-tangles***	***Neurofibrillary tangles***
Cortex				
Frontal	+	+++	-	++
Temporal	+	+++	-	++
Parietal	+	+++	-	++
Occipital	Infarct visual cortex	+	-	-
Cingulate	-	+++	-	+++
Sub-cortical white matter				
Frontal	N/A	+	N/A	N/A
Temporal	N/A	+	N/A	N/A
Parietal	N/A	+	N/A	N/A
Occipital	N/A	+	N/A	N/A
Cingulate	N/A	++	N/A	N/A
Amygdala	-	+++	-	+++
Hippocampus				
Dentate fascia	-	+	-	++
CA4	-	++	+	++
CA3	-	++	-	++
CA2	-	++	-	++
CA1	-	+++	+	+++
Subiculum	-	+++	+	+++
Entorhinal cortex	-	+++	+	+++
Transentorhinal cortex	-	+++	+	+++
Caudate	-	+++	+	++
Putamen	-	++	+	++
Globus pallidus	+	++	-	+
Meynert	+	+++	-	+++
Thalamus	-	++	-	++
Subthalamic nucleus	-	++	-	++
Substantia nigra	+++	++	-	+
Locus coeruleus	+	++	-	+
Pontine tegmentum	-	++	-	++
Pontine nuclei	-	+	-	+
Dorsal motor nucleus of vagus	-	+	-	+
Twelfth nerve nucleus	-	+	-	-
Inferior olive	-	+	-	-
Gracile nucleus	-	+	-	-
Cuneate nucleus	-	+	-	-
Cerebellar Purkinje cells	+	-	-	-
Cerebellar white matter	N/A	-	N/A	N/A
Dentate nucleus	-	+	-	+
N/A: not available				

8.4.5. **Immunoblots**

Tau blots:

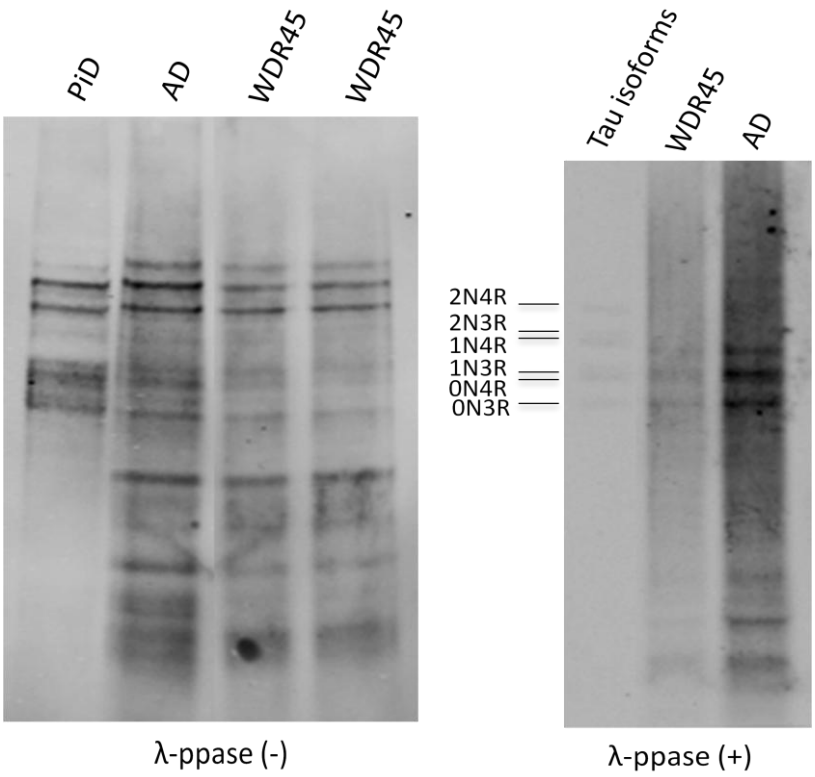

Figure 8.6 Immunoblotting of non-dephosphorylated (left) and dephosphorylated tangle (right) preparations of Pick's disease (PiD), Alzheimer's disease (AD) and WDR45 case. WB of non-dephosphorylated tangle extractions showed the classical triplet band as observed in AD cases (i.e. 3R+4R). When dephosphorylated, the isoform composition is almost identical to the AD with 0N3R, 0N4R, 1N3R and 1N4R tau-isoforms.

Tau blotting of the tangle preparations of WDR45 case showed the classical triplet band as observed in Alzheimer's disease (i.e. 3R + 4R). When dephosphorylated, the isoform composition is almost identical to the AD with 0N3R, 0N4R, 1N3R and 1N4R tau-isoforms.

8.4.6. **Autophagosome associated light chain 3 (LC3) blots**

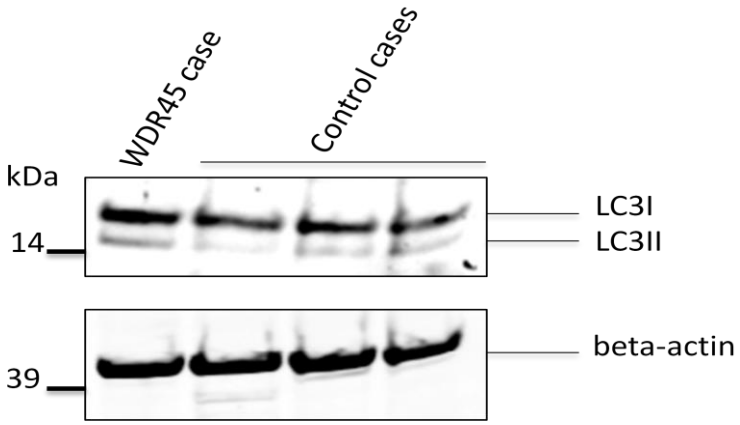

Figure 8.7 Immunoblotting of frontal cortical homogenates from the mutation case and three neurologically normal cases showing LC3I (~18kDa) and LC3II (~16kDa) levels (upper panel). Beta-actin loading control is shown in the bottom panel.

The mutation case shows higher autophagosome associated light chain 3 (LC3)-II formation compared to three control cases. This implies higher levels of autophagic flux in the mutation case compared to the three age and sex matched control cases.

8.5. Discussion

This report describes genetic, clinical and corresponding pathological details of a case with a mutation in *WDR45* gene. *De novo* mutations in the *WDR45* gene have been linked to a subset of NBIA cases, currently known as BPAN and the only X-linked NBIA described in literature. The case is a 51 years old female with disease onset in childhood. The clinical pattern of the case studied here matches to other BPAN cases described which are characterized by global developmental delay and intellectual deficiency in early childhood followed by further neurological and cognitive regression in late adolescence or early adulthood, with parkinsonism, dystonia, and sometimes ocular defects and sleep perturbation (229,237,342). Exome sequencing revealed a de novo mutation in exon 9 of *WDR45*, c.694_703del, p.Leu232Alafs*53 and the mutation in the case and clinical history had been previously published (229).

Consistent with the reports of significant basal ganglia pathology observed in neuroimaging for BPAN cases, iron deposition in the globus pallidus and substantia nigra was evident on brain imaging of this case. Macroscopic examination of the brain suggested atrophy and dark discolouration of the globus pallidus and a markedly abnormal substantia nigra with brown discolouration and a gelatinous texture throughout. The major pathological findings in this case were severe neuronal loss with gliosis affecting the substantia nigra, iron deposition in the substantia nigra and globus pallidus, axonal swellings in the substantia nigra, gracile nucleus and cuneate nucleus and very extensive phospho-tau deposition. Tau

pathology was in the form of neurofibrillary tangles, pre-tangles and neuropil threads and histological studies indicated that many of the tau immunoreactive structures contained fibrillary protein (Gallyas silver positive and AT100 immunoreactive) and contained both 3-and 4-repeat tau isoforms similar to the tau deposits of Alzheimer's disease. This finding was confirmed by immunoblotting of non-dephosphorylated tangle extractions which showed the classical triplet band as observed in AD cases (i.e. 3R+4R). When dephosphorylated, the tau isoform composition is almost identical to the AD case with 0N3R, 0N4R, 1N3R and 1N4R tau-isoforms. Tau pathology was described in BPAN in a post-mortem case in literature but not well documented. The detailed description of the tau pathology and the tau isoform composition adds significantly to the neuropathological findings previously described.

A link between tau pathology, autophagy impairment, and neurodegeneration has been suggested (343). Impairment of protein degradation pathways such as autophagy is emerging as a pathological phenomenon in neurodegenerative diseases, including Alzheimer's, Huntington's and Parkinson's diseases (343). The autophagy pathway is the main degradation route for long-lived proteins, damaged organelles and protein aggregates. It is a highly regulated process, characterized by the formation of double- or multi-membrane vesicles (autophagosomes) that sequester portions of cytosol, which are then delivered for degradation following fusion with lysosomes (343) . However, there is accumulating evidence that protein misfolding disorders involve specific defects in particular steps of the autophagy

process and manipulation of the autophagy in neurodegenerative disease may have unpredictable outcomes.

The *WDR45* gene belongs to the large family of WD40 repeat protein and is one of the four mammalian homologs of yeast Atg18, an important regulator of autophagy. Its involvement in autophagy has been documented in yeast and mammalian cells, where it interacts with ATG2 (244), and in *C. elegans*, where its deletion leads to accumulation of early autophagosomes (245). In lymphoblast cell lines from BPAN patients, the amount of protein is clearly reduced and autophagosome formation is hindered at an early stage as shown by the accumulation of LC3-II protein and its co-localization with ATG9A in enlarged membrane structures (236). This suggests that the mutant protein is structurally unstable and undergoes degradation. These abnormal intracellular structures stained for ATG9A and LC3s, an autophagosome marker which suggests improper autophagosome formation. Accumulation of LC3-II protein was also observed in immunoblot from the brain tissue of our *WDR45* case, where LC3-II accumulation is higher compared to the three normal controls. This implies higher level of autophagic flux in the mutation case compared with controls as previously observed in patient lymphoblasts.

The complexity and multifactorial nature of the neurodegenerative diseases related to iron dysregulation suggests multiple interventions are necessary. For example, treatments for iron accumulation (using iron chelating therapies) are beneficial for

neuroprotection but they may impair cell repair processes (344). When cells are stressed or injured, the autophagic process is induced to clear damaged cellular components and by-products of the stress response. Defective autophagy would leave damaged cells compromised and at risk of perpetuating further damage to neighbouring cells. This cascade, when occurring in post-mitotic tissue such as brain, would present clinically with neurological deterioration after a threshold of cellular functional impairment is exceeded. But the precise mechanism by which the beta-propeller protein that is encoded by *WDR45* serves the autophagic process remains to be elucidated.

In conclusion, significant basal ganglia pathology was observed on histology and immunohistochemistry. The major pathological findings in this case were severe neuronal loss with gliosis affecting the substantia nigra, iron deposition in the substantia nigra and globus pallidus, axonal swellings in the substantia nigra, gracile nucleus and cuneate nucleus and very extensive phospho-tau deposition. Tau isoforms were similar as tau deposits observed in AD cases. The higher autophagy reflux observed in LC3 immunoblotting is consistent with the understanding that the WDR45 protein participates in autophagy. Though the precise steps in autophagy are not known yet, BPAN provides a direct link between autophagy and neurodegeneration. It would be interesting to elucidate the role of iron in this mechanism.

8.6. Neuropathology of Neuroacanthocytosis

8.6.1. Background

NA encompasses a group of genetically heterogeneous disorders characterized by neurologic signs and symptoms associated with acanthocytosis, an abnormality of red blood cells (246). The autosomal recessive type, called chorea-acanthocytosis (ChAc), is the most common form of NA and is linked to the mutations in *VPS13A* gene (251,252,254,255) mapped to chromosome 9q21 and consists of 73 exons encoding chroein (255,256). The degeneration of the basal ganglia is a consistent feature of NA disorder. On autopsy of NA cases, the cerebral cortex appears unaffected.

8.6.2. Aims and Hypothesis

Hypothesis

- The degeneration of the basal ganglia is a consistent feature of NA.

Aim

- To review and characterise the neuropathology of an archival, previously published NA case using modern methods.

8.6.3. Methods

Paraffin blocks representing multiple brain regions from a post mortem case of NA were obtained from QSBB and investigated using routine histological and

immunohistochemical methods as described in Chapter 2. Details of this case had previously been published (case 13 and case 2 respectively)(345,346) but analysis using current IHC techniques had never been performed.

Clinical details and macroscopic description of the brain were obtained from the records of the QSBB. Antibodies used for IHC include: ubiquitin (1:200, Dako, Ely,UK), tau (1:600, AT8, Autogen Bioclear, Calne, UK); AT100 (1:200, Innogenetics, Gent, Belgium), glial fibrillary acidic protein (GFAP; 1:1,000, Dako), Aβ (1:200, Dako), α-synuclein (1:50, Novacastra, Newcastle, UK), α-synuclein (1:1000, BD Transduction Biolabs, Oxford, UK), P62 (1:100, BD Bioscience, Oxford, UK), CD68 (1:150, Dako) and TDP-43 (1:2000, Protein Tech, Manchester, UK).

8.6.4. **Results**

The patient was a 56 year old Caucasian male. He was treated for depression aged 26 and showed behaviour disturbance, personality change and cognitive impairment. He developed progressive generalized chorea from the age of 44 years when on drug treatment. He was admitted to a psychiatric hospital aged 47 years and remained a resident there. He had two generalised tonic-clonic seizures aged 50 and 51 years. On examination aged 51 years, his verbal and performance IQ's were below his estimated average level. There was a mild impairment of saccadic and smooth pursuit eye movements, facial impassivity with mild orofacial dyskinesia, occasional blepharospasm and a brisk jaw reflex. Chorea was mild and generalized while the patient was on Sulpiride and tetrabenazine with additional

severe Parkinsonism and a lurching gait. The small muscles on his hands and feet were wasted, tendon reflexes were absent, plantar responses was flexor and vibration sense was impaired distally. His Parkinsonism had not resolved three months after withdrawal of medication. Laboratory data revealed slightly elevated serum creatine kinase level (261 IU/1) and acanthocytes (30%) in peripheral blood. Computerised tomography (CT) scan showed mild cerebral and caudate atrophy. Electroencephalography (EEG), standard automated perimetry (SAP) and Motor Nerve Conduction Velocities (MNCV) were normal, but MAP's were small and there was evidence of denervation on electromyography (EMG). He had a daughter who is asymptomatic.

The macroscopic appearances were in keeping with the clinical diagnosis of NA. At autopsy, the fixed brain weighed 1505 grams. The leptomeninges were thin. There was no evidence of herniation at the base. Basal vessels showed a few plaques of non-occlusive atheroma. Cranial nerves appeared normal. The caudate nucleus, putamen and pallidum were atrophic with brown pigmentation throughout these nuclei. The ventricular surface of caudate was concave. The lateral ventricles were moderately dilated. Pigmentation of substantia nigra and locus coeruleus was well preserved. The pons, medulla and cerebellum were unremarkable.

Microscopically, neuronal loss and astrocytic gliosis were severe in the caudate nucleus and putamen. The globus pallidus was also gliotic but neuronal loss was not apparent (Figure 8.1). The thalamus was moderately gliotic but neurons were well

preserved. There was mild gliosis and neuronal loss in the substantia nigra and locus coeruleus. In the cerebellum, mild Purkinje cell loss was observed in cerebellar hemisphere and moderate gliosis was observed in the Bergmann layers and white matter. There were occasional empty baskets but no torpedoes. Diffuse iron deposition was detected in the caudate and putamen using Perl's stain. Tau pathology in the form of neurofibrillary tangles and neuropil threads corresponding to Braak and Braak stage I was observed in CA1, entorhinal and transentorhinal cortex of hippocampus. A single ubiquitin positive intraneuronal inclusion of uncertain nature and significance was observed in the subiculum. Sparse diffuse Aβ deposits were observed in cortical regions (frontal, temporal, occipital and cingulate) and sparse diffuse plaques in transentorhinal cortex of hippocampus. Small vessel disease and cerebral amyloid angiopathy were absent. There was no α-synuclein or TDP-43 pathology in brainstem or limbic regions respectively.

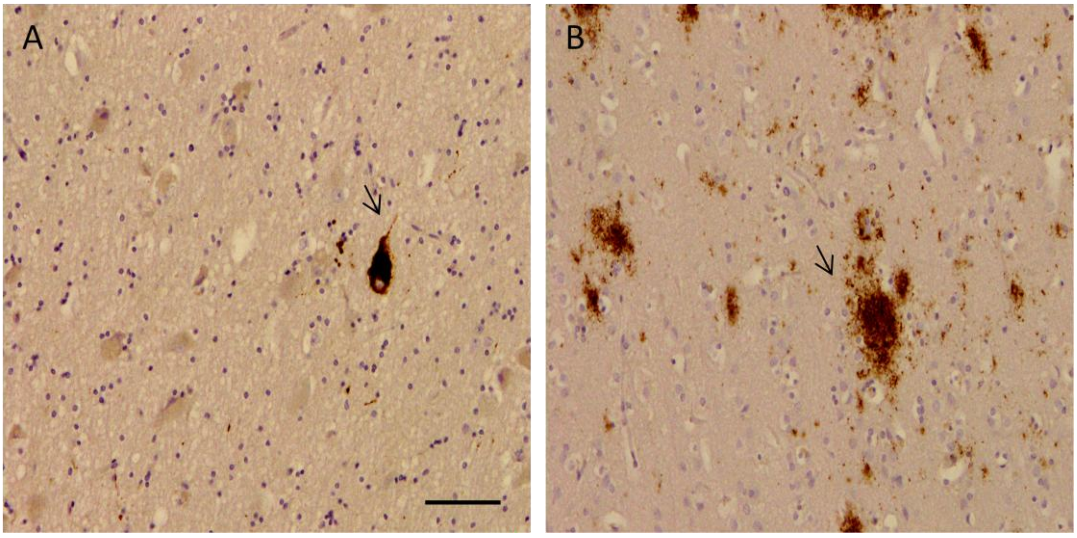

Figure 8.8 Histological findings in hippocampus of neuroacanthocytosis case. Tau pathology in the form of neurofibrillary tangles and neuropil threads was observed in CA1, entorhinal and transentorhinal cortex (A). Sparse diffuse plaques were observed in transentorhinal cortex (B). Scale bar represents 30µm. A: AT8 IHC and B: Aβ IHC.

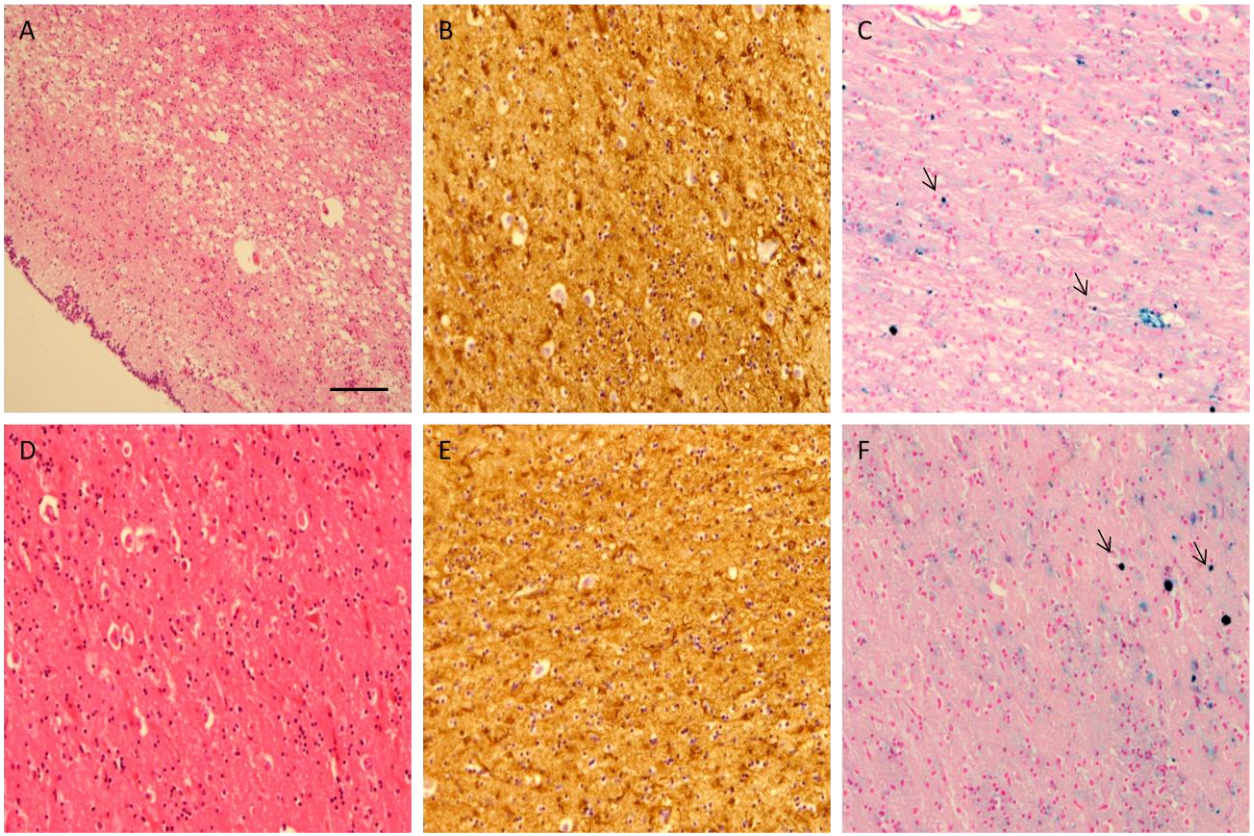

Figure 8.9 Histological findings in caudate (top panel) and putamen (bottom panel) of neuroacanthocytosis case. Neuronal loss and astrocytic gliosis were severe in the caudate nucleus and putamen with iron accumulation. Scale bar: A= 60µm, B-F=30 µm. A and D: H&E; B and E: GFAP IHC and C and F: Perl's stain.

Table 8.2 Semiquantitative analysis of the IHC stains in a Neuroacanthocytosis case

Regions	Neuronal loss	Gliosis	Tau	α-syn	Aβ		Iron deposit-ion	CAA	SVD	Phospo TDP-43
					D	M				
Cortex										
Frontal	-	-	-	-	+	-	-	-	-	-
Motor	-	-	-	-	-	-	-	-	-	-
Temporal	-	-	-	-	+	-	-	-	-	-
Parietal	N/A	N/A	N/A	N/A	N/A	N/A	N/A	N/A	N/A	N/A
Occipital	-	-	-	-	++	-	-	-	-	-
Cingulate	-	-	-	-	++	-	-	-	-	-
Insular	N/A	N/A	N/A	N/A	N/A	N/A	N/A	N/A	N/A	N/A
Amygdala	-	++	-	-	-	-	-	-	-	-
Hippocampus										
Dentate fascia	-	-	-	-	-	-	-	-	-	-
CA4	-	-	-	-	-	-	-	-	-	-
CA3	-	-	-	-	-	-	-	-	-	-
CA2	-	-	-	-	-	-	-	-	-	-
CA1	-	-	+	-	-	-	-	-	-	-
Subiculum	-	-	+	-	-	-	-	-	-	-
Entorhinal cortex	-		+	-	-	-	-	-	-	-
Transentorhinal cortex	-	-	+	-	+	-	-	-	-	-
Caudate	+++	+++	-	-	-	-	+	-	-	-
Putamen	+++	+++	-	-	-	-	+	-	-	-
Globus pallidus	-	+++	-	-	-	-	-	-	-	-
Thalamus	-	-	-	-	-	-	-	-	-	-
Subthalamic nucleus	-	-	-	-	-	-	-	-	-	-
Red nucleus	-	-	-	-	-	-	-	-	-	-
IIIrd nerve nucleus	N/A	N/A	N/A	N/A	N/A	N/A	N/A	N/A	N/A	N/A
Substantia nigra	+	-	-	-	-	-	-	-	-	-
Locus coeruleus	+	-	-	-	-	-	-	-	-	-
Pontine nuclei	-	-	-	-	-	-	-	-	-	-
Pontine base white matter	-	-	-	-	-	-	-	-	-	-
Dorsal motor nucleus of vagus	-	-	-	-	-	-	-	-	-	-
Twelfth nerve nucleus	-	-	-	-	-	-	-	-	-	-
Inferior olive	-	-	-	-	-	-	-	-	-	-
Cerebellar hemisphere Purkinje cells	+	-	-	-	-	-	-	-	-	-
Cerebellar hemisphere white matter	-	++	-	-	-	-	-	-	-	-
Dentate nucleus	-	-	-	-	-	-	-	-	-	-

N/A: not applicable; -: absent; +: sparse/mild; ++: moderate; +++: severe; D: diffuse; M: mature; CAA: cerebral amyloid angiopathy; SVD: small vessel disease

8.6.5. **Discussion**

The neuropathological features of clinically diagnosed ChAc reported previously include marked atrophy, neuronal loss and gliosis of the caudate nucleus and putamen (259,345–351). Chorea is a major clinical feature of AR and AD ChAc but also occurs in HD (352), dentatorubropallidoluysian atrophy (352), HD like-2 (353,354), neuroferritinopathy (232,355) and pantothenate kinase-associated neurodegeneration (222).

Marked atrophy, neuronal loss and gliosis of the striatum and globus pallidus observed in this case is similar to the previous findings in AR and AD-ChAc with mutation in *VPS13A* gene (259,347). Iron accumulation in the brain is a hallmark not only in NBIA diseases but is also found in PD and AD (243), and in Huntington's disease (356). Iron deposition in the striatum was observed in this case with Perl's positive stain. MRI has demonstrated iron deposition in the globus pallidus, substantia nigra, and red nucleus along with caudate and putamen in an AR-ChAc case (357). This feature was linked to the "eye-of-the-tiger" sign described in PKAN and a common pathway responsible for clinical manifestations in both these neuroacanthocytosis syndromes, ChAc and PKAN.

The loss of chorein expression has been suggested as a diagnostic feature of ChAc. Experiments using a gene-targeted mouse model of AR-ChAc revealed an increased level of gene expression of gephyrin, which is known to be a $GABA_A$ receptor-anchoring protein, in comparison to the wild type controls. Hence, chorein

functional loss may lead to a compensatory upregulation of gephyrin and GABRG2 in the pathologic condition in ChAc (262,358,359).

The occurrence of acanthocytes is not known and is very likely due to a distinct primary cause in each syndrome depending on the respective gene defect. The ChAc-associated protein VPS13A apparently plays a role in vesicle tethering along the recycling or late endosomal (RE/LE) pathway; late endosomes/lysosomes will eventually fuse with autophagosomes to autolysosomes (262). Absence or dysfunction of VPS13A may thus interfere with autolysosomal degradation of cargo and may lead to accumulation of aggregates. The protrusions and thorns of acanthocytes could perhaps be viewed as an arrested state among a multitude of continuously changing states of membrane deformation, thus potentially providing insights into basic mechanisms of cell biology (262). To determine the pathomechanisms underlying the neuropathology of AR-ChAc, further studies of ChAc brains are necessary, including analyses of the expression of chorein and related molecules.

Chapter 9. Lewy bodies (LBs) in Lysosomal storage disorders (LSDs)

9.1. Background

Inherited metabolic disorders which have been linked to lysosomal dysfunction belong to a family of diseases identified as sphingolipidoses, a class of LSDs. The main members of sphingolipidoses are NPC, Krabbe disease, Gaucher disease, Fabry disease, Tay-Sachs disease, Sandhoff diasease and metachromatic leukodystrophy. Lysosome is central to the autophagy process, it is not unreasonable to assume this pathway is integral in protecting against neurodegeneration. LSDs occurring due to the enzyme dysfunction in ceramide pathway also develop LB pathology, for example, NPC, Krabbe disease, and Gaucher disease. Hence, a possibility is that LSDs, G_{M1}, Tay-Sachs disease, Sandhoff disease, Fabry disease and metachromatic leukodystrophy which occur due to the enzyme dysfunction in the ceramide pathway may mimic the LB pathology.

9.2. Aims and Hypothesis

Hypothesis

- That LB pathology may be a common feature in the LSDs due to the enzyme dysfunction in the ceramide pathway.

Aim

- To assess LB pathology in the LSDs cases (G_{M1}, Tay-Sachs disease, Sandhoff disease, Fabry disease and metachromatic leukodystrophy).

9.3. Methods

Paraffin blocks (frontal cortex, hippocampus, substantia nigra, pons) for LSDs, Leukodystrophy metachromatic, Sandhoff disease, Fabry's disease, Tay-Sachs disease, and Gangliosidosis GM1 were obtained from BTDBB and investigated using routine histological staining and IHC methods as described in Chapter 2. Antibodies used for IHC include: ubiquitin (1:200, Dako, Ely, UK), α-synuclein (1:50, Novacastra, Newcastle, UK), α-synuclein (1:1000, BD Transduction Biolabs, Oxford, UK) and P62 (1:100, BD Bioscience, Oxford, UK).

9.4. Results

9.4.1. Clinical data

Demographics and clinical history are summarized in Table 9.1.

Table 9.1 Summary of demographics and clinical data for LSD cases					
Cases UMB#	**Sex**	**Ethnicity**	**Age at onset, years**	**Age at death, years**	**Clinical diagnosis and neuropathological data***
1231	M	Caucasian	14	60	Leukodystrophy, Metachromatic
1814	M	Caucasian	N/A	1	Sandhoff Disease • lost developmental milestones at 13 months • macular cherry red spot in both eyes, myopic astigmatism
4299	M	Caucasian	38	50	Fabry's Disease • ruptured basilar aneurysm - subarachnoid hemorrhage, severe brain edema and acute hypoxic ischemic encephalopathy • neuronal storage and small remote cerebral infarcts
5094	M	Caucasian	3	27	Tay-Sachs Disease • learning difficulties, increased agitation, developmental regression and behaviour difficulties • moderate cerebellar atrophy, cerebellar degeneration with storage
5384	M	Caucasian	7	19	Gangliosidosis, GM1 • low beta-galactosidase activity • slow course of neurodegeneration and seizures • global cerebral atrophy (i) neuronal cytoplasmic storage material positive for Luxol fast blue (ii) ultrastructural evidence of myelin and few zebra bodies (iii) extensive cortical neuronal loss, mild to moderate gliosis, moderate white matter gliosis
5596	F	Caucasian	N/A	1	Gangliosidosis, GM1
N/a: not available, *****Derived from the neuropathological report available from BTDBB					

Case 1, Leukodystrophy, Metachromatic – The case is a Caucasian male 60 years old at death. The disease onset was at the age of 14. No further clinical history was available.

Case 2, Sandhoff disease – The case is a Caucasian male 1 year old at death. His chromosomal analysis was normal but had very low lysosomal enzyme (hexosaminidase A) activity. Opthalmologic examination reported macular cherry red spot in both eyes and myopic astigmatism. At 13 months old he lost all the developmental milestones achieved. He died from the complications of the disorder. Detailed neuropathological examination report was not available but was consistent with the presentation of the Sandhoff disease.

Case 3, Fabry's disease – The case is a Caucasian male 50 years old diagnosed with Fabry's disease at the age of 38. Neuropathological examination revealed ruptured basilar aneurysm causing subarachnoid hemorrhage, severe brain edema and acute hypoxic ischemic encephalopathy. Neuronal storage and small remote cerebral infarcts were reported.

Case 4, Tay-Sachs disease - The case is a Caucasian female 27 years old at death with a history of late onset Tay - Sachs disease who had mycolonus, behavioural problems and seizure like activity. Her presentation was at age 3 when she had coordination problems and was diagnosed at age 11. Genetic studies revealed a late-onset genetic mutation in father and an unsual mutation in the mother. She had learning difficulties and at age 17 she had increased agitation, developmental

regression and behaviour difficulties. MRI suggested moderate cerebellar atrophy which is consistent with the parent's clinical history of GM2 deficiency. Neuropathological examination of the brain confirmed the diagnosis of GM2 gangliosidosis. The cerebrum and cerebellum were atrophic and there was neuronal and glial storage. The neuronal storage was most severe in the deep gray nuclei than in the cerebral cortex.

Case 5, Gangliosidosis- GM1 – The case is Caucasian male 19 years old at death. He was diagnosed with type 2 GM1 gangliosidosis by enzyme testing at the age of 7. He developed a slow course of neurodegeneration and seizures. He had no acute illines surrounding his death. Neuropathological examination of the brain confirmed the clinical diagnosis. The brain weighed 679g (expected 980g) showing global cerebral atrophy. Extensive cortical neuronal loss was reported along with mild-moderate gliosis of the cortex and the white matter. Neuronal cytoplasmic storage materials were positive for Luxol fast blue.

Case 6, Gangliosidosis- GM1 – The case is Caucasian female 1 year old at death. She died from complications of the disorder. No further medical history was available.

9.4.2. **Neuropathology**

Using two different α-synuclein antibodies for IHC investigation on all tissues sections available for the five LSD cases no cortical or brainstem LBs could be identified.

Case 1, Leukodystrophy, Metachromatic – Frontal cortex and hippocampus were well preserved. There was mild neuronal cell loss in substantia nigra and locus coeruleus. LB pathology was negative.

Case 2, Sandhoff disease – Cortex was well preserved but white matter was pale. There was mild neuronal cell loss in hippocampus. Neuronal storage in cells was observed in the granule cell layer. LB pathology was negative.

Case 3, Fabry's disease – Frontal cortex was well preserved. LB pathology was negative.

Case 4, Tay Sachs disease – Swollen granule cells with neuronal storage were observed in hippocampus. LB pathology was negative.

Case 5, Gangliosidosis- GM1 – there was mild neuronal cell loss in the frontal cortex with swollen neurons. The hippocampus was well preserved. Substantia nigra showed loss of pigmentation in the neuronal cells. LB pathology was negative.

Case 6, Gangliosidosis- GM1 – There was mild neuronal loss in the frontal cortex. LB pathology was negative.

9.5. Discussion

Deposition of filmentous α-synuclein in the neuronal or glial cytoplasm is a common pathological feature of many neurological diseases, such as PD, dementia with LBs, multiple system atrophy and NBIA. Animal models developed in mice and

flies have shown that the overexpression of α-synuclein leads to the formation of both filamentous and granular aggregates. It has been shown that that cells are capable of clearing preformed α-synuclein aggregates via the lysosomal degradation pathway (360), blocking this pathway causes the accumulation of the α-synuclein aggregates in cells. It is suggested that once formed, the α-synuclein inclusions are refractory to clearance (361). The link between lysosomal malfunction has been associated with age-related neurodegenerative disorders and inhibition of the lysosomal enzymes leads to features such as protein deposition, synaptic loss and neuronal death (361). Lysosomes are a critical component for all forms of autophagy and auto-phagy-mediated clearance of damaged proteins is particularly important for neuronal survival. Impaired autophagy is observed in patients with LSDs (362). LSDs comprise mainly of sphingolipidoses, are a group of monogenic inherited diseases caused by defects in the proteins involved in the lysosomal sphingolipid degradation, with subsequent accumulation of non-degradable storage material in one or more organs (273).

The hypothesis that if LSDs, NPC, Gaucher disease and Krabbe disease in the ceramide pathway have shown LB pathology, other LSDs along the pathway impinging on to ceramide may mimic the pathology. However, neuropathological study of a case each of GM1 gangliosidosis, Tay-Sachs disease, Sandhoff disease, Fabry disease and metachromatic leukodystrophy was negative for alpha-synuclein deposition. The reasons could be (a) the LSDs we included in this study are not directly impinging on to the ceramide where as LSDs which are related to α-

synuclein deposition in the literature (Gaucher disease, NPC and Krabbe disease) are directly related or impinging on to free ceramide synthesis (Figure 1.10). In Gaucher, NPC and Krabbe diseases, the role of the respective metabolic enzyme defect appears to be more crucial for LB formation and these enzymes produce the free ceramide. Hence LB formation may be a response to the direct stress in ceramide synthesis. (b) The life span necessary for LB formation may not be sufficient. The age in the cohort varied from 1 to 60 years old at death. In NPC cases, classic LBs were observed in cases as young as 23 years old at death. Cases below that age showed diffuse immunoreactivity with threads and dots and pre-LBs scattered (283). However, neurodegenerative diseases with tau-based inclusions have been shown to increase the α-synuclein inclusions and tau pathology has been described in NPC cases (283,363). Hence, the GM1 gangliosidosis and Sandhoff cases aged 1 at death may not have enough life span to develop LBs. The absence of LBs in the other cases aged 19, 27, 50 and 60 years at death can also be attributed to the age factors as in normal human controls LBs tend to appear after 60 years old. However, in the latter two cases, if LBs are the hallmark of their respective diseases pre-LBs or diffuse α-synuclein immunoreactivity in the predicted brain regions would have been expected. Hence, this study concludes that LBs cannot be considered as a hallmark of all LSDs with enzyme defects in the ceramide pathway.

Chapter 10. Sumary and future directions

Neuropathology has been the key in understanding the aetiologyl of many neurological disorders such as AD, PD, frontotemporal degeneration and cerebellar ataxias. Dystonia shares many clinical features with these conditions but research in general, has been unrewarding in providing information on disease processes. Neuropathological studies in dystonia cases are few in number and only limited morphological abnormalities have been described. The aim of this project was to understand the neuropathology of rare genetic neurological disorders, in particular dystonia. To address this, we designed experiments to explain the following questions:

- Do perinuclear neuronal inclusions represent a hallmark lesion in primary pure dystonia, DYT1 and DYT6?

- Does a common theme in the pathogenesis of primary dystonia exist?

- Does interaction takes place between the two primary dystonia genes in human CNS?

- Are non-coding mutations important in understanding disease pathology (with an example of primary plus dystonia, DYT5 cohort)?

- Can we draw the relationship between the repeat lengths and disease pathogenesis in secondary dystonia (with an example of SCA8 repeats in ataxia cohort)?

- Does *WDR45* gene provide a link between neurodegeneration and autophagy (with an example of secondary dystonia, BPAN)?

- Can we expect common disease pathology for disorders in a common pathway (with an example of LSDs in ceramide pathway)?

The work performed in this thesis, I have:

- Determined that primary pure dystonia cases lack a neuropathological hallmark and that the perinuclear neuronal cytoplasmic inclusions are not a consistent feature of the disorder.

- Demonstrated that the interaction between two primary dystonia genes may exist in basal ganglia but the cohort is too small to draw a firm conclusion.

- Identified the importance of understanding the pathogeneity of genetic mutations or repeat lengths. In DRD, non-coding mutations in 5'UTR of *GCH1* needs consideration but it is important to understand the functional aspects of the mutation before giving a 'disease causing' status. Repeat lengths in SCA8 may provide a basis to determine the affected individuals

but it should not be the only way to determine the disease in genetic testing.

- Determined that autophagy is directly linked to neurodegeneration in a case of BPAN.

- Demonstrated that even a small change may contribute to the disease pathology and that a common pathology may not exist for disorders due to enzyme dysfunction in the same pathway.

When I began this project, there were limited neuropathological reports available for the DYT1 cases. In addition, the first report demonstrating the perinuclear inclusion in DYT1 cases (129) was published 10 years ago. Between the first paper and when I began to investigate the neuropathology of DYT1 cases, no other pathological reports are available for DYT1 cases. The neuropathology of DYT6 case is the first ever detailed neuropathological investigation carried out to our knowledge. Therefore, the work in this thesis contributes to the field of dystonia.

10.1. Summary for primary pure dystonias (DYT1 and DYT6)

There is accumulating evidence for genetic and clinical heterogeneity in primary dystonia. There has been an unprecedented advance in our understanding of the primary and secondary dystonia syndromes with the speed of genetic discoveries. However, many of the new genes identified have yet to be independently confirmed and their prevalence as a cause of dystonia is as yet unclear to avoid

duplication. For example, mutations in *PRRT2* were identified as the cause of PKD and defined as a locus, DYT10. However, mutation in the gene was also found in the family used to define DYT19 which is a separate form of PKD, suggesting that the initial linkage in this family was incorrect and DYT19 is in fact synonymous with DYT10 (364). Owing to the serious shortcomings with assigning the DYTn loci based on statistical associations (314), the new classification system highlights the importance of biological phenomena in understanding the disorders. By combining phenomenology and biological mechanism in the same classification, it becomes easier for diagnostic testing and clinical recognition of dystonia syndromes. This will also help to keep the clinical practice and scientific discoveries at the same pace. The findings in this thesis will contribute towards classifying primary pure dystonia cases, DYT1 and DYT6 based on etiology.

Neuropathological studies in dystonia are sparse, partly due to the low availability of post-mortem tissue from these patients and the labour intensive nature of exploratory neurological examination of the entire human brain. This study documents a series of neuropathological findings from the largest cohort of genetically confirmed primary pure dystonia (DYT1-7 cases and DYT6-2 cases) cases ever evaluated. Using the immunohistochemical staining battery NFTs, LBs, beta-amyloid plaques, SVD, CAA, neuronal loss, gliosis and axonal swellings noted in both cohorts of DYT1 and DYT6 cases, respectively are comparable to the age and sex matched human control brains and observed in symptomatic and non-manifestating carriers as well. No consistent abnormality or perinuclear inclusions

previously described was detected to link directly to the pathogenicity of the disease in brain regions implicated. The absence of neurodegeneration in primary dystonia, as well as observations that lesions of brain regions other than the basal ganglia can lead to secondary dystonia, have led to the concept of dystonia as a neuro-functional disorder. This study supports the notion that dystonia is a motor system disorder rather than a disease of a particular motor structure.

The increasing knowledge of proteins whose mutant forms cause dystonia has implicated a large number of neurobiological pathways that lead to dystonic movements. A number of themes have emerged that have been identified from abnormal transcription and cell cycle because of the nuclear effects of dystonia genes to endoplasmic reticulum dysfunction and synaptic abnormalities (365). The EFNS dystonia classification system (13) put these dystonia genes (*TOR1A, THAP1, CIZ1, TUBB4,* or *GNAL*) in one class of primary pure dystonia. Hence it seems right to seek common pathways that may represent targets for therapeutic strategies for this movement disorder. However, it may also lead to oversimplification in the search for unifying mechanisms. Most cases of dystonia are primary and not associated with neuronal death. Thus the pathogenic mechanisms may be subtle and only cause relatively mild defects in the relevant pathways, leading to abnormal processing of the motor command within the CNS. A common pathology for dystonias classified based on the clinical characteristics and statistical significance is not always possible as understanding the biological phenomenon is an important aspect in any disorder. The current dystonia classification system may

provide new insights into the disorders by combining the clinical and etiological characteristics of dystonia. For neuropathological diagnostics of dystonia, it is not only necessary to have a good understanding of the functional anatomy of the basal ganglia, but also of a wider network view that includes other structures (amongst others the cerebellum). In case of primary dystonia, subtle changes in the brain need consideration and traditional neuropathological methods may not be sufficient to identify those changes. Hence, there is a need to develop experimental procedures to quantify or analyse these changes.

Protein-protein interactions (PPI) operate at every level of cellular function and are involved in almost all cellular processes. The correct identification of these interactions is important to systematically understand the roles played by cellular proteins in diverse biological functions. Consequently, the prediction of PPI has emerged recently as an important element in the fields of bioinformatics and systems biology. In DYT6 cases, a significant difference in the expression of *TOR1A* and *THAP1* was observed in putamen of a DYT6 cohort supporting the hypothesis that THAP1 represses the expression of *TOR1A* in CNS. However, we also should keep in consideration the surrounding proteins *THAP1* and *TOR1A* are likely to interact with and that these proteins may act as modifiers. THAP1 has been shown to bind to the promoter region of a *TAF1* transcript and it will be interesting to see if *THAP1* and *TAF1* gene show any potential functional link to associate with the clinical phenotype presented for each dystonia type. TorsinA has been shown as having a close association with α-synuclein in LBs (366) where presence of torsinA

in LBs can be a consequence of its role in identifying and interacting with abnormal proteins that must be cleared by the cell. Furthermore, a better understanding of *THAP1* and *TOR1A* protein function and cellular pathogenicity may address the interaction more precisely to improve our understanding of diseases and can also serve as the basis for new therapeutic approaches.

Limitations

The main limitation of the neuropathological investigation in dystonia has been the availability of the post-mortem cases. Hence it would be ideal to increase the number of cases. However, the drawback is more clinical. The low penetrance of primary dystonia genes may leave the cases undiagnosed as the symptoms can be mild. This calls for widening the clinical sprectrum to qualify for genetic testing of DYT1 and DYT6.

The other limitation working with the post-mortem cases is the availability of the brain regions of interest and this hinders the systematic sampling across the cohort. Also the dystonia cohort studied here consisted of cases received from three brainbanks (QSBB, HBB, BTDBB). Each brainbank has its own brain sectioning protocol. Therefore, brain regions available for each case varied and were in variable plane of section. Hence, robust comparision of the neuropathological findings across the cohort was not possible.

The main drawback of the neuropathological study was the unavailability of torsinA and THAP1 antibodies to assess the presence or absence of the torsinA/THAP1 positive inclusions (discussed in detail in Chapter 5). Optimizing new antibodies is always a challenge but reliable human specific antibodies would have given this project a new dimension.

The limitation of using the post-mortem tissue for expression analysis is the preservation of the RNA quality. SYBR green is a cheap and efficient method for analysing the mRNA expression. However, the reliability and accuracy has often been questioned.

10.2. Summary for non-coding 5'UTR mutation in DYT5 dystonia

Medical research has primarily focused on protein-coding variants, due to the difficulty of interpreting non-coding mutations. As technologies evolved over the past century, genetic studies are not limited to studying Mendelian disorders and can tackle more complex phenotypes. For example, genome-wide association studies (GWAS) have provided genome-wide information about the genetic basis of the complex disease across unrelated individuals for common variants associated with complex disease and diverse molecular phenotype (367,368).

In this regard, the hypothesis for this project was established; if the non-coding mutations in the 5'UTR of the *GCH1* gene (181) underlie the clinical manifestation. The cohort consisted of clinically categorized DRD5 cases with *GCH1* mutation spectrum negative for *GCH1* coding mutations. Two unrelated cases were identified

with both -39C>T and -132C>T mutations in the 5' UTR of *GCH1*. However, one of the cases has an affected sibling without these mutations (described in detail in Chapter 6). Functional study identified negligible effect of two mutations (181). Hence, in the DRD cohort studied, there is not enough evidence to conclude that the two non-coding variants underlie the disease manifestation.

Study of evolutionary conservation, functional genomics, sequence motifs, and molecular quantitative trait loci are important in predicting a function of a non-coding variant and relating it to the disease. The list of non-coding variants implicated in human disease will expand from GWAS and whole-genome sequencing technologies. However, there is a need to integrate the genomic data with the functional maps to implicate the pathways and proteins interacting thereby. This will help to replicate the protein interactions experimentally in the scientific laboratories and analyse the pathogenicity of the non-coding variants underlying complex diseases.

Limitation

The unavailability of the recent clinical details for the siblings considered in this study has restricted the current prognosis.

10.3. Summary for SCA8

SCA8 was the first repeat expansion (CAG or CTG) identified in an untranslated region. Potentially pathogenic alleles contain 85 or more combined CTA/CTG

repeats. However, repeats of this size are surprisingly frequent in the general population and also occur in asymptomatic relatives of ataxia individuals (197,204,206,211,340). In the ataxia cohort investigated, the significant difference (p= 0.018) in the occurrence of SCA8 repeat expansions in ataxia patients compared with English controls but not with the diversity controls (p= 0.192) suggests that the pathogenicity of SCA8 repeat expansion is not only dependent on the repeat size but also on the population, environment and the genetic modifiers.

The complex pattern of inheritance has resulted in unaffected carriers commonly having repeat sizes that exceed the pathogenic threshold making it difficult to ascertain clear ranges for pathogenic expansion (199,208). SCA8 may rarely coexist with SCA6 (339) or SCA1 (341) which makes it difficult to assign symptoms to a specific entity. These data demonstrate that the presence of a SCA8 expansion cannot be used to predict whether or not an asymptomatic individual will develop ataxia as the control cases were asymptomatic at the time of study.

However, two cases with SCA8 repeat in the large intermiediate range, 83 and 84 respectively, are in the borderline of the marked pathogenic ranges and were also looked into. They showed all the above clinical criteria for SCA8. The brain MRI in one case showed features consistent with diagnosis of MSA and another case was diagnosed as MSA. Hence, SCA8 expansion may be a susceptibility factor for MSA. This data suggests that SCA8 repeat expansion length should not be the sole

method for diagnostic purposes and patients with progressive cerebellar ataxia may develop other neurodegenerative disease with time.

10.4. Summary for BPAN

This study reports a 51 years old female with a *de novo* mutation in exon 9 of *WDR45*. The disease onset was in childhood characterized by global developmental delay and intellectual deficiency in early childhood then followed by further neurological and cognitive regression in late adolescence or early adulthood, with dystonia, and sometimes ocular defects and sleep perturbation. The clinical pattern of the case studied here matches to other BPAN cases described (229,237,342). BPAN is the only X-linked NBIA described in literature with *de novo* mutations in the *WDR45* gene causing loss of function of the encoded protein; even though the gene is at the chromosome X, males and females present the same clinical phenotype, which seems to be due to somatic mosaicism or skewing of the X chromosome inactivation (229).

PKAN and PLAN are the most common forms of NBIA disorders and PKAN alone accounts for 50% of the all NBIA disorders (342). In PKAN the pathology of the disease was almost exclusively located in the CNS and particularly in the globus pallidus represented by reactive astrocytes, numerous large and granular spheroids, axonal swellings and iron accumulation (223). In PLAN cases, cerebellar cortical atrophy has been a consistent feature in MRI. Iron accumulation in the globus pallidus can be the main feature in atypical cases but is not a consistent

feature in the infantile cases (342). Neuropathological changes have been reported throughtout the CNS, with tau pathology, diffuse α-synuclein positive-LBs in neocortex, depletion of cerebellar granular and Purkinje cells, and numerous axonal swellings and spheroid bodies (342).

Neuropathologically, BPAN and PKAN have similarities with the following characteristics: (a) iron accumulation in basal ganglia is a similar and consistent feature (b) neither are synucleinopathies and (c) tau pathology is present in both. However, BPAN differentiates from PKAN by predominance of substantia nigra iron over that seen in globus pallidus which is reverse in the latter and in PLAN iron accumulates more equally in these structures. In BPAN the substantia nigra is discoloured but in PKAN the globus pallidus is discoloured. The tau pathology observed in BPAN resembles that observed in AD cases (ie. 3R and 4R repeats). However, a close relationship has been suggested between PLAN and PD.

BPAN may provide a link between tau pathology, autophagy impairment, and neurodegeneration. This study supports the involvement of beta–propeller protein (encoded by *WDR45* gene) in autophagy as has been documented in yeast and mammalian cells (245). The increased accumulation of LC3-II protein in brain tissue of the BPAN case compared to the three control cases implies that the autophagosome formation is hindered. However, the role of iron in this process is yet to be understood.

The autophagic process is induced to clear damaged cellular components and by-products of the stress response by cells. Defective autophagy would leave damaged cells compromised and at risk of perpetuating further damage to neighbouring cells. In brain, neurological deterioration is inevitable after a threshold of cellular functional impairment is exceeded. But the precise mechanism by which the beta-propeller protein that is encoded by *WDR45* serves the autophagic process remains to be elucidated.

In conclusion, significant basal ganglia pathology was observed on neuroimaging, histology and IHC. The extensive phospo-tau pathology observed were similar as tau deposits reported in AD cases. The higher autophagy flux indicated by the LC3 blot suggests that the WDR45 protein participates in autophagy. Though the precise steps in autophagy are not known yet, BPAN provides a direct link between autophagy and neurodegeneration. It would be interesting to elucidate the role of iron in this mechanism.

NA

PKAN may be classified as NBIA and NA syndromes as both brain iron accumulation and acanthocytes are found (262). However, in the BPAN case studied acanthocytes were not reported. Cell membrane research may shed light upon the significance of the erythrocyte abnormality, and upon possible connections between PKAN and NA.

10.5. Summary for LSDs and LBs

A great deal of attention has been focused on the assignment of the genetic locus on the clinical basis. However, to identify the pathways of pathogenicity for a given disorder, arguably, one should start by analyzing the genetics of disease based on pathology. The pathological studies are more likely helpful in finding a common pathway if there is a common pathology rather than common clinical characteristics. In this regard, LSDs sharing a role in the ceramide metabolism are discussed based on Figure 1.9.

The hypothesis that if LSDs (NPC disease, Gaucher disease and Krabbe disease) due to mutations encoding enzyme components in the ceramide pathway have LB pathology, other LSDs associated with further components of the same pathway impinging on ceramide may result in similar pathological changes. Alpha-synuclein immunohistochemical staining of a case each of GM1 gangliosidosis, Tay-Sach disease, Sandhoff disease, Fabry disease and metachromatic leukodystrophy was negative for alpha-synuclein deposition.

This study concludes that diseases with gene defects influencing the same pathway may not result in similar pathology. As in the ceramide pathway, metabolic enzymes defective for each of the diseases have a role in breaking down monosaccharides into simpler forms but are not involved directly in producing free ceramide except in NPC, Gaucher and Krabbe disease. This puts an emphasis on a role of free ceramide in LB formation and that LBs are a response to the stress

created by the free ceramide in the cells. If LB pathology is the hallmark of the disease, it may only become apparent in those dying at advanced age. In NPC cases, α-synuclein immunoreactivity has been observed in a case as young as 3 years old. However, neurodegenerative diseases with tau-based inclusions have been shown to increase the α-synuclein inclusions and tau has been described in NPC cases (283,363).

The overall level of ceramides in a cell is a balance between the need for sphingosine and sphingosine derivatives, such as sphingosine-1-phosphate, and the sphingomyelins. With respect to the sphingomyelins they serve a dual purpose of being important membrane phospholipids and as a reservoir for ceramides. In the nervous system, neurons are polarized cells and their normal functions, such as neuronal connectivity and synaptic transmission rely on selective trafficking of molecules across plasma membrane. Small changes in the molecular structure of ceramide can regulate its biological function and can contribute in development of age-related, neurological and neuroinflammatory disease (369,370). The abundance of sphingolipids on neural cellular membranes makes them a potent regulator of brain homeostasis.

10.6. Conclusion

Statistical significance is not sufficient to link a disorder with the genetic mutation. Establishing the pathogenesis bears relevance not only to researchers but also to the clinicians. There are pathological and shared mechanisms which overlap with

dystonia and other common neurological disorders such as tau, α-synucleinopathy and autophagy. For example, torsinA shows a close relationship with α-synuclein in LBs; LBs are a result of the stress created by defective enzyme in free ceramide synthesis; in BPAN, defective autophagy may result in tau accumulation; and autophagic flux may produce acanthocytic protrusion in NA. Hence, understanding the cellular pathology of these shared mechanisms may provide some insights into pathogenesis of each disorder.

10.7. Future directions

In this thesis, I investigated genetics and neuropathology of primary (DYT1, DYT6, DYT5) and secondary (SCA8, BPAN, NA, LSDs) dystonias. Given the obstacles encountered, one might question whether it is worthwhile to further investigate for pathological hallmarks in primary dystonia. This thesis provides a basis for the absence of a pathological hallmark in primary pure dystonia. However, it also highlights that the current histological and IHC methods are not sufficient to identify the subtle changes in the brain leading to neurodegeneration. What is important in the future is to take time and design species-specific antibodies and experiments to identify and quantify these subtle changes in the brain. To investigate the PPI it is important to understand the function of the protein under consideration. The ultrastructural localization and function of torsinA and THAP1 are not known yet. Hence, cellular characteristic and pathology of these proteins should be of prior concern.

A recent technology that has opened new horizons in the generation of cellular disease models in the induction of pluripotent stem (iPS) cells from patient skin fibroblast (321,322). The resultant iPS cells were shown to behave similar to human embryonic system (hES) cells in terms of biomarker expression and differentiation potential but retained any mutations present in the genome of the donor cell (371), which makes them suitable for modelling of genetic diseases. This technology offers breaking down a complex genetic disease involving multiple brain areas into its constituent neurons and studying their particular pathology. A cellular pathology resultant from the particular mutation is essential to understand, as cells and their interactions are the key determinant of the motor output and may provide a link for the genetic defect to the observed motor symptoms. However, high level of control in the *in vitro* system can lead to observations being artefacts of culture conditions and not true features of the disease. Hence, cellular pathology should be integrated with the clinical, molecular and pathological presentations of the genetic disorder to provide a therapeutic approach.

Publications associated with this thesis

- Paudel R, Hardy J, Revesz T, Holton JL, Houlden H. Review: genetics and neuropathology of primary pure dystonia. Neuropathol Appl Neurobiol. 2012 Oct;38(6):520–34.
- Paudel R, Kiely A, Li A, Lashley T, Bandopadhyay R, Hardy J, Jinnah HA, Bhatia K, Houlden H, Holton JL. Neuropathological features of genetically confirmed DYT1 dystonia: investigating disease-specific inclusions. Acta Neuropathol Commun. 2014 Nov 18;2(1):159.
- Neuropathology of genetically confirmed DYT6. Ready to submit.
- Neuropathology of a BPAN case. (Drafting)
- SCA8 repeats in ataxia patients (Drafting)

Co-authored publications during this time

- Pure cerebellar ataxia in an Indian consanguineous family caused by a novel homozygous mutation in PNPLA6 (Drafting).
- Houlden H, Schneider SA, **Paudel R**, Melchers A, Schwingenschuh P, Edwards M, et al. THAP1 mutations (DYT6) are an additional cause of early-onset dystonia. Neurology. 2010 Mar 8; 74 (10):846–50.
- Kruer MC, Salih MA, Mooney C, Alzahrani J, Elmalik SA, Kabiraj MM, Khan AO, **Paudel R**, Houlden H, Azzedine H, Alkuraya F. C19orf12 mutation leads to a pallido-pyramidal syndrome. Gene. 2014 Mar 10;537 (2):352-6.

- Xiromerisiou G, Houlden H, Scarmeas N, Stamelou M, Kara E, Hardy J, Lees AJ, Korlipara P, Limousin P, **Paudel R**, Hadjigeorgiou GM, Bhatia KP. THAP1 mutations and dystonia phenotypes: genotype phenotype correlations. Mov Disord. 2012 Sep 1;27 (10):1290-4.
- Kruer MC, **Paudel R**, Wagoner W, Sanford L, Kara E, Gregory A, Foltynie T, Lees A, Bhatia K, Hardy J, Hayflick SJ, Houlden H.Analysis of ATP13A2 in large neurodegeneration with brain iron accumulation (NBIA) and dystonia-parkinsonism cohorts. Neurosci Lett. 2012 Aug 8;523 (1):35-8.
- Hersheson J, Mencacci NE, Davis M, MacDonald N, Trabzuni D, Ryten M, Pittman A, **Paudel R**, Kara E, Fawcett K, Plagnol V, Bhatia KP, Medlar AJ, Stanescu HC, Hardy J, Kleta R, Wood NW, Houlden H. Mutations in the autoregulatory domain of β-tubulin 4a cause hereditary dystonia. Ann Neurol. 2013 Apr;73 (4):546-53.
- Koutsis G, Pemble S, Sweeney MG, **Paudel R**, Wood NW, Panas M, Kladi A, Houlden H. Analysis of spinocerebellar ataxias due to expanded triplet repeats in Greek patients with cerebellar ataxia. J Neurol Sci. 2012 Jul 15;318 (1-2):178-80.
- Li A, **Paudel R**, Johnson R, Courtney R, Lees AJ, Holton JL, Hardy J, Revesz T, Houlden H. Pantothenate kinase-associated neurodegeneration is not a synucleinopathy. Neuropathol Appl Neurobiol. 2012 Mar 15.

References

1. Azevedo FAC, Carvalho LRB, Grinberg LT, Farfel JM, Ferretti REL, Leite REP, et al. Equal numbers of neuronal and nonneuronal cells make the human brain an isometrically scaled-up primate brain. J Comp Neurol. 2009 Apr 10;513(5):532–41.

2. Kolb B, Whishaw IQ. An introduction to brain and behavior. New York, NY, US: Worth Publishers; 2001. 601 p.

3. Fanh S, Marsden CD, Caine DB. Dystonia 2. Proceedings of the Second International Symposium on Torsion Dystonia. Harriman, New York, 1986. Adv Neurol. 1988;50:1–705.

4. Defazio G, Berardelli A, Hallett M. Do primary adult-onset focal dystonias share aetiological factors? Brain. 2007 May;130(Pt 5):1183–93.

5. Breakefield XO, Blood AJ, Li Y, Hallett M, Hanson PI, Standaert DG. The pathophysiological basis of dystonias. Nature Reviews Neuroscience. 2008;9(3):222–34.

6. Geyer HL, Bressman SB. The diagnosis of dystonia. Lancet Neurol. 2006 Sep;5(9):780–90.

7. Albanese A, Bhatia K, Bressman SB, DeLong MR, Fahn S, Fung VSC, et al. Phenomenology and classification of dystonia: a consensus update. Mov Disord. 2013 Jun 15;28(7):863–73.

8. Nutt JG, Muenter MD, Melton LJ 3rd, Aronson A, Kurland LT. Epidemiology of dystonia in Rochester, Minnesota. Adv Neurol. 1988;50:361–5.

9. Duffey PO, Butler AG, Hawthorne MR, Barnes MP. The epidemiology of the primary dystonias in the north of England. Adv Neurol. 1998;78:121–5.

10. The Dystonia Society - About Dystonia [Internet]. 2012 [cited 2012 Apr 24]. Available from: http://www.dystonia.org.uk/index.php/about-dystonia

11. A prevalence study of primary dystonia in eight European countries. J Neurol. 2000 Oct 1;247(10):787–92.

12. Charlesworth G, Bhatia KP, Wood NW. The genetics of dystonia: new twists in an old tale. Brain. 2013 Jul;136(Pt 7):2017–37.

13. Albanese A, Asmus F, Bhatia KP, Elia AE, Elibol B, Filippini G, et al. EFNS guidelines on diagnosis and treatment of primary dystonias. European Journal of Neurology. 2011;18(1):5–18.

14. Lorincz MT. Neurologic Wilson's disease. Ann N Y Acad Sci. 2010 Jan;1184:173–87.

15. Ross CA, Tabrizi SJ. Huntington's disease: from molecular pathogenesis to clinical treatment. Lancet Neurol. 2011 Jan;10(1):83–98.

16. Schneider SA, Bhatia KP. Secondary dystonia--clinical clues and syndromic associations. Eur J Neurol. 2010 Jul;17 Suppl 1:52–7.

17. Altenmüller E, Müller D. A model of task-specific focal dystonia. Neural Netw. 2013 Dec;48:25–31.

18. Martino D, Berardelli A, Abbruzzese G, Bentivoglio AR, Esposito M, Fabbrini G, et al. Age at onset and symptom spread in primary adult-onset blepharospasm and cervical dystonia. Mov Disord. 2012 Sep 15;27(11):1447–50.

19. Djarmati A, Schneider SA, Lohmann K, Winkler S, Pawlack H, Hagenah J, et al. Mutations in THAP1 (DYT6) and generalised dystonia with prominent spasmodic dysphonia: a genetic screening study. Lancet Neurol. 2009 May;8(5):447–52.

20. Pekmezovic T, Svetel M, Ivanovic N, Dragasevic N, Petrovic I, Tepavcevic DK, et al. Quality of life in patients with focal dystonia. Clin Neurol Neurosurg. 2009 Feb;111(2):161–4.

21. Page D, Butler A, Jahanshahi M. Quality of life in focal, segmental, and generalized dystonia. Mov Disord. 2007 Feb 15;22(3):341–7.

22. Defazio G, Gigante AF. The environmental epidemiology of primary dystonia. Tremor Other Hyperkinet Mov (N Y). 2013;3.

23. Pavese N. Dystonia: hopes for a better diagnosis and a treatment with long-lasting effect. Brain. 2013 Mar;136(Pt 3):694–5.

24. Blood AJ, Kuster JK, Woodman SC, Kirlic N, Makhlouf ML, Multhaupt-Buell TJ, et al. Evidence for altered basal ganglia-brainstem connections in cervical dystonia. PLoS ONE. 2012;7(2):e31654.

25. Lanciego JL, Luquin N, Obeso JA. Functional neuroanatomy of the basal ganglia. Cold Spring Harb Perspect Med. 2012 Dec;2(12):a009621.

26. Obeso JA, Lanciego JL. Past, present, and future of the pathophysiological model of the Basal Ganglia. Front Neuroanat. 2011;5:39.

27. Müller U. The monogenic primary dystonias. Brain. 2009 Jan 8;132(8):2005–25.

28. Albin RL, Young AB, Penney JB. The functional anatomy of basal ganglia disorders. Trends Neurosci. 1989 Oct;12(10):366–75.

29. Alexander GE. Basal ganglia-thalamocortical circuits: their role in control of movements. J Clin Neurophysiol. 1994 Jul;11(4):420–31.

30. Alexander GE, Crutcher MD, DeLong MR. Basal ganglia-thalamocortical circuits: parallel substrates for motor, oculomotor, 'prefrontal' and 'limbic' functions. Prog Brain Res. 1990;85:119–46.

31. Berardelli A, Rothwell JC, Hallett M, Thompson PD, Manfredi M, Marsden CD. The pathophysiology of primary dystonia. Brain. 1998 Jul;121 (Pt 7):1195–212.

32. Hallett M. Pathophysiology of dystonia. J Neural Transm Suppl. 2006;(70):485–8.

33. Hedreen JC, Zweig RM, DeLong MR, Whitehouse PJ, Price DL. Primary dystonias: a review of the pathology and suggestions for new directions of study. Adv Neurol. 1988;50:123–32.

34. McGeer EG, McGeer PL. The dystonias. Can J Neurol Sci. 1988 Nov;15(4):447–83.

35. Marsden CD, Obeso JA, Zarranz JJ, Lang AE. The anatomical basis of symptomatic hemidystonia. Brain. 1985 Jun;108 (Pt 2):463–83.

36. Bhatia KP, Marsden CD. The behavioural and motor consequences of focal lesions of the basal ganglia in man. Brain. 1994 Aug;117 (Pt 4):859–76.

37. Asanuma K, Carbon-Correll M, Eidelberg D. Neuroimaging in human dystonia. J Med Invest. 2005 Nov;52 Suppl:272–9.

38. Carbon M, Eidelberg D. Abnormal structure-function relationships in hereditary dystonia. Neuroscience. 2009 Nov 24;164(1):220–9.

39. Meunier S, Lehéricy S, Garnero L, Vidailhet M. Dystonia: lessons from brain mapping. Neuroscientist. 2003 Feb;9(1):76–81.

40. Niethammer M, Carbon M, Argyelan M, Eidelberg D. Hereditary dystonia as a neurodevelopmental circuit disorder: Evidence from neuroimaging. Neurobiol Dis. 2011 May;42(2):202–9.

41. Jankovic J, Tintner R. Dystonia and parkinsonism. Parkinsonism Relat Disord. 2001 Oct;8(2):109–21.

42. Rivest J, Quinn N, Marsden CD. Dystonia in Parkinson's disease, multiple system atrophy, and progressive supranuclear palsy. Neurology. 1990 Oct;40(10):1571–8.

43. Schneider SA, Bhatia KP, Hardy J. Complicated recessive dystonia parkinsonism syndromes. Mov Disord. 2009 Mar 15;24(4):490–9.

44. Tolosa E, Compta Y. Dystonia in Parkinson's disease. J Neurol. 2006 Dec;253 Suppl 7:VII7–13.

45. Perlmutter JS, Mink JW. Dysfunction of dopaminergic pathways in dystonia. Adv Neurol. 2004;94:163–70.

46. Louis ED, Lee P, Quinn L, Marder K. Dystonia in Huntington's disease: prevalence and clinical characteristics. Mov Disord. 1999 Jan;14(1):95–101.

47. Grabli D, Ewenczyk C, Coelho-Braga M-C, Lagrange C, Fraix V, Cornu P, et al. Interruption of deep brain stimulation of the globus pallidus in primary generalized dystonia. Mov Disord. 2009 Dec 15;24(16):2363–9.

48. Ostrem JL, Starr PA. Treatment of dystonia with deep brain stimulation. Neurotherapeutics. 2008 Apr;5(2):320–30.

49. Guehl D, Cuny E, Ghorayeb I, Michelet T, Bioulac B, Burbaud P. Primate models of dystonia. Prog Neurobiol. 2009 Feb;87(2):118–31.

50. Jinnah HA, Hess EJ, Ledoux MS, Sharma N, Baxter MG, Delong MR. Rodent models for dystonia research: characteristics, evaluation, and utility. Mov Disord. 2005 Mar;20(3):283–92.

51. Richter A, Löscher W. Pathology of idiopathic dystonia: findings from genetic animal models. Prog Neurobiol. 1998 Apr;54(6):633–77.

52. Winkler C, Kirik D, Björklund A, Cenci MA. L-DOPA-induced dyskinesia in the intrastriatal 6-hydroxydopamine model of parkinson's disease: relation to motor and cellular parameters of nigrostriatal function. Neurobiol Dis. 2002 Jul;10(2):165–86.

53. Perlmutter JS, Tempel LW, Black KJ, Parkinson D, Todd RD. MPTP induces dystonia and parkinsonism. Clues to the pathophysiology of dystonia. Neurology. 1997 Nov;49(5):1432–8.

54. Tabbal SD, Mink JW, Antenor JAV, Carl JL, Moerlein SM, Perlmutter JS. 1-Methyl-4-phenyl-1,2,3,6-tetrahydropyridine-induced acute transient dystonia in monkeys associated with low striatal dopamine. Neuroscience. 2006 Sep 1;141(3):1281–7.

55. Fernagut PO, Diguet E, Stefanova N, Biran M, Wenning GK, Canioni P, et al. Subacute systemic 3-nitropropionic acid intoxication induces a distinct motor disorder in adult C57Bl/6 mice: behavioural and histopathological characterisation. Neuroscience. 2002;114(4):1005–17.

56. Cuny E, Ghorayeb I, Guehl D, Escola L, Bioulac B, Burbaud P. Sensory motor mismatch within the supplementary motor area in the dystonic monkey. Neurobiol Dis. 2008 May;30(2):151–61.

57. Ghorayeb I, Fernagut PO, Stefanova N, Wenning GK, Bioulac B, Tison F. Dystonia is predictive of subsequent altered dopaminergic responsiveness in a chronic 1-methyl-4-phenyl-1,2,3,6-tetrahydropyridine+3-nitropropionic acid model of striatonigral degeneration in monkeys. Neurosci Lett. 2002 Dec 19;335(1):34–8.

58. Palfi S, Ferrante RJ, Brouillet E, Beal MF, Dolan R, Guyot MC, et al. Chronic 3-nitropropionic acid treatment in baboons replicates the cognitive and motor deficits of Huntington's disease. J Neurosci. 1996 May 1;16(9):3019–25.

59. Burns LH, Pakzaban P, Deacon TW, Brownell AL, Tatter SB, Jenkins BG, et al. Selective putaminal excitotoxic lesions in non-human primates model the movement disorder of Huntington disease. Neuroscience. 1995 Feb;64(4):1007–17.

60. Burn D. Oxford Textbook of Movement Disorders. Oxford University Press; 2013. 375 p.

61. LeDoux MS, Brady KA. Secondary cervical dystonia associated with structural lesions of the central nervous system. Mov Disord. 2003 Jan;18(1):60–9.

62. Münchau A, Dressler D, Bhatia KP, Vogel P, Zühlke C. Machado-Joseph disease presenting as severe generalised dystonia in a German patient. J Neurol. 1999 Sep;246(9):840–2.

63. Carbon M, Argyelan M, Eidelberg D. Functional imaging in hereditary dystonia. Eur J Neurol. 2010 Jul;17 Suppl 1:58–64.

64. Carbon M, Argyelan M, Habeck C, Ghilardi MF, Fitzpatrick T, Dhawan V, et al. Increased sensorimotor network activity in DYT1 dystonia: a functional imaging study. Brain. 2010 Mar;133(Pt 3):690–700.

65. Carbon M, Ghilardi MF, Argyelan M, Dhawan V, Bressman SB, Eidelberg D. Increased cerebellar activation during sequence learning in DYT1 carriers: an equiperformance study. Brain. 2008 Jan;131(Pt 1):146–54.

66. Teo JTH, van de Warrenburg BPC, Schneider SA, Rothwell JC, Bhatia KP. Neurophysiological evidence for cerebellar dysfunction in primary focal dystonia. J Neurol Neurosurg Psychiatr. 2009 Jan;80(1):80–3.

67. Gerwig M, Kolb FP, Timmann D. The involvement of the human cerebellum in eyeblink conditioning. Cerebellum. 2007;6(1):38–57.

68. Sommer M, Grafman J, Clark K, Hallett M. Learning in Parkinson's disease: eyeblink conditioning, declarative learning, and procedural learning. J Neurol Neurosurg Psychiatr. 1999 Jul;67(1):27–34.

69. Pizoli CE, Jinnah HA, Billingsley ML, Hess EJ. Abnormal cerebellar signaling induces dystonia in mice. J Neurosci. 2002 Sep 1;22(17):7825–33.

70. Neychev VK, Fan X, Mitev VI, Hess EJ, Jinnah HA. The basal ganglia and cerebellum interact in the expression of dystonic movement. Brain. 2008 Sep;131(Pt 9):2499–509.

71. Molinari M, Filippini V, Leggio MG. Neuronal plasticity of interrelated cerebellar and cortical networks. Neuroscience. 2002;111(4):863–70.

72. Manto M-U. On the cerebello-cerebral interactions. Cerebellum. 2006;5(4):286–8.

73. Bostan AC, Dum RP, Strick PL. The basal ganglia communicate with the cerebellum. Proc Natl Acad Sci USA. 2010 May 4;107(18):8452–6.

74. Bostan AC, Strick PL. The cerebellum and basal ganglia are interconnected. Neuropsychol Rev. 2010 Sep;20(3):261–70.

75. Ozelius LJ, Lubarr N, Bressman SB. Milestones in dystonia. Movement Disorders. 2011 May;26:1106–26.

76. Kramer PL, Heiman GA, Gasser T, Ozelius LJ, de Leon D, Brin MF, et al. The DYT1 gene on 9q34 is responsible for most cases of early limb-onset idiopathic torsion dystonia in non-Jews. Am J Hum Genet. 1994 Sep;55(3):468–75.

77. Ozelius LJ, Kramer PL, de Leon D, Risch N, Bressman SB, Schuback DE, et al. Strong allelic association between the torsion dystonia gene (DYT1) andloci on chromosome 9q34 in Ashkenazi Jews. Am J Hum Genet. 1992 Mar;50(3):619–28.

78. Ozelius LJ, Hewett JW, Page CE, Bressman SB, Kramer PL, Shalish C, et al. The early-onset torsion dystonia gene (DYT1) encodes an ATP-binding protein. Nat Genet. 1997 Sep;17(1):40–8.

79. Bressman S. Genetics of dystonia. J Neural Transm Suppl. 2006;(70):489–95.

80. Jamora RDG, Tan EK, Liu CP, Kathirvel P, Burgunder JM, Tan L. < i> DYT1</i> mutations amongst adult primary dystonia patients in Singapore with review of literature comparing East and West. Journal of the neurological sciences. 2006;247(1):35–7.

81. Zirn B, Grundmann K, Huppke P, Puthenparampil J, Wolburg H, Riess O, et al. Novel TOR1A mutation p.Arg288Gln in early-onset dystonia (DYT1). Journal of Neurology, Neurosurgery & Psychiatry. 2008 Dec 1;79(12):1327–30.

82. Calakos N, Patel VD, Gottron M, Wang G, Tran-Viet K-N, Brewington D, et al. Functional evidence implicating a novel TOR1A mutation in idiopathic, late-onset focal dystonia. Journal of Medical Genetics. 2009 Dec 2;47(9):646–50.

83. Opal P, Tintner R, Jankovic J, Leung J, Breakefield XO, Friedman J, et al. Intrafamilial phenotypic variability of the DYT1 dystonia: from asymptomatic TOR1A gene carrier status to dystonic storm. Mov Disord. 2002 Mar;17(2):339–45.

84. Tarsy D, Simon DK. Dystonia. New England Journal of Medicine. 2006;355(8):818–29.

85. Hjermind LE, Werdelin LM, Sørensen SA. Inherited and de novo mutations in sporadic cases of DYT1-dystonia. Eur J Hum Genet. 2002 Mar;10(3):213–6.

86. Kustedjo K, Bracey MH, Cravatt BF. Torsin A and Its Torsion Dystonia-associated Mutant Forms Are Lumenal Glycoproteins That Exhibit Distinct Subcellular Localizations. Journal of Biological Chemistry. 2000;275(36):27933–9.

87. Hewett J, Gonzalez-Agosti C, Slater D, Ziefer P, Li S, Bergeron D, et al. Mutant torsinA, responsible for early-onset torsion dystonia, forms membrane inclusions in cultured neural cells. Hum Mol Genet. 2000 May 22;9(9):1403–13.

88. Gonzalez-Alegre P, Paulson HL. Aberrant Cellular Behavior of Mutant TorsinA Implicates Nuclear Envelope Dysfunction in DYT1 Dystonia. J Neurosci. 2004 Mar 17;24(11):2593–601.

89. Naismith TV, Heuser JE, Breakefield XO, Hanson PI. TorsinA in the nuclear envelope. Proceedings of the National Academy of Sciences of the United States of America. 2004 May 18;101(20):7612–7.

90. Neuwald AF, Aravind L, Spouge JL, Koonin EV. AAA+: A class of chaperone-like ATPases associated with the assembly, operation, and disassembly of protein complexes. Genome Res. 1999 Jan;9(1):27–43.

91. Granata A, Warner TT. The role of torsinA in dystonia. European Journal of Neurology. 2010;17:81–7.

92. Granata A, Schiavo G, Warner TT. TorsinA and dystonia: from nuclear envelope to synapse. Journal of Neurochemistry. 2009;109(6):1596–609.

93. Burdette AJ, Churchill PF, Caldwell GA, Caldwell KA. The early-onset torsion dystonia-associated protein, torsinA, displays molecular chaperone activity in vitro. Cell Stress and Chaperones. 2010 Sep 1;15(5):605–17.

94. McLean PJ, Kawamata H, Shariff S, Hewett J, Sharma N, Ueda K, et al. TorsinA and heat shock proteins act as molecular chaperones: suppression of α-synuclein aggregation. Journal of Neurochemistry. 2002;83(4):846–54.

95. Caldwell GA, Cao S, Sexton EG, Gelwix CC, Bevel JP, Caldwell KA. Suppression of polyglutamine-induced protein aggregation in Caenorhabditis elegans by torsin proteins. Hum Mol Genet. 2003 Jan 2;12(3):307–19.

96. Breakefield XO, Kamm C, Hanson PI. TorsinA: Movement at Many Levels. Neuron. 2001 Jul 19;31(1):9–12.

97. Atai NA, Ryan SD, Kothary R, Breakefield XO, Nery FC. Untethering the nuclear envelope and cytoskeleton: biologically distinct dystonias arising from a common cellular dysfunction. Int J Cell Biol. 2012;2012:634214.

98. Hewett JW, Kamm C, Boston H, Beauchamp R, Naismith T, Ozelius L, et al. TorsinB--perinuclear location and association with torsinA. J Neurochem. 2004 Jun;89(5):1186–94.

99. Shashidharan P, Kramer BC, Walker RH, Olanow CW, Brin MF. Immunohistochemical localization and distribution of torsinA in normal human and rat brain. Brain Res. 2000 Jan 24;853(2):197–206.

100. Konakova M, Huynh DP, Yong W, Pulst SM. Cellular distribution of torsin A and torsin B in normal human brain. Arch Neurol. 2001 Jun;58(6):921–7.

101. Rostasy K, Augood SJ, Hewett JW, Leung JC, Sasaki H, Ozelius LJ, et al. TorsinA protein and neuropathology in early onset generalized dystonia with GAG deletion. Neurobiology of disease. 2003;12(1):11–24.

102. Goodchild RE, Dauer WT. The AAA+ protein torsinA interacts with a conserved domain present in LAP1 and a novel ER protein. The Journal of cell biology. 2005;168(6):855–62.

103. Goodchild RE, Kim CE, Dauer WT. Loss of the dystonia-associated protein torsinA selectively disrupts the neuronal nuclear envelope. Neuron. 2005;48(6):923–32.

104. Hewett JW, Tannous B, Niland BP, Nery FC, Zeng J, Li Y, et al. Mutant torsinA interferes with protein processing through the secretory pathway in DYT1 dystonia cells. Proceedings of the National Academy of Sciences. 2007 Apr 24;104(17):7271–6.

105. Henriksen C, Madsen LB, Bendixen C, Larsen K. Characterization of the porcine TOR1A gene: The first step towards generation of a pig model for dystonia. Gene. 2009 Feb 1;430(1–2):105–15.

106. Nery FC, Armata IA, Farley JE, Cho JA, Yaqub U, Chen P, et al. TorsinA participates in endoplasmic reticulum-associated degradation. Nat Commun. 2011 Jul 12;2:393.

107. Yokoi F, Dang MT, Zhou T, Li Y. Abnormal nuclear envelopes in the striatum and motor deficits in DYT11 myoclonus-dystonia mouse models. Human molecular genetics. 2012;21(4):916–25.

108. Dang MT, Yokoi F, Pence MA, Li Y. Motor deficits and hyperactivity in Dyt1 knockdown mice. Neurosci Res. 2006 Dec;56(4):470–4.

109. Shashidharan P, Sandu D, Potla U, Armata IA, Walker RH, McNaught KS, et al. Transgenic mouse model of early-onset DYT1 dystonia. Hum Mol Genet. 2005 Jan 1;14(1):125–33.

110. Grundmann K, Reischmann B, Vanhoutte G, Hübener J, Teismann P, Hauser T-K, et al. Overexpression of human wildtype torsinA and human DeltaGAG torsinA in a transgenic mouse model causes phenotypic abnormalities. Neurobiol Dis. 2007 Aug;27(2):190–206.

111. Dang MT, Yokoi F, McNaught KSP, Jengelley T-A, Jackson T, Li J, et al. Generation and characterization of Dyt1 DeltaGAG knock-in mouse as a model for early-onset dystonia. Exp Neurol. 2005 Dec;196(2):452–63.

112. Liang C-C, Tanabe LM, Jou S, Chi F, Dauer WT. TorsinA hypofunction causes abnormal twisting movements and sensorimotor circuit neurodegeneration. Journal of Clinical Investigation. 2014 Jul 1;124(7):3080–92.

113. Torres GE, Sweeney AL, Beaulieu J-M, Shashidharan P, Caron MG. Effect of torsinA on membrane proteins reveals a loss of function and a dominant-negative phenotype of the dystonia-associated DeltaE-torsinA mutant. Proc Natl Acad Sci USA. 2004 Nov 2;101(44):15650–5.

114. Giles LM, Li L, Chin L-S. Printor, a Novel TorsinA-interacting Protein Implicated in Dystonia Pathogenesis. Journal of Biological Chemistry. 2009 Jun 17;284(32):21765–75.

115. Nery FC, Zeng J, Niland BP, Hewett J, Farley J, Irimia D, et al. TorsinA binds the KASH domain of nesprins and participates in linkage between nuclear envelope and cytoskeleton. Journal of cell science. 2008;121(20):3476–86.

116. Vander Heyden AB, Naismith TV, Snapp EL, Hodzic D, Hanson PI. LULL1 Retargets TorsinA to the Nuclear Envelope Revealing an Activity That Is Impaired by the DYT1 Dystonia Mutation. Mol Biol Cell. 2009 Jan 6;20(11):2661–72.

117. Zhao C, Brown RSH, Chase AR, Eisele MR, Schlieker C. Regulation of Torsin ATPases by LAP1 and LULL1. Proc Natl Acad Sci USA. 2013 Apr 23;110(17):E1545–54.

118. Waters CH, Faust PL, Powers J, Vinters H, Moskowitz C, Nygaard T, et al. Neuropathology of lubag (x-linked dystonia parkinsonism). Movement disorders. 1993;8(3):387–90.

119. Kaji R, Goto S, Tamiya G, Ando S, Makino S, Lee LV. Molecular dissection and anatomical basis of dystonia: X-linked recessive dystonia-parkinsonism (DYT3). J Med Invest. 2005 Nov;52 Suppl:280–3.

120. Walker RH, Brin MF, Sandu D, Good PF, Shashidharan P. TorsinA immunoreactivity in brains of patients with DYT1 and non-DYT1 dystonia. Neurology. 2002;58(1):120–4.

121. Zweig RM, Hedreen JC, Jankel WR, Casanova MF, Whitehouse PJ, Price DL. Pathology in brainstem regions of individuals with primary dystonia. Neurology. 1988 May;38(5):702–6.

122. Kulisevsky J, Marti MJ, Ferrer I, Tolosa E. Meige syndrome: neuropathology of a case. Mov Disord. 1988;3(2):170–5.

123. Mark MH, Sage JI, Dickson DW, Heikkila RE, Manzino L, Schwarz KO, et al. Meige syndrome in the spectrum of Lewy body disease. Neurology. 1994 Aug;44(8):1432–6.

124. Johnson VE, Stewart W, Smith DH. Widespread tau and amyloid-Beta pathology many years after a single traumatic brain injury in humans. Brain Pathol. 2012 Mar;22(2):142–9.

125. Holton JL, Schneider SA, Ganesharajah T, Gandhi S, Strand C, Shashidharan P, et al. Neuropathology of primary adult-onset dystonia. Neurology. 2008 Feb 26;70:695–9.

126. Gibb WR, Lees AJ, Marsden CD. Pathological report of four patients presenting with cranial dystonias. Mov Disord. 1988;3(3):211–21.

127. Furukawa Y, Hornykiewicz O, Fahn S, Kish SJ. Striatal dopamine in early-onset primary torsion dystonia with the DYT1 mutation. Neurology. 2000 Mar 14;54(5):1193–5.

128. Augood SJ, Keller-McGandy CE, Siriani A, Hewett J, Ramesh V, Sapp E, et al. Distribution and ultrastructural localization of torsinA immunoreactivity in the human brain. Brain Res. 2003 Oct 3;986(1-2):12–21.

129. McNaught KSP, Kapustin A, Jackson T, Jengelley T-A, JnoBaptiste R, Shashidharan P, et al. Brainstem pathology in DYT1 primary torsion dystonia. Annals of Neurology. 2004 Oct;56:540–7.

130. Jungwirth MT, Kumar D, Jeong DY, Goodchild RE. The nuclear envelope localization of DYT1 dystonia torsinA-ΔE requires the SUN1 LINC complex component. BMC Cell Biol. 2011;12:24.

131. Jankovic J. Medical treatment of dystonia. Mov Disord. 2013 Jun 15;28(7):1001–12.

132. Burke RE, Fahn S, Marsden CD. Torsion dystonia: a double-blind, prospective trial of high-dosage trihexyphenidyl. Neurology. 1986 Feb;36(2):160–4.

133. Greene P, Shale H, Fahn S. Analysis of open-label trials in torsion dystonia using high dosages of anticholinergics and other drugs. Mov Disord. 1988;3(1):46–60.

134. Waln O, Jankovic J. Bilateral globus pallidus internus deep brain stimulation after bilateral pallidotomy in a patient with generalized early-onset primary dystonia. Mov Disord. 2013 Jul;28(8):1162–3.

135. Vidailhet M, Vercueil L, Houeto J-L, Krystkowiak P, Benabid A-L, Cornu P, et al. Bilateral deep-brain stimulation of the globus pallidus in primary generalized dystonia. N Engl J Med. 2005 Feb 3;352(5):459–67.

136. Tarlov E. On the problem of the pathology of spasmodic torticollis in man. J Neurol Neurosurg Psychiatr. 1970 Aug;33(4):457–63.

137. Almasy L, Bressman SB, Raymond D, Kramer PL, Greene PE, Heiman GA, et al. Idiopathic torsion dystonia linked to chromosome 8 in two Mennonite families. Ann Neurol. 1997 Oct;42(4):670–3.

138. Fuchs T, Gavarini S, Saunders-Pullman R, Raymond D, Ehrlich ME, Bressman SB, et al. Mutations in the THAP1 gene are responsible for DYT6 primary torsion dystonia. Nat Genet. 2009 Mar;41(3):286–8.

139. Saunders-Pullman R, Raymond D, Senthil G, Kramer P, Ohmann E, Deligtisch A, et al. Narrowing the DYT6 dystonia region and evidence for locus heterogeneity in the Amish-Mennonites. Am J Med Genet A. 2007 Sep 15;143A(18):2098–105.

140. Greene P, Kang UJ, Fahn S. Spread of symptoms in idiopathic torsion dystonia. Mov Disord. 1995 Mar;10(2):143–52.

141. Bessière D, Lacroix C, Campagne S, Ecochard V, Guillet V, Mourey L, et al. Structure-function analysis of the THAP zinc finger of THAP1, a large C2CH DNA-binding module linked to Rb/E2F pathways. J Biol Chem. 2008 Feb 15;283(7):4352–63.

142. Clouaire T, Roussigne M, Ecochard V, Mathe C, Amalric F, Girard J-P. The THAP domain of THAP1 is a large C2CH module with zinc-dependent sequence-specific DNA-binding activity. Proc Natl Acad Sci USA. 2005 May 10;102(19):6907–12.

143. Roussigne M, Cayrol C, Clouaire T, Amalric F, Girard J-P. THAP1 is a nuclear proapoptotic factor that links prostate-apoptosis-response-4 (Par-4) to PML nuclear bodies. Oncogene. 22(16):2432–42.

144. Guo Q, Fu W, Xie J, Luo H, Sells SF, Geddes JW, et al. Par-4 is a mediator of neuronal degeneration associated with the pathogenesis of Alzheimer disease. Nat Med. 1998 Aug;4(8):957–62.

145. Duan W, Zhang Z, Gash DM, Mattson MP. Participation of prostate apoptosis response-4 in degeneration of dopaminergic neurons in models of Parkinson's disease. Ann Neurol. 1999 Oct;46(4):587–97.

146. Pedersen WA, Luo H, Kruman I, Kasarskis E, Mattson MP. The prostate apoptosis response-4 protein participates in motor neuron degeneration in amyotrophic lateral sclerosis. FASEB J. 2000 May;14(7):913–24.

147. Novel death associated proteins, and THAP1 and PAR4 pathways in apoptosis control - Patent - Europe PubMed Central [Internet]. [cited 2014 Feb 19]. Available from: http://europepmc.org/patents/PAT/US2003186337

148. Gavarini S, Cayrol C, Fuchs T, Lyons N, Ehrlich ME, Girard J-P, et al. Direct interaction between causative genes of DYT1 and DYT6 primary dystonia. Ann Neurol. 2010 Oct;68(4):549–53.

149. Kaiser FJ, Osmanoric A, Rakovic A, Erogullari A, Uflacker N, Braunholz D, et al. The dystonia gene DYT1 is repressed by the transcription factor THAP1 (DYT6). Annals of Neurology. 2010 Oct;68:554–9.

150. Bragg DC, Armata IA, Nery FC, Breakefield XO, Sharma N. Molecular pathways in dystonia. Neurobiology of Disease. 2011;42(2):136–47.

151. Kamm C, Uflacker N, Asmus F, Schrader C, Wolters A, Wittstock M, et al. No evidence for THAP1/DYT6 variants as disease modifiers in DYT1 dystonia. Mov Disord. 2011 Sep;26(11):2136–7.

152. Quartarone A, Rizzo V, Morgante F. Clinical features of dystonia: a pathophysiological revisitation. Curr Opin Neurol. 2008 Aug;21(4):484–90.

153. Cayrol C, Lacroix C, Mathe C, Ecochard V, Ceribelli M, Loreau E, et al. The THAP-zinc finger protein THAP1 regulates endothelial cell proliferation through modulation of pRB/E2F cell-cycle target genes. Blood. 2007 Jan 15;109(2):584–94.

154. Palada V, Stiern S, Glöckle N, Gómez-Garre P, Carrillo F, Mir P, et al. Lack of sequence variations in THAP1 gene and THAP1-binding sites in TOR1A promoter of DYT1 patients. Mov Disord. 2012 Jun;27(7):917.

155. Müller U. A molecular link between dystonia 1 and dystonia 6? Annals of Neurology. 2010;68(4):418–20.

156. Mazars R, Gonzalez-de-Peredo A, Cayrol C, Lavigne A-C, Vogel JL, Ortega N, et al. The THAP-zinc finger protein THAP1 associates with coactivator HCF-1 and O-GlcNAc transferase: a link between DYT6 and DYT3 dystonias. J Biol Chem. 2010 Apr 30;285(18):13364–71.

157. Bressman SB. Dystonia update. Clinical neuropharmacology. 2000;23(5):239.

158. Camargos S, Scholz S, Simón-Sánchez J, Paisán-Ruiz C, Lewis P, Hernandez D, et al. DYT16, a novel young-onset dystonia-parkinsonism disorder: identification of a segregating mutation in the stress-response protein PRKRA. Lancet Neurol. 2008 Mar;7(3):207–15.

159. Bressman SB, Raymond D, Fuchs T, Heiman GA, Ozelius LJ, Saunders-Pullman R. Mutations in THAP1 (DYT6) in early-onset dystonia: a genetic screening study. Lancet Neurol. 2009 May;8(5):441–6.

160. Augood SJ, Martin DM, Ozelius LJ, Breakefield XO, Penney JB, Standaert DG. Distribution of the mRNAs encoding torsinA and torsinB in the normal adult human brain. Annals of Neurology. 1999;46(5):761–9.

161. Augood SJ, Penney Jr JB, Friberg IK, Breakefield XO, Young AB, Ozelius LJ, et al. Expression of the early-onset torsion dystonia gene (DYT1) in human brain. Annals of neurology. 1998;43(5):669–73.

162. Balcioglu A, Kim M-O, Sharma N, Cha J-H, Breakefield XO, Standaert DG. Dopamine release is impaired in a mouse model of DYT1 dystonia. J Neurochem. 2007 Aug;102(3):783–8.

163. Page ME, Bao L, Andre P, Pelta-Heller J, Sluzas E, Gonzalez-Alegre P, et al. Cell-autonomous alteration of dopaminergic transmission by wild type and mutant (DeltaE) TorsinA in transgenic mice. Neurobiol Dis. 2010 Sep;39(3):318–26.

164. Zhao Y, DeCuypere M, LeDoux MS. Abnormal motor function and dopamine neurotransmission in DYT1 DeltaGAG transgenic mice. Exp Neurol. 2008 Apr;210(2):719–30.

165. O'Farrell CA, Martin KL, Hutton M, Delatycki MB, Cookson MR, Lockhart PJ. Mutant torsinA interacts with tyrosine hydroxylase in cultured cells. Neuroscience. 2009 Dec 15;164(3):1127–37.

166. Carbon M, Niethammer M, Peng S, Raymond D, Dhawan V, Chaly T, et al. Abnormal striatal and thalamic dopamine neurotransmission: Genotype-related features of dystonia. Neurology. 2009 Jun 16;72(24):2097–103.

167. Ichinose H, Ohye T, Takahashi E, Seki N, Hori T, Segawa M, et al. Hereditary progressive dystonia with marked diurnal fluctuation caused by mutations in the GTP cyclohydrolase I gene. Nat Genet. 1994 Nov;8(3):236–42.

168. Bräutigam C, Wevers RA, Jansen RJ, Smeitink JA, de Rijk-van Andel JF, Gabreëls FJ, et al. Biochemical hallmarks of tyrosine hydroxylase deficiency. Clin Chem. 1998 Sep;44(9):1897–904.

169. Bonafé L, Thöny B, Penzien JM, Czarnecki B, Blau N. Mutations in the sepiapterin reductase gene cause a novel tetrahydrobiopterin-dependent monoamine-neurotransmitter deficiency without hyperphenylalaninemia. Am J Hum Genet. 2001 Aug;69(2):269–77.

170. Segawa M, Hosaka A, Miyagawa F, Nomura Y, Imai H. Hereditary progressive dystonia with marked diurnal fluctuation. Adv Neurol. 1976;14:215–33.

171. Nygaard TG, Wilhelmsen KC, Risch NJ, Brown DL, Trugman JM, Gilliam TC, et al. Linkage mapping of dopa-responsive dystonia (DRD) to chromosome 14q. Nat Genet. 1993 Dec;5(4):386–91.

172. Tassin J, Dürr A, Bonnet AM, Gil R, Vidailhet M, Lücking CB, et al. Levodopa-responsive dystonia. GTP cyclohydrolase I or parkin mutations? Brain. 2000 Jun;123 (Pt 6):1112–21.

173. Steinberger D, Topka H, Fischer D, Müller U. GCH1 mutation in a patient with adult-onset oromandibular dystonia. Neurology. 1999 Mar 10;52(4):877–9.

174. Nygaard TG, Trugman JM, de Yebenes JG, Fahn S. Dopa-responsive dystonia: the spectrum of clinical manifestations in a large North American family. Neurology. 1990 Jan;40(1):66–9.

175. Segawa M, Nomura Y, Nishiyama N. Autosomal dominant guanosine triphosphate cyclohydrolase I deficiency (Segawa disease). Ann Neurol. 2003;54 Suppl 6:S32–45.

176. Cobb SA, Wider C, Ross OA, Mata IF, Adler CH, Rajput A, et al. GCH1 in early-onset Parkinson's disease. Mov Disord. 2009 Oct 30;24(14):2070–5.

177. Trender-Gerhard I, Sweeney MG, Schwingenschuh P, Mir P, Edwards MJ, Gerhard A, et al. Autosomal-dominant GTPCH1-deficient DRD: clinical characteristics and long-term outcome of 34 patients. J Neurol Neurosurg Psychiatr. 2009 Aug;80(8):839–45.

178. Van Hove JLK, Steyaert J, Matthijs G, Legius E, Theys P, Wevers R, et al. Expanded motor and psychiatric phenotype in autosomal dominant Segawa syndrome due to GTP cyclohydrolase deficiency. J Neurol Neurosurg Psychiatr. 2006 Jan;77(1):18–23.

179. Clot F, Grabli D, Cazeneuve C, Roze E, Castelnau P, Chabrol B, et al. Exhaustive analysis of BH4 and dopamine biosynthesis genes in patients with Dopa-responsive dystonia. Brain. 2009 Jul;132(Pt 7):1753–63.

180. Assmann B, Surtees R, Hoffmann GF. Approach to the diagnosis of neurotransmitter diseases exemplified by the differential diagnosis of childhood-onset dystonia. Ann Neurol. 2003;54 Suppl 6:S18–24.

181. Bandmann O, Valente EM, Holmans P, Surtees RA, Walters JH, Wevers RA, et al. Dopa-responsive dystonia: a clinical and molecular genetic study. Ann Neurol. 1998 Oct;44(4):649–56.

182. Furukawa Y. Genetics and biochemistry of dopa-responsive dystonia: significance of striatal tyrosine hydroxylase protein loss. Adv Neurol. 2003;91:401–10.

183. Furukawa Y, Filiano JJ, Kish SJ. Amantadine for levodopa-induced choreic dyskinesia in compound heterozygotes for GCH1 mutations. Mov Disord. 2004 Oct;19(10):1256–8.

184. Wider C, Melquist S, Hauf M, Solida A, Cobb SA, Kachergus JM, et al. Study of a Swiss dopa-responsive dystonia family with a deletion in GCH1: redefining DYT14 as DYT5. Neurology. 2008 Apr 15;70(16 Pt 2):1377–83.

185. Ichinose H, Ohye T, Matsuda Y, Hori T, Blau N, Burlina A, et al. Characterization of mouse and human GTP cyclohydrolase I genes. Mutations in patients with GTP cyclohydrolase I deficiency. J Biol Chem. 1995 Apr 28;270(17):10062–71.

186. Sharma N, Armata IA, Multhaupt-Buell TJ, Ozelius LJ, Xin W, Sims KB. Mutation in 5'upstream region of GCHI gene causes familial dopa-responsive dystonia. Mov Disord. 2011 Sep;26(11):2140–1.

187. Armata IA, Balaj L, Kuster JK, Zhang X, Tsai S, Armatas AA, et al. Dopa-Responsive Dystonia: Functional Analysis of Single Nucleotide Substitutions within the 5' Untranslated GCH1 Region. PLoS ONE. 2013 Oct 4;8(10):e76975.

188. Kurian MA, Gissen P, Smith M, Heales S Jr, Clayton PT. The monoamine neurotransmitter disorders: an expanding range of neurological syndromes. Lancet Neurol. 2011 Aug;10(8):721–33.

189. Furukawa Y, Nygaard TG, Gütlich M, Rajput AH, Pifl C, DiStefano L, et al. Striatal biopterin and tyrosine hydroxylase protein reduction in dopa-responsive dystonia. Neurology. 1999 Sep 22;53(5):1032–41.

190. Schöls L, Bauer P, Schmidt T, Schulte T, Riess O. Autosomal dominant cerebellar ataxias: clinical features, genetics, and pathogenesis. Lancet Neurol. 2004 May;3(5):291–304.

191. Orr HT, Chung MY, Banfi S, Kwiatkowski TJ Jr, Servadio A, Beaudet AL, et al. Expansion of an unstable trinucleotide CAG repeat in spinocerebellar ataxia type 1. Nat Genet. 1993 Jul;4(3):221–6.

192. Kobayashi H, Abe K, Matsuura T, Ikeda Y, Hitomi T, Akechi Y, et al. Expansion of intronic GGCCTG hexanucleotide repeat in NOP56 causes SCA36, a type of spinocerebellar ataxia accompanied by motor neuron involvement. Am J Hum Genet. 2011 Jul 15;89(1):121–30.

193. Wang JL, Yang X, Xia K, Hu ZM, Weng L, Jin X, et al. TGM6 identified as a novel causative gene of spinocerebellar ataxias using exome sequencing. Brain. 2010 Dec;133(Pt 12):3510–8.

194. Serrano-Munuera C, Corral-Juan M, Stevanin G, San Nicolás H, Roig C, Corral J, et al. New subtype of spinocerebellar ataxia with altered vertical eye movements mapping to chromosome 1p32. JAMA Neurol. 2013 Jun;70(6):764–71.

195. Marelli C, Cazeneuve C, Brice A, Stevanin G, Dürr A. Autosomal dominant cerebellar ataxias. Rev Neurol (Paris). 2011 May;167(5):385–400.

196. Ikeda Y, Daughters RS, Ranum LPW. Bidirectional expression of the SCA8 expansion mutation: one mutation, two genes. Cerebellum. 2008;7(2):150–8.

197. Koob MD, Moseley ML, Schut LJ, Benzow KA, Bird TD, Day JW, et al. An untranslated CTG expansion causes a novel form of spinocerebellar ataxia (SCA8). Nat Genet. 1999 Apr;21(4):379–84.

198. Moseley ML, Zu T, Ikeda Y, Gao W, Mosemiller AK, Daughters RS, et al. Bidirectional expression of CUG and CAG expansion transcripts and intranuclear polyglutamine inclusions in spinocerebellar ataxia type 8. Nat Genet. 2006 Jul;38(7):758–69.

199. Moseley ML, Schut LJ, Bird TD, Koob MD, Day JW, Ranum LP. SCA8 CTG repeat: en masse contractions in sperm and intergenerational sequence changes may play a role in reduced penetrance. Hum Mol Genet. 2000 Sep 1;9(14):2125–30.

200. Benzow KA, Koob MD. The KLHL1-antisense transcript (KLHL1AS) is evolutionarily conserved. Mamm Genome. 2002 Mar;13(3):134–41.

201. Andrés AM, Soldevila M, Saitou N, Volpini V, Calafell F, Bertranpetit J. Understanding the dynamics of Spinocerebellar Ataxia 8 (SCA8) locus through a comparative genetic approach in humans and apes. Neurosci Lett. 2003 Jan 23;336(3):143–6.

202. Andrés AM, Soldevila M, Lao O, Volpini V, Saitou N, Jacobs HT, et al. Comparative genetics of functional trinucleotide tandem repeats in humans and apes. J Mol Evol. 2004 Sep;59(3):329–39.

203. Stevanin G, Herman A, Dürr A, Jodice C, Frontali M, Agid Y, et al. Are (CTG)n expansions at the SCA8 locus rare polymorphisms? Nat Genet. 2000 Mar;24(3):213; author reply 215.

204. Worth PF, Houlden H, Giunti P, Davis MB, Wood NW. Large, expanded repeats in SCA8 are not confined to patients with cerebellar ataxia. Nat Genet. 2000 Mar;24(3):214–5.

205. Koob MD, Benzow KA, Bird TD, Day JW, Moseley ML, Ranum LP. Rapid cloning of expanded trinucleotide repeat sequences from genomic DNA. Nat Genet. 1998 Jan;18(1):72–5.

206. Day JW, Schut LJ, Moseley ML, Durand AC, Ranum LP. Spinocerebellar ataxia type 8: clinical features in a large family. Neurology. 2000 Sep 12;55(5):649–57.

207. Mosemiller AK, Dalton JC, Day JW, Ranum LPW. Molecular genetics of spinocerebellar ataxia type 8 (SCA8). Cytogenet Genome Res. 2003;100(1-4):175–83.

208. Silveira I, Alonso I, Guimarães L, Mendonça P, Santos C, Maciel P, et al. High germinal instability of the (CTG)n at the SCA8 locus of both expanded and normal alleles. Am J Hum Genet. 2000 Mar;66(3):830–40.

209. Brusco A, Cagnoli C, Franco A, Dragone E, Nardacchione A, Grosso E, et al. Analysis of SCA8 and SCA12 loci in 134 Italian ataxic patients negative for SCA1-3, 6 and 7 CAG expansions. J Neurol. 2002 Jul;249(7):923–9.

210. Ikeda Y, Shizuka M, Watanabe M, Okamoto K, Shoji M. Molecular and clinical analyses of spinocerebellar ataxia type 8 in Japan. Neurology. 2000 Feb 22;54(4):950–5.

211. Juvonen V, Kairisto V, Hietala M, Savontaus M-L. Calculating predictive values for the large repeat alleles at the SCA8 locus in patients with ataxia. J Med Genet. 2002 Dec;39(12):935–6.

212. Schöls L, Bauer I, Zühlke C, Schulte T, Kölmel C, Bürk K, et al. Do CTG expansions at the SCA8 locus cause ataxia? Ann Neurol. 2003 Jul;54(1):110–5.

213. Juvonen V, Hietala M, Päivärinta M, Rantamäki M, Hakamies L, Kaakkola S, et al. Clinical and genetic findings in Finnish ataxia patients with the spinocerebellar ataxia 8 repeat expansion. Ann Neurol. 2000 Sep;48(3):354–61.

214. Topisirovic I, Dragasevic N, Savic D, Ristic A, Keckarevic M, Keckarevic D, et al. Genetic and clinical analysis of spinocerebellar ataxia type 8 repeat expansion in Yugoslavia. Clin Genet. 2002 Oct;62(4):321–4.

215. Anderson JH, Yavuz MC, Kazar BM, Christova P, Gomez CM. The vestibulo-ocular reflex and velocity storage in spinocerebellar ataxia 8. Arch Ital Biol. 2002 Oct;140(4):323–9.

216. Ikeda Y, Shizuka-Ikeda M, Watanabe M, Schmitt M, Okamoto K, Shoji M. Asymptomatic CTG expansion at the SCA8 locus is associated with cerebellar atrophy on MRI. J Neurol Sci. 2000 Dec 15;182(1):76–9.

217. Cellini E, Nacmias B, Forleo P, Piacentini S, Guarnieri BM, Serio A, et al. Genetic and clinical analysis of spinocerebellar ataxia type 8 repeat expansion in Italy. Arch Neurol. 2001 Nov;58(11):1856–9.

218. Ikeda Y, Dalton JC, Moseley ML, Gardner KL, Bird TD, Ashizawa T, et al. Spinocerebellar ataxia type 8: molecular genetic comparisons and haplotype analysis of 37 families with ataxia. Am J Hum Genet. 2004 Jul;75(1):3–16.

219. Ranum LPW, Daughters RS, Tuttle DL, Gao W, Ikeda Y, Moseley ML, et al. Double the trouble: bidirectional expression of the SCA8 CAG/CTG expansion mutation - evidence for RNA and protein gain of function effects. Rinsho Shinkeigaku. 2010 Nov;50(11):982–3.

220. Vincent JB, Yuan QP, Schalling M, Adolfsson R, Azevedo MH, Macedo A, et al. Long repeat tracts at SCA8 in major psychosis. Am J Med Genet. 2000 Dec 4;96(6):873–6.

221. Vincent JB, Paterson AD, Strong E, Petronis A, Kennedy JL. The unstable trinucleotide repeat story of major psychosis. Am J Med Genet. 2000;97(1):77–97.

222. Gregory A, Hayflick SJ. Neurodegeneration with brain iron accumulation. Folia Neuropathol. 2005;43(4):286–96.

223. Kruer MC. The neuropathology of neurodegeneration with brain iron accumulation. Int Rev Neurobiol. 2013;110:165–94.

224. Kruer MC, Boddaert N, Schneider SA, Houlden H, Bhatia KP, Gregory A, et al. Neuroimaging features of neurodegeneration with brain iron accumulation. AJNR Am J Neuroradiol. 2012 Mar;33(3):407–14.

225. Zhou B, Westaway SK, Levinson B, Johnson MA, Gitschier J, Hayflick SJ. A novel pantothenate kinase gene (PANK2) is defective in Hallervorden-Spatz syndrome. Nat Genet. 2001 Aug;28(4):345–9.

226. Morgan NV, Westaway SK, Morton JEV, Gregory A, Gissen P, Sonek S, et al. PLA2G6, encoding a phospholipase A2, is mutated in neurodegenerative disorders with high brain iron. Nat Genet. 2006 Jul;38(7):752–4.

227. Hartig MB, Iuso A, Haack T, Kmiec T, Jurkiewicz E, Heim K, et al. Absence of an orphan mitochondrial protein, c19orf12, causes a distinct clinical subtype of neurodegeneration with brain iron accumulation. Am J Hum Genet. 2011 Oct 7;89(4):543–50.

228. Hogarth P, Gregory A, Kruer MC, Sanford L, Wagoner W, Natowicz MR, et al. New NBIA subtype: genetic, clinical, pathologic, and radiographic features of MPAN. Neurology. 2013 Jan 15;80(3):268–75.

229. Haack TB, Hogarth P, Kruer MC, Gregory A, Wieland T, Schwarzmayr T, et al. Exome Sequencing Reveals De Novo WDR45 Mutations Causing a Phenotypically Distinct, X-Linked Dominant Form of NBIA. Am J Hum Genet. 2012 Dec 7;91(6):1144–9.

230. Kruer MC, Paisán-Ruiz C, Boddaert N, Yoon MY, Hama H, Gregory A, et al. Defective FA2H leads to a novel form of neurodegeneration with brain iron accumulation (NBIA). Ann Neurol. 2010 Nov;68(5):611–8.

231. Schneider SA, Paisan-Ruiz C, Quinn NP, Lees AJ, Houlden H, Hardy J, et al. ATP13A2 mutations (PARK9) cause neurodegeneration with brain iron accumulation. Mov Disord. 2010 Jun 15;25(8):979–84.

232. Curtis AR, Fey C, Morris CM, Bindoff LA, Ince PG, Chinnery PF, et al. Mutation in the gene encoding ferritin light polypeptide causes dominant adult-onset basal ganglia disease. Nat Genet. 2001 Aug;28(4):350–4.

233. Yoshida K, Furihata K, Takeda S, Nakamura A, Yamamoto K, Morita H, et al. A mutation in the ceruloplasmin gene is associated with systemic hemosiderosis in humans. Nat Genet. 1995 Mar;9(3):267–72.

234. Woodhouse NJ, Sakati NA. A syndrome of hypogonadism, alopecia, diabetes mellitus, mental retardation, deafness, and ECG abnormalities. J Med Genet. 1983 Jun;20(3):216–9.

235. Dusi S, Valletta L, Haack TB, Tsuchiya Y, Venco P, Pasqualato S, et al. Exome sequence reveals mutations in CoA synthase as a cause of neurodegeneration with brain iron accumulation. Am J Hum Genet. 2014 Jan 2;94(1):11–22.

236. Saitsu H, Nishimura T, Muramatsu K, Kodera H, Kumada S, Sugai K, et al. De novo mutations in the autophagy gene WDR45 cause static encephalopathy of childhood with neurodegeneration in adulthood. Nat Genet. 2013 Apr;45(4):445–9, 449e1.

237. Hayflick SJ, Kruer MC, Gregory A, Haack TB, Kurian MA, Houlden HH, et al. β-Propeller protein-associated neurodegeneration: a new X-linked dominant disorder with brain iron accumulation. Brain. 2013 Jun;136(Pt 6):1708–17.

238. Schipper HM. Neurodegeneration with brain iron accumulation — Clinical syndromes and neuroimaging. Biochimica et Biophysica Acta (BBA) - Molecular Basis of Disease. 2012 Mar;1822(3):350–60.

239. Mills E, Dong X, Wang F, Xu H. Mechanisms of Brain Iron Transport: Insight into Neurodegeneration and CNS Disorders. Future Med Chem. 2010 Jan;2(1):51.

240. Pulst SM. Genetics of Movement Disorders. Academic Press; 2002. 586 p.

241. Schipper HM. Brain iron deposition and the free radical-mitochondrial theory of ageing. Ageing Res Rev. 2004 Jul;3(3):265–301.

242. Lillig CH, Berndt C, Holmgren A. Glutaredoxin systems. Biochim Biophys Acta. 2008 Nov;1780(11):1304–17.

243. Zecca L, Youdim MBH, Riederer P, Connor JR, Crichton RR. Iron, brain ageing and neurodegenerative disorders. Nat Rev Neurosci. 2004 Nov;5(11):863–73.

244. Behrends C, Sowa ME, Gygi SP, Harper JW. Network organization of the human autophagy system. Nature. 2010 Jul 1;466(7302):68–76.

245. Lu Q, Yang P, Huang X, Hu W, Guo B, Wu F, et al. The WD40 repeat PtdIns(3)P-binding protein EPG-6 regulates progression of omegasomes to autophagosomes. Dev Cell. 2011 Aug 16;21(2):343–57.

246. BASSEN FA, KORNZWEIG AL. Malformation of the erythrocytes in a case of atypical retinitis pigmentosa. Blood. 1950 Apr;5(4):381–7.

247. Rampoldi L, Danek A, Monaco AP. Clinical features and molecular bases of neuroacanthocytosis. J Mol Med. 2002 Aug;80(8):475–91.

248. Kartsounis LD, Hardie RJ. The pattern of cognitive impairments in neuroacanthocytosis. A frontosubcortical dementia. Arch Neurol. 1996 Jan;53(1):77–80.

249. Medalia A, Merriam A, Sandberg M. Neuropsychological deficits in choreoacanthocytosis. Arch Neurol. 1989 May;46(5):573–5.

250. Tiftikcioglu BI, Dericioglu N, Saygi S. Focal seizures originating from the left temporal lobe in a case with chorea-acanthocytosis. Clin EEG Neurosci. 2006 Jan;37(1):46–9.

251. Critchley EM, Clark DB, Wikler A. Acanthocytosis and neurological disorder without betalipoproteinemia. Arch Neurol. 1968 Feb;18(2):134–40.

252. Levine IM, Estes JW, Looney JM. Hereditary neurological disease with acanthocytosis. A new syndrome. Arch Neurol. 1968 Oct;19(4):403–9.

253. Hardie RJ. Acanthocytosis and neurological impairment--a review. Q J Med. 1989 Apr;71(264):291–306.

254. Estes JW, Morley TJ, Levine IM, Emerson CP. A new hereditary acanthocytosis syndrome. Am J Med. 1967 Jun;42(6):868–81.

255. Rampoldi L, Dobson-Stone C, Rubio JP, Danek A, Chalmers RM, Wood NW, et al. A conserved sorting-associated protein is mutant in chorea-acanthocytosis. Nat Genet. 2001 Jun;28(2):119–20.

256. Ueno S, Maruki Y, Nakamura M, Tomemori Y, Kamae K, Tanabe H, et al. The gene encoding a newly discovered protein, chorein, is mutated in chorea-acanthocytosis. Nat Genet. 2001 Jun;28(2):121–2.

257. Saiki S, Sakai K, Murata K, Saiki M, Nakanishi M, Kitagawa Y, et al. Primary skeletal muscle involvement in chorea-acanthocytosis. Mov Disord. 2007 Apr 30;22(6):848–52.

258. Kurano Y, Nakamura M, Ichiba M, Matsuda M, Mizuno E, Kato M, et al. In vivo distribution and localization of chorein. Biochem Biophys Res Commun. 2007 Feb 9;353(2):431–5.

259. Vital A, Bouillot S, Burbaud P, Ferrer X, Vital C. Chorea-acanthocytosis: neuropathology of brain and peripheral nerve. Clin Neuropathol. 2002 Apr;21(2):77–81.

260. Ishida C, Makifuchi T, Saiki S, Hirose G, Yamada M. A neuropathological study of autosomal-dominant chorea-acanthocytosis with a mutation of VPS13A. Acta Neuropathol. 2009 Jan;117(1):85–94.

261. Bader B, Arzberger T, Heinsen H, Dobson-Stone C, Kretzschmar HA, Danek A. Neuropathology of Chorea-Acanthocytosis. In: Walker RH, Saiki S, Danek A, editors. Neuroacanthocytosis Syndromes II [Internet]. Springer Berlin Heidelberg; 2008 [cited 2013 Jul 26]. p. 187–95. Available from: http://link.springer.com/chapter/10.1007/978-3-540-71693-8_15

262. Prohaska R, Sibon OCM, Rudnicki DD, Danek A, Hayflick SJ, Verhaag EM, et al. Brain, blood, and iron: Perspectives on the roles of erythrocytes and iron in neurodegeneration. Neurobiol Dis. 2012 Jun;46(3):607–24.

263. Schulze H, Sandhoff K. Lysosomal lipid storage diseases. Cold Spring Harb Perspect Biol. 2011 Jun;3(6).

264. Chan SYV, Hilchie AL, Brown MG, Anderson R, Hoskin DW. Apoptosis induced by intracellular ceramide accumulation in MDA-MB-435 breast carcinoma cells is dependent on the generation of reactive oxygen species. Exp Mol Pathol. 2007 Feb;82(1):1–11.

265. Jana A, Hogan EL, Pahan K. Ceramide and neurodegeneration: susceptibility of neurons and oligodendrocytes to cell damage and death. J Neurol Sci. 2009 Mar 15;278(1-2):5–15.

266. Posse de Chaves E, Sipione S. Sphingolipids and gangliosides of the nervous system in membrane function and dysfunction. FEBS Lett. 2010 May 3;584(9):1748–59.

267. Zhang A-S. Control of systemic iron homeostasis by the hemojuvelin-hepcidin axis. Adv Nutr. 2010 Nov;1(1):38–45.

268. Schonberg DL, McTigue DM. Iron is essential for oligodendrocyte genesis following intraspinal macrophage activation. Exp Neurol. 2009 Jul;218(1):64–74.

269. Ogretmen B, Hannun YA. Biologically active sphingolipids in cancer pathogenesis and treatment. Nat Rev Cancer. 2004 Aug;4(8):604–16.

270. De Duve C. The lysosome turns fifty. Nat Cell Biol. 2005 Sep;7(9):847–9.

271. Schneider L, Zhang J. Lysosomal function in macromolecular homeostasis and bioenergetics in Parkinson's disease. Mol Neurodegener. 2010;5:14.

272. Bras J, Singleton A, Cookson MR, Hardy J. POTENTIAL ROLE OF CERAMIDE METABOLISM IN LEWY BODY DISEASE. FEBS J. 2008 Dec;275(23):5767–73.

273. Kolter T, Sandhoff K. Sphingolipid metabolism diseases. Biochim Biophys Acta. 2006 Dec;1758(12):2057–79.

274. Mehta A, Beck M, Linhart A, Sunder-Plassmann G, Widmer U. History of lysosomal storage diseases: an overview. In: Mehta A, Beck M, Sunder-Plassmann G, editors. Fabry Disease: Perspectives from 5 Years of FOS [Internet]. Oxford: Oxford PharmaGenesis; 2006 [cited 2014 Mar 20]. Available from: http://www.ncbi.nlm.nih.gov/books/NBK11615/

275. Vanier MT. Niemann-Pick diseases. Handb Clin Neurol. 2013;113:1717–21.

276. Riccio E, Capuano I, Visciano B, Marchetiello C, Petrillo F, Pisani A. [Enzyme replacement therapy in patients with Fabry disease: state of the art and review of the literature]. G Ital Nefrol. 2013 Oct;30(5).

277. Kohlschütter A. Lysosomal leukodystrophies: Krabbe disease and metachromatic leukodystrophy. Handb Clin Neurol. 2013;113:1611–8.

278. Cox TM. Gaucher disease: clinical profile and therapeutic developments. Biologics. 2010;4:299–313.

279. Hechtman P, Kaplan F. Tay-Sachs disease screening and diagnosis: evolving technologies. DNA Cell Biol. 1993 Oct;12(8):651–65.

280. Sandhoff K, Andreae U, Jatzkewitz H. Deficient hexozaminidase activity in an exceptional case of Tay-Sachs disease with additional storage of kidney globoside in visceral organs. Life Sci. 1968 Mar 15;7(6):283–8.

281. Vanier MT, Millat G. Niemann-Pick disease type C. Clin Genet. 2003 Oct;64(4):269–81.

282. Tamura H, Takahashi T, Ban N, Torisu H, Ninomiya H, Takada G, et al. Niemann-Pick type C disease: novel NPC1 mutations and characterization of the concomitant acid sphingomyelinase deficiency. Mol Genet Metab. 2006 Feb;87(2):113–21.

283. Saito Y, Suzuki K, Hulette CM, Murayama S. Aberrant phosphorylation of alpha-synuclein in human Niemann-Pick type C1 disease. J Neuropathol Exp Neurol. 2004 Apr;63(4):323–8.

284. Smith BR, Santos MB, Marshall MS, Cantuti-Castelvetri L, Lopez-Rosas A, Li G, et al. Neuronal inclusions of α-synuclein contribute to the pathogenesis of Krabbe disease. J Pathol. 2014 Apr;232(5):509–21.

285. Beutler E. Gaucher disease: new molecular approaches to diagnosis and treatment. Science. 1992 May 8;256(5058):794–9.

286. Hruska KS, LaMarca ME, Scott CR, Sidransky E. Gaucher disease: mutation and polymorphism spectrum in the glucocerebrosidase gene (GBA). Hum Mutat. 2008 May;29(5):567–83.

287. Lui K, Commens C, Choong R, Jaworski R. Collodion babies with Gaucher's disease. Arch Dis Child. 1988 Jul;63(7):854–6.

288. Meivar-Levy I, Horowitz M, Futerman AH. Analysis of glucocerebrosidase activity using N-(1-[14C]hexanoyl)-D-erythroglucosylsphingosine demonstrates a correlation between levels of residual enzyme activity and the type of Gaucher disease. Biochem J. 1994 Oct 15;303 (Pt 2):377–82.

289. Aharon-Peretz J, Rosenbaum H, Gershoni-Baruch R. Mutations in the glucocerebrosidase gene and Parkinson's disease in Ashkenazi Jews. N Engl J Med. 2004 Nov 4;351(19):1972–7.

290. Bras J, Paisan-Ruiz C, Guerreiro R, Ribeiro MH, Morgadinho A, Januario C, et al. Complete screening for glucocerebrosidase mutations in parkinson disease patients from portugal. Neurobiol Aging. 2009 Sep;30(9):1515–7.

291. Mata IF, Samii A, Schneer SH, Roberts JW, Griffith A, Leis BC, et al. Glucocerebrosidase Gene Mutations. Arch Neurol. 2008 Mar;65(3):379–82.

292. Bley AE, Giannikopoulos OA, Hayden D, Kubilus K, Tifft CJ, Eichler FS. Natural History of Infantile GM2 Gangliosidosis. Pediatrics. 2011 Nov;128(5):e1233–41.

293. Tanaka A, Ohno K, Sandhoff K, Maire I, Kolodny EH, Brown A, et al. GM2-gangliosidosis B1 variant: analysis of beta-hexosaminidase alpha gene abnormalities in seven patients. Am J Hum Genet. 1990 Feb;46(2):329–39.

294. Willner JP, Grabowski GA, Gordon RE, Bender AN, Desnick RJ. Chronic GM2 gangliosidosis masquerading as atypical Friedreich ataxia: clinical, morphologic, and biochemical studies of nine cases. Neurology. 1981 Jul;31(7):787–98.

295. Kihara H. Genetic heterogeneity in metachromatic leukodystrophy. Am J Hum Genet. 1982 Mar;34(2):171–81.

296. Jakes R, Spillantini MG, Goedert M. Identification of two distinct synucleins from human brain. FEBS Lett. 1994 May 23;345(1):27–32.

297. Ostrerova-Golts N, Petrucelli L, Hardy J, Lee JM, Farer M, Wolozin B. The A53T alpha-synuclein mutation increases iron-dependent aggregation and toxicity. J Neurosci. 2000 Aug 15;20(16):6048–54.

298. Golovko MY, Faergeman NJ, Cole NB, Castagnet PI, Nussbaum RL, Murphy EJ. Alpha-synuclein gene deletion decreases brain palmitate uptake and alters the palmitate metabolism in the absence of alpha-synuclein palmitate binding. Biochemistry. 2005 Jun 14;44(23):8251–9.

299. Patil S, Melrose J, Chan C. Involvement of astroglial ceramide in palmitic acid-induced Alzheimer-like changes in primary neurons. Eur J Neurosci. 2007 Oct;26(8):2131–41.

300. Van Ham TJ, Thijssen KL, Breitling R, Hofstra RMW, Plasterk RHA, Nollen EAA. C. elegans model identifies genetic modifiers of alpha-synuclein inclusion formation during aging. PLoS Genet. 2008 Mar;4(3):e1000027.

301. Xiao J, Uitti RJ, Zhao Y, Vemula SR, Perlmutter JS, Wszolek ZK, et al. Mutations in CIZ1 cause adult onset primary cervical dystonia. Ann Neurol. 2012 Apr;71(4):458–69.

302. Fuchs T, Saunders-Pullman R, Masuho I, Luciano MS, Raymond D, Factor S, et al. Mutations in GNAL cause primary torsion dystonia. Nat Genet. 2013 Jan;45(1):88–92.

303. Hersheson J, Mencacci NE, Davis M, Macdonald N, Trabzuni D, Ryten M, et al. Mutations in the autoregulatory domain of β-tubulin 4a cause hereditary dystonia. Ann Neurol. 2012 Dec 13;

304. Mirra SS, Heyman A, McKeel D, Sumi SM, Crain BJ, Brownlee LM, et al. The Consortium to Establish a Registry for Alzheimer's Disease (CERAD). Part II. Standardization of the neuropathologic assessment of Alzheimer's disease. Neurology. 1991 Apr;41(4):479–86.

305. Braak H, Braak E. Neuropathological stageing of Alzheimer-related changes. Acta Neuropathol. 1991;82(4):239–59.

306. Williams DR, Holton JL, Strand C, Pittman A, de Silva R, Lees AJ, et al. Pathological tau burden and distribution distinguishes progressive supranuclear palsy-parkinsonism from Richardson's syndrome. Brain. 2007 Jun;130(Pt 6):1566–76.

307. McKeith IG, Dickson DW, Lowe J, Emre M, O'Brien JT, Feldman H, et al. Diagnosis and management of dementia with Lewy bodies: third report of the DLB Consortium. Neurology. 2005 Dec 27;65(12):1863–72.

308. Goedert M, Spillantini MG, Cairns NJ, Crowther RA. Tau proteins of alzheimer paired helical filaments: Abnormal phosphorylation of all six brain isoforms. Neuron. 1992 Jan;8(1):159–68.

309. Hanger DP, Betts JC, Loviny TLF, Blackstock WP, Anderton BH. New Phosphorylation Sites Identified in Hyperphosphorylated Tau (Paired Helical Filament-Tau) from Alzheimer's Disease Brain Using Nanoelectrospray Mass Spectrometry. Journal of Neurochemistry. 1998 Dec 1;71(6):2465–76.

310. De Silva R, Lashley T, Gibb G, Hanger D, Hope A, Reid A, et al. Pathological inclusion bodies in tauopathies contain distinct complements of tau with three or four microtubule-binding repeat domains as demonstrated by new specific monoclonal antibodies. Neuropathology and Applied Neurobiology. 2003 Jun 1;29(3):288–302.

311. Paudel R, Hardy J, Revesz T, Holton JL, Houlden H. Review: genetics and neuropathology of primary pure dystonia. Neuropathol Appl Neurobiol. 2012 Oct;38(6):520–34.

312. Paisán-Ruiz C, Ruiz-Martinez J, Ruibal M, Mok KY, Indakoetxea B, Gorostidi A, et al. Identification of a novel THAP1 mutation at R29 amino-acid residue in sporadic patients with early-onset dystonia. Mov Disord. 2009 Dec 15;24(16):2428–9.

313. LeDoux MS, Xiao J, Rudzińska M, Bastian RW, Wszolek ZK, Van Gerpen JA, et al. Genotype-phenotype correlations in THAP1 dystonia: molecular foundations and description of new cases. Parkinsonism Relat Disord. 2012 Jun;18(5):414–25.

314. Marras C, Lohmann K, Lang A, Klein C. Fixing the broken system of genetic locus symbols. Neurology. 2012 Mar 27;78(13):1016–24.

315. Hartmann P, Ramseier A, Gudat F, Mihatsch MJ, Polasek W. [Normal weight of the brain in adults in relation to age, sex, body height and weight]. Pathologe. 1994 Jun;15(3):165–70.

316. Den Dunnen WFA. Neuropathological diagnostic considerations in hyperkinetic movement disorders. Front Neurol. 2013;4:7.

317. Richter-Landsberg C, Leyk J. Inclusion body formation, macroautophagy, and the role of HDAC6 in neurodegeneration. Acta Neuropathol. 2013 Dec;126(6):793–807.

318. Ahmed Z, Tabrizi SJ, Li A, Houlden H, Sailer A, Lees AJ, et al. A Huntington's disease phenocopy characterized by pallido-nigro-luysian degeneration with brain iron accumulation and p62-positive glial inclusions. Neuropathol Appl Neurobiol. 2010 Oct;36(6):551–7.

319. Shashidharan P, Good PF, Hsu A, Perl DP, Brin MF, Olanow CW. TorsinA accumulation in Lewy bodies in sporadic Parkinson's disease. Brain Research. 2000 Sep 22;877(2):379–81.

320. Gordon KL, Gonzalez-Alegre P. Consequences of the DYT1 mutation on torsinA oligomerization and degradation. Neuroscience. 2008 Dec 2;157(3):588–95.

321. Takahashi K, Okita K, Nakagawa M, Yamanaka S. Induction of pluripotent stem cells from fibroblast cultures. Nat Protoc. 2007;2(12):3081–9.

322. Yu J, Vodyanik MA, Smuga-Otto K, Antosiewicz-Bourget J, Frane JL, Tian S, et al. Induced pluripotent stem cell lines derived from human somatic cells. Science. 2007 Dec 21;318(5858):1917–20.

323. Houlden H, Schneider SA, Paudel R, Melchers A, Schwingenschuh P, Edwards M, et al. THAP1 mutations (DYT6) are an additional cause of early-onset dystonia. Neurology. 2010 Mar 8;74(10):846–50.

324. Goto S, Lee LV, Munoz EL, Tooyama I, Tamiya G, Makino S, et al. Functional anatomy of the basal ganglia in X-linked recessive dystonia-parkinsonism. Ann Neurol. 2005 Jul;58(1):7–17.

325. Lashley T, Holton JL, Gray E, Kirkham K, O'Sullivan SS, Hilbig A, et al. Cortical α-synuclein load is associated with amyloid-β plaque burden in a subset of Parkinson's disease patients. Acta Neuropathol. 2008 Apr 1;115(4):417–25.

326. Braak H, Alafuzoff I, Arzberger T, Kretzschmar H, Del Tredici K. Staging of Alzheimer disease-associated neurofibrillary pathology using paraffin sections and immunocytochemistry. Acta Neuropathol. 2006 Oct;112(4):389–404.

327. Braak H, Tredici KD, Rüb U, de Vos RAI, Jansen Steur ENH, Braak E. Staging of brain pathology related to sporadic Parkinson's disease. Neurobiology of Aging. 2003 Mar;24(2):197–211.

328. Fuchs T, Gavarini S, Saunders-Pullman R, Raymond D, Ehrlich ME, Bressman SB, et al. Mutations in the THAP1 gene are responsible for DYT6 primary torsion dystonia. Nat Genet. 2009 Mar;41(3):286–8.

329. Lohmann K, Uflacker N, Erogullari A, Lohnau T, Winkler S, Dendorfer A, et al. Identification and functional analysis of novel THAP1 mutations. Eur J Hum Genet. 2012 Feb;20(2):171–5.

330. Erogullari A, Hollstein R, Seibler P, Braunholz D, Koschmidder E, Depping R, et al. THAP1, the gene mutated in DYT6 dystonia, autoregulates its own expression. Biochim Biophys Acta. 2014 Aug 1;

331. Couchman JR. Commercial Antibodies: The Good, Bad, and Really Ugly. J Histochem Cytochem. 2009 Jan;57(1):7–8.

332. Grundmann K, Glöckle N, Martella G, Sciamanna G, Hauser T-K, Yu L, et al. Generation of a novel rodent model for DYT1 dystonia. Neurobiology of Disease. 2012 Jul;47(1):61–74.

333. Obeso JA, Giménez-Roldán S. Clinicopathological correlation in symptomatic dystonia. Adv Neurol. 1988;50:113–22.

334. Asanuma K, Ma Y, Okulski J, Dhawan V, Chaly T, Carbon M, et al. Decreased striatal D2 receptor binding in non-manifesting carriers of the DYT1 dystonia mutation. Neurology. 2005 Jan 25;64(2):347–9.

335. Herzfeld T, Nolte D, Müller U. Structural and functional analysis of the human TAF1/DYT3 multiple transcript system. Mamm Genome. 2007 Nov;18(11):787–95.

336. Nolte D, Niemann S, Müller U. Specific sequence changes in multiple transcript system DYT3 are associated with X-linked dystonia parkinsonism. Proc Natl Acad Sci USA. 2003 Sep 2;100(18):10347–52.

337. Bandmann O, Nygaard TG, Surtees R, Marsden CD, Wood NW, Harding AE. Dopa-responsive dystonia in British patients: new mutations of the GTP-cyclohydrolase I gene and evidence for genetic heterogeneity. Hum Mol Genet. 1996 Mar;5(3):403–6.

338. Lüdecke B, Dworniczak B, Bartholomé K. A point mutation in the tyrosine hydroxylase gene associated with Segawa's syndrome. Hum Genet. 1995 Jan;95(1):123–5.

339. Izumi Y, Maruyama H, Oda M, Morino H, Okada T, Ito H, et al. SCA8 repeat expansion: large CTA/CTG repeat alleles are more common in ataxic patients, including those with SCA6. Am J Hum Genet. 2003 Mar;72(3):704–9.

340. Sobrido MJ, Cholfin JA, Perlman S, Pulst SM, Geschwind DH. SCA8 repeat expansions in ataxia: a controversial association. Neurology. 2001 Oct 9;57(7):1310–2.

341. Sulek A, Hoffman-Zacharska D, Zdzienicka E, Zaremba J. SCA8 repeat expansion coexists with SCA1--not only with SCA6. Am J Hum Genet. 2003 Oct;73(4):972–4.

342. Levi S, Finazzi D. Neurodegeneration with brain iron accumulation: update on pathogenic mechanisms. Front Pharmacol [Internet]. 2014 May 7 [cited 2014 Aug 19];5. Available from: http://www.ncbi.nlm.nih.gov/pmc/articles/PMC4019866/

343. Nassif M, Hetz C. Autophagy impairment: a crossroad between neurodegeneration and tauopathies. BMC Biol. 2012 Sep 21;10:78.

344. Stephenson E, Nathoo N, Mahjoub Y, Dunn JF, Yong VW. Iron in multiple sclerosis: roles in neurodegeneration and repair. Nat Rev Neurol. 2014 Aug;10(8):459–68.

345. Hardie RJ, Pullon HW, Harding AE, Owen JS, Pires M, Daniels GL, et al. Neuroacanthocytosis. A clinical, haematological and pathological study of 19 cases. Brain. 1991 Feb;114 (Pt 1A):13–49.

346. Rinne JO, Daniel SE, Scaravilli F, Pires M, Harding AE, Marsden CD. The neuropathological features of neuroacanthocytosis. Mov Disord. 1994 May;9(3):297–304.

347. Alonso ME, Teixeira F, Jimenez G, Escobar A. Chorea-acanthocytosis: report of a family and neuropathological study of two cases. Can J Neurol Sci. 1989 Nov;16(4):426–31.

348. Bird TD, Cederbaum S, Valey RW, Stahl WL. Familial degeneration of the basal ganglia with acanthocytosis: a clinical, neuropathological, and neurochemical study. Ann Neurol. 1978 Mar;3(3):253–8.

349. Burbaud P, Vital A, Rougier A, Bouillot S, Guehl D, Cuny E, et al. Minimal tissue damage after stimulation of the motor thalamus in a case of chorea-acanthocytosis. Neurology. 2002 Dec 24;59(12):1982–4.

350. Iwata M, Fuse S, Sakuta M, Toyokura Y. Neuropathological study of chorea-acanthocytosis. Jpn J Med. 1984 May;23(2):118–22.

351. Rinne JO, Daniel SE, Scaravilli F, Harding AE, Marsden CD. Nigral degeneration in neuroacanthocytosis. Neurology. 1994 Sep;44(9):1629–32.

352. Yamada M, Sato T, Tsuji S, Takahashi H. CAG repeat disorder models and human neuropathology: similarities and differences. Acta Neuropathol. 2008 Jan;115(1):71–86.

353. Greenstein PE, Vonsattel J-PG, Margolis RL, Joseph JT. Huntington's disease like-2 neuropathology. Mov Disord. 2007 Jul 30;22(10):1416–23.

354. Margolis RL, O'Hearn E, Rosenblatt A, Willour V, Holmes SE, Franz ML, et al. A disorder similar to Huntington's disease is associated with a novel CAG repeat expansion. Ann Neurol. 2001 Dec;50(6):373–80.

355. Crompton DE, Chinnery PF, Fey C, Curtis ARJ, Morris CM, Kierstan J, et al. Neuroferritinopathy: a window on the role of iron in neurodegeneration. Blood Cells Mol Dis. 2002 Dec;29(3):522–31.

356. Bartzokis G, Lu PH, Tishler TA, Fong SM, Oluwadara B, Finn JP, et al. Myelin breakdown and iron changes in Huntington's disease: pathogenesis and treatment implications. Neurochem Res. 2007 Oct;32(10):1655–64.

357. Goyal V, Shukla G, Srivastava A, Garg A, Bader B, Danek A, et al. Mineral deposition on magnetic resonance imaging in chorea-acanthocytosis: A pathogenic link with pantothenate kinase-associated neurodegeneration? Neurology India. 2013;61(2):169.

358. Dobson-Stone C, Velayos-Baeza A, Filippone LA, Westbury S, Storch A, Erdmann T, et al. Chorein detection for the diagnosis of chorea-acanthocytosis. Ann Neurol. 2004 Aug;56(2):299–302.

359. Kurano Y, Nakamura M, Ichiba M, Matsuda M, Mizuno E, Kato M, et al. Chorein deficiency leads to upregulation of gephyrin and GABA(A) receptor. Biochem Biophys Res Commun. 2006 Dec 15;351(2):438–42.

360. Lee H-J, Khoshaghideh F, Patel S, Lee S-J. Clearance of alpha-synuclein oligomeric intermediates via the lysosomal degradation pathway. J Neurosci. 2004 Feb 25;24(8):1888–96.

361. Tanik SA, Schultheiss CE, Volpicelli-Daley LA, Brunden KR, Lee VMY. Lewy body-like α-synuclein aggregates resist degradation and impair macroautophagy. J Biol Chem. 2013 May 24;288(21):15194–210.

362. Takamura A, Higaki K, Kajimaki K, Otsuka S, Ninomiya H, Matsuda J, et al. Enhanced autophagy and mitochondrial aberrations in murine G(M1)-gangliosidosis. Biochem Biophys Res Commun. 2008 Mar 14;367(3):616–22.

363. Popescu A, Lippa CF, Lee VM-Y, Trojanowski JQ. Lewy bodies in the amygdala: increase of alpha-synuclein aggregates in neurodegenerative diseases with tau-based inclusions. Arch Neurol. 2004 Dec;61(12):1915–9.

364. Charlesworth G, Bhatia KP. Primary and secondary dystonic syndromes: an update. Curr Opin Neurol. 2013 Aug;26(4):406–12.

365. LeDoux MS, Dauer WT, Warner TT. Emerging common molecular pathways for primary dystonia. Movement Disorders. 2013;28(7):968–81.

366. Sharma N, Hewett J, Ozelius LJ, Ramesh V, McLean PJ, Breakefield XO, et al. A Close Association of TorsinA and ?-Synuclein in Lewy Bodies. Am J Pathol. 2001 Jul;159(1):339–44.

367. McCarthy MI, Abecasis GR, Cardon LR, Goldstein DB, Little J, Ioannidis JPA, et al. Genome-wide association studies for complex traits: consensus, uncertainty and challenges. Nat Rev Genet. 2008 May;9(5):356–69.

368. Ward LD, Kellis M. Interpreting non-coding variation in complex disease genetics. Nat Biotechnol. 2012 Nov;30(11):1095–106.

369. Mencarelli C, Martinez-Martinez P. Ceramide function in the brain: when a slight tilt is enough. Cell Mol Life Sci. 2013 Jan;70(2):181–203.

370. Gault CR, Obeid LM, Hannun YA. An overview of sphingolipid metabolism: from synthesis to breakdown. Adv Exp Med Biol. 2010;688:1–23.

371. Mohamadnejad M, Swenson ES. Induced pluripotent cells mimicking human embryonic stem cells. Arch Iran Med. 2008 Jan;11(1):125–8.